

Drinking Water Biofiltration: Removal of Antibiotics and Behaviour of Antibiotic Resistance Genes

Like Xu

This dissertation is submitted to University College London for the
degree of Doctor of Philosophy

University College London, 2020

Declaration

I, Like Xu, confirm that the work presented in this thesis is my own. Where information has been derived from other sources, I confirm that this has been indicated in the thesis.

Abstract

This research investigated the effectiveness of biofiltration systems for the attenuation of antibiotics and antibiotic resistance genes (ARGs) from drinking water. Five antibiotics, including amoxicillin, clarithromycin, oxytetracycline, sulfamethoxazole, and trimethoprim, and the relevant resistance genes (*bla_{CTX-M}*, *bla_{OXA-1}*, *bla_{TEM}*, *ermB*, *tetA*, *tetG*, *tetQ*, *tetW*, *tetX*, *sul 1*, *sul 2*, *dfrA1* and *dfrA12*) as well as integrase genes (*intl 1* and *intl 2*) were targeted. In addition, the role the biofilm plays as a gene transfer site was also investigated. Both chemical (LC-MS/MS) and molecular biology (real-time qPCR, high-throughput qPCR and 16S rRNA amplicon sequencing) methodologies were used. A total of three biofiltration experiments using sand, granular activated carbon (GAC) and anthracite as filter media were set-up at bench-scale. Results showed that the target antibiotics were substantially removed (> 90%) by GAC-associated biofilters and partially removed (< 20%) by sand and anthracite-sand dual media biofilters. The position of GAC layer within the sand filter bed showed no effect on antibiotic removal. The absolute abundance of ARGs decreased (1.0-log reduction on average) after biofiltration, while ARGs' normalised copy number remained unchanged or showed an increasing trend in the filtered water, especially when exposed to the target antibiotics, indicating that the biofilters did not contribute greatly to the elimination of ARG pollution from the feedwater despite the effective removal of antibiotics. Exposure to the target antibiotics affected the bacterial community in biofilm samples and the differences in bacterial community structure were correlated with the changes in the resistome. Plasmid conjugative transfer experiment based on biofiltration showed that the GAC media is more conducive to the horizontal transfer of ARGs in biofilms and the transfer occurred more frequently in biofilms than in the influents and effluents. Overall, the results of this study could enhance our understanding of the prevalence of ARGs during drinking water treatment.

Keywords

Biofiltration; Antibiotic Resistance; Drinking water treatment; Biofilm.

Impact Statement

Inside academia

1) This research established in-house qPCR assays using chemically synthesised oligonucleotides as standards for the quantification of thirteen ARGs and two integron genes. The qPCR assays have been successfully applied to different types of environmental samples and are suitable for research projects that has several ARGs of interest. In addition, this method is of particular importance for the analysis of those very rare or newly-discovered ARGs.

2) A solid phase extraction coupled with liquid chromatography tandem mass spectrometer method was developed and verified for the extraction and quantification of amoxicillin, clarithromycin, oxytetracycline, sulfamethoxazole, and trimethoprim from aqueous samples. This method can be used as a reference for research projects regarding the prevalence of antibiotic residues in aquatic environment.

3) This research may help to further understand the persistence of ARGs and their association with the microbial community in drinking water biofiltration system.

Outside academia

1) The research on the overall performance of biofilters could provide useful information for optimising or updating the biofiltration process for industry. In addition, the GAC sandwich modification to slow sand filtration could be considered as a promising and cost-effective technology for both improved quality of drinking water and enhanced removal of the target antibiotics.

2) The assessment of ARGs transfer in biofilms could provide an insight into biofilter management strategies in order to find an appropriate way for the disposal of used filter media. Considering the persistence of ARGs during biofiltration, land application of drinking water waste products may act as an environmental exposure route for trace level ARGs and introduce a source for diffuse pollution in previously unexposed regions.

3) This study provides experimental evidence based on the persistence of ARGs during biofiltration treatment and highlights the need to reduce environmental pollution of drinking water by antibiotics. For policymakers and environmental regulators, there is a need to establish a comprehensive framework in the field of water policy for assessing the risk of antibiotic resistance in potable water. For instance, in addition to the several antibiotics and ARGs selected in the current surveillance systems in aquatic environment, more targets should be included to monitor antibiotic resistance both regionally and globally.

Acknowledgements

Undertaking this PhD has been a truly life-changing experience for me. It is a pleasure to thank all those who made this journey possible.

I would like to first thank my supervisor Dr Lena Ciric for all the support and encouragement she gave me during my time at UCL. Her enthusiasm on research is contagious, during our many discussions, her constant feedback on my research questions has always motivated me. Her guidance helped me in all the time of my research and writing of this thesis. Without her help, this PhD would not have been achievable. I really appreciate the positive influence she's had on my life.

My sincere thanks also goes to my second supervisor, Dr Luiza Campos, for her invaluable advice during the start-up of my experiment. She provided me the opportunity to visit Coppermill Drinking Water Treatment Works, where I could attain more knowledge beyond laboratory study.

Thanks to all my lovely colleagues who helped me so much. A very special thank you to Dr Melisa Canales, our technical officer, for always being so supportive of my work throughout these 4 years. A big thank you to Dr Asrah Mohamad, who is not only a colleague but also a lifetime friend of mine, helped me to get familiar with the life at UCL and in London when I started my PhD. Also of course a big thank you to my lovely colleagues, Stacey Harbot, Ruby Matharu, Stanislaw Makarchuk, Claire Bankier for all the fun we have had in the last four years. Thanks to Dr Elaine Cloutman-Green, who always brought tea and cakes for us all.

Many thanks to Mr Ian Seaton, who gave me access to the laboratory and research facilities, especially out of the working hours. More importantly, he constructed those perfect columns for my experiment. I am also very grateful to Dr Judith Zhou and Dr Utku Solpuker, the managers of Environmental Engineering laboratory, who were always so helpful in numerous ways and provided me with their assistance. Thanks to Dr Kersti Karu, who trained me to use the LC-MS/MS facilities in her lab and helped me to develop the analytical method. Thanks to Dr Jianqiang Su and Dr Xinyuan Zhou for the help with the high-throughput qPCR.

Thanks to all my friends in London who were always so helpful. A massive thanks to Zhuojun Li and Fan Huang, who helped me with my experiment and data analysis and have been always by my side during my ups and downs throughout this PhD. Thanks for being there for me when I really needed you. A special thanks to Shuqiong Luo for all her delicious food I ate during these 4 years. Also thanks to my many housemates: Yu Liu, Jingyi Sheng, Rui Zhou, Hao Xu, Danqing Wang, Ling Tong (to name a few), I'll always remember their kindness and support. Special thanks to Biao Song, who helped me continuously throughout these years. And also thanks to my old friends in China, Ran Tao, Linchun Tang and Runbo Shi for being so supportive. Thanks to Catherine, Anna, Jianan Li, who all helped me in numerous ways during various stages of my PhD.

I would also like to say a heartfelt thank you to my mum Jiaolian Lv, dad Qing Xu, my sisters Lijie Xu, Yamin Xu and brothers in law for always believing in me and encouraging me to follow my dreams. Without my family, I would not have had the courage to embark on this journey in the first place. My nieces and nephew, Zhipu Lu, Yihe Teng, Zhixu Lu, Ninghan Xu and Haobo Lu, thanks for supporting me with all your lovely smiles. Also thanks to my uncles, aunts and cousins for their help and support.

I gratefully acknowledge the funding received towards my PhD from Chinese Scholarship Council (CSC).

Table of contents

Declaration.....	1
Abstract.....	2
Impact Statement.....	3
Acknowledgements.....	5
Table of contents	7
List of figures	13
List of tables.....	18
List of abbreviations	20
1 INTRODUCTION	24
1.1 Problem statement	24
1.2 Research gaps	25
1.3 Aims and Objectives.....	25
1.4 Thesis outline	26
2 LITERATURE REVIEW.....	28
2.1 An overview of antibiotic pollution.....	28
2.1.1 The usage of antibiotics	28
2.1.2 The occurrence of antibiotics in the aquatic environment	30
2.1.3 The elimination of antibiotics during water treatment works.....	33
2.1.4 The selection of target antibiotics	34
2.2 Antibiotic resistance genes (ARGs) as emerging micropollutants	38
2.2.1 The prevalence of ARGs in the aquatic environment.....	38

2.2.2 The potential risk of ARG pollution	39
2.2.3 The selection of target ARGs for this study	43
2.3 Biological filtration.....	47
2.3.1 The application of biological filtration.....	47
2.3.2 Factors affecting biofiltration	50
2.3.3 Antibiotic resistance associated with biofiltration	51
2.4 Analytical methods	56
2.4.1 Detection methods for antibiotics	56
2.4.2 Methods for ARG detection and bacterial community analysis	57
3 METHODOLOGY.....	62
3.1 Introduction.....	62
3.2 Biofiltration experiment	63
3.2.1 Design of biofiltration columns.....	63
3.2.2 Operation of biofiltration columns	68
3.2.3 Sampling of biofiltration columns.....	72
3.2.4 GAC adsorption kinetics.....	74
3.3 General water quality parameters	75
3.3.1 pH, conductivity, turbidity, DO, absorbance and COD	75
3.3.2 DOC and ion characterisation	76
3.3.3 Microbial characterisation.....	76
3.4 Antibiotic quantification method development	77
3.4.1 Chemicals	77
3.4.2 LC-MS/MS detection	77

3.4.3 Solid Phase Extraction	79
3.4.4 Method validation	84
3.5 ARGs quantification method development	89
3.5.1 DNA extraction	89
3.5.2 qPCR	89
3.5.3 High-throughput qPCR	94
3.6 Bacterial community analysis	95
3.7 Conjugative gene transfer experiment	96
3.7.1 Characteristics of bacterial strains and plasmid	96
3.7.2 RP1 plasmid transfer in pure <i>E. coli</i> cultures	97
3.7.3 RP1 plasmid transformation	100
3.7.4 Conjugation experiment based on biofiltration	100
3.8 Statistics	102
4 BIOFILTER PERFORMANCE	105
4.1 Biofiltration experiment 1 - different types of filter media	105
4.1.1 pH, conductivity and dissolved oxygen	105
4.1.2 Turbidity	108
4.1.3 Absorbance and dissolved organic carbon	109
4.1.4 Nitrate, nitrite and phosphate	113
4.1.5 Total coliforms and <i>E. coli</i>	114
4.2 Biofiltration experiment 2 – difference types of GAC sandwich biofilters	116
4.2.1 Maturation stage	116
4.2.2 Experimental stage	118

4.2.3 The effect of cleaning process.....	123
4.3 Summary.....	125
5 REMOVAL OF ANTIBIOTICS	127
5.1 Biofiltration experiment 1 – different types of filter media	127
5.1.1 Matrix-matched standard.....	127
5.1.2 Overview of the target antibiotic removals	127
5.1.3 Antibiotic removal by sand and anthracite-sand dual biofilters.....	128
5.1.4 Antibiotic removal by GAC and GAC sandwich biofilters	134
5.1.5 Removal mechanism by GAC adsorption.....	137
5.2 Biofiltration experiment 2 – different types of GAC sandwich biofilters.....	141
5.2.1 The occurrence of antibiotic in River Thames.....	141
5.2.2 The removal of antibiotics	141
5.3 Summary.....	142
6 ANTIBIOTICS RESISTANCE GENES AND BACTERIAL COMMUNITY	145
6.1 Biofiltration experiment 1 – different types of filter media	145
6.1.1 ARGs in the biofilm samples	145
6.1.2 ARGs in the aqueous samples	153
6.1.3 Comparison of ARGs profiles in biofilm and aqueous samples.....	156
6.1.4 Bacterial community in filter biofilm	158
6.1.5 Relationship between water quality, antibiotics, ARGs and bacterial community.....	161
6.1.6 Summary	166
6.2 Biofiltration experiment 2 – different types of GAC sandwich biofilters.....	167
6.2.1 The occurrence of ARGs in the River Thames	167

6.2.2 ARGs in biofilm samples	168
6.2.3 ARGs in influent and effluent.....	178
6.2.4 Comparison of ARGs profiles in biofilm and aqueous sample	180
6.2.5 Bacterial community in <i>schmutzdecke</i> and GAC biofilms	181
6.2.6 Relationship among the water quality parameters and ARGs.....	185
6.2.7 Correlation between bacterial community and antibiotic resistome.....	187
6.2.8 Summary	194
7 IMPACT OF BIOFILTRATION ON PLASMID CONJUGATIVE TRANSFER	196
7.1 Conjugative transfer model construction.....	196
7.1.1 Antibiotic susceptibility testing.....	196
7.1.2 Transfer frequency of RP1 plasmid in pure <i>E. coli</i> cultures	197
7.1.3 Transconjugants identification.....	197
7.2 Plasmid conjugative transfer in biofilter.....	198
7.2.1 Plasmid conjugative transfer in media (biofilm) samples	198
7.2.2 Plasmid conjugative transfer in biofilter aqueous samples.....	203
7.3 Overall discussion	206
7.3.1 Mechanisms underlying the RP1 plasmid conjugative transfer	206
7.3.2 Reduction of conjugative transfer in drinking water treatment process	207
7.3.3 Environmental implications.....	208
7.4 Summary.....	209
8 CONCLUSION AND FUTURE WORK	211
8.1 Summary and Conclusions.....	211
8.1.1 Biofilter performance	211

8.1.2 Removal of antibiotics by biofiltration	212
8.1.3 Behaviour of ARGs during biofiltration.....	213
8.1.4 Association of ARGs with bacterial community in biofilms	213
8.1.5 Horizontal gene transfer during biofiltration	214
8.2 Limitations and suggestions for future research.....	216
References	220
Appendix – Chapter 3	252
Appendix – Chapter 4	268
Appendix – Chapter 5	276
Appendix – Chapter 6	278
Appendix – Chapter 7	298

List of figures

Figure 2. 1 Mechanisms of action of the target antibiotics..	34
Figure 2. 2 Mechanisms of DNA transfer between and within bacteria.....	40
Figure 2. 3 Schematic representation of a slow sand filter.	48
Figure 3. 1 Systematic diagram of the biofiltration experiment.	62
Figure 3. 2 Systematic diagram of the conjugative transfer system based on biofiltration ...	63
Figure 3. 3 The design of the biofilters setup.....	64
Figure 3. 4 SEM image of the surface structure of sand, GAC and anthracite.....	65
Figure 3. 5 Schematic of biofilter composition.	66
Figure 3. 6 Schematic of biofilter column set-up.....	67
Figure 3. 7 Schematic of the GAC sandwich biofilter composition.	68
Figure 3. 8 The GAC sandwich biofilter system setup.	68
Figure 3. 9 Recoveries of the selected antibiotics at different pH-values and Na ₂ EDTA concentration.	81
Figure 3. 10 Recoveries of the selected antibiotics at different elution conditions.....	83
Figure 3. 11 Recoveries of the selected antibiotics at different loading rates.....	83
Figure 3. 12 SPE-LC-MS/MS protocol in this study.	88
Figure 3. 13 Electrophoresis bands of target genes.	92
Figure 3. 14 RP1 plasmid conjugative transfer.....	98
Figure 3. 15 Bench-scale biofilters schematic..	101
Figure 4. 1 pH and the variations of pH in the influent and effluent.....	106
Figure 4. 2 Conductivity and the variations of conductivity in the influent and effluent.	107
Figure 4. 3 DO and the consumption of DO during phase I, II, and III of biofilter run.	108
Figure 4. 4 The reduction of turbidity during phase I and phase II; and before and after backwashing/cleaning.	109

Figure 4. 5 DOC concentrations in the influent and effluent samples..	110
Figure 4. 6 DOC removal and UV ₂₅₄ reduction in biofilters.	110
Figure 4. 7 DOC removal and UV ₂₅₄ reduction before and after backwashing/cleaning process.	113
Figure 4. 8 Nitrate and the variation of nitrate in the influent and effluent..	114
Figure 4. 9 Phosphate and the variation of phosphate in the influent and effluent..	114
Figure 4. 10 Mean removal of total coliforms and <i>E. coli</i> .	115
Figure 4. 11 Removal of total coliforms and <i>E. coli</i> after backwashing/cleaning..	115
Figure 4. 12 The concentration of DO, nitrate and nitrite in the influent and effluent samples; The reduction of turbidity, DOC, UV ₂₅₄ and COD during maturation stage.....	117
Figure 4. 13 The concentration of nitrate in influents from Set A and Set B during experimental stage.....	120
Figure 4. 14 The removal of turbidity, COD, absorbance, and DOC by GAC sandwich biofilters during experimental period.....	121
Figure 4. 15 Levels of DO in the influent and effluent of GAC sandwich biofilters during the experimental period.	122
Figure 4. 16 The increase of nitrate levels in the effluents of GAC sandwich biofilters during experimental period.	123
Figure 5. 1 Mean removal efficiencies of antibiotics in different biofilters.....	128
Figure 5. 2 Removal efficiencies of antibiotics by sand biofilter.	129
Figure 5. 3 Removal efficiencies of antibiotics by anthracite-sand dual biofilter.....	131
Figure 5. 4 Removal efficiencies of antibiotics by GAC biofilter..	135
Figure 5. 5 Removal efficiencies of antibiotics by GAC sandwich biofilter.	136
Figure 5. 6 Effect of contact time on the adsorption removal of antibiotics	138
Figure 5. 7 Effect of GAC dosage on the adsorption removal of antibiotics.	140

Figure 6. 1 Absolute abundance of <i>16S rRNA</i> gene, ARGs and integrons in media samples at 4-weeks and 11-weeks of system run.	146
Figure 6. 2 The correlations between the absolute abundance of ARGs and the corresponding <i>16S rRNA</i> gene and integrons in all biofilm samples.	147
Figure 6. 3 Absolute abundance of <i>16S rRNA</i> gene and total ARGs; and relative abundance of ARG and integron at each sampling site of sand biofilter.	148
Figure 6. 4 Absolute abundance of <i>16S rRNA</i> gene and total ARGs; and relative abundance of ARG categories and integron at each sampling site of GAC biofilter.	148
Figure 6. 5 Absolute abundance of <i>16S rRNA</i> gene and total ARGs; and relative abundance of ARG categories and integron at each sampling site of GAC sandwich biofilter.	149
Figure 6. 6 Absolute abundance of <i>16S rRNA</i> gene and total ARGs; and relative abundance of ARG categories and integron at each sampling site of anthracite-sand dual biofilter.	149
Figure 6. 7 Relative abundance of ARGs in biofilm samples from different biofilters.	152
Figure 6. 8 Comparison of sand biofilms collected at 20 cm.	153
Figure 6. 9 Absolute abundance and relative abundance of ARGs and integrons in the influent and effluent samples.	155
Figure 6. 10 The correlations between the absolute abundance of ARGs and the corresponding <i>16S rRNA</i> gene and integron in influent and effluent samples.	155
Figure 6. 11 The reduction of the copy numbers of ARGs in all biofilters.	156
Figure 6. 12 A heatmap showing the distinct patterns of the relative abundance of ARGs.	158
Figure 6. 13 Structure of surface biofilm microbial community at phylum level.	159
Figure 6. 14 Relative abundance of taxonomic genus in the surface biofilm samples.	160
Figure 6. 15 PCoA showing the distribution of bacterial communities in surface biofilm samples; and Venn diagram showing the number of OTUs in surface biofilm samples.	161
Figure 6. 16 RDA of the correlation between ARGs/ <i>intl 1</i> and environmental variables and VPA differentiating effects of environmental factors and <i>intl 1</i> on the ARGs variation.	162
Figure 6. 17 RDA of the correlation between major phyla and target ARGs and integron genes in surface biofilm samples.	164

Figure 6. 18 VPA differentiating effects of microbial community and integron on the ARGs variation in surface biofilm samples.....	165
Figure 6. 19 The concentration of <i>16S rRNA</i> , ARGs and integron genes in raw water.	167
Figure 6. 20 Absolute and relative abundance of ARGs and <i>intl 1</i> in B-sand and B-GAC..	169
Figure 6. 21 Absolute abundance of ARGs and <i>intl 1</i> in B- <i>schm</i> , B-sand and B-GAC samples collected at 11-week	170
Figure 6. 22 Relative abundance of ARGs and <i>intl1</i> in B- <i>schm</i> , B-sand and B-GAC samples collected at 11-week.	171
Figure 6. 23 Richness of detected ARGs and Shannon index in B- <i>schm</i> and B-GAC.	173
Figure 6. 24 Relative abundance of ARGs in B- <i>schm</i> and B-GAC.....	175
Figure 6. 25 PCoA of ARGs in B- <i>schm</i> and B-GAC.	177
Figure 6. 26 Venn diagram showing the number of detected ARGs among B- <i>schm</i> and B-GAC.	178
Figure 6. 27 Behaviour of ARGs and integron in the influent and effluent samples.	179
Figure 6. 28 The correlations between the absolute abundance of ARGs and the corresponding <i>16S rRNA</i> and integron in influent and effluent samples.	179
Figure 6. 29 The reduction of the concentration of ARGs in all GAC sandwich biofilters. ..	180
Figure 6. 30 A heatmap showing the distinct patterns of the relative abundance of ARGs and integron genes in all samples.....	181
Figure 6. 31 Bacterial phyla composition in B- <i>schm</i> and B-GAC samples	182
Figure 6. 32 Bacterial class composition in B- <i>schm</i> and B-GAC samples	182
Figure 6. 33 PCoA of bacterial communities in B- <i>schm</i> and B-GAC samples.....	183
Figure 6. 34 Heatmap showing the distribution of major genera in B- <i>schm</i> and B-GAC	184
Figure 6. 35 RDA and VPA showing the correlation between ARGs/ <i>intl 1</i> and environmental variables in effluent samples.....	186
Figure 6. 36 RDA of the correlation between major genera and relative abundance of ARGs types in biofilm samples.	188

Figure 6. 37 VPA differentiating effects of bacterial community and MGEs on the variations of ARGs in biofilm samples.....	190
Figure 6. 38 Network analysis revealing the co-occurrence patterns between ARG subtypes, MGEs and bacterial taxa.....	192
Figure 6. 39 Network analysis revealing the co-occurrence patterns between ARG subtypes and top taxonomic genera.....	193
Figure 7. 1 Petri dishes showing different zone of inhibition	196
Figure 7. 2 Transconjugants colony PCR amplification plots and electrophoresis bands...	198
Figure 7. 3 Impact of sand biofiltration on the plasmid conjugative transfer.....	199
Figure 7. 4 Impact of GAC biofiltration on the plasmid conjugative transfer.....	200
Figure 7. 5 Impact of anthracite biofiltration on the plasmid conjugative transfer.....	201
Figure 7. 6 Dynamic changes of RP1 plasmid transfer frequency in media samples.....	202
Figure 7. 7 Comparisons of plasmid conjugative transfer frequency in Set A and Set B:...	203
Figure 7. 8 Number of donor and recipient cells in the influent samples.....	204
Figure 7. 9 The removal of donor and recipient by biofilters.. ..	205
Figure 7. 10 Conjugative transfer of RP1 plasmid within stationary phase; between stationary and planktonic phase; and in planktonic phase.....	207
Figure 8. 1 Mind map showing the overall structure of the biofiltration experiment.	215

List of tables

Table 2. 1 The most frequently prescribed antibiotics in humans and sold for animal use in the UK, 2013 – 2017	30
Table 2. 2 The occurrence of antibiotics of interest in drinking waters.....	32
Table 2. 3 Major physical-chemical properties of the selected antibiotics.....	37
Table 2. 4 Antibiotic resistance genes and mobile genetic elements selected in this study.	44
Table 2. 5 Removal of the target antibiotics by biofiltration process.	52
Table 3. 1 Typical media properties for sand, GAC and anthracite.....	64
Table 3. 2 Sampling strategy of the first biofiltration experiment.....	72
Table 3. 3 Sampling strategy of the second biofiltration experiment.....	74
Table 3. 4 Methods and instruments used for the determination of general water quality parameters.....	75
Table 3. 5 Summary of the precursor and product ions, retention time, MS/MS parameters observed for the target antibiotics.	78
Table 3. 6 Solid Phase Extraction cartridges tested in this study.....	80
Table 3. 7 A comparison of recoveries observed for different cartridges.	80
Table 3. 8 The regression equations, correlation coefficients and linear range of target antibiotics.....	84
Table 3. 9 Linear regression parameters of the target antibiotics in reference matrices.	85
Table 3. 10 Recoveries, repeatability, matrix effects and method detection limits for the selected antibiotics in reference matrices.....	87
Table 3. 11 Primers and amplicon size of target ARGs in this study.....	90
Table 3. 12 Standard curves, amplification efficiency, R ² value of each qPCR array.....	93
Table 3. 13 Bacteria strains/plasmid used.....	96
Table 3. 14 Selective LB plate/broth used.....	97

Table 4. 1 SUVA ₂₅₄ values of biofilter influent and effluent samples.	112
Table 4. 2 SUVA ₂₅₄ values of GSB influent and effluent samples.	118
Table 4. 3 Mean values of water quality parameters during the experimental stage.	119
Table 4. 4 Variation of water quality parameters before and after biofilter cleaning.	124
Table 5. 1 Removal of antibiotics by sand biofilters.	130
Table 5. 2 Removal of antibiotics by anthracite-sand biofilters.	132
Table 5. 3 Removal of antibiotics by GAC biofilters.	135
Table 5. 4 Removal of antibiotics by GAC sandwich biofilters.	136
Table 5. 5 Comparison of the pseudo-first-order and pseudo-second-order adsorption rate constants.	138
Table 5. 6 Comparison of the Freundlich and Langmuir isotherm.	140
Table 5. 7 Overall mean removal of antibiotics by GAC sandwich biofilters.	142
Table 6. 1 The correlation of the relative abundance of ARGs between raw water, influent, effluent and biofilm samples.	157
Table 6. 2 The percentage relative abundance of genera associated with opportunistic human pathogens.	160
Table 6. 3 Richness of ARGs in biofilm samples.	168
Table 7. 1 The transfer frequency of RP1 plasmid in agar and broth mating systems.	197
Table 7. 2 The transfer frequency of RP1 plasmid in the influent and effluent samples.	206

List of abbreviations

AMOX	Amoxicillin
Amp	Ampicillin
AOPs	Advanced oxidation processes
ARB	Antibiotic resistant bacteria
ARGs	Antibiotic resistance genes
ASB	Anthracite-sand biofilter
B-GAC	Biofilm of GAC media
B-sand	Biofilm of sand media
B- <i>schm</i>	Biofilm of <i>schmutzdecke</i> layer
CFU	Colony forming units
CTM	Clarithromycin
COD	Chemical oxygen demand
Dfr	Dihydrofolate reductase
DHPS	Dihydropteroate synthase
DO	Dissolved oxygen
DOC	Dissolved organic carbon
DWTPs	Drinking water treatment plants
EBCT	Empty bed contact time
EDTA	Ethylenediamine tetraacetate
ESI	Electrospray ionisation
EUCAST	European Committee on Antimicrobial Susceptibility Testing
FCA	Fluoroquinolone, quinolone, florfenicol, chloramphenicol and amphenicol
GAC	Granular activated carbon
GB	GAC biofilter
GSB	GAC sandwich biofilter
HGT	Horizontal gene transfer
HLB	Hydrophilic lipophilic balance

HLR	Hydraulic loading rate
HPLC	High-performance liquid chromatography
HT-qPCR	High-throughput qPCR
HTS	High-throughput sequencing
IT	Ion trap
Kan	Kanamycin
K _{ow}	Octanol-water partition coefficient
LB	Luria-Bertani
LC-MS/MS	Liquid chromatography-tandem mass spectrometry
LOQ	Limit of quantification
LOD	Limit of detection
MCE	Mixed cellulose ester
MDR	Multi-drug resistance
MDL	Method detection limit
ME%	Matrix effect percentage
MGEs	Mobile genetic elements
MH	Mueller-Hinton
MLSB	Macrolide-Lincosamide-Streptogramin B
MRM	Multiple reaction mode
MSC	Minimal selective concentration
NPOC	Non-purgeable organic carbon
NTU	Nephelometric turbidity unit
OD ₆₀₀	Absorbance at a wavelength of 600 nm
OTC	Oxytetracycline
OTU	Operational taxonomic unit
PCoA	Principal coordinate analysis
PCR	Polymerase chain reaction
PhACs	Pharmaceutically active compounds

pK _a	Acidity coefficient
pK _b	Alkalinity coefficient
PPCPs	Pharmaceuticals and personal care products
qPCR	Quantitative real-time PCR
QqQ	Triple quadrupole
RDA	Redundancy analysis
RSD	Relative standard deviation
SB	Sand biofilter
SEM	Scanning electron microscopy
SMX	Sulfamethoxazole
SPE	Solid phase extraction
STD	Standard deviation
Str	Streptomycin
SUVA ₂₅₄	Specific UV ₂₅₄ absorbance
Tc	Tetracycline
TMP	Trimethoprim
UV	Ultraviolet
UV ₂₅₄	Absorbance of ultraviolet light at a wavelength of 254 nm
WHO	World Health Organisation
WWTPs	Wastewater treatment plants
VPA	Variation partitioning analysis

Chapter 1

INTRODUCTION

1 INTRODUCTION

1.1 Problem statement

The widespread misuse and overuse of antibiotics in both humans and veterinary settings over the past decades have led to the rapid spread of antibiotic resistant bacteria (ARB) and antibiotic resistance genes (ARGs) throughout the environment. Among the various ARB and ARG reservoirs, the aquatic environment is considered to be the most important due to the high mobility of microorganisms. Antibiotic residues and ARGs are being detected at increasing concentrations in the aquatic environment, including water bodies used as drinking water sources, constituting a major public health issue. However, there is currently no legislation or guidance for the removal of antibiotics during drinking water treatment. ARGs are recognised as emerging environmental micropollutants and their association with mobile genetic elements (MGEs) has accelerated the proliferation of ARGs in the aquatic environment. Recent studies have shown that ARGs are persistent in treated drinking water and the distribution systems that may have direct contact with human beings, raising concerns from both researchers and the public.

Biological filtration (biofiltration) is a viable drinking water treatment technology which allows microorganisms in the source water to attach to the filter media surface and develop a biofilm. Most granular media filters, including sand, granular activated carbon (GAC) and anthracite can be converted into biological filters (biofilters). In addition to the conventional aspects of biofiltration in reducing suspended solids, natural organic matters and waterborne pathogens, this process has shown the ability to remove a variety of micropollutants, including antibiotic residues, from the source water. Considering the ubiquitous presence of ARGs in natural water, the biofilm may be underestimated as a long-term reservoir harbouring various ARGs during the biofiltration process. Additionally, as a biologically active layer, the biofilm may facilitate the horizontal transfer of ARGs, contributing to their proliferation in drinking water. Considering the persistence of antibiotic residues and ARGs in natural water

environments, it is of great importance to find an economical and effective way to reduce the risk of antibiotic resistance dissemination in drinking water.

1.2 Research gaps

Thus far, most of the studies regarding the removal of antibiotics have been based on the investigation of municipal and drinking water treatment plants. Only a few research projects have focused on the underlying removal mechanisms of antibiotics and ARGs through widely-used biofiltration systems, especially when related to biofilms. For the biofilm developed on the filter media surface during the course of drinking water biofiltration period, recent research has either focused on the behaviour of ARGs or the structure of microbial communities. A sound understanding of microbial community structure of biofilm and its association with ARGs profiles may provide insights into the mechanism of persistent bacterial antibiotic resistance in drinking water treatment and thus minimise antibiotic resistance pollution. With the increasing concern of antibiotic and ARG pollution in drinking water, this study examines the hypothesis that the drinking water biofilter has the potential to treat antibiotics from the feed and the biofilms may harbour high abundance and diversity of ARGs, contributing to the spread of ARGs during the biofiltration process.

1.3 Aims and Objectives

This study aims to explore the effectiveness of biofiltration systems for the attenuation of antibiotics and ARGs from drinking water. This was achieved through the following objectives:

- set-up lab-scale biofiltration systems consisting of sand, GAC, GAC sandwich and sand-anthracite dual biofilters to mimic this process in real drinking water treatment works; explore the performance of GAC sandwich biofilter with different thicknesses and positions of the GAC layers in filter bed;

- evaluate the removal of five antibiotics (amoxicillin, clarithromycin, oxytetracycline, sulfamethoxazole, and trimethoprim) and their removal mechanisms during the biofiltration process;
- understand the fate of ARGs during the biofiltration process and their associations with bacterial communities in biofilms;
- explore the impact of filter media (sand, GAC and anthracite) on the horizontal transfer of resistance genes in biofilms and filtered water.

1.4 Thesis outline

This thesis consists of eight chapters. Chapter 1 and 2 are introduction and literature review, where motivations and background information behind this research are provided. Chapter 3 includes the set-up of all biofiltration experiments and the methodologies used throughout this study. Chapter 4 - 7 are results and discussions. Chapter 4 summarises the performances of the biofilters depending on the variations of general water quality parameters; Chapter 5 describes the removal efficiencies of antibiotics by different types of biofilters; Chapter 6 presents the results of ARGs analysis and further explores the relationship between ARGs and bacterial communities during biofiltration. Chapter 7 discusses the impact of filter media on plasmid conjugative transfer. Chapter 8 summarises the main findings in this study and provides possible directions for future studies.

Chapter 2

LITERATURE REVIEW

2 LITERATURE REVIEW

2.1 An overview of antibiotic pollution

The discovery of antibiotics was a revolution in the development of medicine in the twentieth century. The impact of antibiotics on public health is incomparable, especially at the early stage after the discovery and application of these chemical substances. 1945-1960 was the 'golden era' of antibiotic discovery, during which most of the chemical classes of antibiotics now in clinical use were first characterised and more than 20 new classes reached the market [1-3]. Antibiotics are commonly classified based on their mechanism of action, chemical structure, or spectrum of activity [4]. In general, antibiotics are classified into different sub-groups such as β -lactams, fluoroquinolones, quinolones, aminoglycosides, macrolides, lincosamides, streptogramins, chloramphenicol, tetracyclines, trimethoprim and sulfonamides [5-7]. Besides their fundamental application in human health, antibiotics have also been used for the prevention and treatment of animal and plant infections and as growth promoters in animal husbandry [8-12].

2.1.1 The usage of antibiotics

2.1.1.1 Antibiotic usage worldwide

Global antibiotic consumption has been increasing in recent years. Between 2000 and 2015, the global antibiotic consumption rate (defined daily doses per 1000 inhabitants per day) has increased by 39% based on the data obtained from 76 countries [13]. By contrast, the consumption rate increased 36% between 2000 and 2010 [14], suggesting a much slower increasing trend compared to the early 21st century. India and China were the largest consumers of antibiotics in 2010, however, very high antibiotic consumption per person was also observed in Australia and New Zealand [14]. Aarestrup reported that the global consumption of antibiotics in animals is almost twice that of humans [15]. As antibiotic consumption is a primary driver of antibiotic resistance, the rise of antibiotic consumption in human and food-producing animals and the increase in use of last-resort drugs raise serious

concerns for public health. For example, in the European Union alone, 400,000 resistant infections are estimated to occur every year, leading to about 25,000 patients deaths [16]. Similarly, a report by the US Centers for Disease Control and Prevention conservatively estimated that at least 23,000 deaths a year in the USA were caused by antibiotic-resistant infections [17]. With the rise in antibiotic resistance expected to result in more deaths due to antibiotic treatment failure than due to cancer by the year 2050 [18].

2.1.1.2 Antibiotic usage in the UK

In 2017, the UK was in the mid-range for antibiotic consumption in humans and animals among Europe: the UK was ranked 10th of 30 in the total amount of antibiotics sold for use in food-producing animals within Europe; and ranked 19th of 28 in the antibiotics administered in the community and hospital sector within Europe [19]. The English surveillance programme for antimicrobial utilisation and resistance (ESPAUR) report from Public Health England summarises the total consumption of antibiotics in primary and secondary care in the UK during 2014 to 2018 [20]. According to the report, the most commonly used groups of antibiotics for humans were penicillins, tetracyclines and macrolides. Amoxicillin was the most frequently used penicillin in humans and 94% of amoxicillin consumption was in General Practice, which is responsible for the largest share of inappropriate antibiotic prescribing in primary care. Doxytetracycline and clarithromycin were the most frequently used tetracyclines and macrolides, respectively. Considering high antibiotic usage allocated for animals, although it is not directly comparable to the usage in humans, assessment of antibiotic prescription and sales data enables some understanding of the impact of antibiotic use on the resistance patterns. In 2017, the total antibiotic use/sales in humans and animals was 773 tonnes in the UK; 64% of total use/sales was in humans. The most frequent antibiotic groups prescribed for humans and sold for animal use in the UK in 2013 and 2017 are summarised in Table 2.1. Compared to 2013, the total amount of the most prescribed antibiotic groups has reduced by 7.1% and 39.4% in human and animal use in 2017, respectively. Among the four antibiotic groups, tetracyclines sold for animal use contributed considerably (reduced by 45.9%) to the overall reduction of antibiotic usage in 2017.

Table 2.1 The most frequently prescribed antibiotics in humans and sold for animal use in the UK, 2013 – 2017 [19, 21]

Antibiotic group	Antibiotics prescribed in humans ^a (tonnes) (% of total)		Antibiotics sold for animal ^b use (tonnes) (% of total)	
	2013	2017	2013	2017
Penicillins	339.1 (65)	330.2 (67)	87.5 (20)	72.5 (26)
Tetracyclines	54.6 (10)	48.2 (10)	194 (44)	104.9 (37)
Macrolides	54.5 (10)	43.5 (9)	40.3 (9)	23.3 (8)
Trimethoprim/ Sulfonamides	24.0 (5)	17.4 (4)	60.7 (14)	31.0 (11)

^a Antibiotics used in humans including primary and secondary prescription; ^b Antibiotics sold for animals including livestock, companion animals and horses.

2.1.2 The occurrence of antibiotics in the aquatic environment

2.1.2.1 Sources of antibiotics in the aquatic environment

Antibiotics in the aquatic environment have various sources according to their usage in clinics, husbandry, agriculture and aquaculture. For the antibiotics administered to humans or animals, they can be more or less completely metabolised. Excretion rates (via urine and feces) for the unchanged active compound cover a broad range (10–90%) [4, 22, 23]. These compounds are released into municipal sewage (e.g. hospital and domestic wastewater) either as non-metabolised parent or as metabolites, or a mixture of parent and metabolites forms [4, 24, 25]. Antibiotics are only partially eliminated in wastewater treatment plants (WWTPs) and may end up in the environment, constituting a large amount of antibiotic residue in natural water environments [4]. Furthermore, the adoption of liquid manure as fertiliser in agriculture which can be washed off from the top soil by runoff, resulting in the release of active substances remaining in manure to the natural environment [26]. The direct discharge from pharmaceutical factories, poultry processing, meat processing and aquaculture also contributes to an increase in the total antibiotic residues in aquatic environments [4, 27]. To tackle this issue, the EU Water Framework Directive includes a list of potential water pollutants that must be carefully monitored in surface waters to determine the risk they pose to the aquatic environments. The updated Watch List in 2018 includes the macrolides erythromycin,

clarithromycin and azithromycin, the β -lactam amoxicillin and the fluoroquinolone ciprofloxacin [19].

2.1.2.2 Antibiotic residues in the aquatic environment

The concentrations of antibiotic in typical aquatic environments are well documented: in the high $\mu\text{g/L}$ range in hospital effluent, in the low $\mu\text{g/L}$ range in municipal waste water, and in the ng/L range in surface water, ground water, sea water and tap water [28-31]. Singer *et al.* reported mean river concentration of antibiotics (17–74 ng/L) [19], with clarithromycin (max = 292 ng/L) yielding the highest single measure in the River Thames catchment samples. Jiang *et al.* investigated the occurrence and seasonal variation of 22 antibiotics, including four tetracyclines, two macrolides, three chloramphenicols, six fluoroquinolones, six sulfonamides and trimethoprim, with the detection frequencies ranging from 5.3% to 100% in 19 sampling sites along Huangpu River in Shanghai, China [32]. The concentrations of detected antibiotics were typically in the ng/L level, which represented moderate antibiotic contamination level when compared to other sites globally. Similarly, a total of 28 antibiotics was detected quite frequently in the low ng/L range, up to 2 $\mu\text{g/L}$ (sulfamethoxazole) in the surface waters of six rivers including freshwater, estuarine and marine samples within watersheds of South–East Queensland, Australia [33].

Despite the presence of antibiotics in surface waters, few studies have reported the contamination of drinking water by antibiotics in different countries and regions. Table 2.2 lists the concentrations of antibiotics of interest in drinking water, including finished water from drinking water treatment plants (DWTPs) and tap water. In Spain, four antibiotics out of 54 targeted pharmaceuticals, *i.e.*, azithromycin, clarithromycin, erythromycin and sulfamethoxazole, were detected at measurable levels in finished drinking water [31]. Sulfamethoxazole and trimethoprim were detected (lower than 3.0 ng/L) in both finished drinking water and tap water from 19 U.S. water utilities [34]. Leung *et al.* monitored 32 pharmaceuticals in Chinese tap water from 13 cities and 17 pharmaceuticals were detected in 89% samples [35]. According to their research, the authors suggested that sulfamethazine and clarithromycin should both be considered as high priority for management. The study of

amoxicillin in drinking water has been scarce due to the instability of amoxicillin and the limitation of available analytical methods. In fact, there are few comprehensive, systematic studies on the occurrence of antibiotics in drinking water and the limited data are a challenge in assessing potential human health risks. The effect of chronic, low-level exposure to antibiotics on the human body is still unknown (WHO, 2012) [36].

Table 2.2 The occurrence of antibiotics of interest in drinking waters.

Antibiotics	Sample matrix	LOQ (ng/L)	Max (ng/L)	Mean (ng/L)	Ref.
Amoxicillin	finished water	20	ND	ND	[33]
	treated drinking water before final chlorination	120	ND	ND	[37]
	finished water	115	ND	ND	[23]
Clarithromycin	tap water	0.2	2.2	0.2	[31]
	treated drinking water before final chlorination	0.2	ND	ND	[37]
	tap water	0.7	11.9	6.7	[35]
Oxytetracycline	finished water	2.0	ND	ND	[38]
	finished water	4.4	ND	ND	[39]
	finished water	10	ND	ND	[33]
Sulfamethoxazole	tap water	1.0	1.4	< LOQ	[31]
	treated drinking water before final chlorination	1.0	ND	ND	[37]
	tap water	0.25	3.0	0.39	[34]
	finished water	0.9	ND	ND	[38]
	tap water	2.7	21.2	8.0	[35]
	finished water	7.1	< 5.0	< 5.0	[39]
Trimethoprim	tap water	0.25	< 0.25	< 0.25	[34]
	treated drinking water before final chlorination	0.9	ND	ND	[37]
	tap water	5.2	14.2	10.2	[35]
	finished water	1.3	ND	ND	[39]

Finished water: water samples collected after the final treatment step in drinking water treatment plant; tap water: water samples collected directly from taps; LOQ: limit of quantification; ND: not detected.

2.1.3 The elimination of antibiotics during water treatment works

Several antibiotics can be naturally biodegraded as they have been in contact with environmental microbiota for millions of years, and the degradation can even serve as a food source for several microorganisms [40]. By contrast, synthetic antibiotics (e.g. quinolones) can be more recalcitrant to degradation in the natural environment [10]. The elimination of antibiotics is the result of different processes, both biotic (biodegradation by bacteria and fungi) and abiotic (sorption, hydrolysis, photolysis, oxidation and reduction) [4].

The removal of antibiotics during conventional wastewater treatment processes is highly variable due to the treatment technologies and the physiochemical and biological properties of the antibiotic itself. Reungoat *et al.* summarised the technologies which have proven to be effective in removing antibiotics in water treatment works, including activated carbon adsorption, ozonation, advanced oxidation processes (AOPs) and membrane filtration [41]. The combination of activated carbon and ozonation can be very effective in removing organic micropollutants in both wastewater and drinking water treatment processes [42-44]. Biofiltration represents an alternative technology for the removal of organic micropollutants due to its stability and low energy requirements [41]. Among which sand filtration and biological activated carbon filtration are two of the most common biofiltration technologies. Activated carbon displays several advantages due to its great potential to adsorb micropollutants of different types while sand biofiltration is considered a promising technology due to the low cost of sand [41, 45]. AOPs like Fenton oxidation, or photocatalytic oxidation have been shown to effectively remove antibiotics with high removal efficiencies (>90%) [46]. The major concern of applying oxidation processes is the formation of a wide number of oxidation by-products (or transformation products) from micropollutants. To further reduce parent compounds and oxidation by-products, biological post-filtration (sand filtration or activated carbon filtration) can be considered [46].

2.1.4 The selection of target antibiotics

The selection of the target antibiotics was based on three main criteria: 1) presence in surface waters used as source of drinking water; 2) differences in physico-chemical properties, and 3) availability of a reliable analysis method. Five antibiotics, including amoxicillin, clarithromycin, oxytetracycline, sulfamethoxazole and trimethoprim were selected in this study. Table 2.3 summarises the major physico-chemical properties of the selected antibiotics. Mechanisms of action of the target antibiotics is shown in Figure 2.1.

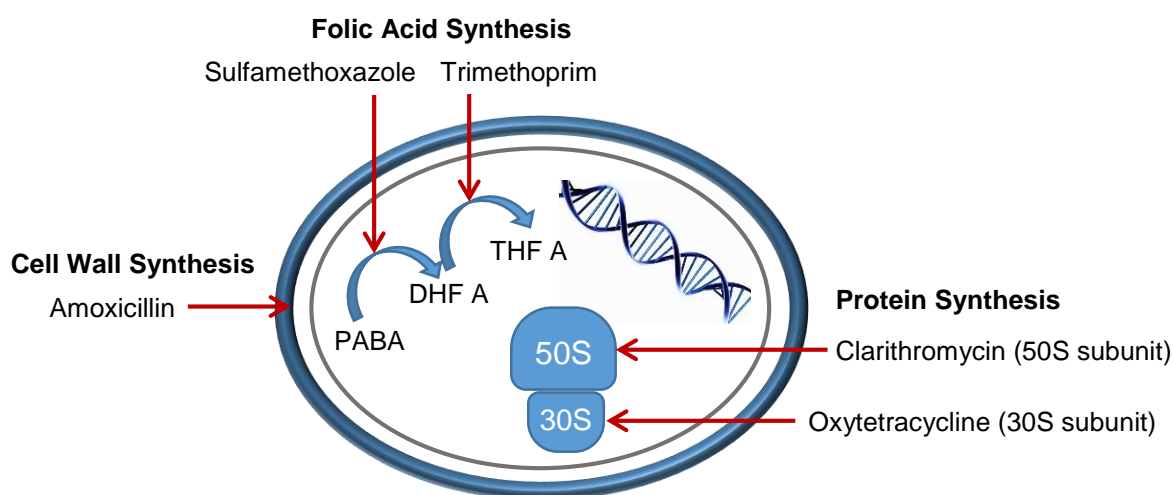


Figure 2.1 Mechanisms of action of the target antibiotics.

PABA: para-aminobenzoic acid; DHF A: dihydrofolic acid; THF A: tetrahydrofolic acid.

2.1.4.1 Amoxicillin

Amoxicillin is a broad spectrum amino-penicillin antibiotic, widely used in human and veterinary medicine. It is usually the drug of choice within the class as it is better absorbed, following oral administration, than other β -lactam antibiotics [47]. This β -lactam antibiotic belongs to a group of drugs excreted by the body unmetabolised (present in the form of amoxicillin rather than a transformation product), and it is predicted to have heavy environmental load due to high usage [48]. A difficulty for the study of amoxicillin in the natural environment is its poor stability in aqueous solution and the low sensitivity of available analytical methods [48, 49]. Meanwhile, β -lactams are not generally thought to be of concern as environmental pollutants due to the ability to be degraded through hydrolytic cleavage and

ultimate mineralisation to CO₂ and water [33]. However, low concentrations of a number of β -lactam drugs (e.g. amoxicillin, penicillin G and penicillin V) were sporadically reported in the effluent of WWTPs ranging from 10 ng/L to 200 ng/L [33, 48]. This may indicate that although the reports of these antibiotics are scarce and they are not considered persistent in the classic sense, a pseudo-persistence may be occurring due to their continual discharge to aquatic systems via WWTPs, albeit in small quantities [50].

2.1.4.2 Clarithromycin

Clarithromycin is a macrolide antibiotic used to treat skin, throat and lung infections. Clarithromycin binds to the microbial 50S ribosomal sub-unit, thereby inhibiting protein synthesis. Up to 40% of the consumed clarithromycin is excreted unchanged as the parent compound and about 60% is excreted metabolised [51]. Its major metabolite, 14-hydroxy(R)-clarithromycin is pharmacologically active and has also been found in surface waters [51]. Clarithromycin was recently added to a watch list of priority pollutants by the European Union and has been constantly detected in wastewater, surface and ground water at concentrations ranging from ng/L to low μ g/L [52, 53]. The drug was detected in concentrations ranging from 5 to 360 ng/L in German rivers and up to high μ g/L levels in a small river of southern France [54]. Clarithromycin was also present along all selected river water samples in Italy [55].

2.4.4.3 Oxytetracycline

In most countries, tetracyclines are the most commonly used veterinary antibiotics [56, 57], among which oxytetracycline was widely administered to farm animals to control intestinal and respiratory infections [58]. Oxytetracycline targets the microbial 30s ribosomal sub-unit to inhibit protein synthesis. This antibiotic has been in use since the 1960s and has been overused or misused in the past decades in applications aimed at preventing and treating diseases and improving growth rates in poultry [59]. Sebastine and Wakeman identified that oxytetracycline may accumulate and lead to problems in the aquatic environment due to its poor biodegradability [60]. Oxytetracycline has been detected in the effluent of oxytetracycline production facilities at extremely high concentrations (20-800 mg/L) [61, 62], which could be considered as a point discharge affecting a limited area but may pose a long-term effect on

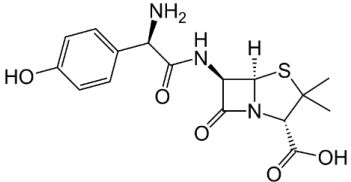
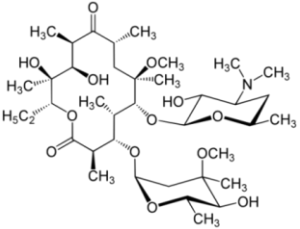
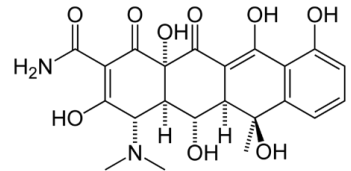
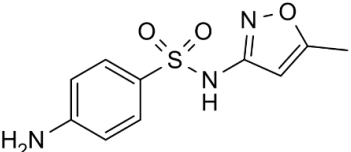
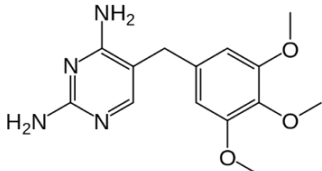
the aquatic environment, as high concentrations of oxytetracycline (0.38-2.0 mg/L) were still detected in the receiving surface water.

2.4.4.4 Sulfamethoxazole/trimethoprim

The combination of trimethoprim and sulfamethoxazole, also known as co-trimoxazole, is an antibiotic used to treat a variety of bacterial infections such as those of the urinary and respiratory tract. Sulfamethoxazole is a typical sulfonamide antibiotic which entered the market in the 1970s and inhibits an enzyme involved in the synthesis of tetrahydrofolic acid (part of the thymidine metabolic pathway in DNA synthesis) [63]. Trimethoprim belongs to the class of chemotherapeutic agents known as dihydrofolate reductase inhibitors. Trimethoprim acts by targeting an enzyme involved in the tetrahydrofolic acid pathway and so sulfamethoxazole and trimethoprim have often been used together in therapy since 1974 [63].

Sulfamethoxazole is among the most widely detected antibiotic in aquatic environments [64]. It was found to be incompletely removed by WWTPs, with the median concentration of 290 ng/L in the final effluent. The principal sulfamethoxazole metabolite, acetyl-sulfamethoxazole has been reported to occur at low concentrations in a small percentage of samples collected from rivers receiving WWTP effluent [65]. Similarly, trimethoprim has been frequently detected in surface waters in Europe, Canada and USA with a maximum measured concentration of 0.71 µg/L [66].

Table 2.3 Major physical-chemical properties of the selected antibiotics.

Antibiotics	Family	Mechanism	Formula	Mass	Structure *	pK _a , pK _b *	logK _{OW} *
Amoxicillin (AMOX)	β-lactam	Cell wall synthesis inhibitor	C ₁₆ H ₁₉ N ₃ O ₅ S	365.4		3.23, 7.43	0.87
Clarithromycin (CTM)	Macrolide	Protein synthesis inhibitor	C ₃₈ H ₆₉ NO ₁₃	747.9		12.46, 8.38	3.16
Oxytetracycline (OTC)	Tetracycline	Protein synthesis inhibitor	C ₂₂ H ₂₄ N ₂ O ₉	460.4		0.24, 7.75	-0.90
Sulfamethoxazole (SMX)	Sulfonamide	Folic Acid synthesis inhibitor	C ₁₀ H ₁₁ N ₃ O ₃ S	253.3		6.16, 1.97	0.89
Trimethoprim (TMP)	Trimethoprim	Folic Acid synthesis inhibitor	C ₁₄ H ₁₈ N ₄ O ₃	290.3		17.33, 7.16	0.91

pK_a: acidity coefficient; pK_b: alkalinity coefficient. K_{OW}: octanol-water partition coefficient. * Structures of antibiotics, pK_a, pK_b and logK_{OW} values were obtained from <https://www.drugbank.ca/documentation/search>.

2.2 Antibiotic resistance genes (ARGs) as emerging micropollutants

Along with the extensive use of antibiotics worldwide, antibiotic resistance has become a growing issue. This problem has been described as 'the best-known example of rapid adaption of bacteria to a new ecosystem' [67]. Antibiotic resistance in bacteria has been recognised as one of the greatest threats to human health by the WHO [68]. Pruden *et al.* defined antibiotic resistance genes (ARGs) as emerging environmental contaminants in 2006. Antibiotic resistance is ancient, however, it is the increase in the numbers and diversity of resistant organisms that has made resistance a huge clinical problem [69]. Superbugs, some of which are resistant to multiple antibiotics, are now one of the biggest challenges faced by modern medicine [70, 71].

2.2.1 The prevalence of ARGs in the aquatic environment

ARGs are diverse and ubiquitous in natural environments [72]. Hundreds of ARGs are detected in various environmental samples, including wastewater and drinking water treatment plants, livestock, aquaculture, surface water, tap water, soil and sediment [73-77]. As a result of extensive use of human and veterinary antibiotics, hospital wastewater and livestock manure are considered as the major sources of environmental ARGs [78, 79]. ARGs can enter into aquatic environments by direct discharging of untreated wastewater or into WWTPs through wastewater collection systems and subsequently into the environments with effluents and discharged sludge [80-82]. Furthermore, aquaculture [77, 83] and agriculture [84] also contribute to the dissemination of ARGs in aquatic environments. Surface water and shallow groundwater are commonly used as sources of drinking water, however, the high concentrations of ARGs remaining in source waters may enter water supply pipelines through drinking water treatment and distribution systems and increase the potential for antibiotic resistance pollution in drinking water [85].

2.2.2 The potential risk of ARG pollution

2.2.2.1 Mechanisms of antibiotic resistance

Bacterial antibiotic resistance can be attained through intrinsic or acquired mechanisms. Intrinsic mechanisms are those specified by naturally occurring genes found on the host's chromosome, which are independent of antibiotic selective pressure. The conventional example of intrinsic antibiotic resistance is the multi-drug resistant (MDR) phenotype exhibited by Gram-negative bacteria, which are resistant to many classes of antibiotics due to the presence of Gram-negative outer membrane [86, 87]. Acquired resistance is of greater concern where initially susceptible bacteria can become resistant to an antibiotic via mutations in chromosomal genes and by horizontal gene transfer (HGT) [69]. The resistant mechanisms were summarised by Poole [88] as:

1) *target alteration*, which changes in drug targets that interfere with or limit antibiotic interaction also prevent the bacteriostatic/bactericidal effects of these agents and, thus, promote resistance;

2) *impermeability*, which antibiotics must access intracellular targets in order to exert their bacteriostatic or bactericidal actions on bacteria. The outer membrane barrier is a major resistance mechanism among Gram-negative bacteria;

3) *enzymatic modification or destruction*, which the acquisition of genes encoding enzymes enables the organisms to destroy antibiotics before they can have an effect. This is the predominant mechanism of resistance to β -lactams;

4) *efflux*, which the acquisition of efflux pumps can extrude the antibiotic from the cell before they reach target sites and exert their effect. Efflux mechanism can be widely found in tetracycline resistant bacteria [89].

2.2.2.2 Horizontal transfer of ARGs

In bacteria, HGT is widely recognized as the mechanism responsible for the widespread distribution of ARGs [90, 91]. The association of ARGs and mobile genetic elements (MGEs) can accelerate the proliferation of ARGs through HGT mechanisms. Genetic

mechanisms involved in horizontal transfer of ARGs among environmental bacteria include conjugation, transduction, and transformation (Figure 2.2) [1, 91].

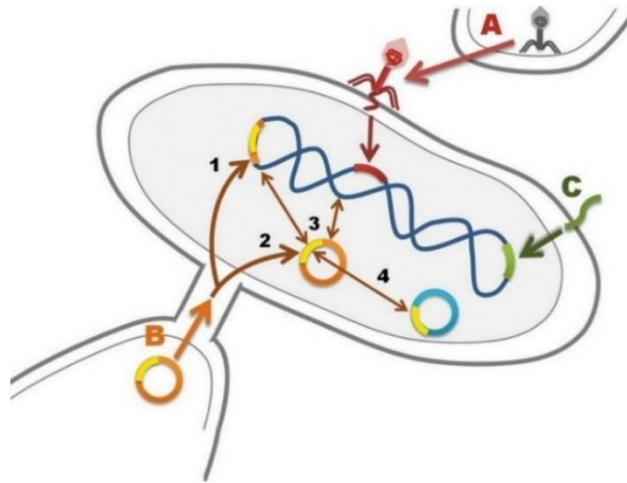


Figure 2.2 Mechanisms of DNA transfer between and within bacteria (adapted from [91]).

(A) Transduction: injection of DNA into a bacterium by a phage. (B) Conjugation: plasmid in a donor bacterium is transferred through a pilus into a recipient bacterium; plasmid may integrate into the chromosome (1) or remain in the cytoplasm (2); plasmid may be transferred between cytoplasmic and chromosomal locations (3); plasmid may exchange insertion sequences or transposons with other plasmids (4) or the chromosome. (C) Transformation: uptake of naked DNA from the environment.

1) Conjugation

Conjugative MGEs include plasmids, transposons, and integrons on plasmids or transposons. Conjugation occurs more frequently between closely related strains (within genera) or species of bacteria and at a relatively low frequency across genera. Of all the mechanisms and MGEs that mediate HGT between bacteria, conjugation by self-transferable plasmids is by far the most common mechanism of HGT [92-94]. Conjugative plasmid transfer occurs in various environments and the frequencies often vary significantly. Generally, the efficiency of plasmid transfer (expressed as number of transconjugants/number of recipient cells) in bulk environments such as bulk water and bulk soil is low (typically $< 10^{-5}$) [94]. By contrast, the transfer frequency can typically be as high as 10^{-3} or even 10^{-1} for indigenous and introduced plasmids in biofilm-supporting environments [94, 95].

A number of studies evaluating the possibility of conjugative ARG transfer in natural aquatic systems suggested that this process can account for significant frequencies of HGT

in environmental bacterial populations. Alcaide and Garay observed that ARG plasmid transfer (conferring resistance to amoxicillin, chloramphenicol, tetracycline, and ampicillin) occurred readily in wastewaters and polluted surface waters, with transfer frequencies ranging from 10^{-7} to 10^{-3} [96]. In addition, conjugative plasmids isolated from a natural river exhibited transfer frequencies ranging from 10^{-7} to 10^{-1} to the recipient strain *Escherichia coli* (*E. coli*) J53 [97], and the majority of these plasmids showed multi-resistant phenotypes, most of which were tetracycline and sulfonamide resistance.

Transposons are MGEs that can exist on plasmids or integrate into other transposons or the host's chromosome. Transposons and insertion sequences often jump randomly and occasionally on genome or plasmid, among which conjugative transposons are unique in having qualities of plasmids and can facilitate the transfer of endogenous plasmids from one organism to another [87, 98]. An integron is not capable of moving itself but can capture, integrate, and express resistance gene cassettes in their variable regions and can be transmitted via transposons and conjugative plasmids [87]. Gene cassettes carried on the integrons contained miscellaneous ARGs encoding resistance to β -lactams, aminoglycosides, sulfonamides, trimethoprim, tetracycline, streptomycin, chloramphenicol and quaternary ammonium compounds in the drinking water [99].

2) Transduction

Transduction is achieved through injection of DNA by a bacteriophage. Numerous studies examining DNA transfer from phage donors to recipients under environmentally relevant conditions have conclusively demonstrated the relevance of transduction as a general means of HGT amongst environmental bacterial populations in a wide variety of aquatic compartments, such as WWTPs, rivers and lakes [100]. Several more recent investigations have highlighted the presence of a wide variety of phage-borne ARGs conferring resistance to β -lactams and other antibiotics in municipal wastewater and surface water samples [101, 102], suggesting that transduction could represent an important mechanism for ARG dissemination in the relevant environmental matrixes [103].

3) Transformation

Through the process of natural transformation, extracellular plasmid or chromosomal DNA originating from a donor cell can be taken up from the environment and incorporated into naturally competent recipient cells (e.g. *Acinetobacter*) [103, 104]. Once lysis occurs, free DNA can remain stable for a certain period and be incorporated by transformation. However, free DNA is quite susceptible to environmental degradation. DNA exchange by natural transformation occurs more frequently amongst cells of the same species, but has also been observed to occur amongst diverse species [105]. For instance, transformation is believed to represent a key means of gene exchange amongst the streptococci, meningococci, and related genera [93].

Some antibiotic-like environmental pollutants, such as heavy metals (e.g. Cd, Hg, Cu, and Zn), disinfectants and disinfection by-products, are considered to have cross- or co-resistance to antibiotics in terms of the selection of bacterial resistance, and may be important contributors to the spread of antibiotic resistance in the environment [99, 106, 107]. These co-selection mechanisms are partly due to the fact that the genes encoding resistance to antibiotics are located on the same MGE as genes encoding resistance to antibiotic-like elements such as disinfectants and heavy metals [99, 108].

2.2.2.3 HGT in aquatic biofilms

Biofilms consist of microorganisms, their excreted metabolic products (known as extracellular polymeric substances), various organic and inorganic particles, and water [94]. Biofilms are particularly suited for HGT, as they sustain high bacterial density and metabolic activity. The extensive research on HGT and biofilms in environmental microbiology leads to the recognition of their high relevance for bacterial adaptation and evolution. Bacteria and their plasmids have co-evolved to provide key mechanisms for gene transfer and to ensure their own survival as components of the horizontal gene pool [94]. In addition, the products of conjugational genes could further promote cell-to-cell contact, which can facilitate biofilm formation [109].

Aquatic biofilms are long-term reservoirs for ARGs in the environment and they have been shown to facilitate HGT of ARGs under environmental conditions due to the nutritional richness and high bacterial density and diversity [110]. Schwartz *et al.* detected the presence of bacteria exhibiting elevated resistance to vancomycin, ceftazidime, ceftazolin, and penicillin G in drinking water biofilms compared to the raw water supply [111]. In addition, they demonstrated that a vancomycin resistant gene, *vanA*, was detected in drinking water biofilms in the absence of bacterial host enterococci, suggesting possible gene transfer to autochthonous drinking water bacteria [111]. Farkas *et al.* reported that biofilm community in a drinking water treatment plant is a reservoir of class 1 integrons, suggesting that drinking water biofilm has the potential to accumulate resistance determinants [112]. Furthermore, research mimicking natural receiving water bodies revealed that tetracycline resistance genes migrated rapidly to biofilms and persisted longer than adjacent water [113]. The above observations suggest that biofilm may be an optimum site for ARG transfer in aquatic environments.

2.2.3 The selection of target ARGs for this study

The selection of the target ARGs was based on: 1) the antibiotic to which they confer resistance; 2) the mechanism of resistance and, 3) their presence in surface waters. Thirteen ARGs encoding resistance to different antibiotics and two integron-integrase genes (*intl 1* and *intl 2*) were selected for this study (Table 2.4). In particular, 40% of the targeted genes, *i.e.*, β -lactam ARGs, *bla*_{CTX-M} and *bla*_{TEM}; sulfonamide ARGs, *sul1* and *sul2*; macrolide ARG, *ermB* and the class 1 integron, *intl 1*) have been selected by the European COST (Cooperation in Science and Technology) Action DARE (Detecting Evolutionary Hotspots of Antibiotic Resistance in Europe, TD 0803) as genetic determinants to assess the antibiotic resistance status in environmental setting [114].

Table 2.4 Antibiotic resistance genes and mobile genetic elements selected in this study.

Gene Classification	ARGs	Mechanism	Associated MGEs *
β-lactams	<i>bla_{TEM}</i>	inactivation	plasmids [115, 116] insertion sequences [117]
	<i>bla_{OXA-1}</i>	inactivation	plasmids [118, 119] insertion sequences [119]
	<i>bla_{CTX-M}</i>	inactivation	plasmids [116], insertion sequences [117] integrons [120]
Macrolides	<i>ermB</i>	protection	conjugative transposons [121]
Tetracyclines	<i>tetA</i>	efflux	conjugative transposons [122] plasmids [79]
	<i>tetG</i>	efflux	conjugative transposons, integrons [123]
	<i>tetQ</i>	protection	conjugative transposons [124]
	<i>tetW</i>	protection	conjugative transposons [125]
	<i>tetX</i>	inactivation	conjugative transposons [126]
Sulfonamides	<i>sul1</i>	protection	plasmids [127], integrons [123]
	<i>sul2</i>	protection	plasmids [77]
Trimethoprim	<i>dfrA1</i>	inactivation	integrons [79]
	<i>dfrA12</i>	inactivation	integrons [128]
Mobile genetic elements	<i>int1</i>	integrase	-
	<i>int2</i>	integrase	-

*: ARGs locate on or commonly link to mobile genetic elements (MGEs).

2.2.3.1 ARGs related to β-lactam antibiotics

The mechanisms of β-lactam resistance include inaccessibility of the antibiotics to their target enzymes, modifications of target enzymes, and/or direct deactivation of the antibiotics by β-lactamases [129]. Resistance to β-lactams in Gram-negative bacteria is mediated by two

major types of β -lactamases: the chromosomally-encoded enzymes of the Amber class C (e.g. AmpC β -lactamase in *Citrobacter*, *Enterobacter* and *Pseudomonas aeruginosa*) or by plasmid-encoded enzymes of the Amber class A, in species that do not produce AmpC β -lactamases, such as *E. coli*, *Salmonella spp.*, and *Shigella spp.* [67]. A variety of genes (*ampC*, *bla_{TEM}*, *bla_{CTX-M}* and *bla_{SHV}*) encoding resistance to β -lactams have been identified in bacteria derived from wastewater, surface water and drinking water samples [97, 111, 130-132]. These environmental compartments may further serve as reservoirs for β -lactam resistance genes. For instance, *bla_{TEM}*, one of the most widespread antibiotic resistance genes in the environment and associated mainly with *Enterobacteriaceae*, is considered as an indicator of anthropogenic antibiotic resistance contamination [130, 133]. Plasmid-mediated *ampC* and *bla_{TEM-1}* have been frequently detected in drinking water [99], which further increases the environmental dissemination of resistance.

2.2.3.2 ARGs related to macrolide

The *erm* genes encode resistance to macrolides associated with ribosomal RNA (rRNA) methylation, efflux, and inactivation [79]. *Erm* genes are persistent in wastewater, surface water and drinking water [81, 99]. Among the macrolide resistance genes, *ermB* is considered as the most prevalent gene in environmental microorganisms [79] and confers cross-resistance to macrolide, lincosamide and streptogramin B antibiotics. *Erm* genes can easily be transferred from one host to another, as they are usually acquired and associated with mobile elements, such as plasmids and transposons [134, 135]. For instance, the *ermB* gene is carried by transposons Tn917 and Tn1545 in pathogenic Gram-positive bacteria (e.g. *Streptococcus pneumoniae* and *Enterococcus faecalis*) [136, 137]. In addition, *erm* genes were reported to be positively correlated with *tet* genes in clinical- and environmental-related samples [136, 138], as these genes are often co-located on the same MGEs.

2.2.3.3 ARGs related to tetracyclines

Resistance mechanisms among the *tet* genes involve efflux pump (e.g. *tetA*, *tetG*), ribosomal protection (target modification, e.g. *tetM*, O, S, Q and W) and enzyme inactivation (e.g. *tetX*). *Tet* genes in the environment have been extensively studied in WWTPs [139],

DWTPs [140], agriculture [141] and aquaculture [77]. In particular, Harnisz *et al.* studied the prevalence of *tet* genes in the Lyna River in Poland and suggested that *tet* genes (especially *tetB*) could be used as molecular indicators of anthropogenic changes in aquatic environments [142]. Many *tet* genes are located on non-mobile plasmids or incomplete transposons in the chromosome [89]. However, some genes encoding efflux enzymes and ribosomal protection have a broad host range and have been found in several environmental genera [79]. *TetA*, *D*, and *M* can be transferred horizontally by plasmids encoding tetracycline resistance from environmental microorganisms to *E. coli* strains isolated from chickens, pigs, and humans [143].

2.2.3.4 ARGs related to sulfonamides/trimethoprim

Resistances to sulfonamides is often encoded by mutations located on highly conserved regions of dihydropteroate synthase (DHPS) genes [144]. Such chromosomal mutations in the DHPS gene has been identified in pathogens such as *E. coli*, *Staphylococcus aureus* and *Streptococcus pneumoniae* [144]. Plasmid-borne genes that encode alternative drug-resistance variants of the DHPS enzymes, such as *sul1* and *sul2*, are mediated by MGEs. *Sul1* was one of the first discovered plasmid-borne sulfonamide resistance genes [145] and is typically associated with class 1 integrons, while *sul2* is mostly found on small non-conjugative plasmids or large transmissible multi-resistant plasmids [144]. *Sul* genes have been widely reported in aquatic environments [125, 140]. In addition, mediated by MGEs, *sul* genes can be disseminated and transferred horizontally within and between bacterial species in various water samples [79]. The most widespread trimethoprim resistance mechanism is the replacement of a trimethoprim-sensitive dihydrofolate reductase (*dfr*) gene by a plasmid-, transposon-, or cassette-borne trimethoprim-resistant *dfr* [146]. *Dfr* gene cassettes are frequently found in the variable regions of integrons and are often the only gene cassettes present in environmental isolates. Several *dfrA* genes encoding resistance to trimethoprim are commonly found in various environmental isolates [122, 147], among which *dfrA1* is one of the static resistance genes located on class II integrons [148, 149].

2.2.3.5 Class 1 and class 2 integrons

Two mobile elements, class 1 and class 2 integron-integrase genes (*intl 1* and *intl 2*) were targeted in this study. Class 1 integrons are ubiquitous in environmental microbiomes and used as a proxy for antibiotic resistance in the environment [123]. *Intl1* was reported to integrate and express more than 100 types of resistance genes by gene cassettes, most of which were aminoglycoside and trimethoprim resistance genes and β -lactamases [123, 150]. As another contributor to the wide spread of antibiotic resistance in microorganisms, class 2 integrons have been commonly reported in some species of Gram-negative organisms such as *Acinetobacter*, *Enterobacteriaceae* and *Pseudomonas* [151]. In contrast, class 2 integrons are less commonly found in environmental samples. For instance, detection frequencies of *intl1* and *intl2* were 85% and 1.2% in drinking water samples, respectively [99].

2.3 Biological filtration

2.3.1 The application of biological filtration

Biological filtration (biofiltration) is a traditional drinking water treatment technology which is widely used in Europe [152]. Most granular media filters, including sand, granular activated carbon (GAC), anthracite and ceramic can be converted into biological filters (biofilters) simply by not carrying a disinfection residual through the filter, which allows indigenous microbial communities in the source water to attach and colonise the surface of media and develop a biofilm. In addition to single medium biofilters, combinations of different filter materials with proper gradation is also common practice in DWTPs.

2.3.1.1 Sand biofiltration

Slow sand filtration is one of the earliest forms of drinking water treatment. Schematic of a typical slow sand filter is shown in Figure 2.3. The major function of the sand biofilter occurs at the surface layer (known as the *schmutzdecke*) of the sand bed in which biological activities are the highest [153]. The nature of the *schmutzdecke* varies based on source water characteristics, but a typical *schmutzdecke* consists of a gelatinous biofilm matrix made up of bacteria, fungi, protozoa, plankton, diatoms, rotifers and algae and their extracellular material.

Suspended solids and waterborne pathogens are removed by sand filtration via both physical processes and biological processes.

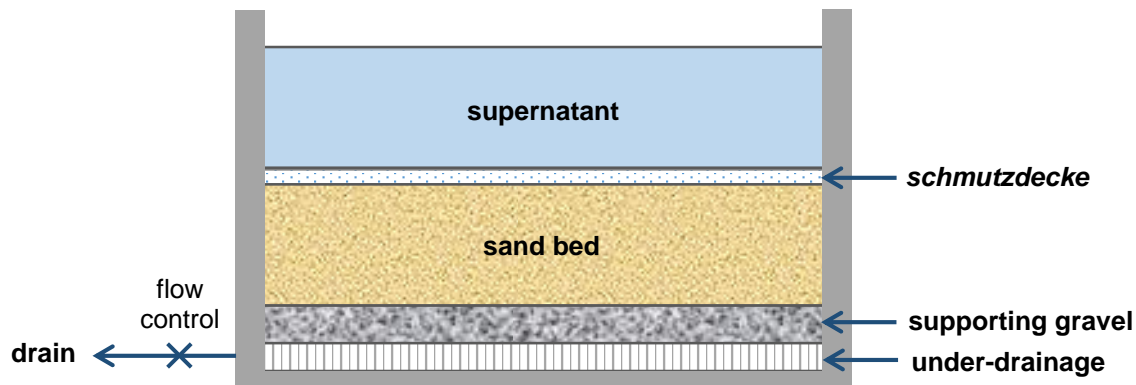


Figure 2.3 Schematic representation of a slow sand filter.

In contrast to rapid sand filtration, slow sand filtration can provide an efficient single-stage treatment for raw water within certain water quality limits of turbidity and other parameters such as organic carbon, *Cryptosporidium*, pesticides and nitrate [154]. Organic micropollutants can be partly removed both in lab-scale and pilot/full-scale biological sand filtration treatment process, however, the removal of different compounds can be sporadic and limited. Campos *et al.* found an average of 23% organic carbon removal by full-scale drinking water slow sand filters [155]. However, much higher removals (50% - 80%) of biodegradable compounds can also be found by conventional sand biofilters [156]. As an energy-efficient drinking water treatment technology, sand biofiltration shows the possibility to remove trace level micropollutants (e.g. antibiotics) from the source water. For instance, Zearley *et al.* reported removal efficiencies of 4.2% for sulfamethoxazole and 92% for trimethoprim by lab-scale sand filtration [152]. One of the major drawbacks of slow sand filtration is the requirement of a large land area, which may add considerably to the capital cost and limit the application of this treatment technology in the water industry [157].

2.3.1.2 GAC biofiltration

BAC filtration consists of a fixed bed of GAC supporting the growth of bacteria on the GAC surface and has been widely used in DWTPs. Adsorption and biodegradation are main

mechanisms contributing to the removal of organic compounds during the GAC biofiltration process. The unique porous surface structure and high surface area of GAC enable its capacity for the adsorption of organic compounds and other non-polar contaminants; while the bacteria immobilised on the surface of the GAC can remove organics via the process of biodegradation. It has been proven that GAC biofiltration can effectively remove a number of organic micropollutants (including antibiotics) from drinking water and wastewater treatment processes [41, 158, 159]. For example, a wide range of natural organic matter fractions (e.g. hydrophilic, hydrophobic and humic substances fractions) were effectively removed by full-scale GAC biofilter due to adsorption and biodegradation [160]. One drawback of GAC biofilters is that the continuous loading of natural organic matters causes a reduction of the GAC media lifespan and consequently reduces its adsorption capacity.

2.3.1.3 Dual media biofiltration

The most commonly used dual-media configurations are anthracite/sand and GAC/sand. Generally, a GAC/sand biofilter produces better performance than an anthracite/sand biofilter for the removal of natural organic matter, taste and odour compounds from the source water [153, 161]. Introducing a layer of GAC to the traditional sand biofilter (GAC sandwich biofilter) has been shown to be a promising process for drinking water purification. The GAC sandwich biofilter was first studied by Bauer *et al.* to remove pesticides [162]. Compared to single medium filters, the GAC sandwich biofilter is multi-functional: the upper layer of sand ensures the biological treatment process and hosts the *schmutzdecke* layer which plays an important role in water purification; the middle GAC layer further removes contaminants that cannot be biodegraded within the *schmutzdecke*; and the lower sand layer minimises the potential of biological particles and GAC fines entering the filtrate [162]. A recent study based on a lab-scale GAC sandwich biofilter has shown its capacity to remove DEET, paracetamol, caffeine and triclosan [163]. GAC sandwich biofilters have been widely used in Thames Water, including Coppermills, Hampton, Kempton, Ashford Common, Walton and Fobney Water Treatment Works [164], with the GAC layer ranging between 10-15 cm in a total bed depth of 80-90 cm.

2.3.2 Factors affecting biofiltration

2.3.2.1 Type of media

The selection of media type is a critical biofiltration design consideration as there is no single medium that can be applied universally for all waters. The selection of media is dependent on the physical characteristics such as effective size, uniformity coefficient, surface roughness and density; and also dictated by specific treatment objectives such as extended filter run time and removal of organics. In theory, a smaller media size slows down the rate of infiltration, reduces the size of pore space passages, and supports a larger biofilm surface area [165]. Media commonly used for drinking water treatment are adsorptive media such as GAC and non-adsorptive media such as sand and anthracite, among which activated carbon displays several advantages to adsorb different types of organic micropollutants [41]. The irregular GAC surface is suitable for bacterial attachment and offers protection against shear stress. Alternative media such as ceramic, crushed glass, expanded clay, pumice and compressible rubber granules are also used in biofiltration [166-169].

2.3.2.2 Hydraulic loading rate

Hydraulic loading rate (HLR, or filtration rate) may vary to some degree with demand in drinking water treatment plants. In general, sand media with a HLR of 0.04 – 0.4 m/h is recommended for drinking water purification [170, 171]. In laboratory-scale biofiltration studies, empty bed contact time (EBCT) is sometimes used as an alternative operational parameter to indicate how much contact occurs between particles, such as sand and GAC, and water as the water flows through a bed of the particles. EBCT is directly influenced by the HLR and the filter depth, it has been reported that EBCTs between 4 and 25 minutes may be optimal for drinking water treatment [172]. HLR can significantly affect the removal of chemicals and should be considered to predict and maximise biofilter performance [156]. The extent to which HLR affects removal efficiency is variable. For example, according to Reungoat's research, an increasing removal of several target compounds was observed with decreasing HLR [41] while Paredes *et al.* found there was no direct correlation between HLR and removal efficiency in biofilters [45]. In addition, microbial community structure in the drinking water biofilters is

also affected by HLR [173]. Prolonged contact time in the filters may promote gene transfer and consequently increase the percentage of resistant bacteria during biofiltration [174].

2.3.2.3 Characteristics of influent water

Biofilms developed on the media surface to acclimatise and biodegrade compounds are highly dependent on source water, which may vary significantly due to geographical and seasonal variations as well as upstream processes (e.g. flocculation/coagulation and ozonation). Temperature is also an important environmental factor affecting microbial biofilm formation. In general, a higher temperature tends to shorten the maturation stage, when surface biofilm develops gradually and forms a functional layer. Recommendation of turbidity in the influent for sand filtration is below 10 NTU to reduce filter clogging caused by flocs and particles [154]. Nutrient level in source water is also an important factor, where excess biomass accumulation causes reduced performance, such as clogging, pressure drop and proliferation of undesirable microorganisms [175]. The combination of ozonation followed by biofiltration is common practice for maximum natural organic matter removal as well as to reduce the formation of disinfection by-products [42, 173, 176].

2.3.3 Antibiotic resistance associated with biofiltration

For most biodegradable micropollutants, the main removal mechanism through biofilters is attributed to the metabolic activities of microorganisms grown on biofilms attached to the filtration media [41, 152, 177]. The type of biofiltration material (e.g. sand and GAC) does not affect the development of the biofilm [45], that is to say, the biofilm can form easily on all media in the presence of microorganisms. However, biofilters may also serve as a potential antibiotic resistance reservoir associated with horizontally transferable genetic elements.

2.3.3.1 Removal of antibiotics by biofiltration

Removal of emerging micropollutants of concern, such as insecticides and herbicides, pharmaceuticals and personal care products (PPCPs), and industrial and commercial chemicals by biofiltration has been well documented in recent years given their widespread

occurrence in water supplies [156]. In particular, removal of antibiotics of interest by various biofiltration processes is reviewed and summarised in Table 2.5, including lab-scale, pilot-scale, single-stage and multi-stage biofiltration. Removal efficiencies vary greatly with respect to media characteristics and HLR. Generally, a longer contact time increases removal of antibiotics. By contrast, effect of media size on antibiotic removal is unclear due to the fact that various sizes of media have been used in different research and the results are not comparable. Research has shown that smaller sand particle size does result in a larger surface area for microorganisms to colonise within the column compared to larger particle sizes [178].

Table 2.5 Removal of the target antibiotics by biofiltration process.

Antibiotic	Media	Effective size (range) (mm)	EBCT	Influent concentration	Removal (%)	Reference
SMX	sand	0.45	7.9 min	230 ± 33 ng/L	2.4	[152]
		0.45	15.8 min		4.1	
		1.0-2.0	0.8 d	1 – 40 µg/L	70	[45]
		1.0-2.0	0.2 d		55	
		0.3	-	200 µg/L	3.1-26.4	[179]
		0.7-1.2	14 d	0.25 – 4.2 µg/L	0-60	[180]
		-	-	< 10 ng/L	0	[43]
		-	-	443 ± 172 ng/L	-3 ± 14	[159]
		-	-	39.9 ng/L	26.8	[181]
		GAC		1.0-1.2	18 min	2.47 µg/L
	10 min				60-90	
0.8-1.0	6 min			2.85 µg/L	50	[183]
1.0-2.3	35 min			1 – 40 µg/L	98	[45]
1.0-2.3	17 min				65	
0.6-0.7, mean 1.0	44.7 min			26 ng/L	12	[184]
-	30 min			-	>99	[159]
-	15 min			1 – 43 ng/L	100	[43]
anthracite-sand		anthracite: 0.8-2.0	10 min	2.5 µg/L	20-55	[182]
		sand: 0.55-0.65	18 min		20-80	
GAC-sand		-	4.2 min	1.77 ± 0.68 µg/L	2-40	[156]
		-	8.4 min		30-87	

Continued Table 2.5 Removal of the target antibiotics by biofiltration process.

Antibiotic	Media	Effective size (range) (mm)	EBCT	Influent concentration	Removal (%)	Reference		
TMP	sand	0.45	7.9 min	175 ± 98	83	[152]		
		0.45	15.8 min		92			
		-	-	620 ± 89 ng/L	30 ± 5	[159]		
		-	120 min	10 – 180 ng/L	40	[41]		
		-	-	16.3 ng/L	66.2	[181]		
		1.0-2.0	0.8 d	1 – 40 µg/L	50	[45]		
		1.0-2.0	0.2 d		25			
		0.3	-	200 µg/L	>99.5	[179]		
		GAC	GAC	1.0-1.2	18 min	681 ng/L	>95	[182]
				1.0-1.2	10 min		>95	
0.6-1.6	120			10 – 180 ng/L	95	[41]		
0.8-1.0	6 min			1.45 µg/L	92	[183]		
1.0-2.3	35 min			1 – 40 µg/L	100	[45]		
1.0-2.3	17 min				98			
0.6-0.7, mean 1.0	44.7 min			20 ng/L	12	[184]		
-	30 min			-	>99	[159]		
anthracite-sand	anthracite-sand			anthracite: 0.8-2.0	10 min	681 ng/L	70-100	[182]
				sand: 0.55-0.65	18 min		65-100	
OTC	sand	-	-	< 10 ng/L	15	[43]		
		GAC	15 min	1 – 43 ng/L	54			
CTM	sand	-	-	135 ng/L	0	[181]		
		GAC	0.6-0.7, mean 1.0	44.7 min	46 ng/L	70	[184]	
AMOX	sand	-	-	< 10 ng/L	0	[43]		
		GAC	-	15 min	1 – 43 ng/L	60		

SMX: sulfamethoxazole; TMP: trimethoprim; OTC: oxytetracycline; CTM: clarithromycin; AMOX: amoxicillin. EBCT: empty bed contact time.

Sulfamethoxazole and trimethoprim are frequently selected as targets for research in biofiltration. The removal of sulfamethoxazole was much lower than trimethoprim by sand biofiltration, while GAC showed relatively higher removals than sand and anthracite-sand dual media. According to a comparative pilot-scale research, the mean removals of selected antibiotics were 30-50% by sand filters and above 90% by GAC biofilters [41]. Some organic

micropollutants tend to be recalcitrant to removal by biological filters, such as erythromycin, with a removal efficiency below 27%. Whereas trimethoprim was effectively removed (92%) in the same study [152]. This could be explained by the biodegradability of different compounds. Zearley *et al.* found that the removal of target compounds was independent of the influent concentration based on the data obtained from a 12-month study [152]. Research on amoxicillin in aquatic environment is scarce due to its poor stability in aqueous solution and the low sensitivity of the available analytical methods [48, 49]. Based on an investigation of antibiotics in industrial-scale DWTP, amoxicillin was moderately removed (60%) by GAC biofilters while no removal was observed by sand biofilter [43].

In addition to the biodegradability of antibiotics, factors such as the concentration of micropollutants and GAC adsorbent, contact time, pH, temperature may also affect the removal efficiency [185]. An increased dosage of GAC used in biofiltration and increased contact time could enhance adsorption removal. The adsorption removal of micropollutants, especially hydrophilic compounds (e.g. sulfamethoxazole), was affected by pH [185]. Lowering the solution pH lead to increase the hydrophobicity of ionisable compounds and subsequently their tendency of adsorption [186]. The dependence of sorption and metabolic activity on temperature is responsible for the variation of removal efficiencies among different micropollutants. Hai *et al.* found that the removal of most hydrophobic compounds was stable under the temperature range of 10–35 °C but the removal of less hydrophobic micropollutants was significantly influenced by temperature variation below and above 20 °C [187]. Nam *et al.* also reported that a low temperature (5 °C) decreases the adsorption removal of micropollutants, and affects hydrophobic compounds more than hydrophilic compounds [185].

2.3.3.2 Behaviour of ARGs during biofiltration

ARGs have been observed to establish and proliferate in drinking water biofilms [111, 188]. Behaviour of ARGs during traditional biofiltration process was inconsistent in previous studies. Guo *et al.* investigated the prevalence of sulfonamide and tetracycline resistance genes in DWTPs, and sand filtration showed an approximately 1 log unit of ARG reduction in effluent [140]. The application of sand filtration in water reuse systems in agriculture showed

significant reduction of ARGs, with removal values of 0.9 ± 0.7 log units for *tetA*, 1.1 ± 0.7 log units for *ermB*, 1.1 ± 0.8 log units for *sul1* and 1.3 ± 0.8 log units for *sul2*, however, limited or no decrease of the relative abundance of ARGs (normalised to *16S rRNA* gene) was observed [189]. These findings suggest that the removal of total bacteria is the main mechanism of ARGs reduction in biofiltration treatment. Similarly, by using high-throughput qPCR, Xu *et al.* reported a reduction of ARGs by sand and GAC filtration while the proportions of ARGs to bacteria numbers increased, especially after GAC treatment, suggesting that gene exchanges may occur not only in bacteria adsorbed by biofilm but also in bacteria contained in the water phase near the biofilm [75, 190].

2.3.3.3 ARGs associated with bacterial community

Liao *et al.* have summarised that the bacterial community compositions in biofilter media are dependent on the availability of nutrients and carbon substrates in the feedwater, as well as the operational conditions such as HRT and temperature [173]. Recent studies have shown that the variation of antibiotic resistome during drinking water treatment processes is generally associated with the bacterial community. The phylum *Firmicutes* has been shown to be closely related to the ARG composition in waterbodies [191]. Zheng *et al.* reported that *Firmicutes* were mostly related to persistent ARGs in activated carbon biofilms in a case study in a DWTP [192]. Moreover, they discovered the *Firmicutes* was able to communicate with each other through quorum sensing in GAC biofilms in response to selective pressure from the environment and accelerating the ARG conjugative transfer [192]. A lab-scale sand biofiltration study has suggested that the difference in bacterial community composition was likely the main reason for the variation in antibiotic resistome in sand biofilms, with 90 % of the most abundant genera significantly correlated with the relative abundance of ARGs [193]. In addition, the authors found that the organic carbon in the influent shaped the bacterial community structure of the sand filter and indirectly affected the antibiotic resistome in biofilm, which may help explain the persistence of ARGs in drinking water treatment and distribution systems.

2.4 Analytical methods

2.4.1 Detection methods for antibiotics

2.4.1.1 Antibiotic detection

The simultaneous analysis of different antibiotics requires chromatographic separation using gas (GC) or liquid chromatography (LC). Due to the polarity, low volatility and thermal stability of several antibiotics, derivatization is required when using GC, which limits its applicability in antibiotic analysis [194]. Therefore, LC has been primarily implemented for multiclass analysis, especially when coupled to mass spectrometry (LC-MS) and tandem MS (LC-MS/MS). For the majority of LC analysis, reverse-phase chromatography with stationary phases based on octadecyl (C18) or octyl (C8) silane is used [194].

Different types of mass spectrometers, including the single quadrupole (q), triple quadrupole (QqQ), and ion trap (IT) mass analysers have been used to detect multiclass antibiotics in various water matrix [194, 195]. The QqQ is the one that is the most widely used due to its high specificity and sensitivity, especially when operated in the multiple reaction monitoring (MRM) mode [194], but its cost usually limits its accessibility. The q is the simplest and least expensive of the three, but its inability to perform tandem mass spectrometry does not allow it the selectivity of the QqQ and IT. According to EU criteria (2002/657/EC) [196], for the confirmation of veterinary drug residues in foodstuffs, at least two MRM transitions (in the correct ion ratios) must be recorded, usually corresponding to those from the most abundant precursors to the most abundant product ions. While the IT does not provide the same sensitivity as the q or QqQ for trace analysis, the high selectivity of the IT can improve signal-to-noise ratios which enables the quantification of environmentally relevant concentrations of contaminants [195]. Furthermore, the MS^n (multiple-stage fragmentation) data provided by IT increase the number of identification points and provide valuable information in the analysis of complex environmental samples at an affordable cost.

2.4.1.2 Antibiotic extraction

For environmental aqueous samples, the concentration of antibiotic residues is mostly in the ng/L- μ g/L or pg/g-ng/g ranges depending on the sample matrix. Analytes, therefore, need to be extracted and concentrated for the detection by modern instruments. For aqueous samples, the most universal extraction method for antibiotics is Solid Phase Extraction (SPE) [194, 197]. The basic principle of SPE is using cartridges with specific sorbent materials to retain the analytes. The sorbent selected is based on the physiochemical properties (e.g. pK_a, functional group, polarity, stability, etc.) of the analytes as the ability of different sorbents to interact with a target analyte and other sample components can vary. Polymer-based materials are the most applicable sorbent for the simultaneous extraction of multiple classes of antibiotics from various environmental matrices. Numerous studies have applied SPE to extract diverse compounds from aqueous samples. For instance, a total of 60 pharmaceuticals, including all of the target antibiotics, were extracted from wastewater effluents using SPE [198]. Similarly, different SPE methods were tested for the extraction of amoxicillin, sulfamethoxazole and trimethoprim from surface and ground waters [199].

2.4.2 Methods for ARG detection and bacterial community analysis

To date, the methods used for the detection and characterization of ARGs include (but are not limited to) specific and multiplex polymerase chain reaction (PCR), quantitative real-time PCR (qPCR), high-throughput qPCR and metagenomic sequencing.

2.4.2.1 PCR

Conventional PCR analysis has been widely used in both pure culture and mixed environmental samples for the identification of specific ARGs encoding resistance to different antibiotic [77, 139, 188, 200]. Environmental target DNA at low concentrations can be amplified and detected by PCR-based methods. By using conventional PCR, Gao *et al.* investigated the presence/absence of sulfonamide and tetracycline resistance genes in resistant bacterial isolates from aquaculture environments, among which *sul1* and *sul2* were detected in most of the resistant bacteria with detection frequency ranging from 71.4-100% in

sediment and 60%-100% in water samples [77]. Multiplex PCR methods have been developed for the simultaneous detection of more than one environmental ARG. However, there are several limitations of PCR, including low-throughput, limited availability of primers, amplification bias, false-negative results due to inhibition in PCR and false-positive results due to nonspecific amplification [201].

2.4.2.2 qPCR

Quantitative real-time PCR (qPCR) is able to provide an approximation of the dissemination of known ARGs in environmental samples [114]. In addition, this method is also applied to study the effects of environmental factors or treatment process on the removal of ARGs [79]. Conventional qPCR has been extensively applied over the last decade to quantify both ARGs and markers of MGEs in soil, water, vegetables and food-producing animals [73, 202-204]. By using absolute copy number per microliter of DNA, it is possible to compare results between batch samples for long-term ARG-related research. As was suggested by Berendonk *et al.*, it is necessary to improve the comparability between studies worldwide for a comprehensive understanding and global perspective on the antibiotic resistome irrespective of geographical, temporal or environmental constraints [114]. Additionally, in accordance with WHO's initiatives for the surveillance of antibiotic resistance, more data across countries are needed to fully assess ARG prevalence worldwide [205]. Despite the wide application, a major drawback of qPCR is that only a limited number of ARGs can be targeted in a given study [206].

2.4.2.3 High-throughput qPCR (HT-qPCR)

High-throughput qPCR (HT-qPCR) performs thousands of nanoliter qPCR reactions and has been developed to simultaneously track hundreds of ARGs and other genes of interest [207]. The HT-qPCR approach has recently been applied to comprehensively investigate ARG profiles in various environmental compartments, including soil [74], drinking water [75, 99], sediment [76] and vegetables [208]. QIAGEN has also recently developed an ARG Microbial DNA qPCR array, which contains assays for 87 ARGs targeting multiple resistance gene families. The QIAGEN qPCR assay has been successfully applied to recent

studies [209-211]. An illustrative example is cited here. Zhao *et al.*, found the antibiotic resistance in mariculture sediment samples was co-driven by nutrients, heavy metals and microbial communities by using the QIAGEN microbial ARGs qPCR Assay kit [209]. Although HT-qPCR is a promising method for the rapid detection and quantification of the diversity and abundance of ARGs in environmental samples, one drawback is the inability to optimise each individual qPCR array as the PCR protocol (e.g. annealing temperature) is uniform throughout the array [206]. Furthermore, the costs of HT-qPCR platforms or qPCR Assay kits for ARG analysis are generally very high, for example, a QIAGEN microbial ARGs qPCR Array plate costs around £750 for one DNA sample.

2.4.2.4 16S rRNA gene sequencing

High-throughput sequencing (HTS) provides unparalleled insight into community structures among various environmental samples [74, 212]. Amplicons (sequence reads) of variable 16S rRNA gene regions are quantified and subsequently assigned to microbial taxonomies. Among the nine hypervariable 16S rRNA gene regions, V3-V4, V4, and V4-V5 regions are commonly selected for the analysis of bacterial community in environmental-related samples. For instance, V3-V4 region was selected for biofilter media (biofilm) and activated sludge samples [193, 213]; V4 region was selected for drinking water, biofilm, compost and sediment samples [73, 209, 214, 215]; V4-V5 region was selected for water, GAC biofilm and lettuce samples [192, 208].

2.4.2.5 Metagenomic analysis

Metagenomics approach is a powerful tool to describe the genetic potential of a community and to identify the types of microbes present in a community, as well as the presence or absence of genes or genetic variations responsible for antibiotic resistance [216]. In contrast to PCR-based methods, metagenomics analysis enables the discovery of novel resistance determinants and the improved understanding of resistance mechanisms in diverse environments. Using metagenomics, novel ARGs encoding resistance to β -lactams and tetracycline have been identified [217, 218]. In addition, this approach has been recently

applied for the analysis of antibiotic resistome in environmental samples such as surface and drinking water, soil, vegetable and compost samples [219-222].

2.4.2.6 Correlation between bacterial community and ARGs

Combined with network analysis tools, the co-occurrence patterns between ARGs and microbial taxa could be assessed in complex environmental samples across spatial gradients [201]. Many studies suggest that differences in bacterial community structure are the leading cause of differences in antibiotic resistome in various environments. Some representative examples are cited here. Metagenomic sequencing has been applied for the establishment of antibiotic resistome catalogue in drinking water samples collected from 25 cities over the world and to explore the potential hosts of ARGs [219]. In this survey, *Acidovorax*, *Acinetobacter*, *Aeromonas*, *Methylobacterium*, *Methyloversatilis*, *Mycobacterium*, *Polaromonas*, and *Pseudomonas* were identified as the hosts of ARGs in drinking water. By using metagenomic and 16S rRNA gene sequencing, Jia *et al.* have reported that *Salmonella* is considered as the major host of sulfonamide resistance genes while *Pseudomonas* and *Escherichia* carry most of aminoglycoside resistance genes during drinking water chlorination [223]. The combination of HT-qPCR and 16S rRNA gene sequencing approaches revealed that *Rhodospirillaceae* is thought to be the possible host of a β -lactam resistance gene (*bla_{CTX-M-02}*) whereas *Solirubrobacteraceae* carry more diverse ARGs in soil samples applied with sewage sludge [220]; *Rhodobacteraceae* and *Comamonadaceae* host diverse ARGs (*bla_{TEM}*, *ermK-01*, *tetPB-03* and *mepA*) in lettuce sample. qPCR and metagenomic analysis have suggested that 18 bacterial genera are possible hosts for 13 ARGs in sludge samples during anaerobic digestion [224].

Chapter 3

METHODOLOGY

3 METHODOLOGY

3.1 Introduction

In this chapter, methodologies used throughout this study, including the design and operation of the biofiltration columns (Section 3.2), methods developed for sample analysis (Section 3.3, 3.4, 3.5, and 3.6) and the set-up of a horizontal gene transfer experiment based on biofiltration (Section 3.7) are summarised. Two biofiltration experiments were set-up at bench-scale (Figure 3.1): the first biofiltration experiment comprised four types of biofilters, including sand, granular activated carbon (GAC), GAC sandwich (a layer of GAC loaded in the middle of sand bed), and anthracite-sand dual biofilters; the second biofiltration experiment consisted of GAC sandwich biofilters with different thicknesses and positions of the GAC layers. Furthermore, a conjugative gene transfer system was set-up to explore the impact of filter media on plasmid conjugative transfer frequency (Figure 3.2).

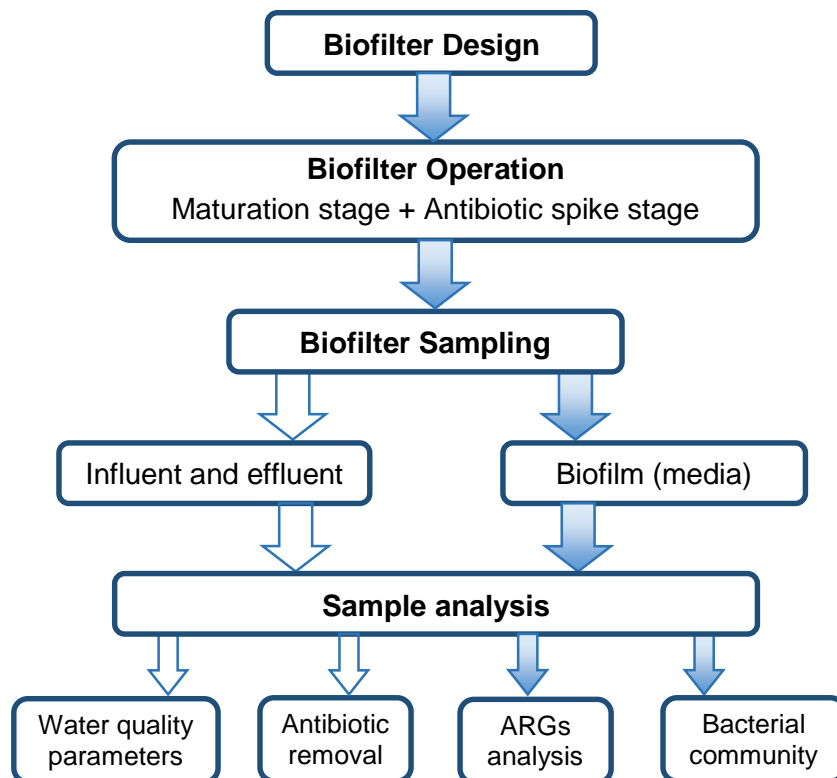


Figure 3.1 Systematic diagram of the biofiltration experiment.

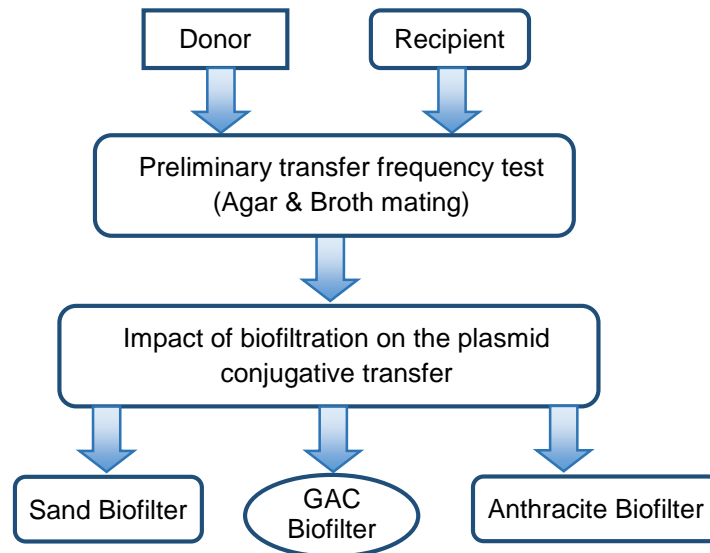


Figure 3.2 Systematic diagram of the conjugative transfer system based on biofiltration.

3.2 Biofiltration experiment

3.2.1 Design of biofiltration columns

3.2.1.1 Column construction

Biofilters were constructed using eight 62 cm lengths of acrylic (Plastic Shop, UK) columns with a 36-mm inner diameter (ID) and 2-mm wall thickness. Each filter column had three sampling ports, located along the length of the column at 27, 36 and 39 cm from the top. A stainless steel tube (3 mm ID, 46 mm length) was horizontally screwed through the external surface of sampling port into the column centre (Figure 3.3). The support base using polyvinyl chloride (PVC) was placed at the bottom of the column, each embedded with a stainless steel tube (5 mm ID) as the water outlet port. An overflow port (5 mm ID) was installed in line with the sampling ports at 5 cm from the top of the column. All eight columns were placed in a specially-designed half circle stand which allowed easy handling and changing position.

3.2.1.2 Biofilter media

Sand, GAC and anthracite were selected as the filter media in this study. The surface characteristics of the selected media were obtained either from the supplier or determined by microscopy. Typical properties of the selected media are shown in Table 3.1. The fine sand was purchased from Mineral Marketing (UK) and had an effective size of 0.20 mm and a

uniformity coefficient of 1.82. The values are within the typical range of grain size, between 0.15 mm and 0.35 mm, and uniformity coefficient, between 1.5 and 3.6, in use in slow sand filtration [157, 225]. GAC with a particle size of 0.62 – 1.60 mm was purchased from Chemviron Carbon (UK); and anthracite with effective size of 0.90 mm was purchased from EGL Puracite (UK). Scanning electron microscopy (SEM, JSM-6700F, UCL Chemistry) was used to characterise surface morphology of the filter media. Figure 3.4 shows the three-dimensional SEM images of the sand, GAC and anthracite. The surface of the sand is non-porous and smooth, while the GAC shows a much rougher surface with widely-distributed crevasses and ridges. Both smooth and rough surfaces with edge areas can be seen on the anthracite, which provide solids holding capacity and sufficient flow path for the water filtration.

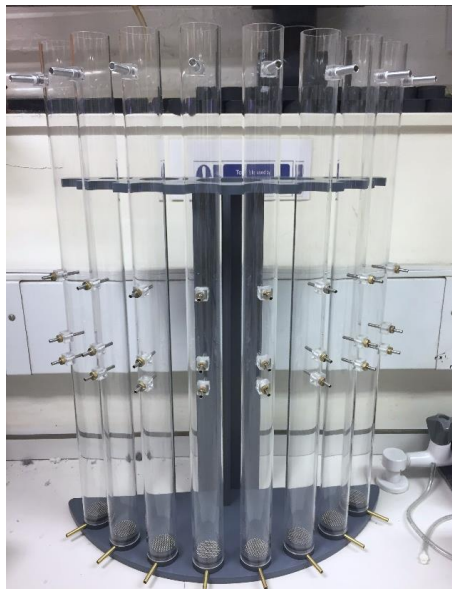


Figure 3.3 The design of the biofilters setup.

Table 3.1 Typical media properties for sand, GAC and anthracite.

Media	Effective Size (d_{10} , mm)	Uniformity Coefficient	Size Range (mm)	Bulk Density (kg/m^3)	Surface area (m^2/g)
Sand	0.20	1.82	0.16 – 0.50	1645	-
GAC	0.72	1.68	0.62 – 1.60	518	556 *
Anthracite	0.90	1.32	0.85 – 1.46	712	-

Effective size (d_{10}) is defined as the size of the sieve through which 10% of the filter media (by weight) will pass. Uniformity coefficient is defined as the ratio of the sieve size through which 60% (d_{60}) of the filter media passes to the sieve size that allows 10% (d_{10}) of the media to pass. Bulk density: the mass of the media related to a specific volume. * Value of the surface area of GAC is obtained from [163].

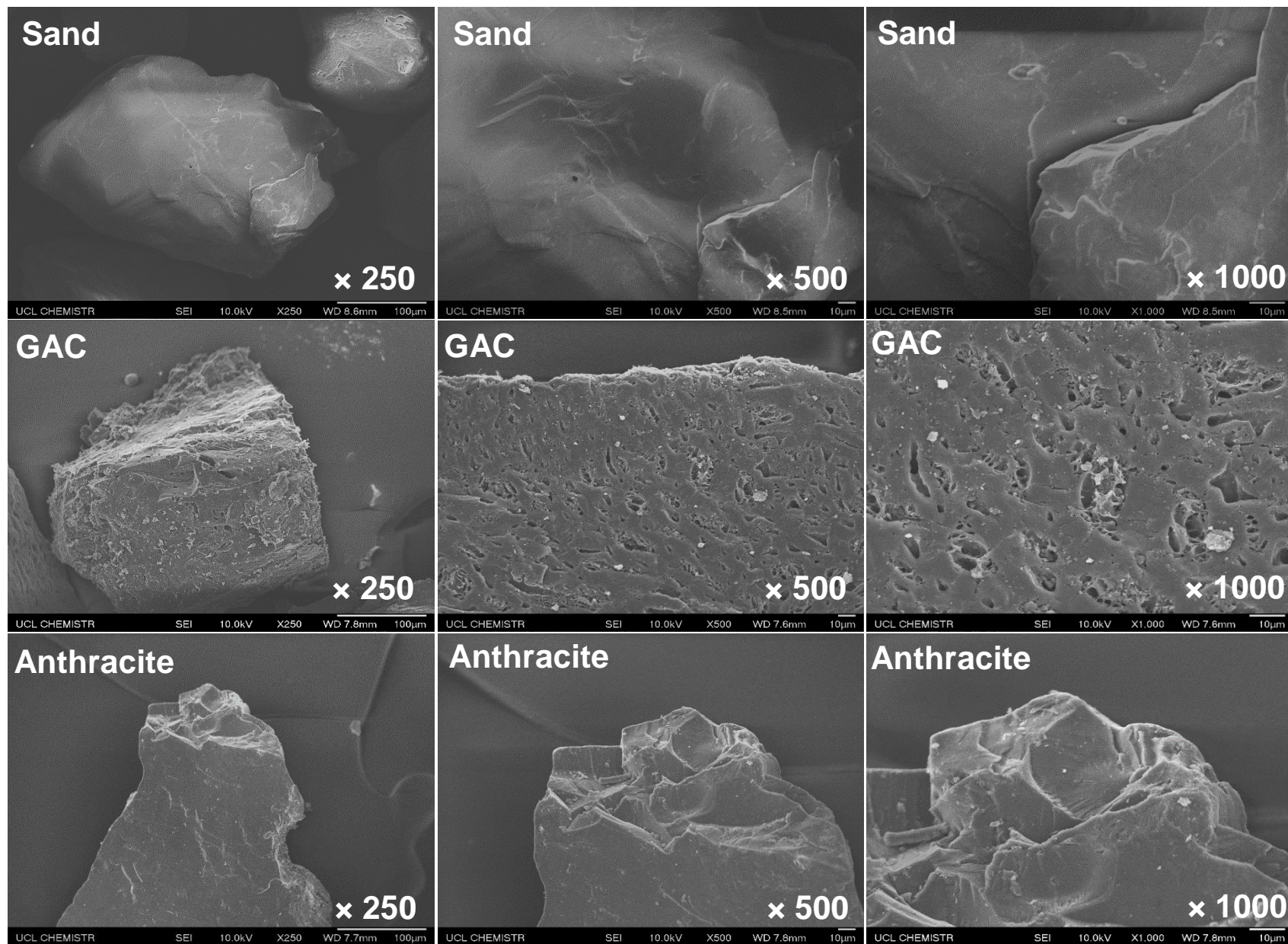


Figure 3.4 SEM (Scanning electron microscope) image of the surface structure of sand, GAC and anthracite.

3.2.1.3 Design of the Biofiltration experiment 1 – different types of filter media

Sand, GAC, GAC sandwich, and anthracite-sand representing four types of biofilter were set-up in parallel at bench scale in September 2017. Each biofilter type was run in duplicate. The composition of the biofilters is shown in Figure 3.5. All of the biofilters had 5 cm of under-drainage (0.6–3 mm gravel) to allow free drainage of filtered water from the columns. The overall media depth was 41 cm.

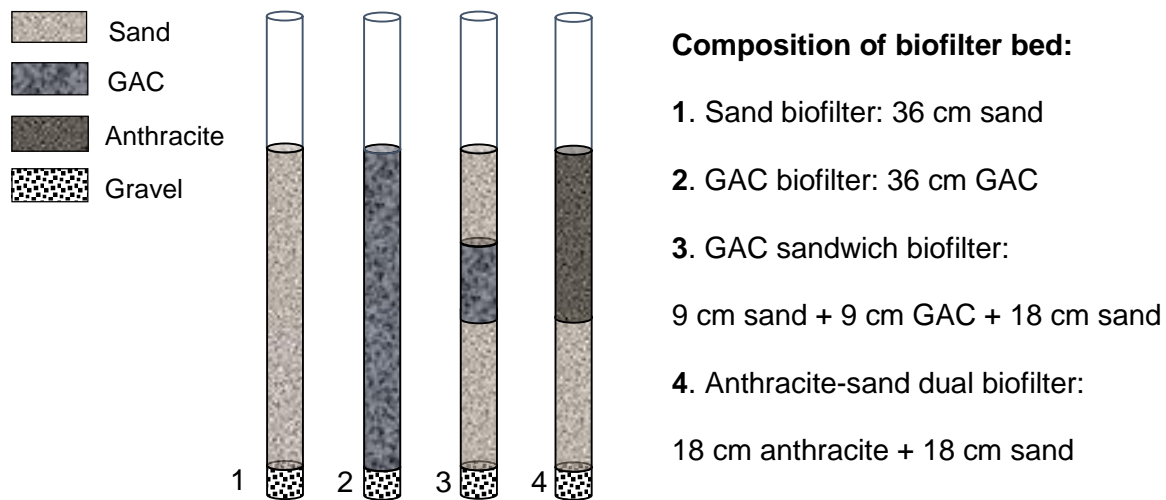


Figure 3.5 Schematic of biofilter composition.

Prior to packing the filter columns, all the media were repeatedly washed with tap water and deionised water to remove fines, and then dried at 105 °C overnight. A round-shape stainless steel wire mesh with 1.5 mm openings was placed at the bottom of each column to stop the gravel from escaping. For pure media filters, 36 cm of sand or GAC were placed onto the gravel. For mixed media filters, the bottom layer of sand was placed first and then the GAC/anthracite was gently placed on the top of the sand. The top of the media was level in all columns. A dual head peristaltic pump (Watson-Marlow 323 U) with 10 channels was introduced to simultaneously deliver feedwater to biofilters from the reservoir. The system was setup using both PVC and silicone tubing with different specifications (Table A3.1). Each sampling port had a stopping clip to prevent the media and water from leaking. A needle valve was used to adjust the effluent flow. After all the tubing and valves were installed, the biofilters

were initially fed with dechlorinated tap water to test the stability of the system for a week. During the system start-up, filters were re-checked every day to ensure that the influent and effluent flow were balanced and ran smoothly. No water leaks should be observed and the head of water above the filter bed remained constant at all times. All the columns were installed with overflow to prevent water from rising above the walls of the filters. An overview of the biofilter system setup is shown in Figure 3.6.



Figure 3.6 Schematic of biofilter column set-up. Sand, GAC, GAC sandwich, and anthracite-sand dual biofilters were set-up in duplicate (from left to right).

3.2.1.4 Design of biofiltration experiment 2 – different types of GAC sandwich biofilters

Only sand and GAC were used as filter media in this study. The design of the GAC sandwich biofilters is shown in Figures 3.7 and 3.8. Eight biofilters comprising four types of GAC sandwich were set-up at bench scale, each biofilter type run in duplicate. Media packing and tubing installation followed the first biofiltration experiment (as described in Section 3.2.1.3). Except for the bottom layer sand, the design of biofilter (a) is a replicate of GAC sandwich biofilter from previous biofiltration experiment.

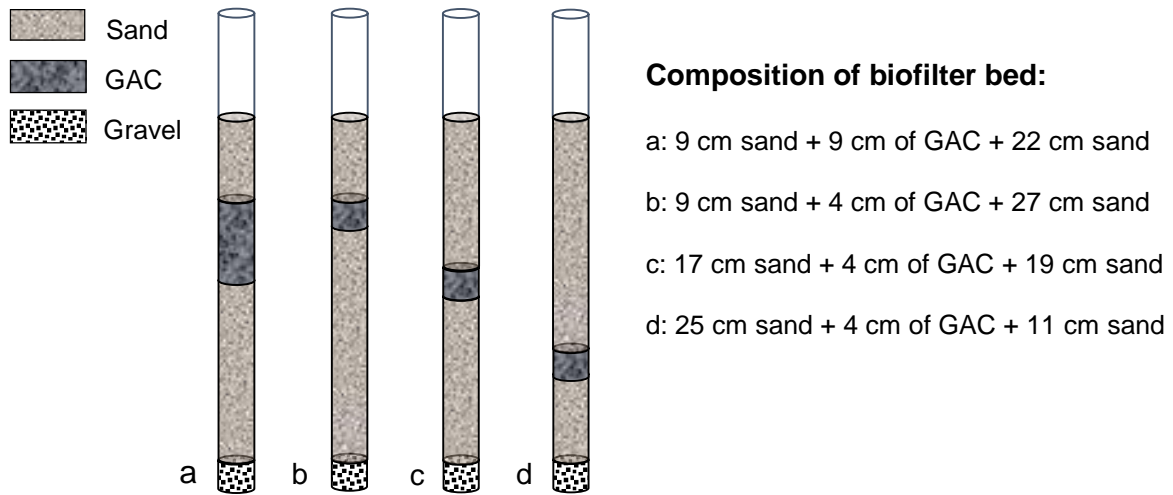


Figure 3.7 Schematic of the GAC sandwich biofilter composition.



Figure 3.8 The GAC sandwich biofilter system setup.

3.2.2 Operation of biofiltration columns

3.2.2.1 Biofiltration experiment 1 – different types of filter media

To ensure that the comparison of biofilters' performance was as objective and reliable as possible, all of the biofilters were operated under identical conditions (regarding feedwater quality, temperature, HLR, etc.). The system was operated continuously for 12 weeks, including 4 weeks of biofilter maturation and 8 weeks' exposure to antibiotics followed by a backwash step at the end.

1) Feedwater preparation

The feedwater for all biofilters was natural surface water from Regent's Park Lake, London. A total of 25 L of raw water was collected from the lake twice a week from October 2017 to January 2018. For convenience, raw water was aliquotted equally into two separate feed barrels, each barrel supplied feedwater for four biofilters (left four and right four shown in Figure 3.6). The feed barrels were emptied and washed each time before refilling with fresh raw water.

Five antibiotics, sulfamethoxazole (SMX), clarithromycin (CTM), amoxicillin (AMOX), oxytetracycline (OTC) and trimethoprim (TMP) stock solutions were prepared at a concentration of 1 mg/mL. Details of the preparation of antibiotic stock are provided later in this chapter (Section 3.4.1). Biofilter feedwater was spiked with the target antibiotics at 2 µg/L, except for amoxicillin which was spiked at 5 µg/L due to the analytical method constraints. The concentration selected in this study was based on relevant environmental concentrations and projected removal. Once the antibiotics were added to the feedwater (after 4 weeks of operation), their addition continued for the remainder of the study.

2) Hydraulic loading rate (HLR)

A hydraulic loading rate of 0.06 m/h to the biofilters was used throughout the study, which was within the typical range of 0.04 to 0.4 m/h in use for slow sand filtration [171, 225]. Based on the area of the column circular base, the specific flow rate was calculated by the following equation:

$$\text{Flow Rate (mL/min)} = \frac{0.06 \times 3.14 \times 1.8^2 \times 100}{60} = 1.0 \text{ mL/min}$$

KCl was used as an indicator to estimate the travel time of water through the biofilters as well as to verify the target HLR. The travel time was between 10 h – 11 h from the feedwater reservoir to the bottom of the filter, which was in accordance with the target HLR of 0.06 m/h. A needle valve was used to adjust the flow for each filter. The flow was monitored daily by measuring the amount of water collected in a graduated cylinder. If required, the flow rate was re-adjusted to the target HLR. At the early stages of the biofilter run, the regulating valve

controlling the flow rate only needed very little adjustment. As the biofilter run continued, the valve needed to be checked and opened fractionally to compensate for the clogging of the filter and to maintain a constant flow.

3) Biofilter maturation

Once the natural water was introduced to the system, the filter was run continuously without interruption under the target HLR of 0.06 m/h. As filter maturation proceeded, the microorganisms in the feedwater built up gradually on the medium surface and formed a visible biofilm layer. The filter maturation took approximately 4 weeks in this study, when turbidity of effluent was < 1 NTU and total coliforms and *E. coli* achieved 2-log reduction [157].

4) Backwash and biofilter cleaning

A backwash was conducted once after 11 weeks of system operation. Except for the GAC sandwich, biofilters were backwashed using filtered water to achieve a 20-30% bed expansion [226]. Each biofilter was backwashed for 10 min. Due to the restrictions of lab-scale columns, the GAC sandwich was cleaned by stirring the top layer of sand and withdrawing water from above the filter at the same time [41]. After backwashing/cleaning, the filters continued to run for another 24 h before the resumption of sampling.

5) Trouble shooting

When media are loaded into the columns, the filter must first be filled with dechlorinated water introduced from the bottom to drive out the air bubbles from the interstices of the media, ensuring that the whole surface of every medium grain is in contact with water. Water then continues to be pumped from below until the filter bed is covered and reached overflow position, where a sufficient depth above the filter bed is necessary to prevent the bed surface being disturbed by the turbulence from the admission of feedwater. For the GAC sandwich, the top layer of sand is only introduced when the air bubbles are removed from the GAC and the bottom layer of sand and the column is filled with water in order not to disturb the GAC layer.

The peristaltic pump tubing needs to be replaced regularly due to the continuous compression pressure from the moving rotor when operating the pump. The worn-out tubing

may cause water leakage and contaminate the inside of the pumphead as well as reducing the water inlet flow. The filter bed may have drained owing to not enough feedwater pumping in, eventually affecting the biofilter performance. The water inlet tubing needs to be replaced once every two weeks to avoid the excess growth of biofilm inside the tubes. As the feedwater is rich in nutrients and dissolved oxygen, the inner surface of the tube creates a desirable environment for biofilm growth, which is visually apparent along the tube. When the biofilm grows thicker, it might have shed over time and flown into the biofilters, affecting the indigenous biofilm formed on the filter media surface.

3.2.2.2 Biofiltration experiment 2 – different types of GAC sandwich biofilters

All of the biofilters were operated under identical conditions during the start-up stage, which took approximately 3 weeks until all biofilters reached maturation. Once matured, the system was divided into Set A and B, each consisting of four biofilters with different GAC thickness or position (as shown in Figure 3.7). Set A was operated with the addition of antibiotics while Set B was operated as control (without the addition of antibiotics). The system run continuously for another 8 weeks, and a cleaning procedure (described below) was conducted after 11 weeks' operation.

A total of 15 L raw water was collected from the River Thames twice a week from June to September 2018. Raw water was diluted with dechlorinated tap water at a ratio of 1:2 and used as feedwater for all biofilters throughout this study. A minimum of 6 hours was allowed to precipitate the raw water and only the supernatant was diluted to reduce biofilter clogging caused by particles. During the maturation stage, all biofilters were seeded with the same source water for approximately 3 weeks. Then, the antibiotic mixture was added to Set A at 10 µg/L continuously for 8 weeks. The spike concentration was higher than the previous experiment in order to increase the detectability of target antibiotics in the effluents. Set B was operated as a control and supplied with only diluted raw water during the experimental period. Except for the difference in feedwater, all other operational parameters (including cleaning technique) followed the previous study (Section 3.2.2.1).

3.2.3 Sampling of biofiltration columns

3.2.3.1 Biofiltration experiment 1 – different types of filter media

Biofilter sampling was divided into two stages: the maturation stage and the antibiotic spike stage. During the maturation stage, which took approximately 4 weeks after the start of biofilter operation, influent and effluent samples were taken weekly for the determination of general water quality parameters. During the antibiotic spike stage, influent and effluent samples were taken once a week for water quality parameters and antibiotic removal determination over a period of eight weeks. Influent and effluent were also collected the first week after antibiotic spike and every two weeks thereafter for ARGs analysis. Media samples at different depths of the filter bed were withdrawn from the sampling ports at the end of the maturation stage and before biofilter backwashing/cleaning, respectively. Table 3.2 summarises the sampling strategy during biofilter operation.

Table 3.2 Sampling strategy of the first biofiltration experiment.

Phase	Duration	Sample type	Frequency	Analysis
Maturation	4 weeks	influent/effluent	weekly	general water quality parameters
		biofilm (media)	once (after 4 weeks)	ARGs
Antibiotic spike	7 weeks	influent/effluent	weekly	general water quality parameters; antibiotics
		influent/effluent*	every two weeks	ARGs
		biofilm (media)	once (after 7 weeks)	ARGs; bacterial community**
Backwash/cleaning	24 hours	influent/effluent	once	general water quality parameters, ARGs

* Influent/effluent samples were collected the first week after antibiotic spike, and then every two weeks afterwards; ** Only surface biofilm samples were selected for bacterial community analysis.

Prior to sampling, the flow was rechecked and adjusted as needed. Samples were collected only after a constant dripping flow was established. The influent samples were taken immediately before the biofilters and mixed as one sample to capture an accurate influent concentration, while the effluents were collected in drainage pipes located in the bottom of the biofilter and led by gravity to the outlets. Paired influent and effluent samples were taken at all

times. Media samples were withdrawn from the top layer and the sampling ports and subjected to DNA extraction. Specifically, DNA extracted from the eight surface biofilm samples (taken at the end of the run) was sent for high-throughput sequencing of the *16S rRNA* gene using the Illumina HiSeq2500 platform (Novogene, Beijing, China) to investigate the bacterial community structure. Details are provided later in this chapter (Section 3.6).

3.2.3.2 Biofiltration experiment 2 – different types of GAC sandwich biofilters

The sampling strategy for the general water quality parameters and antibiotic analysis followed the previous study (Section 3.2.3.1). Only influent and effluent collected from Set A were processed for the analysis of antibiotic removal. Raw water from the River Thames without antibiotic addition was used as environmental background. Paired influent and effluent samples of all biofilters were collected the week before and after the addition of antibiotics, and then every two weeks afterwards for ARGs analysis. Influent and effluent were continuously collected 24 h after biofilter cleaning. Surface biofilm and middle GAC layer samples were collected before the addition of antibiotics (3 weeks) and before biofilter cleaning (11 weeks). Specifically, to further investigate the behaviour of ARGs in surface biofilms after 11-weeks' operation, the *schmutzdecke* layer was separated from the top layer of sand and subject to DNA extraction and qPCR analysis. A sterile pipette was used to randomly take the *schmutzdecke* samples from five points of the cross section and then mixed as one sample. Excess water was carefully removed from the *schmutzdecke* samples using a needle syringe and 0.5 g (wet) of the *schmutzdecke* were then subjected to DNA extraction.

In addition to the qPCR analysis, the eight *schmutzdecke* and eight GAC samples collected at the end of the system run were sent for high-throughput qPCR (HT-qPCR) analysis. A total of 296 primer sets were used. Details of the method used for HT-qPCR and the classification of the 296 genes are provided later in this chapter (Section 3.5.3). DNA from the 16 biofilm samples (eight *schmutzdecke* and eight GAC taken at the end of the run) was also sent for high-throughput sequencing of the *16S rRNA* gene to investigate the bacterial community structure. Table 3.3 summarises the sampling strategy during biofilter operation.

Table 3.3 Sampling strategy of the second biofiltration experiment.

Phase	Duration	Sample type	Frequency	Analysis
Maturation	3 weeks	influent/effluent	weekly	general water quality parameters
		influent/effluent	once (after 3 weeks)	ARGs
		biofilm (media)	once (after 3 weeks)	ARGs
Antibiotic spike	7 weeks	influent/effluent	weekly	general water quality parameters; antibiotics (Set A only)
		influent/effluent*	every two weeks	ARGs
		biofilm (media)	once (after 7 weeks)	ARGs**, bacterial community***
Backwash/ cleaning	24 hours	influent/effluent	once	general water quality parameters, ARGs

*: influent/effluent samples were collected the week before and after antibiotic spike, and then every two weeks afterwards; **: both normal qPCR and high-through qPCR were conducted for ARGs quantification. ***: only *schmutzdecke* and GAC biofilms were selected for bacterial community analysis.

3.2.4 GAC adsorption kinetics

In addition to the biofiltration experiment, isothermal experiments and adsorption kinetics of the five antibiotics on GAC were determined in lake water samples. The initial concentration of five antibiotics were set at 5 µg/L by adding stock solution to aqueous samples. For contact time test, 0.5 g GAC was added into glass bottles filled with 1 L lake water. Bottles were placed in a rotary mixer at the speed of 30 rpm. Reaction time was set at 1 h, 3 h, 6 h, 9 h, 12 h, 24 h, and 48 h, respectively. For the GAC dosage test, 0.025 g, 0.05 g, 0.1 g, 0.25 g, 0.5 g, and 1 g GAC were added into 1 L lake water. Bottles were placed in a rotary mixer at the speed of 30 rpm for 24 h. For each test, surface water spiked with 5 µg/L of antibiotics without GAC was used as a control. All bottles were prepared in triplicate. When finished, samples were processed for the determination of antibiotic residues in the reaction bottle. Analytical methods are provided in a separate section later in this chapter.

3.3 General water quality parameters

The determination of general water quality parameters followed standard methods (APHA) [227]. Table 3.4 lists the methods and instruments used in this study.

Table 3.4 Methods and instruments used for the determination of general water quality parameters.

Sampling parameters	Method/Instrument/Model
Particulate characterisation	
pH	Mettler Toledo SevenMulti
Conductivity	Mettler Toledo SevenMulti
Dissolved oxygen (DO)	Jenway 9200
Turbidity	HACH 2100AN IS turbidmeter (ISO Method 7027) [228]
Organic precursors characterisation	
Dissolved organic carbon (DOC)	Shimadzu TOC-L (NPOC method)
Chemical oxygen demand (COD)	Hanna C 9800
UV absorbance (254 nm)	Camspec M550
Microbial characterisation	
Total coliforms	ISO 9308-1:2014 (January, 2017) [229]
<i>Escherichia coli</i>	ISO 9308-1:2014 (January, 2017) [229]
Ion characterisation	
Phosphate (PO ₄ ³⁻)	IC, Dionex ICS 1100
Nitrite (NO ₂ ⁻)	IC, Dionex ICS 1100
Nitrate (NO ₃ ⁻)	IC, Dionex ICS 1100

3.3.1 pH, conductivity, turbidity, DO, absorbance and COD

For the measurement of pH, conductivity, turbidity, dissolved oxygen (DO) and absorbance (254 nm), no sample pre-treatment was required. Chemical oxygen demand (COD) was measured using the Hach COD TNT digestion solution (0-150 mg/L, HACH Company, UK). Two mL of aqueous samples were added to the digestion solution vials according to the manufacturer's instructions. Deionised water was used as a blank. All vials

were then put inside a COD digestion reactor (Hanna C 9800) at 150 °C for 2 h. A DR 890 Colorimeter was used to measure the final COD value.

3.3.2 DOC and ion characterisation

For the analysis of dissolved organic carbon (DOC), phosphate (PO_4^{3-}), nitrite (NO_2^-) and nitrate (NO_3^-), aqueous samples were pre-filtered through 0.45 μm mixed cellulose esters (MCE) membrane (Millipore, UK). 15 mL and 5 mL of the filtered aqueous samples were transferred into sample vials for DOC and Ion chromatography analysis, respectively. The Shimadzu TOC-L machine was used to determine DOC using NPOC (non-purgeable organic carbon) method by removing the portion of inorganic carbon first and then measuring the leftover carbon. An ion chromatography (Dionex ICS 1100, US) system was used to determine phosphate, nitrite and nitrate. The method used the AS234 \times 250 mm carbonate eluent anion-exchange column (Dionex). Anion mode analysis was carried out according to the manufacturer's recommendations, using a mobile phase of 4.5 mM Na_2CO_3 . The flow rate was set at 1 mL/min, with a total run time of 30 min and column temperature held at 30 °C. The spectra were analysed using a set of standards and software provided by Dionex.

3.3.3 Microbial characterisation

The standard membrane filtration method was used for the enumeration of *E. coli* and coliform bacteria following ISO 9308-1:2014 (<https://www.iso.org/standard/55832.html>). 50 mL of aqueous samples or dilutions were filtered through a sterile 0.45 μm membrane (GILSON, UK) and the membrane was then placed on the Chromogenic Coliform Agar (ThermoFisher SCIENTIFIC, UK). The plates were incubated at 37 °C for 24 h. *E. coli* K12 was used as a positive control.

3.4 Antibiotic quantification method development

3.4.1 Chemicals

Amoxicillin (AMOX, Cat. No. 61336-70-7), clarithromycin (CTM, Cat. No. 81103-11-9), oxytetracycline (OTC, Cat. No. 2058-46-0), sulfamethoxazole (SMX, Cat. No. 723-46-6), trimethoprim (TMP, Cat. No. 738-70-5) standards ($\geq 99.0\%$) were purchased from Sigma-Aldrich, UK. HPLC grade acetonitrile (Cat. No. 75-05-8) and methanol (Cat. No. 67-58-1) were obtained from Fisher Scientific. Ultrapure (Milli-Q) water, analytical grade formic acid (Sigma-Aldrich, Cat. No. 64-18-6), acetone (Fisher Scientific, Cat. No. 67-64-1) and disodium ethylenediamine tetraacetate (Na_2EDTA) (Acros Organics, Cat. No. 6381-92-6) were used during the experiment. Individual stock standards were prepared in methanol at 1 mg/mL, except for amoxicillin, which was dissolved in acetonitrile/water (50:50, v/v). A working solution was prepared by diluting the stock solutions in Milli-Q water into 1 mg/L. All the stock solutions were stored at $-20\text{ }^\circ\text{C}$ and working solutions were preserved at $4\text{ }^\circ\text{C}$. Antibiotic stock solutions were prepared every three months and working solutions were prepared daily.

3.4.2 LC-MS/MS detection

3.4.2.1 Mass spectrometry

An Accela 1100 HPLC system coupled to a LTQ ion-trap mass spectrometer (Thermo Finnigan LTQ) was used for the detection of target antibiotics. This system provides capillary LC-MS and $-\text{MS}^n$ analyses in electrospray ionisation (ESI) mode. The mass spectrometer setting was optimised with a direct infusion of working standard solutions prepared at 1 mg/L. All standard solutions were infused with the syringe pump at $20\text{ }\mu\text{l}/\text{min}$. For each analyte, mass spectra from 110 to 1000 were recorded in positive ionisation mode with the protonated molecular ion of each compound $[\text{M}+\text{H}]^+$ chosen as precursor ion (see Appendix Figure A3.1). The two most abundant product ions produced from each precursor ion were chosen as the ion transitions which is required by the 2002/657/EC decision [196]. In general, the most abundant product ion was selected for quantification and the retention time and the second

most abundant ion was used for the identification of the compound. The optimised mass spectrometer parameters including precursor ion, product ions, and collision energy for each antibiotic are summarised in Table 3.5.

Table 3.5 Summary of the precursor and product ions, retention time, MS/MS parameters observed for the target antibiotics.

Compound	Precursor ion (m/z)	Product ion 1 (m/z)	Product ion 2 (m/z)	Retention time (min)	Collision energy (eV)
Amoxicillin	366.1	349.1	208.0	1.63	28
Clarithromycin	748.4	590.3	558.4	9.22	30
Oxytetracycline	461.3	443.2	426.2	5.25	44
Sulfamethoxazole	254.2	188.1	156.0	6.95	34
Trimethoprim	291.5	230.1	123.1	5.07	44

3.4.2.2 Liquid chromatography systems

In order to optimise the chromatographic separation of target antibiotics from the possible matrix interferences, different LC parameters were tested. A Hypersil GOLD C18 column (100 mm × 2.1 mm, 1.9 µm) was used for the chromatographic separation of antibiotic compounds. For the optimisation of chromatographic separation, different mobile phases were tested. Acidic additives (formic or acetic acid) are known to promote the protonation of basic molecules and increase the signal in ESI+ interface [230]. Initially, mobile phases consisting of methanol (mobile phase A) and water with 0.1 % formic acid (mobile phase B) were tested. A linear gradient from 5% to 95% of mobile phase A in 20 min and a flow rate of 250 µl/min were selected as starting conditions. The result showed poor chromatographic separation in terms of peak shape and signal intensity. The addition of formic acid (0.1%) to both methanol and water was then tested and the signal responses were improved due to the protonation of the basic compounds. Furthermore, acetonitrile with 0.1 % formic acid as the organic phase was tested and both resolution and peak shapes were improved and better chromatographic separation was achieved when acetonitrile was used. Therefore, acetonitrile with 0.1 % formic acid (mobile phase A) and water with 0.1 % formic acid (mobile phase B) were selected as the mobile phases in this study.

After the establishment of mobile phase composition, the gradient elution was then optimised in order to improve chromatographic resolution and to reduce total run time. The flow rate of the mobile phase was increased from 250 $\mu\text{l}/\text{min}$ to 300 $\mu\text{l}/\text{min}$ as the higher flow rate can reduce retention times and enhance peak heights by narrowing them [231]. For improving the peak separation quality and avoiding time gaps throughout the chromatogram, the gradient program of the mobile phase from 1% to 99% of A in 16 min was finally selected. Under these conditions, the total run time was reduced by 4 mins and an increase from 30% to 60% in peak responses was achieved. The chromatographic separation of target antibiotic is shown in Appendix (Figure A3.2).

3.4.3 Solid Phase Extraction

Solid Phase Extraction (SPE) is the most applicable method for the pre-concentration of analytes from the aqueous samples. A typical SPE procedure includes 1) pH adjustment of water sample; 2) condition and equilibration of extraction cartridges; 3) sample loading; 4) washing and drying of cartridges; 5) elution of analytes; 6) evaporation of eluent; and 7) final reconstitution. Milli-Q water spiked with antibiotic working solutions was used to test the recoveries under different SPE conditions. In general, a validated SPE method should achieve 70%-120% recovery of the analytes according to EU requirements [232, 233]. However, the lower recovery (<50%) for an analyte may be considered when it is repeatedly and reliably obtained [194]. During the development of the SPE methods, recovery optimization remains an important but secondary issue, because the main goal is the simultaneous extraction of as many analytes from multiple classes as possible.

3.4.3.1 Different cartridges

In this study, seven SPE cartridges were tested to optimise the efficiency of simultaneous extraction for target antibiotics. Specifications of the cartridges selected are summarised in Table 3.6. Recoveries for different types of cartridges are summarised in Table 3.7.

Table 3.6 Solid Phase Extraction (SPE) cartridges tested in this study.

SPE Cartridge	Cartridge type	Application	Particle size	Sorbent weight	Barrel size	Supplier
HyperSep Retain PEP	Mixed-mode anion exchange	polarity and non-polarity	30 – 50 μm	60 mg	6 mL	Thermo Fisher Scientific, USA
Supel TM -Select SPE	Polymer Reverse-phase	acids, neutrals and bases	50 – 70 μm	200 mg	6 mL	Supelco, USA
Oasis HLB	Copolymer Reverse-phase/polar interactions	acids, neutrals and bases	30 μm 60 μm	200 mg 500 mg	6 mL	Waters, UK
Oasis MCX	Strong cation exchange Reverse-phase	bases	30 μm	30 mg	1 mL	Waters, UK
Oasis WAX	Weak anion exchange Reverse-phase	strong acids	30 μm	30 mg	1 mL	Waters, UK
Oasis MAX	Strong anion exchange Reverse-phase	acids	30 μm	30 mg	1 mL	Waters, UK
Oasis WCX	Weak cation exchange Reverse-phase	strong bases	30 μm	30 mg	1 mL	Waters, UK

Table 3.7 A comparison of recoveries observed for different cartridges (n = 3).

Antibiotics	HyperSep Retain PEP	Supel TM -Select SPE	Oasis HLB	Oasis MCX	Oasis WAX	Oasis MAX	Oasis WCX
Amoxicillin	NA	NA	12 \pm 3	53 \pm 3	NA	8 \pm 3	NA
Clarithromycin	84 \pm 5	82 \pm 3	109 \pm 7	7 \pm 3	102 \pm 4	82 \pm 5	71 \pm 6
Oxytetracycline	85 \pm 6	72 \pm 8	80 \pm 13	32 \pm 7	15 \pm 5	70 \pm 8	5 \pm 2
Sulfamethoxazole	87 \pm 3	84 \pm 6	91 \pm 2	72 \pm 4	95 \pm 3	71 \pm 5	10 \pm 4
Trimethoprim	43 \pm 12	33 \pm 4	80 \pm 8	97 \pm 7	32 \pm 6	71 \pm 2	99 \pm 5

Given the structural differences of the target antibiotics and the wide range of $\log K_{OW}$ (log of the octanol-water partition coefficient), the sorbent that gave better overall recoveries was Oasis HLB. $\log K_{OW}$ values are typically between -3 (very hydrophilic) and $+10$ (extremely hydrophobic), a compound is considered hydrophobic when $\log K_{OW} > 2$ [186]. Due to the presence of the macrocyclic lactone ring in the molecule of CTM, it is the most hydrophobic compound (CTM, $\log K_{OW} = 3.16$) among the selected antibiotics (AMOX $\log K_{OW} = 0.87$; OTC $\log K_{OW} = -0.90$; SMX $\log K_{OW} = 0.89$; and TMP $\log K_{OW} = 0.91$). The result was expected to be the Oasis HLB which has a wide range of extraction targets, including acidic, basic and neutral compounds from various matrices. Despite of the better recovery (53%) observed for AMOX

using the Oasis MCX cartridges, better recoveries for the majority of compounds were still achieved by Oasis HLB cartridges. In most cases, the use of one cartridge is preferred in order to simplify the sample preparation procedure, rather than using more complex procedures (e.g. two or more SPE cartridges in tandem or in parallel) that yield higher recovery rates [194].

3.4.3.2 pH and Na₂EDTA

The pH is a critical part of the sample preparation and SPE process as the pK_a (negative log of the acid dissociation constant) values of analytes are in the range of 0.24-17.33, which affects the efficiency of analytes to be ionised and retained by the sorbent. In this study, the water samples were adjusted to pH 3.0, 5.0 and also left without pH adjustment before being loaded onto the HLB cartridge. The results of recoveries are shown in Figure 3.9a. The antibiotics selected in this study exhibited pH-dependent recoveries. Except for AMOX, all of the selected antibiotics had higher recoveries in an acidic environment than in a neutral environment. For CTM, OTC and TMP, the highest recoveries can be obtained in strongly acidic conditions (pH=3.0). SMX had relatively stable recoveries in both acidic and neutral environment (80.7%~95.4%). It was difficult to find a compromise between AMOX and the other antibiotics, for which the isolation was better in acidic solution. The most satisfactory overall recoveries were achieved at pH=3.0.

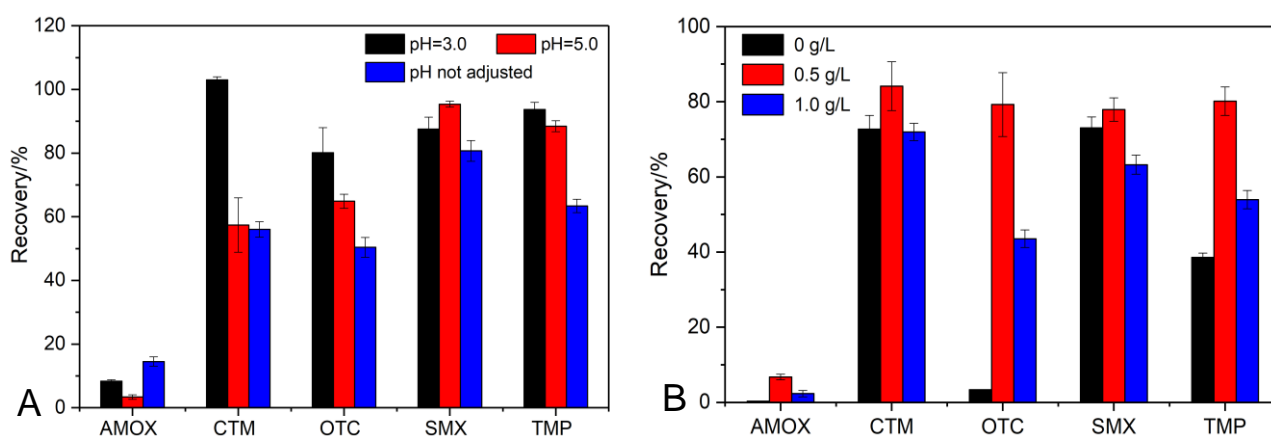


Figure 3.9 Recoveries of selected antibiotics (spiked at 1 µg/L) at different A: pH-values and B: Na₂EDTA concentration. AMOX: amoxicillin; CTM: clarithromycin; OTC: oxytetracycline; SMX: sulfamethoxazole; TMP: trimethoprim. The error bar represents one standard deviation from the mean value (n = 3).

Some organic compounds may chelate with metal ions (e.g. Ca^{2+} , Mg^{2+}) existing in natural water, which may reduce the recoveries of target analytes. To improve the extraction efficiency, three Na_2EDTA concentrations were tested (at 0, 0.5, 1.0 g/L) and the results are shown in Figure 3.9b. All of the selected antibiotics had the highest recoveries at Na_2EDTA 0.5 g/L. It has been reported that the addition of EDTA to water samples is necessary to increase the recovery of tetracyclines [49], which is consistent with this study as the recovery of OTC increased considerably (from 3.36% to 79.25%) when Na_2EDTA was added. For those compounds yielded low extraction recoveries without the addition of EDTA, the possible reason is these compounds can potentially bind residual metals present in the sample matrix and glassware [234]. By adding Na_2EDTA , soluble metals are bound to the chelating agent, increasing the extraction efficiency.

3.4.3.3 Elution solvents

A suitable eluent is important for the analytical performance of the SPE procedure. The selection of eluent is based on appropriate chemical polarities and good applicability for the extraction of analytes from various environmental matrices. Methanol and acetonitrile were first tested as extraction solvents in multiclass analysis of the selected antibiotics according to the previous research [198, 233, 235]. The optimisation of the elution condition was to get the maximum recovery of the antibiotic with the minimum volume of the elution solvent. Results showed that methanol, as a single extraction solvent, achieved the highest overall recoveries of the selected antibiotics (Figure 3.10).

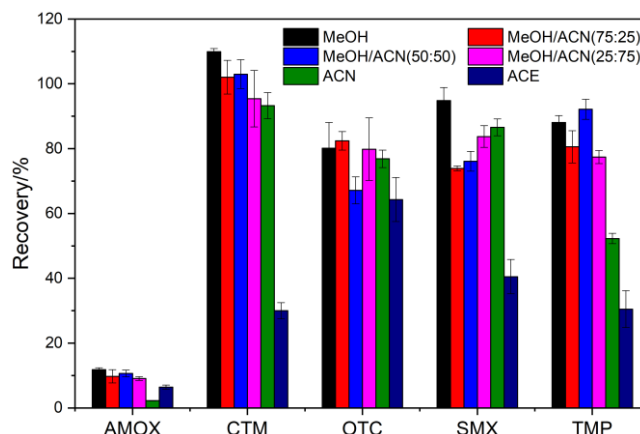


Figure 3.10 Recoveries of the selected antibiotics (spiked at 1 $\mu\text{g/L}$) at different elution conditions. MeOH: methanol; ACN: Acetonitrile; ACE: acetone. AMOX: amoxicillin; CTM: clarithromycin; OTC: oxytetracycline; SMX: sulfamethoxazole; TMP: trimethoprim. The error bar represents one standard deviation from the mean value ($n = 3$).

3.4.3.4 Sample loading rate

A fast loading rate is desirable to reduce instrument operation time but it may also reduce the capacity of the sorbent retaining analytes as the interaction time is reduced. Four sample loading rates were tested in this study, 1 mL/min, 3 mL/min, 5 mL/min and 10 mL/min using the automatic SPE system (Dionex Autotrace 280). Results showed similar overall recoveries for the tested loading rates (Figure 3.11). The average recovery ranged from 64.3% at 10 mL/min to 73.0 % at 5 mL/min. Therefore, 5 mL/min was selected as the final sample loading rate.

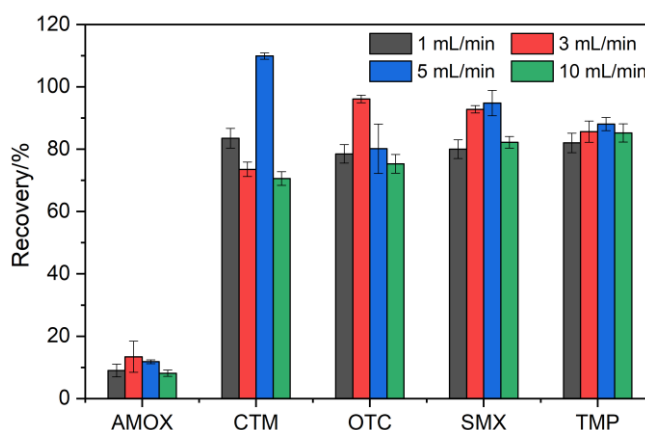


Figure 3.11 Recoveries of selected antibiotics (spiked at 1 $\mu\text{g/L}$) at different loading rates. AMOX: amoxicillin; CTM: clarithromycin; OTC: oxytetracycline; SMX: sulfamethoxazole; TMP: trimethoprim. The error bar represents one standard deviation from the mean value ($n = 3$).

3.4.4 Method validation

Surface water free from the target antibiotics were used for method validation. Two sampling sites, a pond in Regent's Park (central London) and the New River (North London) were selected. Geographical location of the sampling sites is provided in the appendix (Figure A3.3). Water samples were collected at each sampling point in amber glass bottles and kept refrigerated at 4 °C without preservatives until they were processed within 24 h of sampling.

3.4.4.1 Calibration curve

For the calibration curves for each antibiotic, individual antibiotic solutions at different concentrations (0.05, 0.1, 0.5, 1, 5 ng/μl) were injected into the LC-MS/MS system to obtain the peak area of each analyte at different concentrations; Linear fitting curves were obtained for each antibiotic standard and R² values were all above 0.99 (Table 3.8).

Table 3.8 The regression equations, correlation coefficients (R²) and linear range of target antibiotics.

Antibiotics	Regression equation	Linearity (R ²)	Linear range (ng/mL)
Amoxicillin	$y=3049.9x - 100219$	1.0000	5-5000
Clarithromycin	$y=14672x + 237714$	0.9974	5-5000
Oxytetracycline	$y=1874.3x - 272102$	0.9943	5-5000
Sulfamethoxazole	$y=3602.9x + 42531$	0.9994	5-5000
Trimethoprim	$y=6603.9x - 498483$	0.9990	5-5000

3.4.4.2 Matrix-matched calibration

When detection is performed using the ESI mass spectrometer, it is very common to have signal enhancement or suppression occur in environmental samples. It is well documented that reliable calibration can be achieved using internal standards [195, 198, 234], external standards [236] and standard addition methods [237, 238]. In general, isotopically labelled analytes or structurally similar compounds are usually chosen as an internal standard. However, when analysing a mixture of very different analytes, it is impractical and costly to find an appropriate internal standard which is suitable for all analytes. The traditional external

calibration uses serial standard solutions in pure solvent to obtain the linear relationship between concentration and peak area. This method is neither suitable nor reliable due to the matrix effect occurring in the ESI process. In this study, the external calibration method with matrix-matched standards was used. This method can minimise the influence of interfering substances from different environmental samples and has been widely used in previous research [199, 232, 239]. The matrix-matched standards were prepared as follows: the same surface water matrix was initially extracted, and the analytes were added at levels of 0.05, 0.1, 0.25, 0.5, 1, 5 µg to 1 mL of the final reconstituted extract. The linearity of the calibration curves is shown in Table 3.9. Within the selected range, all target antibiotics achieved good linearity ($R^2 > 0.99$), indicating the applicability of the matrix-matched standard method.

Table 3.9 Linear regression parameters of the target antibiotics in reference matrices.

Antibiotics	Matrix-matched calibration curves for RW			Matrix-matched calibration curves for PW		
	Regression equation	R^2	Range (µg/mL)	Regression equation	R^2	Range (µg/mL)
Amoxicillin	$y = 568332x + 172720$	0.9985	0.05-5	$y = 473907x + 85858$	0.9916	0.05-5
Clarithromycin	$y = 5E+06x - 230015$	0.9994	0.05-5	$y = 4E+06x - 590363$	0.9991	0.05-5
Oxytetracycline	$y = 1E+06x + 96520$	0.9994	0.05-5	$y = 954773x - 21766$	0.9998	0.05-5
Sulfamethoxazole	$y = 1E+06x + 7471.3$	0.9998	0.05-5	$y = 1E+06x - 182202$	0.9948	0.05-5
Trimethoprim	$y = 7E+06x + 386801$	1.0000	0.05-5	$y = 6E+06x - 100258$	0.9997	0.05-5

RW: river water; PW: pond water.

3.4.4.3 Matrix effect

The matrix effect percentage (%ME), which represents how the matrix may interfere with the analyte's signal, was calculated by the ratio of the signal response of spiked post-extracted matrix sample to that of analyte in solvent. The equation is shown below [232, 240]:

$$\% ME = \left(1 - \frac{\text{signal response of spiked post - extracted reference matrix sample}}{\text{signal response of analyte in solvent}} \right) \times 100$$

Based on the equation, 0% ME indicated no matrix interference with the analyte's signal. The matrix effect was tested at the concentration of 100 ng/mL and the results are

shown in Table 3.10. Even though the matrix effect was not pertinent to one class of antibiotics but specific to each antibiotic [232], different reference matrices will also interfere with the signal intensity for the same analyte. This may be attributed to the amount of interfering substances in various water samples being different and their mechanisms of interaction with analytes being unknown. For river water samples, the signal was not significantly affected for most antibiotics, as the matrix effect was less than 22%. However, for OTC, significant signal enhancement was observed (- 50%). Results obtained from pond water showed that the signal of all analytes was suppressed. Low interference levels (5%~23%) were observed for CTM, OTC, and AMOX and high interference levels (30%~46%) for TMP and SMX. The higher matrix effect could lead to inaccurate quantification, therefore, the use of matrix-matched standard was necessary.

3.4.4.4 Validation of analytical method

The optimised SPE-LC-MS/MS method was finally validated using surface water samples. A total volume of 1 L for each sample was filtered through a 0.45 µm membrane filter (Whatman, Cat. No. 7184-004) and antibiotics were spiked at a final concentration of 0.5 and 5.0 µg/L into the reference matrix samples. In addition, the final reconstituted SPE extracts were vortexed and filtered through 0.2 µm PTFE syringe filters (Whatman, Cat. No. 7582-002) prior to LC injection. Recoveries and repeatability of the method, expressed as the relative standard deviation (RSD), were determined by the analysis of three replicate sample. Results are summarised in Table 3.10.

Except for AMOX, the recoveries of the four antibiotics ranged from 66 % to 122 % for river water samples and from 61% to 124 % for pond water. These recoveries were comparable to those of published methods for the detection of selected antibiotics in surface water with a relatively similar matrix (e.g. lake water, river water and ground water) [37, 199, 238]. The overall method precision (RSD) was determined to be within the range of 2 – 13% for all the investigated antibiotics, which is less than 20% as recommended by the U.S. Environmental Protection Agency [232]. No statistical difference was found ($p > 0.05$) at the two spiking levels. The recoveries for AMOX were between 19 – 31% in both pond and river water, which were

similar to the results obtained by previous research ranging from 17 – 22% in ground water [199]. It was common that β -lactam antibiotics were expected to achieve relatively low recoveries when using a single SPE method for the simultaneous analysis of different classes of antibiotics. This could be attributed to β -lactams being related structurally though the presence of a chemically unstable β -lactam ring [241]. Overall, the validation experiment indicated that the optimised SPE-LC-MS/MS method (Figure 3.12) was suitable for the simultaneous extraction of target antibiotics from natural water samples.

Table 3.10 Recoveries, repeatability, matrix effects and method detection limits for the selected antibiotics in reference matrices.

Antibiotics	Spiked Con. ($\mu\text{g/L}$)	Recovery, % (RSD)		% ME _{RW}	% ME _{PW}	MDL (ng/L)
		RW	PW			
Amoxicillin	0.5	31 (3)	30 (2)	17	15	50
	5.0	26 (12)	19 (6)			
Clarithromycin	0.5	66 (5)	61 (10)	11	5	3
	5.0	88 (6)	67 (4)			
Oxytetracycline	0.5	122 (6)	124 (4)	-50	23	20
	5.0	119 (2)	70 (8)			
Sulfamethoxazole	0.5	89 (2)	72 (3)	22	46	7
	5.0	85 (13)	78 (5)			
Trimethoprim	0.5	94 (3)	74 (3)	16	30	2
	5.0	88 (3)	68 (3)			

RSD: relative standard deviation (n = 3); RW: river water; PW: pond water; % ME: matrix effect percentage; MDL: method detection limit.

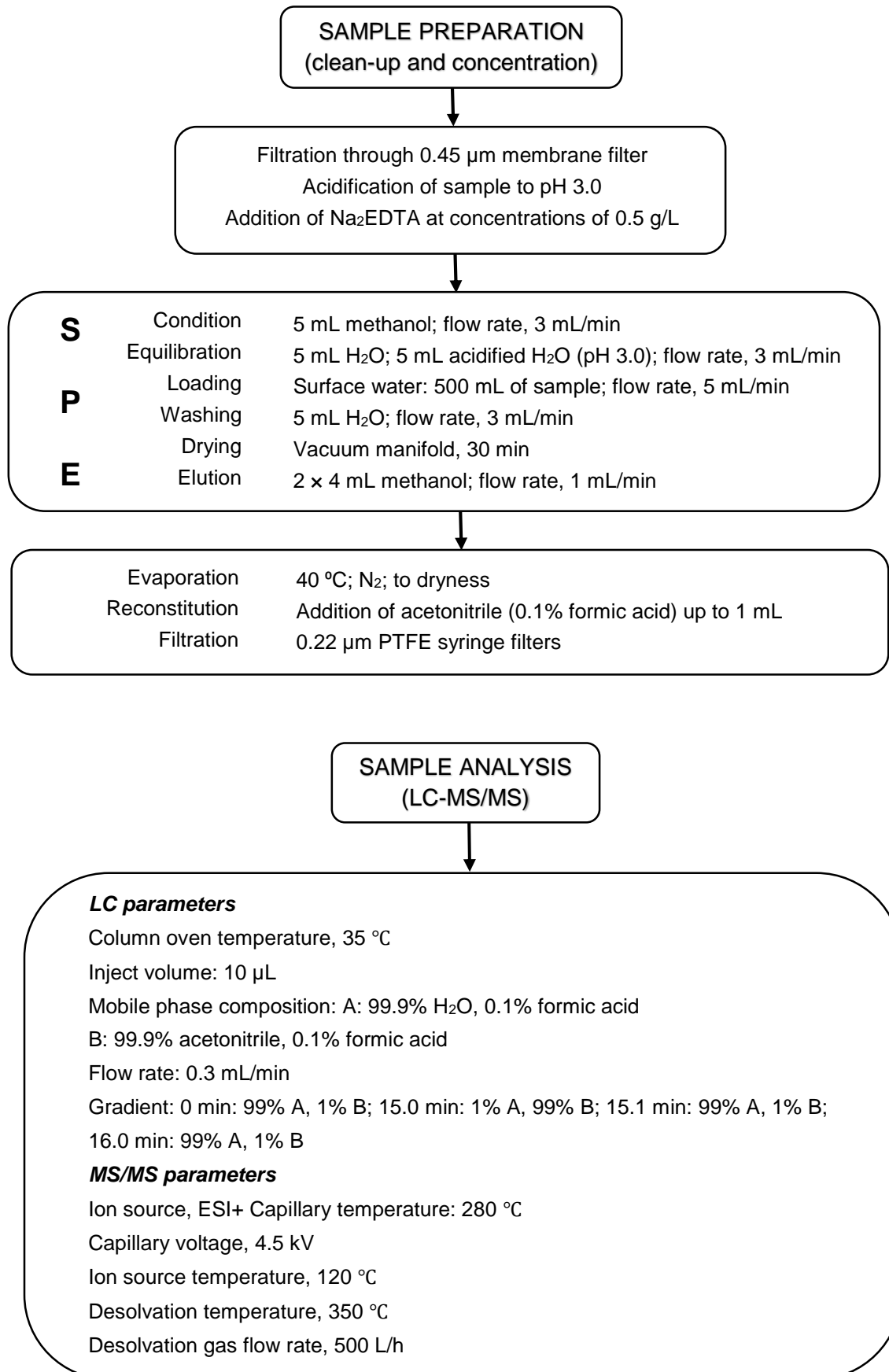


Figure 3.12 SPE-LC-MS/MS protocol in this study.

3.5 ARGs quantification method development

3.5.1 DNA extraction

Biofilter influent and effluent samples were filtered through 0.22 µm mixed cellulose ester (MCE) membrane filters (Millipore, UK) to capture the bacteria. Media (biofilm) samples were added to sterile saline (NaCl, 0.85 g/L) and ultrasonicated at 80 kHz, 100 W for 20 min to suspend the biofilm's DNA [242]. The ultrasonication was repeated three times with 5 min intervals. The biofilm suspensions were then concentrated onto 0.22 µm MCE filters. All of the membranes were stored at - 20 °C until DNA extraction. Genomic DNA was extracted using the FastDNA Spin Kit for Soil (MP Biomedicals, UK) according to the manufacturers' instructions. The concentration of the purified DNA was quantified spectrophotometrically using the NanoDrop (Thermo Scientific, UK) and Qubit Fluorometer (Invitrogen, UK) and stored at - 85 °C until further analysis.

3.5.2 qPCR

In this study, chemically synthesised double-stranded gene fragments were modified and used as quantitative PCR standards in order to establish in-house qPCR assays for the quantification of the target ARGs. The *ermB* gene from a naturally occurring plasmid was used to compare the performance of the qPCR assay with the chemically synthesised *ermB*. This work has been published as "Use of synthesized double-stranded gene fragments as qPCR standards for the quantification of antibiotic resistance genes." *Journal of Microbiological Methods*, 2019. 164: p. 105670.

3.5.2.1 ARG fragment design

Nucleic acid sequences for individual ARG were downloaded from the NCBI website (<https://www.ncbi.nlm.nih.gov/nucleotide>). Specific pair of primers for each ARG (Table 3.11) was used to trim both sides of the sequence obtained from the NCBI website. ARG sequences selected in this study are supplied in Table A3.2. Chemically synthesised double-stranded ARGs (referred to hereafter as 'gBlocks' gene fragments) were obtained from Integrated DNA Technology (UK). Once received, gBlocks gene products were re-suspended in Tris-EDTA

buffer (pH 8.0, Sigma-Aldrich, UK) according to the manufacturers' instructions to reach a final concentration of 10 or 20 ng/ μ L and stored at -20°C for further processes.

Table 3.11 Primers and amplicon size of target ARGs in this study.

Target Gene	Primer	Sequence	Amplicon Size (bp)	Reference
<i>bla_{CTX-M}</i>	Forward	CTATGGCACCACCAACGATA	103	[243]
	Reverse	ACGGCTTTCTGCCTTAGGTT		
<i>bla_{OXA-1}</i>	Forward	ACCAAAGACGTGGATGCAAT	325	[244]
	Reverse	TGCACCAGTTTTCCCATACA		
<i>bla_{TEM}</i>	Forward	CCCCGAAGAACGTTTTTC	516	[245]
	Reverse	ATCAGCAATAAACCAGC		
<i>ermB</i>	Forward	ACGACGAAACTGGCTAAAATAAGT	412	This study
	Reverse	CTGTGGTATGGCGGGTAAGT		
<i>tetA</i>	Forward	GCTACATCCTGCTTGCCTTC	210	[246]
	Reverse	CATAGATCGCCGTGAAGAGG		
<i>tetG</i>	Forward	GCTCGGTGGTATCTCTGCTC	468	[246]
	Reverse	AGCAACAGAATCGGGAACAC		
<i>tetQ</i>	Forward	AGAATCTGCTGTTTGCCAGTG	169	[247]
	Reverse	CGGAGTGCAATGATATTGCA		
<i>tetW</i>	Forward	GAGAGCCTGCTATATGCCAGC	168	[247]
	Reverse	GGGCGTATCCACAATGTTAAC		
<i>tetX</i>	Forward	CAATAATTGGTGGTGGACCC	468	[246]
	Reverse	TTCTTACCTTGGACATCCCG		
<i>sul 1</i>	Forward	CACCGGAAACATCGCTGCA	158	[248]
	Reverse	AAGTTCCGCCGCAAGGCT		
<i>sul 2</i>	Forward	CTCCGATGGAGGCCGGTAT	190	[248]
	Reverse	GGGAATGCCATCTGCCTTGA		
<i>dfrA1</i>	Forward	TGGTAGCTATATCGAAGAATGGAGT	425	[249]
	Reverse	TATGTTAGAGGCCGAAGTCTTGGGTA		
<i>dfrA12</i>	Forward	GAGCTGAGATATACTCTGGCACT	155	[249]
	Reverse	GTACGGAATTACAGCTTGAATGGT		
<i>intl 1</i>	Forward	CCTCCCGCACGATGATC	280	[250]
	Reverse	TCCACGCATCGTCAGGC		
<i>intl 2</i>	Forward	TTATTGCTGGGATTAGGC	233	[250]
	Reverse	ACGGCTACCCTCTGTTATC		
16S rRNA	1369-Forward	CGGTGAATACGTTTCYCGG	143	[251]
	1492-Reverse	GGWTACCTTGTTACGACTT		

3.5.2.2 gBlocks Cloning

As gBlocks are blunt-end DNA fragments, it is necessary to add adenosine (A) overhangs to gBlocks for compatibility with T/A cloning vectors. The gBlocks DNA suspensions were incubated at 50°C for 20 minutes prior to use. The A-tailing experiment was conducted at room temperature. 0.6 µL Taq DNA polymerase (5 units/µL), 1.5 µL 10× PCR buffer (Taq PCR Core Kit, QIAGEN, UK), 0.05 mM dATP (BIOLINE, UK), 50 ng gBlocks DNA fragments, and PCR grade water were combined to a final volume of 15 µL. A reaction tube adding PCR grade water instead of gBlocks was used as a negative control. After 30 minutes' incubation at 70°C, the A-tailing products were ready for T/A cloning.

In order to compare the performance of gene fragments originating from both chemical synthesis and a naturally occurring resistance plasmid, the plasmid pMTL9301 carrying *ermB* was also used for gene cloning. Fresh PCR product with the confirmed presence of the *ermB* gene was excised and purified using the QIAquick Gel Extraction Kit (QIAGEN, UK). 1 µL purified PCR product or A-tailed gBlocks was ligated into pGEM Easy Vector and then transformed into *E. coli* JM109 competent cells using the pGEM Easy Vector Systems (Promega, UK) according to the manufacturers' instructions.

Successful recombinant cells (blue colonies) were picked from Luria-Bertani (LB) agar containing 100 mg/L Ampicillin (Sigma-Aldrich, UK) and Blue/White Select Screening reagent (Sigma-Aldrich, UK) and screened by PCR (TECHNE, UK) using the primers listed in Table 3.11 to evaluate cloning of the target genes. Details about PCR conditions can be found in the appendix (Chapter 3 appendix, Section A3.1). Six µL of each PCR product were verified by 1.5% agarose gel electrophoresis and then visualised with a AlphasMager Mini System (Protein Simple, UK). As can be seen from Figure 3.13, all of the target genes were amplified and formed a single band. The size of each ARG band as it appeared on the gel was in accordance with the amplicon size specified in Table 3.11. Both *ermB* gene bands were the same size and intensity. In addition, all PCR products were sequenced by Source Bioscience (London, UK) for the verification of the presence of ARGs. The sequence results were compared with existing sequences using BLAST alignment tool

(<https://blast.ncbi.nlm.nih.gov/Blast.cgi>). Plasmid DNA were extracted from the vector containing the insert using the QIAprep Spin Miniprep Kit (QIAGEN, UK) and the concentration of plasmid DNA was measured by the Qubit 3.0 Fluorometer.

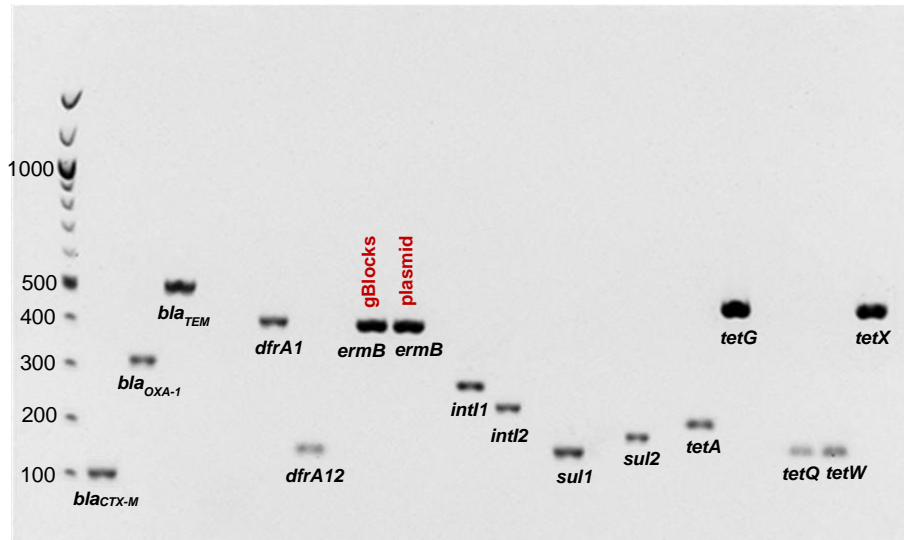


Figure 3.13 Electrophoresis bands of target genes.

(*ermB* - left: originated from gBlocks; right: originated from plasmid)

3.5.2.3 qPCR Procedures

Plasmid DNA containing target genes were used to generate standard curves. The numbers of copies of plasmid DNA per microliter were calculated using the following formula [252]:

$$\frac{\text{Copies}}{\mu\text{L}} = \frac{\text{DNA mass concentration (ng}/\mu\text{L}) \times 10^{-9} \times 6.022 \times 10^{23}}{(3015 \text{ bp}^* + \text{amplicon size bp}) \times 660}$$

* The length of the pGEM Easy vector is 3015 bp.

Seven-point standard curves with copy numbers ranging from 10^2 to 10^8 for qPCR were generated using 10-fold serial dilutions of the plasmid DNA carrying target ARGs. A final volume of 20 μL reaction mixture was used, consisting of 10 μL of Luna Universal qPCR Master Mix (New England Biolabs, UK), 0.5 μL of each primer (10 μM), 1 μL DNA template, and 8 μL of PCR grade water. The PCR cycling conditions were as follows: 1 min at 95°C, followed by 40 cycles of 15 s at 95°C, 30 s at 60°C, and then a final melt curve stage with temperature ramping from 60 to 95°C. Each reaction was run in triplicate and a non-template

control was included. All the qPCR assays were performed in 96-well plates under standard conditions, as per the instructions of the manufacturer, in a 7500 Real-Time PCR system (Applied Biosystems). Amplification efficiencies for all target genes ranged from 82.0% to 107.4% with good linearity (Table 3.12), indicating the reliability of synthetic gene fragments as qPCR standards. Ideally, the qPCR efficiency should be 1.0, however, if consistent, a lower efficiency value is also acceptable due to the potential PCR inhibitors in DNA extracts [206]. The variation in amplification efficiency could also be attributed to the uniform annealing temperature used throughout the qPCR array.

Table 3.12 Standard curves, amplification efficiency, R² value of each qPCR array.

Target Gene	Standard curve	R ²	Amplification efficiency	LOD (GC/μL)
<i>bla_{CTX-M}</i>	Y = -3.44X + 39.19	0.999	95.3%	9.6
<i>bla_{OXA-1}</i>	Y = -3.53X + 38.05	0.999	92.1%	7.3
<i>bla_{TEM}</i>	Y = -3.16X + 36.66	0.993	107.4%	6.1
* <i>ermB</i> (gBlocks)	Y = -3.30X + 41.55	0.997	100.9%	9.2
* <i>ermB</i> (plasmid)	Y = -3.55X + 36.30	0.995	91.3%	4.6
<i>tetA</i>	Y = -3.44X + 36.72	0.999	95.4%	3.2
<i>tetG</i>	Y = -3.84X + 40.25	0.983	82.0%	6.8
<i>tetQ</i>	Y = -3.26X + 35.25	0.999	102.8%	2.0
<i>tetW</i>	Y = -3.31X + 35.89	0.998	100.3%	7.1
<i>tetX</i>	Y = -3.38X + 40.51	0.997	97.6%	6.3
<i>sul I</i>	Y = -3.43X + 38.11	0.997	95.8%	5.1
<i>sul II</i>	Y = -3.81X + 39.01	0.999	83.0%	7.3
<i>dfrA1</i>	Y = -3.63X + 36.45	0.997	88.5%	4.5
<i>dfrA12</i>	Y = -3.34X + 39.42	0.997	99.4%	6.1
<i>intl 1</i>	Y = -3.51X + 43.04	0.995	92.8%	3.1
<i>intl 2</i>	Y = -3.10X + 39.65	0.998	96.8%	3.8
16S	Y = -3.39X + 36.34	1.000	97.3%	3.9

**ermB* (gBlocks): chemically-synthesised *ermB*; *ermB* (plasmid): plasmid-carrying *ermB*.

LOD: Limit of detection; GC/μL: gene copies/μL.

The calculation of the limit of detection followed previous research by performing eight replicates of each dilution of the standard for each gene, and the lower gene copies gave results that were accurately reproducible was considered as limit of detection [253]. Only runs resulting in gene copies higher than the detection limit were applied for the calculation of resistance gene concentrations. Both gBlocks-*ermB* and plasmid-*ermB* achieved good amplification efficiency and linearity (100.9%, 0.997 and 91.3%, 0.995, respectively). Sequence alignment results also showed 100% similarity for both *ermB* gene fragments, indicating the performance of gBlocks-*ermB* qPCR assay was comparable with plasmid-harboured *ermB*. In general, gBlocks standards enable more independent qPCR assay development which is not limited to the availability of the positive isolates or plasmids, especially when a research project has several ARGs of interest.

Different types of environmental samples (Figure A3.4), including surface water, soil and faeces were used to validate the qPCR assays prior to the application for ARGs quantification during biofiltration experiment. Details are provided in appendix (Chapter 3 appendix, Section A3.2).

3.5.3 High-throughput qPCR

High-throughput qPCR (HT-qPCR) analysis was conducted in the Key Laboratory of Urban Environment and Health, Institute of Urban Environment, Chinese Academy of Sciences. The SmartChip Real-time PCR System (Warfengen Inc., USA) was used to perform HT-qPCR as previously described [75, 220]. A total of 296 primer sets were used, including 285 ARGs conferring resistance to all major classes of antibiotics, including aminoglycoside, beta-lactams, FCA (fluoroquinolone, quinolone, florfenicol, chloramphenicol and amphenicol), MLSB (Macrolide-Lincosamide-Streptogramin B), multidrug, sulfonamide, tetracycline and vancomycin; eight transposases; *16S rRNA* gene; *intl 1*; and the clinical *intl 1* (*intl1*). PCR mixtures (100 nL per well) consisted of 1 × LightCycler 480 SYBR Green I Master (Roche Applied Sciences, Indianapolis, IN), nuclease free PCR-grade water, 1 mg/mL bovine serum albumin (New England Biolaboratories, Beverly, MA), 500 nM of each primer and a DNA

template of 5 ng/ μ L. The qPCR conditions included initial enzyme activation at 95 °C for 10 min, and 40 cycles of denaturation at 95 °C for 30 s and annealing at 60 °C for 30 s for amplification. The melting process was automatically generated by Wafergen software and the qPCR results were analysed using SmartChip qPCR Software. Data with multiple melting peaks or with amplification efficiency beyond the range (1.8–2.2) were discarded. A threshold cycle (CT) of 31 was used as the detection limit, and only samples with detected amplification of ARGs in all replicates were regarded as positive. Details of the classification of the 296 genes can be found in appendix (Table A3.3). HT-qPCR and the preliminary data analysis were done by the researchers in the Key Laboratory of Urban Environment and Health, China.

3.6 Bacterial community analysis

DNA samples were sent for amplicon sequencing using the Illumina Hiseq2500 platform (Novogene, Beijing, China). The V3-V4 region of the *16S rRNA* gene was selected for amplification with primers 341F: CCTAYGGGRBGCASCAG and 806R: GGACTACNNGGGTATCTAAT. All PCR reactions were carried out with Phusion High-Fidelity PCR Master Mix (New England Biolabs). PCR conditions were as follows: 98 °C for 30 s, followed by 35 cycles of 98 °C for 5 s, 56 °C for 20 s and 72 °C for 20 s and a final extension of 72 °C for 5 min. Details of PCR method were provided by the sequencing company.

Paired-end reads were assigned to samples based on their unique barcode and truncated by cutting off the barcode and primer sequence. Paired-end reads were merged using FLASH (V1.2.7, <http://ccb.jhu.edu/software/FLASH/>). Quality filtering on the raw tags were performed under specific filtering conditions to obtain the high-quality clean tags according to the Quantitative Insights Into Microbial Ecology (QIIME, V1.7.0, <http://qiime.org/index.html>) quality controlled process. The open-reference operational taxonomic unit (OTU) picking was performed following the online instruction of QIIME. OTU was defined at the 97% similarity level using Uparse software (Uparse v7.0.1001, <http://drive5.com/uparse/>). Representative sequence for each OTU was screened based on

RDP classifier (<http://sourceforge.net/projects/rdp-classifier/>) for annotate taxonomic information. The above bioinformatic analysis was performed by the sequencing company.

3.7 Conjugative gene transfer experiment

A small biofiltration system was setup at bench-scale to investigate changes in the conjugative transfer frequency during different drinking water biofiltration processes and the underlying mechanisms. *E. coli* strains were used to establish the conjugative transfer model using the RP1 plasmid. Transferability of the plasmid in agar and broth mating systems was tested prior to the set-up of biofilters.

3.7.1 Characteristics of bacterial strains and plasmid

3.7.1.1 *E. coli* strains and RP1 plasmid

The donor strain used in this study was *E. coli* J53, which harbours the conjugative RP1 plasmid that confers resistance to ampicillin, tetracycline and kanamycin. The *E. coli* HB 101 strain resistant to streptomycin was used as the recipient. The donor strain was provided by Prof. Matthew Avison and Dr Jacqueline Findlay from the University of Bristol; Recipient *E. coli* HB 101 was gifted by Prof. Laura Piddock and Dr Maria Laura Ciusa from the University of Birmingham. Table 3.13 summarises the characteristics of the *E. coli* strains and the RP1 plasmid.

Table 3.13 Bacteria strains/plasmid used.

Strain	Usage	Genotype	Resistance
<i>E. coli</i> J53 (RP1)	Donor	<i>aphA</i>	Kanamycin
		<i>tetA</i> and <i>tetR</i>	Tetracycline
		<i>bla</i> genes	Ampicillin
<i>E. coli</i> HB101	Recipient	Mutation * <i>rpsL</i> 20	Streptomycin

* *rpsL*: Ribosomal Protein Small subunit. Genotype information was provided by strains/plasmid provider.

3.7.1.2 Antibiotic susceptibility testing

The standard disk diffusion test according to EUCAST (European Committee on Antimicrobial Susceptibility Testing) [254] was performed with the *E. coli* strains J53 and HB101, for antibiotic resistance against kanamycin, tetracycline, ampicillin, and streptomycin. Freshly overnight culture was picked from LB plate to make a suspension of the strains in 0.9% saline to the density of a 0.5 McFarland turbidity standard (approximately 1.5×10^8 CFU/mL). A sterile cotton swab was used to spread the suspension evenly onto the Mueller-Hinton (MH) agar plate. Kanamycin (30 µg), tetracycline (30 µg), ampicillin (2 µg), and streptomycin (25 µg) disks purchased from Thermo Scientific OXOID, UK were applied firmly to the surface of the MH agar plate and incubated at 37 °C for 24 h.

3.7.2 RP1 plasmid transfer in pure *E. coli* cultures

3.7.2.1 Antibiotic resistance phenotypes

Kanamycin sulfate (Kan), tetracycline hydrochloride (Tc), ampicillin (Amp), streptomycin sulfate (Str) were purchased from Thermo Scientific, UK. All antibiotic stock solutions were prepared in deionised water and filtered through a 0.22 µm PTFE membrane. Once prepared, aliquots of the stocks were stored at -20 °C freezer. Recipients carrying the RP1 plasmid were recognised as transconjugants. LB medium containing different antibiotics was used to select and count donor, recipient and transconjugant colonies. Details are shown in Table 3.14. In order to confirm that the donor and recipient strains can be distinguished, they were cross cultivated on selective LB plate/broth supplemented with the appropriate antibiotics. Strains only grew in the presence of antibiotics to which they confer resistance.

Table 3.14 Selective LB plate/broth used.

Strains	Selective LB medium
Donor (RP1)	Amp (100 µg/mL), Kan (50 µg/mL), Tc (10 µg/mL)
Recipient	Str (30 µg/mL)
Transconjugant	Amp (100 µg/mL), Kan (50 µg/mL), Tc (10 µg/mL) Str (30 µg/mL)

Amp: ampicillin; Kan: kanamycin; Tc: tetracycline; Str: streptomycin.

3.7.2.2 Mating system

An overview of the establishment of agar and broth mating systems based on the RP1 plasmid conjugative transfer is shown in Figure 3.14. For each experiment, donor and recipient strains were cultured separately overnight at 37 °C in selective LB broth supplemented with corresponding antibiotics. The overnight cultures were then used for agar and broth mating experiments.

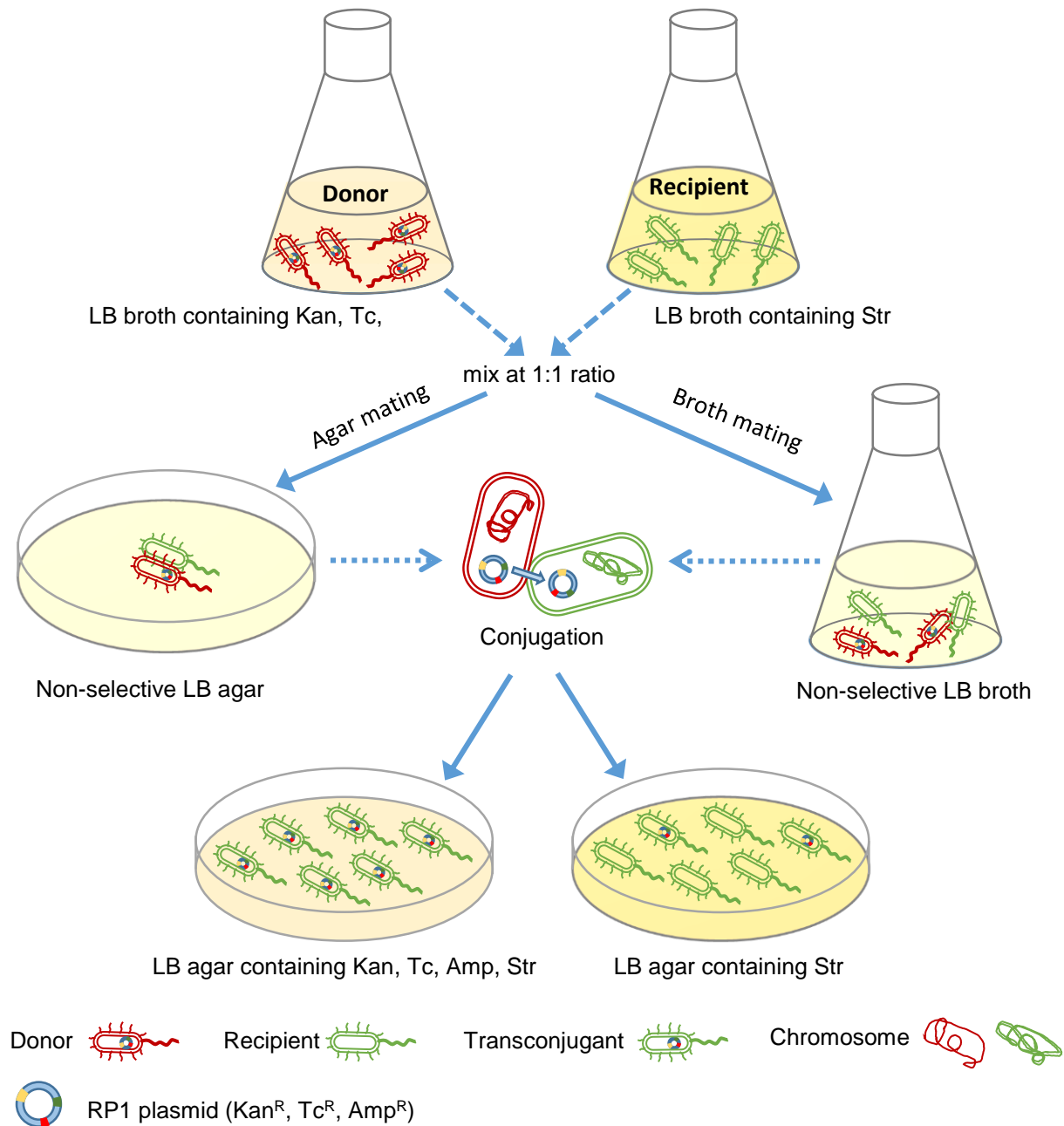


Figure 3.14 RP1 plasmid conjugative transfer.

Kan: kanamycin; Tc: tetracycline; Amp: ampicillin; Str: streptomycin.

A) Agar mating system

1) The overnight culture was centrifuged at 5000 × g at room temperature for 5 min, then washed twice with 1 mL of saline solution (NaCl, 8.5%). The resulting pellets were resuspended in 5 mL of saline and the cell density adjusted to an OD₆₀₀ (absorbance at 600 nm wavelength) value of 0.1; 2) The donor and recipient were mixed at 1:1 ratio and 20 µL of the mixture was dropped to non-selective LB agar plate. The plate was kept inside an incubator at 37 °C overnight; 3) The mixed culture was harvested from the plate and suspended in 5 mL saline. The bacterial suspension was then serially diluted and plated on selective LB plates.

B) LB broth mating system

1) The overnight culture was centrifuged at 5000 × g at room temperature for 5 min, then washed twice with 1 mL of saline. The resulting pellets were resuspended in 10 mL of non-selective LB broth and the cell density adjusted to OD₆₀₀ values of 0.1 and 0.5, respectively; 2) The donor and recipient were mixed at 1:1 ratio (10 mL each) and cultivated at 37 °C with shaking at 150 rpm overnight; 3) The overnight cultures were vigorously mixed and appropriate dilutions were plated on selective LB plates.

Plates obtained from agar and broth mating were cultivated at 37 °C for 48 h, colonies were counted and results presented as colony forming units per millilitre culture (CFU/mL). The transfer frequency was calculated by the following formula:

$$\text{Conjugative frequency} = \frac{\text{transconjugants (CFU/mL)}}{\text{recipients (CFU/mL)}}$$

3.7.2.3 Determination of RP1 plasmid genotype

Based on the antibiotic resistance phenotype of the RP1 plasmid, four pairs of ARG primers, *bla*_{CTX-M}, *bla*_{OXA-1}, *bla*_{TEM} and *tetA* were used to determine the antibiotic resistance genotype of the RP1 plasmid. Transconjugants were randomly selected from the plate and subjected to colony PCR to confirm the presence of the transferred plasmid. All the colony PCR assays were carried out using MutiGene Mini Thermal Cycler (Labnet International, UK). Details of PCR protocols are provided in appendix (Section A3.1). Plasmid DNA carrying

*bla*_{CTX-M}, *bla*_{OXA-1}, *bla*_{TEM} and *tetA* were used as positive controls and PCR grade water was used as the negative control in every run. Six μ L of the PCR products were verified by 1.5 % agarose gel electrophoresis. All PCR products were sequenced by Source Bioscience (London, UK) and the results were compared with existing sequences using BLASTn alignment tool (<https://blast.ncbi.nlm.nih.gov/Blast.cgi>).

3.7.3 RP1 plasmid transformation

To rule out the natural transformation of naked plasmid DNA to the recipient, a natural transformation experiment [255, 256] was used as the negative control for the transfer of the RP1 plasmid to the recipient *E. coli* HB101. RP1 plasmid DNA was extracted from fresh *E. coli* J53 culture using a QIAprep Spin Miniprep Kit according to the manufacturer's instructions. Freshly grown *E. coli* HB101 cultures were centrifuged and washed and adjusted to 0.5 McFarland turbidity standard (approximately 1.5×10^8 CFU/mL). the RP1 plasmid DNA was added to the recipient cells to a final concentration of 100 ng/mL in a total volume of 1.0 mL. The transformation experiment was performed under the same conditions as those used for conjugation (as described in Section 3.7.2.2). Recipient *E. coli* HB101 was plated onto selective LB agar separately as negative controls to rule out the spontaneous mutation of the recipient strains.

3.7.4 Conjugation experiment based on biofiltration

3.7.4.1 System set-up

A small-scale biofiltration system was established to explore its impact on the plasmid conjugative transfer using *E. coli* strains J53 and HB101 as donor and recipient, respectively. A modified 50 mL centrifuge tube was used as a filter column for easy operation and maintenance. An overview of the system setup is shown in Figure 3.15. Two sets of biofiltration systems (set A and set B), each consisting of three columns loaded with sand, GAC and anthracite up to 7 cm were installed in parallel. All the materials, including filter media, feedwater reservoir, tubing and columns were autoclaved prior to system set-up. The

feedwater reservoirs (2 L Duran glass bottle) and columns were covered to avoid contamination throughout the study. All the columns were fed with sterile water using a peristaltic pump for 48 h to check the stability of the system prior to inoculation with donor and recipient strains.

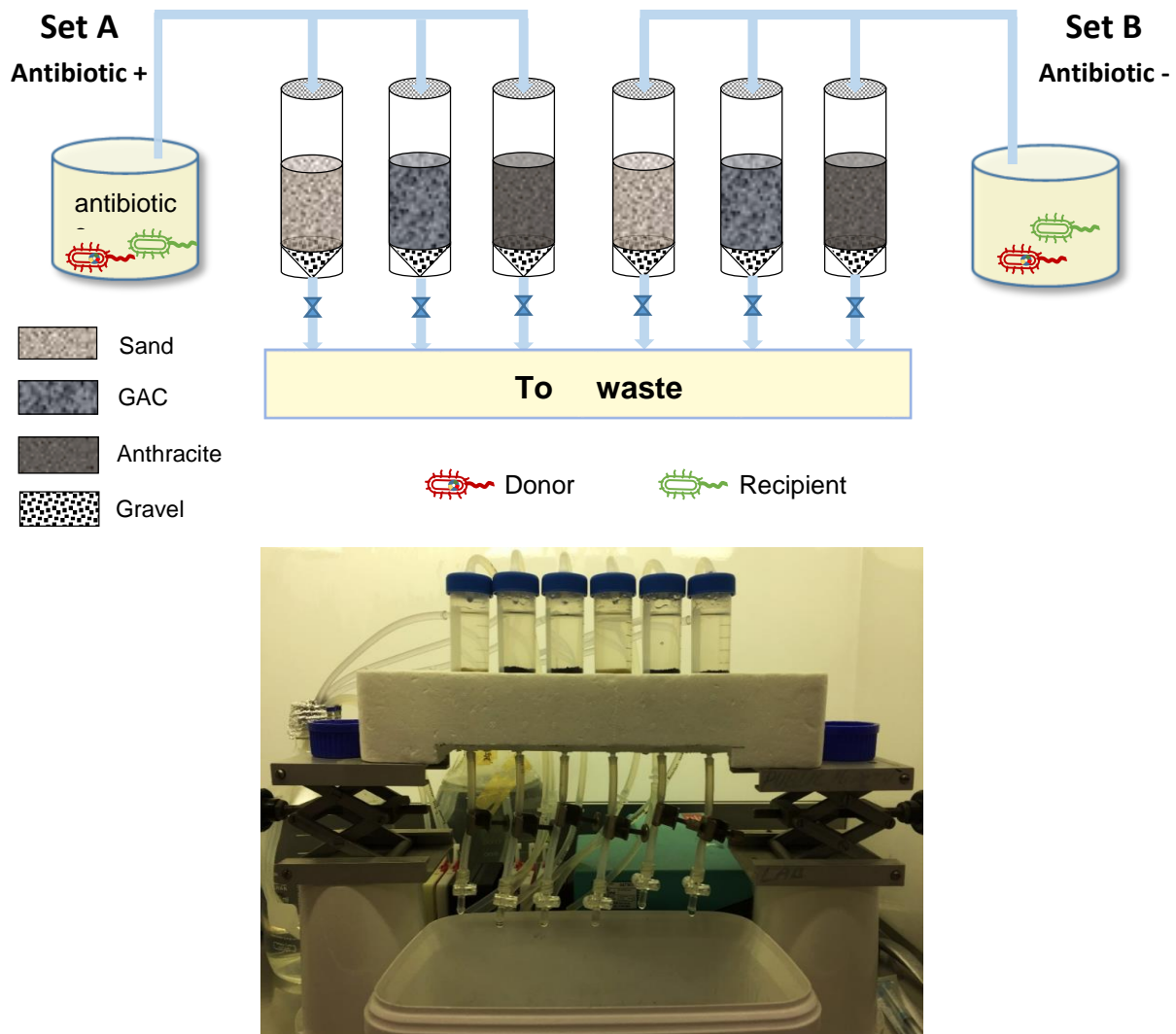


Figure 3.15 Bench-scale biofilters schematic.

Set A: biofilters exposed to antibiotics; Set B: biofilters without antibiotics addition.

3.7.4.2 System operation

The system was run at room temperature and continued for two weeks including a backwash step at the end of the study. The six biofilters were operated in parallel under identical conditions at a HLR of 0.06 m/h. The flow rate was controlled by valves installed at the water outlet. Freshly prepared LB broth (1:1000 diluted, DOC = 6 mg/L) was refilled to the

feedwater reservoirs every day. Set A was fed with diluted LB broth spiked with the target antibiotics at 2 µg/L, while Set B was only fed with diluted LB broth. Both Set A and B were inoculated with the equal amount of fresh culture of *E. coli* J53 and HB101 at approximately 1.0×10^7 CFU/mL every day. The flow rate was checked and re-adjusted when necessary. The whole system was operated inside a biosafety cabinet. After two weeks' operation, the system was backwashed once by pumping sterile water in counter current through the columns at 30% fluidisation for 5 min.

3.7.4.3 Sampling strategy

Prior to inoculation with the *E. coli* strains, biofilter media and effluents were collected to ensure that the system was free of contamination. Influent, effluent and surface media samples (sand, GAC and anthracite) were collected 24 h after first inoculation and then every two days afterwards. Once collected, media samples were suspended in sterile saline and then ultrasonicated at 80 kHz for 20 min to wash off the bacteria attached to the media surface. Influent, effluent and media bacteria suspension samples were serially diluted using saline and plated on selective LB agar to count the numbers of donors, transconjugants and recipients. Recipient *E. coli* HB101 was plated onto selective LB agar separately as negative controls to rule out the spontaneous mutation of the recipient strain. One to three transconjugant colonies obtained from each batch sample were randomly picked up from LB agar plates and subjected to colony PCR to confirm the transfer of RP1 plasmid.

3.8 Statistics

Removal/reduction of DOC, turbidity, UV₂₅₄, total coliforms, *E. coli* and antibiotics were calculated based on influent and effluent concentrations. The qPCR results were analysed using 7500 software v2.3 (Applied Biosystems, UK). OriginPro 2018 was used to draw histogram and line graphs.

The absolute abundance of ARGs was defined as the ARG copies per litre in aqueous samples (copies/L) or per gram in medium samples (copies/g). The relative abundance of

ARG was defined as the normalised ARG copies to the *16S rRNA* gene copies. The richness of ARGs is defined as the number of the detected ARGs in different samples. Mean and standard deviation calculations were performed with Microsoft Excel 2016. One-way analysis of variance (ANOVA), Pearson correlation analysis and ARGs' profile heatmap were performed using OriginPro 2018.

Principal coordinate analysis (PCoA) based on Bray-Curtis dissimilarity matrix was used to evaluate both the ARGs and bacterial community profiles between different biofilm samples. Redundancy analysis (RDA) was performed to analyse the correlation between the abundance of detected ARGs and bacterial communities/environmental factors. Variation partitioning analysis (VPA) was performed for the determination of the contributions of environmental factors, bacterial communities and integrons to the variations of persistent ARGs. PCoA, RDA and VPA were performed using Canoco 5.0 software (USA). Venn diagram analysis was conducted to assess the numbers of shared and unique ARGs in biofilm samples using OriginPro 2018. Network analysis of the co-occurrence patterns (similarity of location) among ARGs and bacterial taxa was performed using an online analysis pipeline at <http://ieg4.rccc.ou.edu/mena/main.cgi> and Cytoscape 3.7.1 was used to visualise the network graphs [208, 221, 224].

Chapter 4

BIOFILTER PERFORMANCE

4 BIOFILTER PERFORMANCE

Biofilter influent and effluent were collected and analysed weekly for general water quality parameters, including pH, conductivity, turbidity, dissolved organic carbon (DOC), chemical oxygen demand (COD), specific ultraviolet absorbency (UV_{254}), dissolved oxygen (DO), phosphate (PO_4^{3-}), nitrite (NO_2^-), nitrate (NO_3^-), total coliforms and *E. coli*. In this chapter, biofilter performances regarding general water quality parameters in the two biofiltration experiments are summarised and discussed.

4.1 Biofiltration experiment 1 - different types of filter media

The biofiltration system was operated continuously for 12 weeks, including 4 weeks of biofilter maturation and 8 weeks' exposure to antibiotics followed by a backwash/cleaning process at the end, which generated a total of 12 batch samples. Accordingly, the biofiltration process was divided into three phases, phase I (maturation), phase II (antibiotics spike) and phase III (backwash/cleaning) for the following data analysis and discussion. The effect of the sand biofilter (SB1 and SB2), GAC biofilter (GB1 and GB2), GAC sandwich biofilter (GSB1 and GSB2) and anthracite-sand biofilter (ASB1 and ASB2) on water quality parameters is discussed in this section. The main physico-chemical characteristics of the raw waters are summarised in Table A4.1. Raw data of each parameter in different batch samples are provided in Table A4.2 – A4.10. The characteristic difference of feedwater between two reservoirs was negligible ($p > 0.05$).

4.1.1 pH, conductivity and dissolved oxygen

4.1.1.1 pH

The raw water samples were slightly alkaline, with a pH ranging from 7.85 – 8.35. In general, pH in the effluents showed little variation compared to the influent ($p > 0.05$), with pH variations from -0.15 ± 0.02 to 0.09 ± 0.01 (Figure 4.1). When the biofilm gradually built up, the respiration of microorganisms consumed oxygen and produced carbon dioxide continuously. During phase I, the pH of the effluents decreased after filtration, among which

the GAC filters had the lowest pH values (7.94 on average). A slight increase of pH in the effluent was observed in phase II, suggesting reduced respiration or carbon dioxide production compared to phase I. After backwashing/cleaning (phase III), the change of pH across the columns was significantly different ($p < 0.01$) compared to phase II, indicating the removal of surface biofilms affected the microorganism respiration.

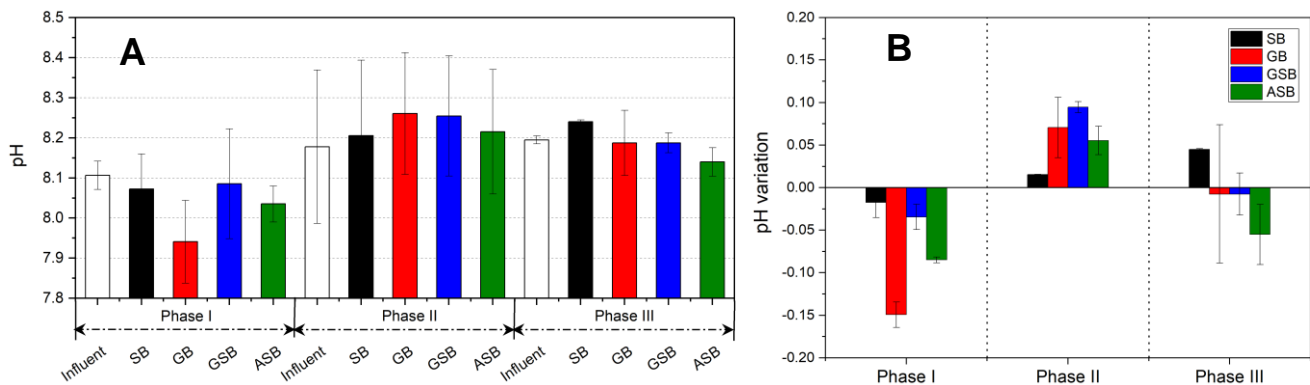


Figure 4.1 A: pH and B: the variations of pH during Phase I, II and III of biofilter run. The error bars represent STD from the mean value of duplicate biofilters in different Phase samples ($n = 8, 14$ and 2 for Phase I, II and III, respectively). SB: sand biofilter; GB: GAC biofilter; GSB: GAC sandwich biofilter; ASB: anthracite-sand dual biofilter.

4.1.1.2 Conductivity

Mean conductivity values were between 1035 to 1060 $\mu\text{S}/\text{cm}$ in raw water. The variation of conductivity in the effluent compared to influent is shown in Figure 4.2. No statistically significant differences ($p > 0.05$) were found between the effluent samples during phase I and II. After filtration, the effluent conductivity decreased from 1061 $\mu\text{S}/\text{cm}$ to 1050 $\mu\text{S}/\text{cm}$ in the sand filter and 1045 $\mu\text{S}/\text{cm}$ in the GAC filter during phase I, indicating a reduced concentration of ions in the filtered water. The trend for the variation of conductivity is consistent with previous slow sand filtration study using the same source water [257]. Similar as with pH variation, during phase III, a significant difference ($p < 0.01$) of effluent conductivity was observed before and after backwashing/cleaning was conducted.

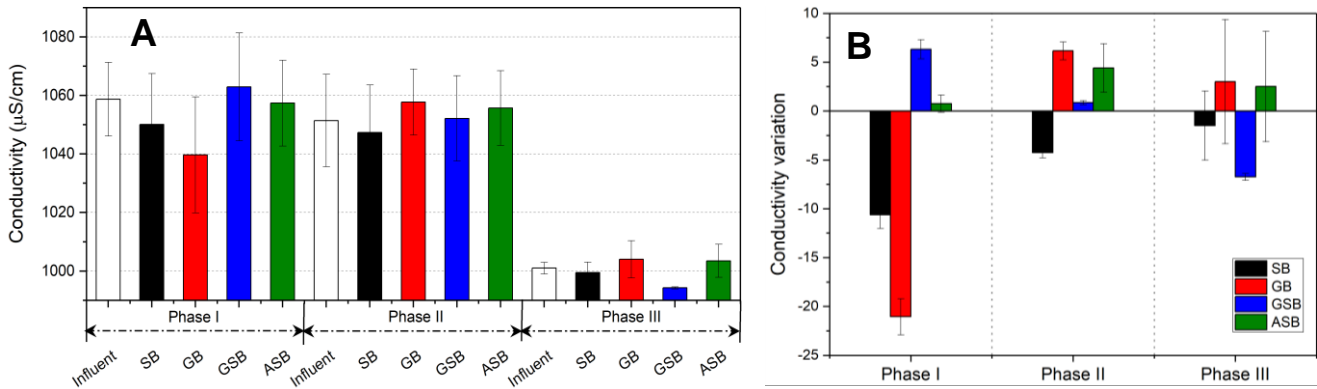


Figure 4.2 A: Conductivity and B: the variations of conductivity during Phase I, II, and III of biofilter run. The error bars represent STD from the mean value of duplicate biofilters in different Phase samples ($n = 8, 14$ and 2 for Phase I, II and III, respectively). SB: sand biofilter; GB: GAC biofilter; GSB: GAC sandwich biofilter; ASB: anthracite-sand dual biofilter.

4.1.1.3 Dissolved oxygen

Influent DO concentrations varied as a function of the season with approximately 5.15 mg/L in October to 7.88 mg/L in January. The levels of DO present in the effluent are above the recommend value of 3 mg/L for slow sand filtration, suggesting an aerobic environment in the aqueous phase throughout the biofilter columns [157]. The variations of DO across the columns were consistent in phase I and phase II (Figure 4.3). The aerobic respiration of the microorganisms in the biofilters caused the reduction in DO concentration. The reduction of DO during phase I was 0.41 mg/L (on average), and then dropped to 0.29 mg/L during phase II, suggesting a higher extent of microbial respiration in the earlier stages of the system run. SB revealed the greatest oxygen consumption, while ASB showed the least oxygen consumption. No difference of oxygen reduction was found between the two GAC-associated biofilters. Zhang *et al.* reported a 0.84 mg/L oxygen consumption by GAC biofilters and 0.43 mg/L by anthracite-sand media with a similar influent DO concentration [182], which were within the range of oxygen consumption in this study. Much higher oxygen consumptions were observed in a different study by Zhang *et al.*, though the trend was similar, where 2.5 mg/L, 2.3 mg/L, and 2.1 mg/L DO consumption were found in quartz sand, activated carbon, and anthracite, respectively [258]. An increased DO level was observed after

backwashing/cleaning was conducted for all biofilters. The biofilm became thinner after backwashing/cleaning, which favoured the diffusion of oxygen [226]. The time needed for the re-establishment of a new biofilm was not investigated in the present study. Therefore, the mechanism underlying the increased DO levels in the effluent after backwashing/cleaning process is unclear.

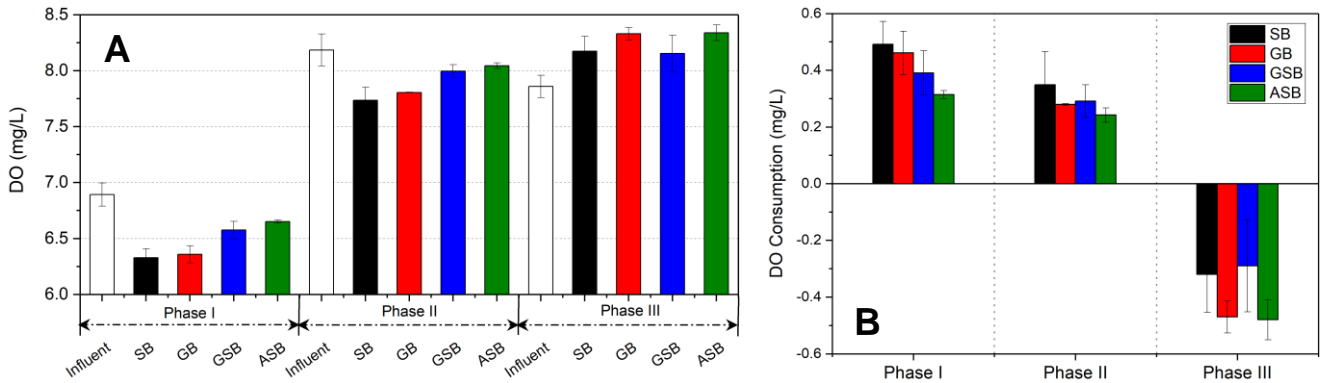


Figure 4.3 A: DO and B: the consumption of DO during Phase I, II, and III of biofilter run. The error bars represent STD from the mean value of duplicate biofilters in different Phase samples ($n = 8, 14$ and 2 for Phase I, II and III, respectively). SB: sand biofilter; GB: GAC biofilter; GSB: GAC sandwich biofilter; ASB: anthracite-sand dual biofilter.

4.1.2 Turbidity

The turbidity levels of biofilter influent varied between 0.56 ± 0.23 NTU during the study period. Mean turbidity of the effluent ranged from 0.18 to 0.42 NTU during phase I and from 0.14 to 0.22 during phase II. The reduction in turbidity (in percentage) for biofilters during phase I and phase II is shown in Figure 4.4A. The GSB was found to be the most effective in removing turbidity-causing particles. Although the ASB had a better removal at the later stage of the filter run, it generally exhibited the worst performance in terms of turbidity reduction compared to other biofilter types. The principal mechanisms responsible for turbidity removal from the feedwater are direct sieving or straining; and sedimentation [259]. As anthracite media had the biggest particle size, it was expected that both sand and GAC would perform better than anthracite in reducing turbidity. High variability in turbidity was observed in this study, presumably due to detachment of precipitates or the inherent variations in turbidity in

the source water [166, 260]. As biofilms accumulating on the medium surface, when they reached a certain size, non-biological particles may have shed from the media surface from time to time and been transported by the water, resulting in increased turbidity in the effluent. No statistical difference in turbidity reduction was observed between the four types of biofilters ($p > 0.05$). This may likely be a function of the inherent low turbidity in the source water (< 1 NTU) [166]. When the biofilm layer was removed by backwashing/cleaning, a significant increase in effluent turbidity ($p < 0.01$) was observed for all biofilters (Figure 4.4B).

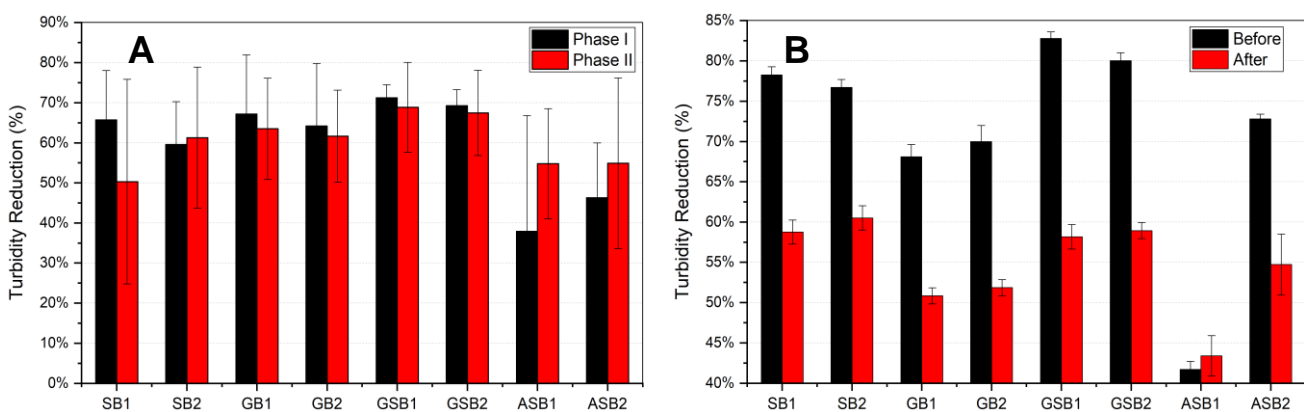


Figure 4.4 The reduction of turbidity (A) during phase I and II; (B) before and after backwashing/cleaning (B). The error bars in A represent STD from the mean value in Phase I ($n = 4$) and Phase II ($n = 7$); and the error bars in B represent STD from the mean value of triplicate samples ($n = 3$). SB: sand biofilter; GB: GAC biofilter; GSB: GAC sandwich biofilter; ASB: anthracite-sand dual biofilter.

4.1.3 Absorbance and dissolved organic carbon

In this study, raw water DOC ranged between 3.51 mg/L to 4.24 mg/L and the difference between the two feedwater reservoirs was consistently below 0.6 mg/L ($p > 0.05$). DOC concentrations in the influent and effluent of the biofilters are shown in Figure 4.5. The GAC-associated biofilters showed much lower DOC levels in the filtered water compared to sand and anthracite. Similar trends were found for the removal of DOC and UV_{254} across all biofilters but to slightly different extents (Figure 4.6). Phase I showed a better removal of organic compounds compared to phase II, however no statistical difference ($p > 0.05$) was found between them.

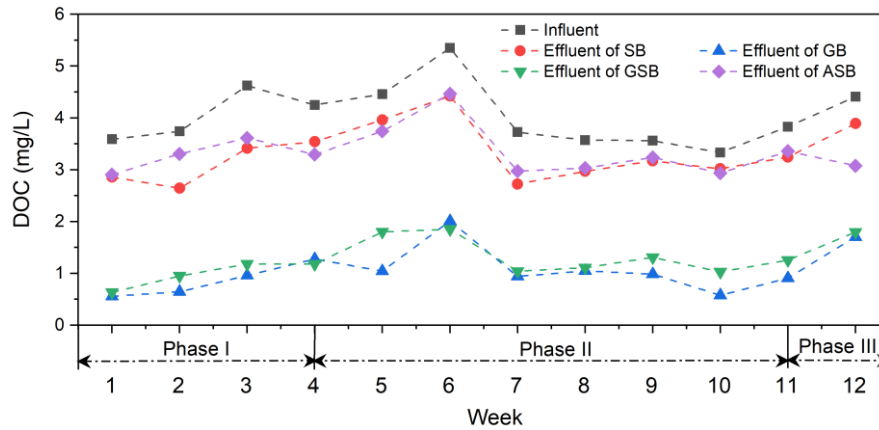


Figure 4.5 DOC concentrations in the influent and effluent samples. SB: sand biofilter; GB: GAC biofilter; GSB: GAC sandwich biofilter; ASB: anthracite-sand dual biofilter.

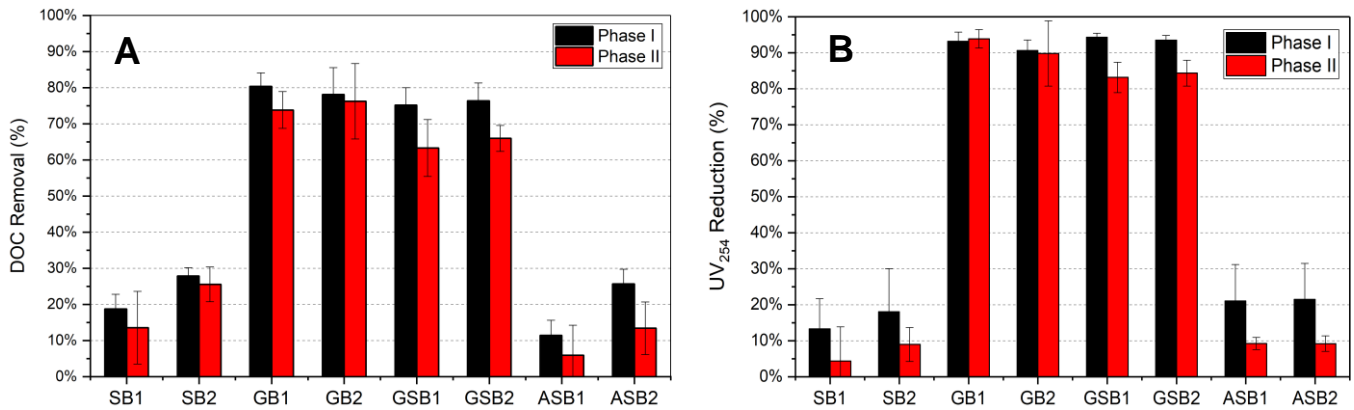


Figure 4.6 DOC removal (A) and UV₂₅₄ reduction (B) in biofilters. The error bars represent STD from the mean value ($n = 4$ and 7 for Phase I and II, respectively). SB: sand biofilter; GB: GAC biofilter; GSB: GAC sandwich biofilter; ASB: anthracite-sand dual biofilter.

From phase I to II, the DOC removal (on average) dropped from 23% to 20% by SB; 79% to 75% by GB; 76% to 65% by GSB; and 19% to 10% by ASB (Figure 4.6A). These findings are in agreement with Gibert's research, where the DOC removal progressively declined over time [160]. GAC-associated filters revealed significantly greater DOC removal efficiencies ($p < 0.001$) than SB and ASB during the operational period of 3 months, attributed to the adsorption of organic matter by the porous GAC structure. This process was more important on DOC removal than biodegradation. Nevertheless, it is usually difficult to identify the relative importance of the adsorption and biodegradation mechanisms at different operational stages of GAC filters, especially when an active biofilm is present. In general, it is

presumed that once the adsorption mode of GAC has been exhausted, biodegradation would act as the predominant mechanism for organics removal [178]. The GAC media used in this study did not reach its service life end, as it typically requires years of operation until GAC sorption capacity becomes exhausted. The sandwich biofilter showed a similar initial DOC removal compared to the whole GAC-bed filter, although a reduced removal rate (by 11%) was observed at the later stage of the system run. This was somewhat expected, because of the sorption capacity of GAC gradually declines over time [160]. Sand media performed slightly better than anthracite, with removals ranging between 14% - 28% and 6% - 26% by sand and anthracite, respectively. Previous research has also reported that by using anthracite-sand dual media (similar grain size with this study), partial DOC removal (< 27%) was observed and after 6 months of operation, the removal plateaued at 7.6% [182]. Campos *et al.* have found an average of 23% DOC removal by full-scale drinking water slow sand filters [155]. However, much higher removal (50% - 80%) of biodegradable compounds can be found by conventional sand or anthracite-sand biofilters [156], this may potentially be attributed to differences in the attached microbial community and the upstream treatment process (e.g. ozonation, flocculation/coagulation). It is worth mentioning that higher DOC levels were observed occasionally in the effluent than the influent in this study. As the biofilm may form along the walls of the biofilters, it may have been shedding over time, which would explain the increased DOC after filtration.

Reduction in UV_{254} absorbance is consistent with DOC removal (Figure 4.6B). A specific UV_{254} absorbance ($SUVA_{254}$) parameter is used here to discuss the preferable removal of organic components by the biofilters. $SUVA_{254}$ is defined as the UV_{254} absorbance divided by the DOC concentration and often related to the dissolved aromatic carbon content in a water sample [261]. A higher value of $SUVA_{254}$ generally indicates greater molecular complexity, for example increased aromaticity, that may result in reduced biodegradability [262]. The $SUVA_{254}$ values of influent and effluent (on average) are provided in Table 4.1. The aromatic compounds were adsorbed favourably by GAC media, evidenced by the influent $SUVA_{254}$ being reduced from 2.16 ± 0.31 to 0.73 ± 0.28 $L\ mg^{-1}\ m^{-1}$ and 0.94 ± 0.39 $L\ mg^{-1}\ m^{-1}$

by the GB and GSB, respectively. On the contrary, elevation in $SUVA_{254}$ values by SB and ASB suggests that the aliphatic dissolved organic matters can be removed more efficiently than the aromatic substances by those filters. Previous study has also demonstrated similar trend, where the $SUVA$ values increased from 0.8 ± 0.3 to 1.5 ± 0.4 $L\ mg^{-1}\ m^{-1}$ after slow sand filtration as a result of biodegradation of aliphatic organic matter [263].

Table 4.1 $SUVA_{254}$ values of biofilter influent and effluent samples.

Samples	$SUVA_{254}$ ($L\ mg^{-1}\ m^{-1}$) Mean value \pm STD (n = 11)
Influent	2.16 ± 0.31
Sand biofilter	2.38 ± 0.32
GAC biofilter	0.73 ± 0.28
GAC sandwich biofilter	0.94 ± 0.39
Anthracite-sand dual biofilter	2.28 ± 0.49

$SUVA_{254}$: specific UV_{254} absorbance. STD is calculated based on all 11 batch samples.

In real practice, biofilters are backwashed periodically to restore the hydraulic capacity as the filters are usually used to remove both DOC and particles. In this study, the overall DOC removal and UV_{254} reduction were not affected significantly ($p > 0.05$) by backwashing/cleaning. Figure 4.7 shows the variation of DOC removal and UV_{254} reduction before and after backwashing/cleaning was conducted. Backwashing can significantly reduce the biomass concentration in filters, which may lower the rate of biodegradation and the extent of organic carbon removal [262]. Surprisingly, the performance of ASB was partially restored as shown by the increased DOC removal (16% on average) and UV_{254} reduction (8% on average) after backwashing. The above findings indicated that the DOC removal was insensitive to backwash/cleaning, whereas other conventional performance parameters (e.g. pH, conductivity, and turbidity) were significantly affected by this process. These variations are similar to those reported by Emelko *et al.*, in full-scale biofilters, allowing conventional performance parameters to be optimised without compromising DOC removal [264].

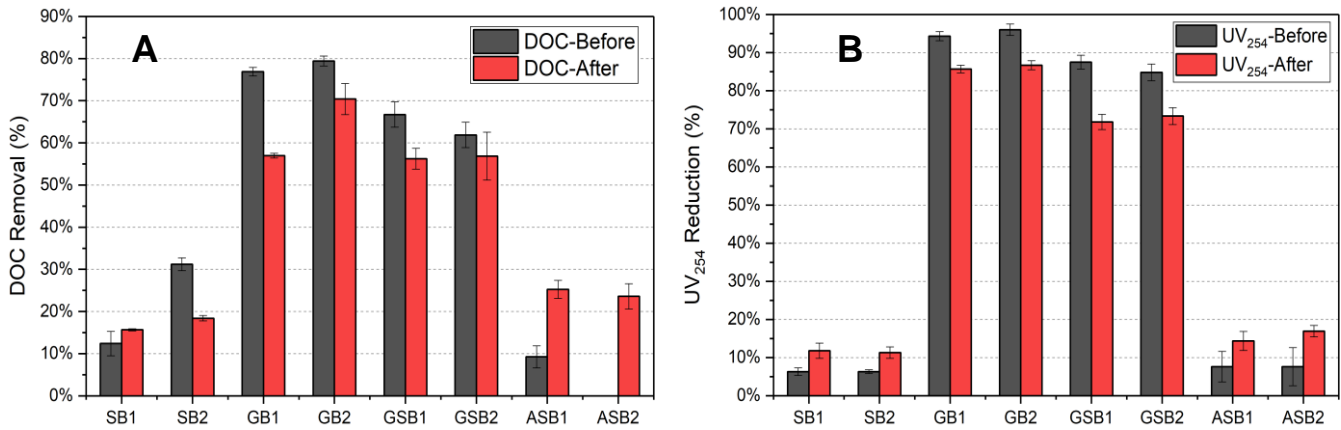


Figure 4.7 DOC removal (A) and UV₂₅₄ reduction (B) across all biofilters before and after backwashing/cleaning process. The error bars represent STD from the mean value of triplicate samples (n = 3). SB: sand biofilter; GB: GAC biofilter; GSB: GAC sandwich biofilter; ASB: anthracite-sand dual biofilter.

4.1.4 Nitrate, nitrite and phosphate

Biofiltration is the most popular approach to treat $\text{NH}_4^+\text{-N}$ in source water, through nitrification in most cases [265]. In this pathway, ammonia is oxidised to nitrite ($\text{NO}_2^-\text{-N}$) by ammonia oxidising bacteria (AOB) and further oxidised to nitrate ($\text{NO}_3^-\text{-N}$) by nitrite oxidising bacteria (NOB). Variations of nitrate concentrations in the influent and effluent of the biofilters are shown in Figure 4.8. Nitrate concentration increased after sand and dual media biofiltration during phase I and II, which means the extent of nitrification in the two biofilters was greater than that in GAC-associated biofilters. No nitrite was found except on only a few days in the effluent, indicating a relatively complete nitrification. After biofiltration, Phosphate-P (PO_4^{3-}) remained stable (ranged between 0.31 mg/L and 0.35 mg/L) in phase I and increased moderately from 0.32 mg/L to 0.41 mg/L (on average) in phase II (Figure 4.9), with no statistical difference ($p > 0.05$). The increase in nitrate and phosphate may be due to algal respiration which converts algal nitrogen to inorganic nitrogen and algal phosphorus to inorganic phosphorus [266].

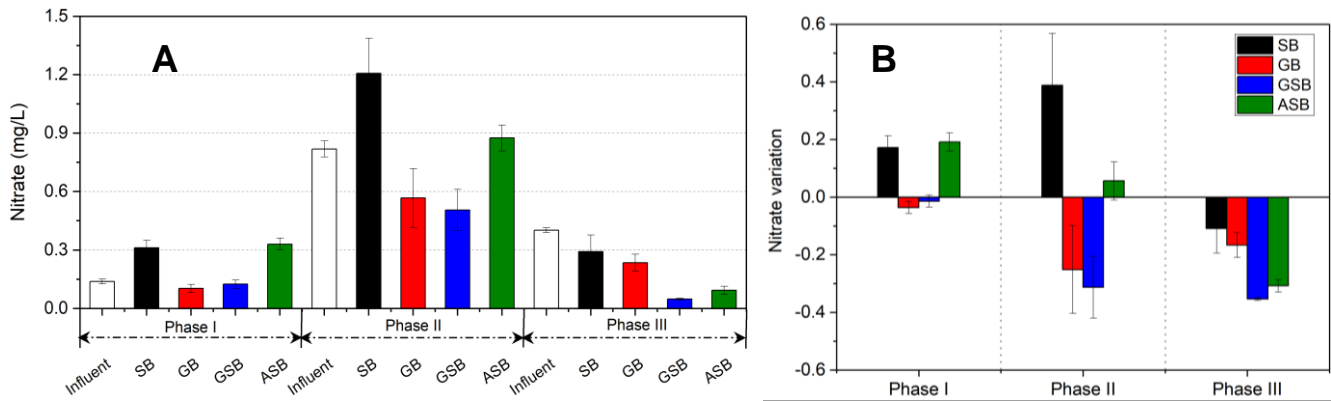


Figure 4.8 A: Nitrate and B: the variation of nitrate in the influent and effluent. The error bars represent STD from the mean value of duplicate biofilters in different Phase samples ($n = 8, 14$ and 2 for Phase I, II and III, respectively). SB: sand biofilter; GB: GAC biofilter; GSB: GAC sandwich biofilter; ASB: anthracite-sand dual biofilter.

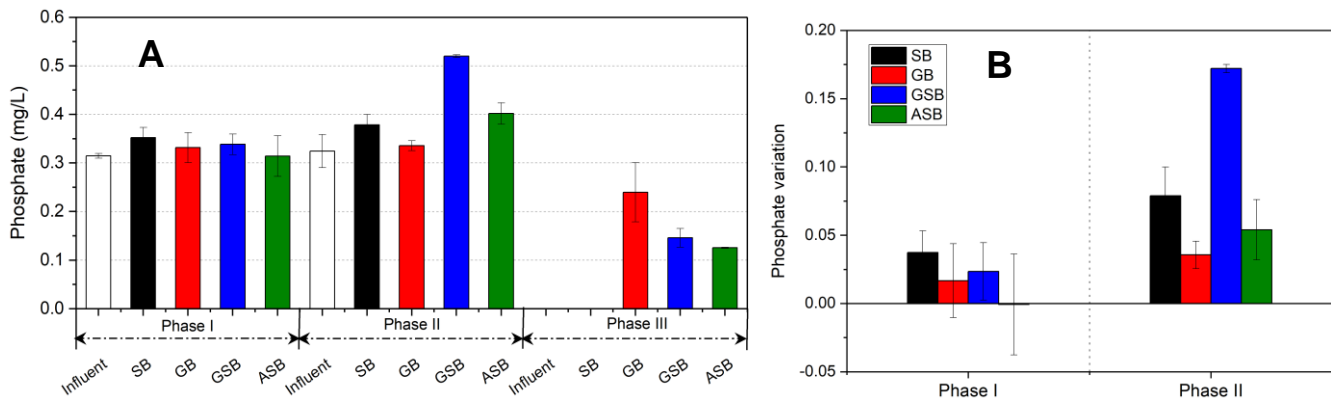


Figure 4.9 A: Phosphate and B: the variation of phosphate in the influent and effluent. The error bars represent STD from the mean value of duplicate biofilters in different Phase samples ($n = 8, 14$ and 2 for Phase I, II and III, respectively). SB: sand biofilter; GB: GAC biofilter; GSB: GAC sandwich biofilter; ASB: anthracite-sand dual biofilter.

4.1.5 Total coliforms and *E. coli*

Mean removals of total coliforms and *E. coli* are presented in Figure 4.10. After four weeks' operation, both total coliforms and *E. coli* achieved 99% removal by all of the biofilters, indicating that a matured biofilm has been established. The removal slightly fluctuated between week 5 to 11, probably due to the detachment of biofilm either from the media surface or from the water outlet tubing. The removals of total coliforms and *E. coli* were consistently above 90% (Table A4.9 and A4.10), which was within the typical removal range of between 90% and 99.9% required by conventional slow sand filters [267].

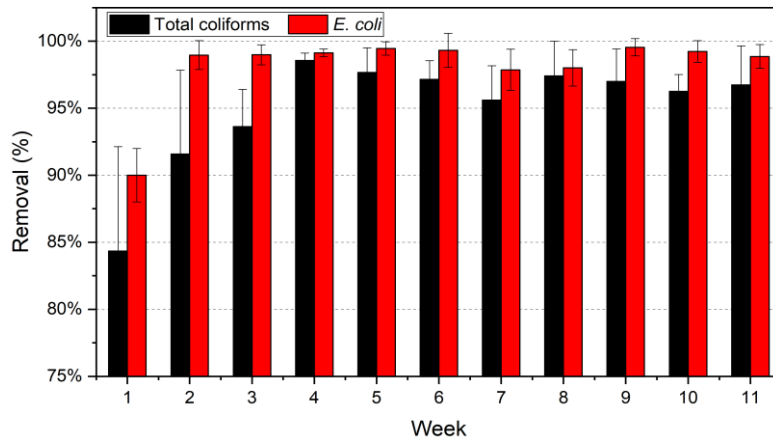


Figure 4.10 Mean removal of total coliforms and *E. coli*. The error bars represent STD from the mean value of all biofilter effluents ($n = 8$).

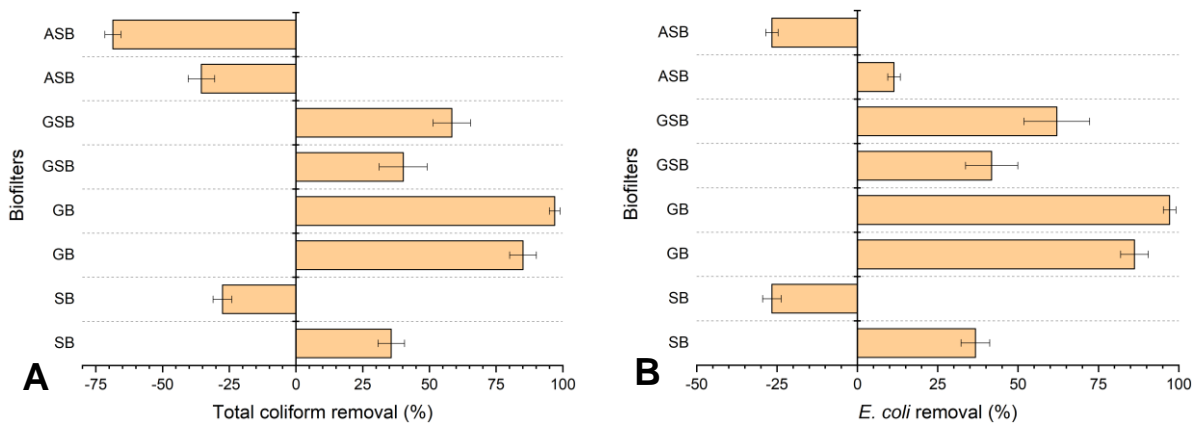


Figure 4.11 Removal of A: total coliforms and B: *E. coli* after backwashing/cleaning. The error bars represent STD from the mean value of triplicate samples ($n = 3$). SB: sand biofilter; GB: GAC biofilter; GSB: GAC sandwich biofilter; ASB: anthracite-sand dual biofilter.

Figure 4.11 shows the removal of total coliforms and *E. coli* after backwashing/cleaning of the biofilters. Except for GB, significantly reduced removals ($p < 0.01$) were observed for the other three types of biofilters. GSB showed higher removals of total coliforms and *E. coli* (ranging from 35% to 60%) than SB after the top layer of sand was removed along with the biofilm. This could be attributed to the introduction of the GAC layer within the GSB column, evidenced by 80% - 99% removal achieved in the pure GAC column after filter backwashing. Another possible reason is that the biofilm was removed to a lesser extent by stirring compared to backwashing. The tightly attached biofilm remained on the surface of top layer sand and it was the basis for the fast-regrowth of the new biofilm after the

backwashing/cleaning [226]. The results suggested that a certain degree of restoration time is needed to allow the re-growth of the new biofilm to the previous thickness.

4.2 Biofiltration experiment 2 – difference types of GAC sandwich biofilters

All GAC sandwich biofilters were run continuously for 11 weeks. After maturation, which took approximately 3 weeks, biofilters in Set A were exposed of antibiotics for 8 weeks, while Set B was run as a control. Biofilters were labelled as GSB-1 to GSB-4 in Set A and as GSB-5 to GSB-8 in Set B for the following data analysis. The performance of all biofilters in the maturation stage is summarised and presented together. For the experimental period, when antibiotics were added to Set A, performance of biofilters in Set A and B is discussed separately. The general water quality parameters of raw water collected from June to September 2018 are listed in Table A4.11. Raw water showed variations in all parameters, however no statistical differences ($p > 0.70$) were found across the sampling period. The turbidity of the raw water varied from a low of 5.72 NTU to a high of 26.7 NTU, therefore, big particles in raw water were separated by gravity sedimentation and only the supernatant was used as the feedwater source and diluted with dechlorinated tap water to reduce filter clogging caused by flocs and particles. This was also in order to comply with the recommendations of turbidity in the influent for sand filtration (< 10 NTU) [154].

4.2.1 Maturation stage

Average removals of 99.1% of total coliforms and 99.6% of *E. coli* by all biofilters were observed after 3-weeks' operation, indicating the biofilms had reached maturity in the filter columns. During the maturation stage, the effluents of all biofilters showed similar values for conventional chemical parameters (Table A4.12) such as pH, conductivity, DO and phosphate but differed slightly with respect to turbidity, nitrate, nitrite and organics-related parameters (i.e. DOC, UV_{254} and COD). Biofilters with 9 cm GAC layer revealed the greatest oxygen

consumption, turbidity reduction, and removal of organic matters during the first 3 weeks (Figure 4.12).

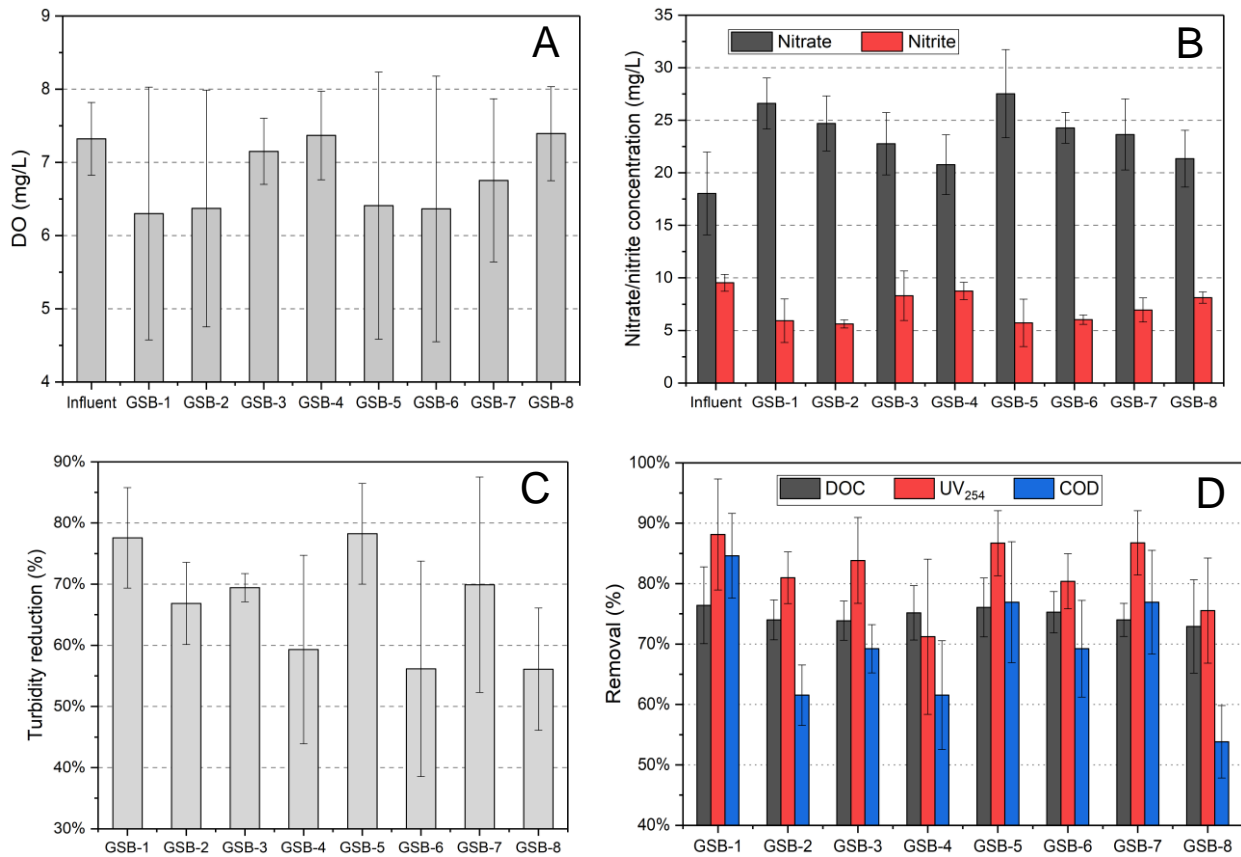


Figure 4.12 The concentration of (A): dissolved oxygen (DO); and (B): nitrate and nitrite in the influent and effluent samples; The reduction of (C): turbidity; and (D): dissolved organic carbon (DOC), UV₂₅₄ absorbance, and chemical oxygen demand (COD) during maturation stage (3 weeks). The error bars represent STD from the mean value of all batch samples (n = 3).

It is interesting to note that the biofilters with 4 cm GAC in the middle of the column showed better removal of organics, albeit not significant, than in the upper or lower position (Figure 4.12 D). Assuming that the biodegradation rate within the *schmutzdecke* layer was the same for all biofilters, the differences in organic removals can only be attributed to the position of GAC in the column. SUVA₂₅₄ was calculated here to discuss the preferable removal of organic components by the GAC adsorption. The comparison of SUVA₂₅₄ among GSBs with 4 cm GAC layers (Table 4.2) indicated that aromatic compounds were adsorbed favourably by GAC media loaded in the middle of filter bed. Water samples were not collected at the specific positions of GAC layers in this study, therefore, the reason behind this observation is

unclear. A possible explanation is that the biofilm within middle-layer GAC was likely to be moderately competitive compared to the upper or lower layer GAC. Wan *et al.* found that the upper layer of sand bed (1-10 cm) provided the maximum DOC removal and consumed the most of oxygen from the influent, while the deeper layer of sand (10-50 cm) had limited effect on DOC removal [193]. When reaching the middle layer GAC, the levels of oxygen and nutrients in the planktonic phase may be more favourable for the growth of aromatic organics-degrading bacterial communities within the biofilm, contributing to the additional removal of organics when the water flowed. The nitrate concentration increased in all filter columns, among which filters with 9 cm GAC increased the most (Figure 4.12 B). The indigenous nitrifying bacterial community in raw water may contribute to the increased nitrate level owing to nitrification process. This process occurred not only during biofiltration, but also in the feedwater bottles, evidenced by the absence of nitrite in the raw water and the presence in the influent.

Table 4.2 SUVA₂₅₄ values of biofilter influent and effluent samples.

Samples	SUVA ₂₅₄ (L mg ⁻¹ m ⁻¹) Mean value ± STD (n = 3)
Influent	2.25 ± 0.11
GSB (9-cm upper GAC layer)	1.26 ± 0.01
GSB (4-cm upper GAC layer)	1.73 ± 0.11
GSB (4-cm middle GAC layer)	1.36 ± 0.08
GSB (4-cm lower GAC layer)	2.10 ± 0.25

SUVA₂₅₄: specific UV₂₅₄ absorbance. GSB: GAC sandwich biofilter. STD is calculated based on all 3 batch samples.

4.2.2 Experimental stage

4.2.2.1 Differences in feedwater

Influent for Set A and B showed variations in the general parameters over time, despite the fact that all biofilters received the same source water, possibly the antibiotics added to Set A could influence the biological activity in the feedwater bottle. The slightly lower pH value and dissolved oxygen observed in the influents of Set A indicated a greater extent of bacterial respiration (Table 4.3).

Table 4.3 Mean values \pm STD (n = 8) of water quality parameters during the experimental stage (8 weeks).

Parameters	Set-A					Set-B				
	Influent	GSB-1	GSB-2	GSB-3	GSB-4	Influent	GSB-5	GSB-6	GSB-7	GSB-8
pH	7.98 \pm 0.17	7.95 \pm 0.17	7.94 \pm 0.19	7.92 \pm 0.20	7.99 \pm 0.18	8.08 \pm 0.16	8.05 \pm 0.15	8.01 \pm 0.17	7.99 \pm 0.18	8.01 \pm 0.15
Conductivity (mS/cm)	1.50 \pm 0.42	1.52 \pm 0.42	1.51 \pm 0.42	1.52 \pm 0.42	1.52 \pm 0.42	1.51 \pm 0.41	1.52 \pm 0.41	1.52 \pm 0.41	1.52 \pm 0.41	1.52 \pm 0.41
Turbidity (NTU)	0.88 \pm 0.53	0.24 \pm 0.08	0.26 \pm 0.12	0.25 \pm 0.11	0.21 \pm 0.11	0.64 \pm 0.28	0.15 \pm 0.08	0.16 \pm 0.07	0.19 \pm 0.07	0.19 \pm 0.07
Absorbance (254 nm)	0.089 \pm 0.011	0.020 \pm 0.004	0.029 \pm 0.007	0.028 \pm 0.008	0.031 \pm 0.010	0.082 \pm 0.005	0.014 \pm 0.003	0.022 \pm 0.008	0.022 \pm 0.006	0.022 \pm 0.009
COD (mg/L)	18 \pm 4	8 \pm 2	8 \pm 2	9 \pm 2	9 \pm 2	17 \pm 4	6 \pm 2	7 \pm 1	8 \pm 2	7 \pm 3
DO (mg/L)	5.51 \pm 0.59	5.48 \pm 0.41	5.45 \pm 0.45	5.30 \pm 0.50	5.40 \pm 0.49	5.56 \pm 0.54	5.55 \pm 0.32	5.51 \pm 0.36	5.38 \pm 0.38	5.50 \pm 0.42
Nitrate (mg/L)	7.84 \pm 3.67	4.90 \pm 1.85	3.58 \pm 1.80	2.50 \pm 2.08	1.67 \pm 1.62	17.23 \pm 5.84	8.87 \pm 3.19	6.61 \pm 3.42	6.64 \pm 3.76	5.61 \pm 3.66
Phosphate (mg/L)	3.08 \pm 0.42	3.17 \pm 0.38	3.06 \pm 0.33	3.11 \pm 0.38	3.13 \pm 0.50	3.34 \pm 0.35	3.57 \pm 0.24	3.48 \pm 0.26	3.51 \pm 0.22	3.52 \pm 0.24
DOC (mg/L)	4.13 \pm 0.63	1.96 \pm 0.19	2.22 \pm 0.28	2.02 \pm 0.22	2.18 \pm 0.28	3.94 \pm 0.37	1.30 \pm 0.28	1.70 \pm 0.27	1.61 \pm 0.29	1.69 \pm 0.21
Total coliforms removal (%)	n.a.	97.1 \pm 1.6	97.9 \pm 1.5	96.4 \pm 2.9	97.2 \pm 1.9	n.a.	97.2 \pm 1.3	96.5 \pm 2.4	97.5 \pm 2.2	95.4 \pm 3.3
<i>E. coli</i> removal (%)	n.a.	99.2 \pm 0.7	98.6 \pm 1.3	97.5 \pm 3.6	95.6 \pm 4.5	n.a.	99.0 \pm 0.7	98.8 \pm 0.6	98.8 \pm 0.7	97.3 \pm 1.2

COD: chemical oxygen demand; DOC: dissolved organic carbon; GSB: GAC sandwich biofilter.

It should be noted that the influents showed a significant difference ($p < 0.01$) in nitrate concentration, especially at the early stage after the addition of antibiotics (Week 1 and 2, Figure 4.13). It has been reported that effluents from WWTP containing antibiotics have the potential to disrupt nitrification/denitrification processes in aquatic ecology [268]. For instance, Costanzo *et al.* found that bacterial denitrification rates were reduced significantly after short term exposure to clarithromycin and amoxicillin at 1000 $\mu\text{g/L}$ [268]; Klaver and Matthews reported that antibiotics such as oxytetracycline could inhibit nitrification process in surface water [269]. However, in some cases, when a complex mixture of bacteria (e.g. soil or activated sludge) is exposed to antibiotics, increased nitrification activity can be observed [270]. Though much lower concentrations of antibiotics (10 $\mu\text{g/L}$) were used in the present study, the difference in nitrate concentration observed between the two influents indicated that the addition of antibiotics interferes with the nitrification/denitrification processes.

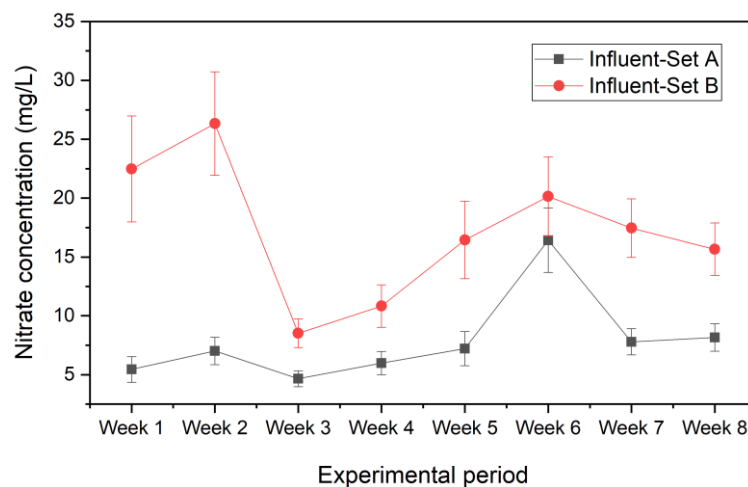


Figure 4.13 The concentration of nitrate in influents from Set A and Set B during experimental stage. The error bars represent STD from the mean value of triplicate samples ($n = 3$).

4.2.2.2 Biofilter performance in Set A and Set B

Slightly higher pH and conductivity were found in influents from Set B, however, the effluents did not show variations from both Sets. Raw data of all parameters during the experimental stage are summarised in Table 4.3. The removal/reduction of key parameters is shown in Figure 4.14.

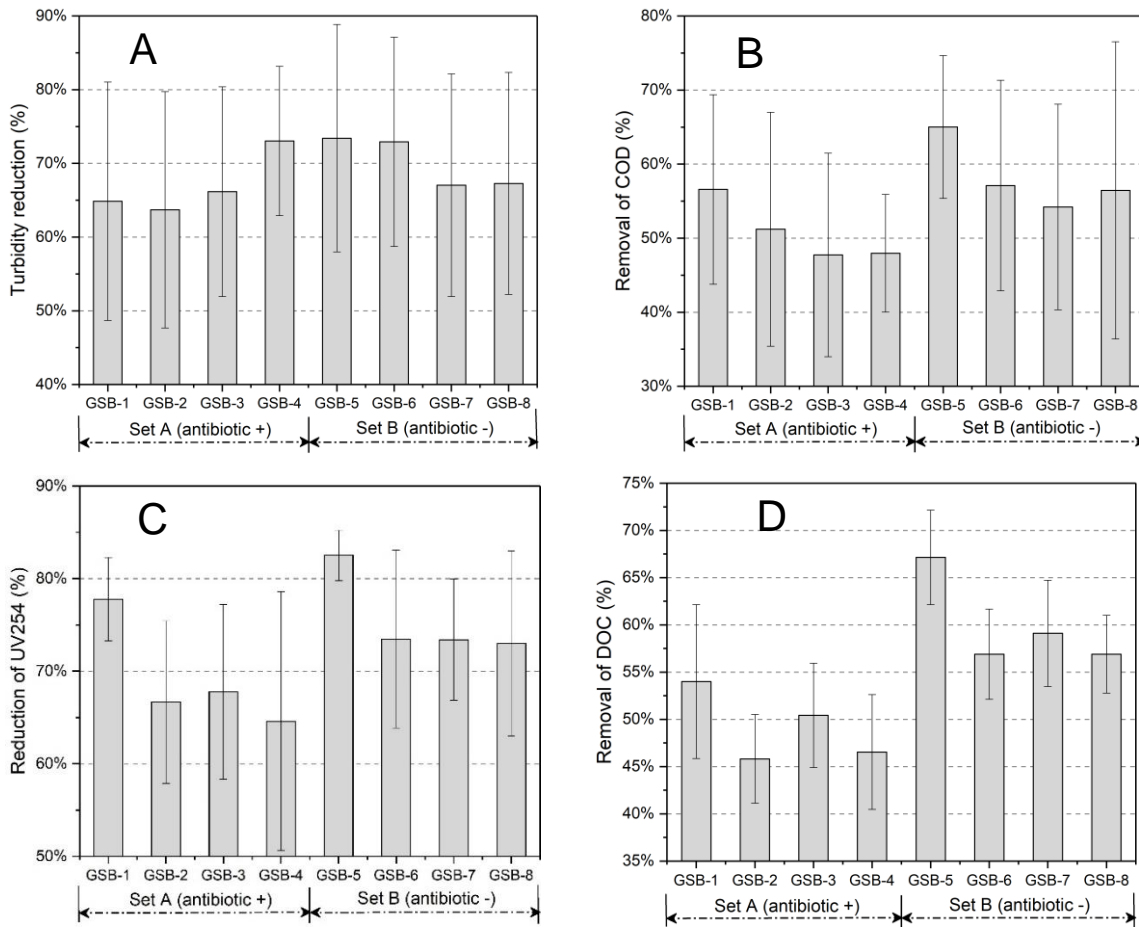


Figure 4.14 The reduction of turbidity (A), and the removal of COD (B), absorbance (C), and DOC (D) by GAC sandwich biofilters during the experimental period (8 weeks). The error bars represent STD from the mean value of all batch samples (n = 8).

In this study there did not appear to be a consistent trend in performance between biofilters with different GAC thickness or depth with respect to turbidity reduction. Turbidity achieved removals ranging from 65% to 75% (Figure 4.14 A), and the values are in accordance with the observations of GAC sandwich biofilters from previous study (68% on average; Section 4.1.2). In general, biofilters from Set B showed a better performance for eliminating organics, higher removals were consistently found in organics-related parameters (Figure 4.14 B, C & D). The average reduction of DOC was 2.06 mg/L by biofilters in Set A and 2.36 mg/L in Set B, respectively. This maybe due to the discrepancy in water quality in the influents. In addition to the adsorption of organic compounds by the GAC layer, higher oxygen levels observed in the influent of Set B could enhance the biodegradation process (Figure 4.15), contributing to higher organics removals in Set B.

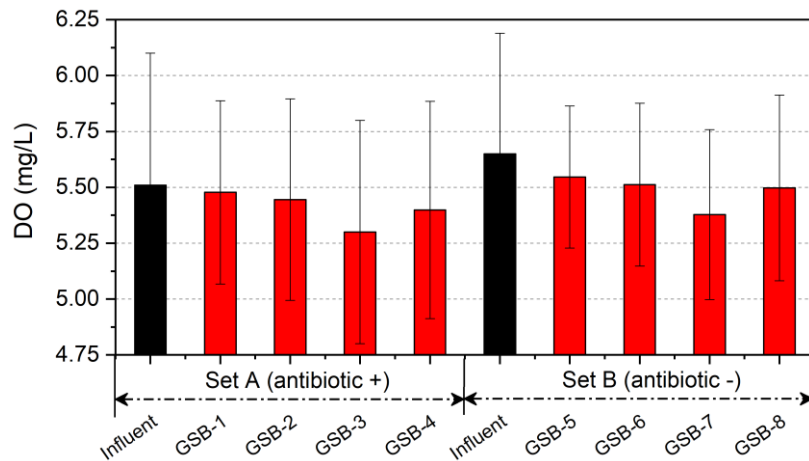


Figure 4.15 Levels of dissolved oxygen (DO) in the influent and effluent of GAC sandwich biofilters during the experimental period (8 weeks). The error bars represent STD from the mean value of all batch samples ($n = 8$).

Despite the differences in the influent, biofilters with 9 cm GAC revealed highest removals of organics as expected. For the amount of oxidisable organic compounds, biofilters with a 4 cm GAC layer at different depth showed no variations (less than 3.5%) of COD reduction (Figure 4.14 b). UV_{254} removal efficiencies ranged from 50.0 to 90.5%, averaging 72.9%, while DOC removal efficiencies varied from 41.8 to 74.3% with an average of 54.6%. Consistent with the maturation stage, a trend for a higher removal of DOC by biofilters loaded with 4 cm GAC in the middle than other positions was observed during the experimental stage, albeit not significant. This is possibly related to oxygen variation, as GSB-3 and GSB-7 consumed highest oxygen than other types of sandwich biofilters (Figure 4.15). The removal of DOC decreased from 78.4% during the start-up and then plateaued at around 53.0% after 7-weeks' operation (Figure A4.1), which is much higher than the removal observed by pure sand (21.3%) in the previous study (Section 4.1.3). Once again, the GAC sandwich biofilter outperformed the sand biofilter achieving better organic matter removal under the same filtration rate.

A higher concentration of nitrate was consistently found in the filtered water, suggesting that the nitrification process of transforming ammonium to nitrate is dominant over denitrification during filtration. Figure 4.16 shows the increase of nitrate in all biofilters, among which filters with 9 cm GAC (GSB-1 and GAB-5) increased the most. The levels of nitrate

decreased with the increase of GAC layer in filter depth, indicating that under a given filtration rate, nitrification process is affected by both the GAC amount and position. Nitrification occurs in both sand and GAC biofilters [271, 272]. Nakhla and Farooq reported that nitrification exhibits the most sensitivity to filtration rate and media size, and this process occurs not only in *schmutzdecke* layer but also in the deep beds [271], which further supported the findings in this study as the GAC layer underlying the sand bed affected the filter performance. Nitrite only presented in few batch water samples collected from Set B (< 1.6 mg/L, data not shown).

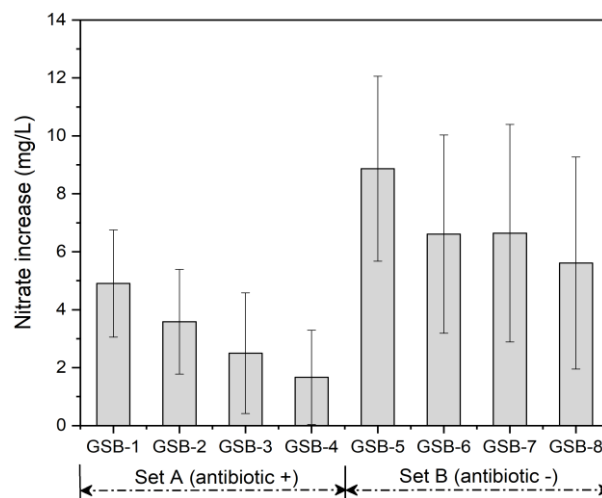


Figure 4.16 The increase of nitrate levels in the effluents of GAC sandwich biofilters during the experimental period (8 weeks). The error bars represent STD from the mean value of all batch samples (n = 8).

4.2.3 The effect of cleaning process

The cleaning process affected biofilter performance to various extents as seen in the effluents of Set A and Set B. This may relate to the removal of functional biofilms developed in the *schmutzdecke* layer. The variation of water quality parameters in batch samples before and after cleaning is summarised in Table 4.4. The greater oxygen reduction after cleaning indicates more dynamic microbiological activities as the new *schmutzdecke* was developing. Interestingly, the performance of biofilters in Set A was partially restored, evidenced by higher removal of organic matters and turbidity. By contrast, disturbance of the *schmutzdecke* showed less effect on biofilters in Set B in terms of organics (except for COD) and turbidity removal.

Table 4.4 Variation of water quality parameters (mean value \pm STD, n = 3) in batch samples before and after biofilter cleaning.

Parameters	Set A (antibiotic +)		Set B (antibiotic -)	
	Before	After	Before	After
pH reduction	0.09 \pm 0.07	0.01 \pm 0.05	0.03 \pm 0.05	0.11 \pm 0.06
Conductivity reduction (μ S/cm)	-12 \pm 4	8 \pm 10	6 \pm 7	-20 \pm 8
Oxygen consumption (mg/L)	0.15 \pm 0.33	-0.14 \pm 0.38	0.35 \pm 0.17	0.81 \pm 0.27
Turbidity reduction (%)	63.6 \pm 11.6	86.8 \pm 1.8	76.6 \pm 2.4	83.9 \pm 2.2
UV ₂₅₄ reduction (%)	61.6 \pm 9.8	67.2 \pm 4.8	72.2 \pm 7.6	65.6 \pm 6.6
COD reduction (%)	47.5 \pm 6.8	71.4 \pm 17.5	57.8 \pm 13.9	46.4 \pm 14.9
DOC removal (%)	44.5 \pm 4.0	47.9 \pm 3.6	59.1 \pm 8.9	55.3 \pm 7.4
Nitrite increase (mg/L)	n.a.	2.17 \pm 1.87	n.a.	0.09 \pm 0.26
Nitrate reduction (mg/L)	2.20 \pm 1.13	15.33 \pm 1.12	1.89 \pm 1.69	6.32 \pm 6.19
Phosphate reduction (mg/L)	0.09 \pm 0.08	0.35 \pm 0.07	-0.02 \pm 0.03	0.09 \pm 0.12
Total coliforms removal (%)	97.4 \pm 1.1	82.6 \pm 7.5	96.3 \pm 1.9	78.7 \pm 3.8
<i>E. coli</i> removal (%)	98.4 \pm 1.6	70.0 \pm 7.8	98.5 \pm 0.8	52.2 \pm 21.1

COD: chemical oxygen demand; DOC: dissolved organic carbon.

Higher nitrate removals were observed after cleaning, and this may be due to the denitrification microbes transforming nitrate to nitrite, resulting in reduced nitrate levels in the filtered water. This is further confirmed by the presence of nitrite in the effluents after biofilter cleaning. It is possible that some functional nitrifiers/denitrifiers were removed along with the *schmutzdecke* layer and therefore, microbiological activities in the lower positions of the column (especially within the GAC layer) dominated the denitrification process, contributing to the removal of nitrate from the feed. Consistent with the previous biofiltration experiment (Section 4.1.5), the cleaning process lowered the removal of total coliforms and *E. coli* (from 97.7% to 70.9%). This is conflicting with the slow sand filter performance measured by Jenkins *et al.*, where the filter cleaning showed no effect on total coliforms and *E. coli* removal [165]. This is likely related to the extent of cleaning and the restoring time needed for the re-

establishment of new biofilms. In their study, the top 2 cm of sand were gently rubbed and the filter was allowed to mature for one week before sampling, whereas, the whole slimy *schmutzdecke* layer was removed and samples were collected 24 hours after the cleaning process.

4.3 Summary

- Microbiological activities were more dynamic in maturation stage by the evidence of greater oxygen consumption, increased pH drop, and greater organic carbon removal.
- GAC-associated biofilters exhibited superior performance in reducing organic carbon from the feed compared to the non-adsorptive sand and anthracite biofilters.
- The addition of antibiotics (at 10 µg/L) to the feed has the potential to interrupt with the nitrification/denitrification processes.
- GAC sandwich biofilters with the GAC layer loaded in the middle of filter bed showed a better removal of organic carbons than in the upper or lower position.
- Biofilter backwashing/cleaning had a considerable impact on pH, conductivity, DO, turbidity, nitrate, total coliforms and *E. coli*, while organic carbon-related parameters were not sensitive to backwashing/cleaning, allowing conventional performance parameters to be optimised without compromising DOC removal.

Chapter 5

REMOVAL OF ANTIBIOTICS

5 REMOVAL OF ANTIBIOTICS

After the spike of antibiotics (amoxicillin, clarithromycin, oxytetracycline, sulfamethoxazole, and trimethoprim) to the biofiltration systems, paired influent and effluent were collected weekly for the determination of antibiotics. Removals were calculated based on influent and effluent concentrations. The removals of five antibiotics from the two biofiltration experiments are presented and discussed in this chapter. In addition, adsorptive removal of antibiotics by GAC is also included in this chapter to further explore the underlying removal mechanism.

5.1 Biofiltration experiment 1 – different types of filter media

5.1.1 Matrix-matched standard

For the qualification of antibiotics, a matrix-matched calibration method was used throughout this study. Normal standard mixtures were also run in parallel with the matrix-matched standards to assess instrumental stability. The effect of the environmental matrix on each antibiotic (based on 1 µg/mL) from different batch samples is provided in Table A5.1. The higher matrix effect could lead to inaccurate quantification, therefore, the use of matrix-matched standards was necessary. Lake water spiked with 1 µg/L of antibiotic mixture was used to check the method recovery rate. Mean recoveries and limits of detection (LOD) are presented in Table A5.2. The recoveries for SMX, TMP, OTC and CTM ranged from 66.7% to 115.9% throughout this study, while recoveries for AMOX were consistently below 40%.

5.1.2 Overview of the target antibiotic removals

The overall removals (mean value) of the five antibiotics over the entire course of the experiment were 20.3% by sand biofilter (SB), 97.4% by GAC biofilter (GB), 96.6% by GAC sandwich biofilter (GSB), and 17.7% by anthracite-sand dual biofilter (ASB) (Figure 5.1). GAC-associated biofilters exhibited considerably superior performance in eliminating all of the five antibiotics than conventional sand or anthracite media biofilters and the mean removals of

each antibiotic were all above 90%. Except for TMP, which was removed significantly more effectively ($p < 0.05$) by SB (55.4% on average) than ASB (12.9% on average), the remaining four antibiotics showed comparable removal rates by the two biofilters.

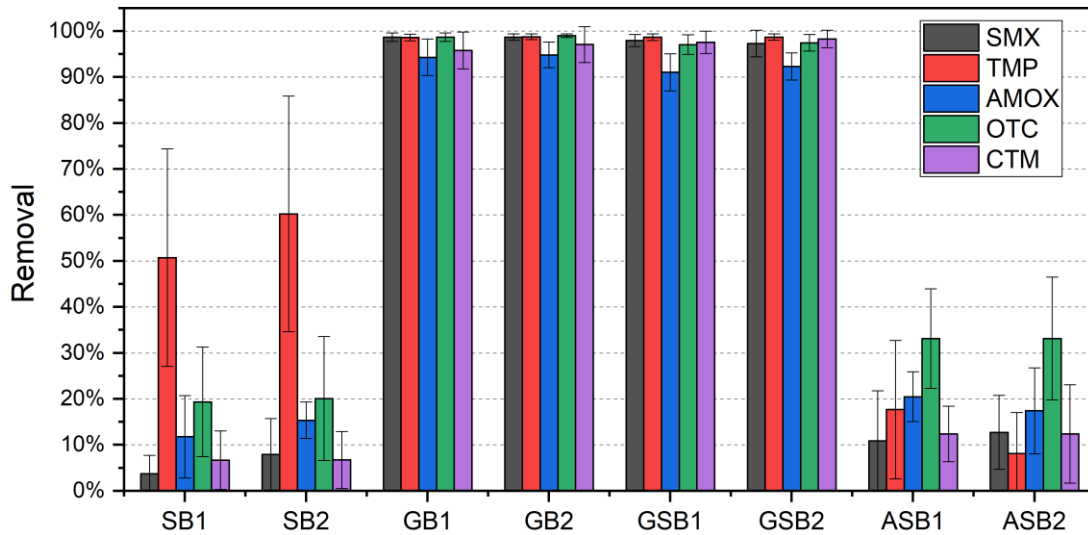


Figure 5.1 Mean removal efficiencies (%) of antibiotics in different biofilters over the operation period. The error bars represent STD from the mean value of all batch samples ($n = 8$). SMX, sulfamethoxazole; TMP: trimethoprim; AMOX: amoxicillin; OTC: oxytetracycline; CTM: clarithromycin. SB: sand biofilter; GB: GAC biofilter; GSB: GAC sandwich biofilter; ASB: anthracite-sand dual biofilter.

5.1.3 Antibiotic removal by sand and anthracite-sand dual biofilters

Figure 5.2 and Table 5.1 show the removal efficiencies of the five antibiotics by SB; and Figure 5.3 and Table 5.2 summarise the removals by ASB. Week 5-12 represented all 8 sampling periods (2 months in total), among which week 12 was after backwashing/cleaning was performed to the biofilters. The removal efficiencies of the selected antibiotics were highly variable among the batch samples.

5.1.3.1 Removal efficiencies by the sand biofilter

The overall removal (mean value) of the five antibiotics was 20.3% by sand biofilters, with TMP being the most efficiently removed antibiotic (55.5%) followed by OTC (20.0%), AMOX (13.6%), CTM (6.7%), and SMX (5.8%). The removal of TMP ranged from 38.9% to 74.8% at the earlier stage (5-8 weeks) after antibiotics spike and from 59.6% to 87.2% at the

later stage (9-11 weeks). This observation is consistent with a previous study where TMP was reported to be readily biodegradable (removal ranged from 50% to 92%) in the sand biofilter [152]. These results suggest that conventional biologically-active sand filters are an effective way to eliminate TMP in drinking water treatment. SMX and CTM showed very limited removals (< 10%) in this system, which were similar to the ranges reported in previous papers. For instance, only 4.1% of SMX was removed by laboratory biological sand filters [152], and no removal of CTM was found during sand filtration in a pilot-scale plant [181]. No obvious trend of increasing or decreasing removal was found for antibiotics over the two-month study period. TMP removal was considerably reduced ($p < 0.01$) from 68.9% to 7.2% after backwashing. This further confirmed that the sand biofilm layer contributed to the elimination of TMP from the source water. The backwash did not exert a noticeable effect ($p > 0.05$) on the remaining antibiotics, possibly due to the already low removal rate before backwashing occurred.

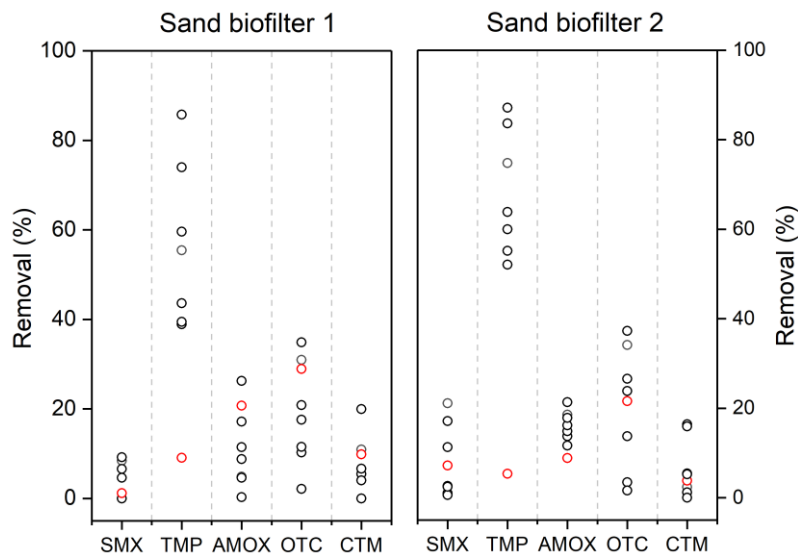


Figure 5.2 Removal efficiencies of antibiotics by sand biofilter 1 and 2. Red dots indicate the removal after backwashing process. SMX, sulfamethoxazole; TMP: trimethoprim; AMOX: amoxicillin; OTC: oxytetracycline; CTM: clarithromycin

Table 5.1 Removal of antibiotics by sand biofilters.

Week	Biofilter	SMX	TMP	AMOX	OTC	CTM
5	SB1	8.4 ± 2.3	55.4 ± 3.3	4.9 ± 1.4	31.0 ± 0.9	10.9 ± 1.5
	SB2	21.1 ± 1.2	74.8 ± 2.9	18.5 ± 3.8	34.1 ± 2.6	2.4 ± 0.8
6	SB1	6.6 ± 1.4	38.9 ± 1.7	11.4 ± 0.4	34.9 ± 0.5	19.9 ± 0.6
	SB2	7.2 ± 1.5	52.1 ± 0.1	21.4 ± 2.0	37.3 ± 1.4	16.4 ± 4.8
7	SB1	4.6 ± 1.9	39.5 ± 1.2	8.8 ± 0.7	20.9 ± 4.5	5.5 ± 1.0
	SB2	1.0 ± 2.2	60.0 ± 3.7	13.7 ± 1.4	23.9 ± 3.2	1.2 ± 0.8
8	SB1	-8.0 ± 3.7	43.6 ± 2.8	0.2 ± 0.5	2.1 ± 0.6	-1.6 ± 1.4
	SB2	0.6 ± 1.5	55.2 ± 3.1	11.7 ± 2.0	13.7 ± 1.1	15.9 ± 1.7
9	SB1	-1.8 ± 2.7	59.6 ± 0.2	4.6 ± 2.4	10.3 ± 2.2	4.0 ± 2.0
	SB2	2.7 ± 0.9	83.7 ± 1.4	14.8 ± 1.8	3.5 ± 1.1	3.8 ± 3.7
10	SB1	-8.8 ± 3.4	85.8 ± 3.6	17.2 ± 2.7	11.5 ± 0.8	-4.3 ± 2.0
	SB2	2.4 ± 2.4	87.2 ± 2.9	16.2 ± 1.8	1.6 ± 1.4	-5.5 ± 0.9
11	SB1	9.2 ± 1.9	74.0 ± 1.2	26.3 ± 0.9	17.6 ± 2.5	6.6 ± 2.4
	SB2	11.3 ± 4.7	63.8 ± 5.3	17.8 ± 3.1	26.6 ± 1.9	5.4 ± 3.7
12	SB1	1.2 ± 0.8	9.1 ± 0.7	20.7 ± 3.2	28.9 ± 3.5	9.8 ± 0.8
	SB2	12.7 ± 2.6	5.3 ± 1.9	8.9 ± 1.4	21.6 ± 5.5	5.2 ± 2.0
Mean value*		5.8 ± 6.4	55.5 ± 24.3	13.6 ± 6.9	20.0 ± 11.9	6.7 ± 6.3

Results are presented as removal (%) ± STD (n = 3). SB1 and SB2: duplicate sand biofilters. * All negative removals were corrected to 0% when calculating mean removal. SMX, sulfamethoxazole; TMP: trimethoprim; AMOX: amoxicillin; OTC: oxytetracycline; CTM: clarithromycin

5.1.3.2 Removal efficiencies by anthracite-sand biofilter

In general, anthracite-sand filtration was not effective in removing the target antibiotics, with an average removal of 17.7% observed in this study. This is consistent with previous research which showed limited removal efficiencies (generally less than 55%) for antibiotics by dual-media filtration [156, 182, 183, 273]. OTC was removed more effectively than other antibiotics, ranging from 18.3% to 60.4%, followed by AMOX with an average of 18.9% removal. Compared to sand, limited TMP removal was observed in dual media. The removals ranging from 4.4% to 44.7% in ASB1 and from 0% to 19.7% in ASB2. These variable removals

in duplicate biofilters may be due to the different microbial communities developed on the anthracite surface. A much higher (> 75%) TMP removal in the ASB was observed by Zhang *et al.*, when 2-year-old media from a drinking water treatment facility were used [182]. As TMP was found to be readily biodegradable in non-adsorptive sand biofilters under the identical operational conditions, it is likely that 3 months were not sufficient to develop an effective biofilm for biodegrading TMP within the dual media filter. Zhang *et al.* reported that the removals of erythromycin, sulfamethoxazole, and trimethoprim in the ASB were generally less than 55% [182]. Research on CTM removal in drinking water treatment is scarce, however research focused on CTM removal in WWTPs has shown that biological treatments are normally insufficient for the removal of such recalcitrant compound from raw water [53]. All of these observations, as well as the results found in this study, indicate that the conventional biologically-active anthracite-sand filters are ineffective for the elimination of the target antibiotics in drinking water treatment. Same removal efficiencies (15.1% on average) were found before and after backwashing, indicating that the removal of the target antibiotics was not affected ($p > 0.05$) by backwashing.

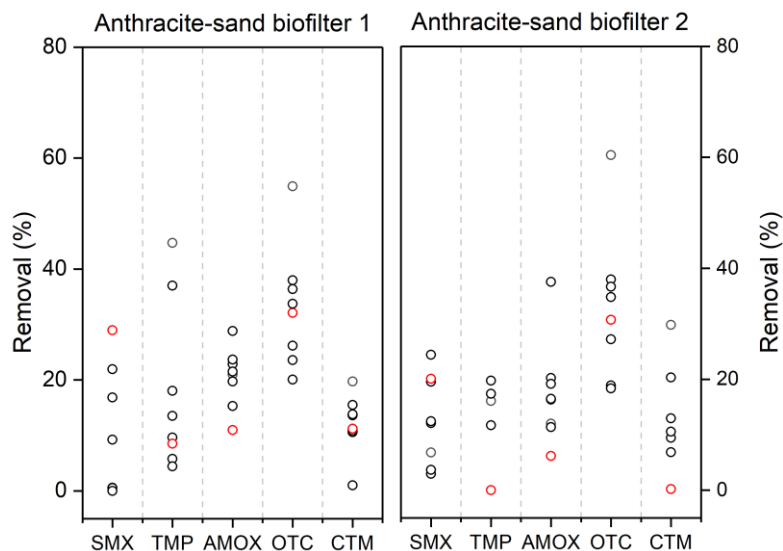


Figure 5.3 Removal efficiencies of antibiotics by anthracite-sand dual biofilter 1 and 2.

Red dots indicate the removal after backwashing process. SMX, sulfamethoxazole; TMP: trimethoprim; AMOX: amoxicillin; OTC: oxytetracycline; CTM: clarithromycin.

Table 5.2 Removal of antibiotics by anthracite-sand biofilters.

Week	Biofilter	SMX	TMP	AMOX	OTC	CTM
5	ASB1	9.2 ± 3.3	44.7 ± 5.2	21.0 ± 5.0	54.9 ± 1.1	19.7 ± 0.8
	ASB2	6.8 ± 2.9	16.1 ± 2.7	12.0 ± 3.7	60.4 ± 0.4	29.8 ± 1.4
6	ASB1	16.8 ± 4.6	9.6 ± 1.6	22.8 ± 2.0	32.1 ± 1.7	10.6 ± 1.9
	ASB2	19.5 ± 2.5	11.7 ± 4.8	37.5 ± 3.7	34.8 ± 1.2	20.3 ± 2.7
7	ASB1	0.6 ± 1.0	5.8 ± 3.0	19.7 ± 2.2	23.6 ± 2.9	13.6 ± 0.4
	ASB2	12.1 ± 5.8	17.4 ± 5.7	11.4 ± 0.8	18.9 ± 3.2	6.8 ± 1.5
8	ASB1	9.2 ± 5.6	13.5 ± 3.5	21.5 ± 1.5	26.2 ± 2.2	13.8 ± 3.4
	ASB2	24.4 ± 1.7	19.7 ± 2.8	16.3 ± 2.3	38.0 ± 1.6	9.5 ± 2.1
9	ASB1	0.5 ± 0.6	4.4 ± 1.1	15.3 ± 1.9	36.4 ± 3.1	10.9 ± 0.9
	ASB2	12.4 ± 7.5	-7.8 ± 1.8	20.2 ± 4.2	36.7 ± 2.4	10.6 ± 1.6
10	ASB1	21.9 ± 2.2	37.0 ± 2.0	23.7 ± 0.4	20.1 ± 4.0	1.0 ± 1.0
	ASB2	3.0 ± 1.7	-4.7 ± 0.7	16.5 ± 1.9	18.3 ± 2.6	0.2 ± 0.8
11	ASB1	-7.2 ± 0.9	18.1 ± 1.0	28.8 ± 2.8	38.0 ± 1.9	15.5 ± 2.2
	ASB2	3.7 ± 1.2	-5.4 ± 0.8	19.2 ± 3.7	27.2 ± 2.4	13.0 ± 1.2
12	ASB1	29.0 ± 3.0	8.5 ± 2.2	11.0 ± 4.4	33.7 ± 3.7	11.2 ± 3.4
	ASB2	20.1 ± 3.8	-0.8 ± 1.3	6.2 ± 5.0	30.7 ± 4.2	0.2 ± 1.1
Mean value*		11.8 ± 9.3	12.9 ± 12.9	18.9 ± 7.5	33.1 ± 11.7	11.7 ± 7.8

Results are presented as removal (%) ± STD (n = 3). ASB1 and ASB2: duplicate anthracite-sand dual biofilters. * All negative removals were corrected to 0% when calculating mean removal. SMX, sulfamethoxazole; TMP: trimethoprim; AMOX: amoxicillin; OTC: oxytetracycline; CTM: clarithromycin.

The removals by duplicate biofilters were not statistically different ($p > 0.05$), however, removal efficiency varied greatly for individual antibiotics. For example, in week 9 effluent samples, 83.7% of TMP was removed by SB2, while a much lower removal of 59.6% was found in SB1; the removals of SMX by ASB1 and 2 were 21.9% and 3.0%, respectively, in week 10 samples. These differences may attribute to the dynamic changes of bacterial community developed on the media surface. Although duplicate biofilters were operated under identical conditions, the microorganisms in the feedwater entering duplicate columns may not be the same, resulting in a different microbial composition in the biofilm layer.

5.1.3.3 Removal mechanisms of antibiotics by sand and anthracite-sand dual biofilters

For the non-adsorptive media, biodegradation is the only significant removal mechanism for the antibiotics from the feedwater [41, 152]. The antibiotics exhibited different levels of biodegradability in this study. Based on the mean removal by SB and ASB, the antibiotics were classified as follows [152]: SMX and CTM had removals of less than 15% and were classified as recalcitrant to biodegradation, AMOX and OTC had removals between 15% and 50% and were classified as having slow biodegradation rates (moderately biodegradable), and TMP had removals between 50 and 85% (only in SB) and were classified as having fast biodegradation rates (readily biodegradable). Except for TMP, no significant difference in antibiotic removal was found between SB and ASB.

Sand biofiltration works through a slime layer that accumulates above the sand surface (known as the *schmutzdecke*) and within the upper layers of the sand bed [155, 157, 274]. This layer is highly biologically active and has been shown to have the ability to biodegrade many trace level micropollutants [152, 178, 275]. Maeng *et al.* investigated the role of biodegradation in the removal of selected pharmaceutically active compounds (PhACs) during passage through sand columns under biotic and abiotic conditions. They concluded that biodegradation represents an important mechanism for removing PhACs during sand filtration [276]. The sand biofilters showed fluctuations in removing the target antibiotics in different batch samples. This may be due to the dynamics of the microbial community within the *schmutzdecke* layer. The biofilm developed to acclimatise and biodegrade compounds was highly depending on the characteristics of the source water, which may vary over time and be affected by the indigenous antibiotic-degrading bacteria in the *schmutzdecke* layer.

The biodegradation rate of antibiotics is possibly affected by their initial concentrations in the raw water. For instance, the initial SMX concentration is a driving factor for its biodegradation [273]. It was hypothesised that SMX degradation would only occur if a threshold concentration of 0.3 µg/L was exceeded [277]. This was further confirmed by a laboratory column experiment, where a higher concentration of SMX (4 µg/L) in the feed water can be removed more effectively than at 0.25 µg/L [180]. Furthermore, the sorption of

antibiotics onto the *schmutzdecke*, or within the filter column might also contribute to their removal. Previous research has shown that TMP had higher sorption potential onto the *schmutzdecke* than SMX and their sorption kinetics were comparable to those previously found for soils [179]. For hydrophilic antibiotics (AMOX, OTC, SMX and TMP), their removal through sand filtration might also attribute to the removal of the fine suspended particles adsorbing to these compounds [157, 181]. Filter substrate plays an important role in determining bacterial community composition. Smaller sand particle size would result in a larger surface area for microorganisms to colonise within the column compared to larger particle sizes [178]. Furthermore, the different elemental compositions of sand and anthracite surfaces may also have influenced bacterial attachment [178]. These factors could provide some answers as to why different antibiotic removal efficiencies have been observed through this study.

5.1.4 Antibiotic removal by GAC and GAC sandwich biofilters

The overall mean removals of the five antibiotics during the whole operational period were 97.4% and 96.6% for GB and GSB, respectively. Figure 5.4 and Table 5.3 show the removal efficiencies by GB; and Figure 5.5 and Table 5.4 summarise the removals by GSB. The GSB achieved considerably higher removals ($p < 0.01$) than the conventional SB, indicating the applicability of GSB in eliminating trace organic compounds from drinking water. This observation is in agreement with the results reported by Li *et al.*, where an average removal of 95% was observed for DEET, paracetamol, caffeine, and triclosan in GSB with various GAC layer depths [163]. Comparing the results obtained from SB (as shown in Figure 5.2), it can be assumed that the removal of target antibiotics in the sandwich biofilter could be attributed to both adsorption by the GAC layers and biodegradation within the *schmutzdecke* and upper sand layer. However, the contribution of biodegradation could not be elucidated in sandwich biofilter since the overall removal of antibiotics was similar to that obtained in the pure GAC column. The removal was not affected by filter backwashing/ cleaning in the GAC-associated biofilters.

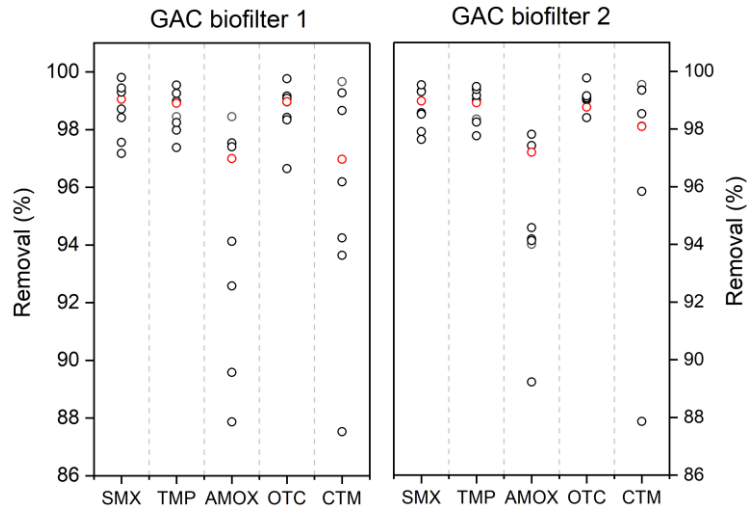


Figure 5.4 Removal efficiencies of antibiotics by GAC biofilter 1 and 2. Red dots indicate the removal after backwashing/cleaning process. SMX, sulfamethoxazole; TMP: trimethoprim; AMOX: amoxicillin; OTC: oxytetracycline; CTM: clarithromycin.

Table 5.3 Removal of antibiotics by GAC biofilters.

Week	Biofilter	SMX	TMP	AMOX	OTC	CTM
5	GB1	99.1 ± 0.4	98.4 ± 0.4	98.4 ± 0.9	99.0 ± 0.3	99.7 ± 0.1
	GB2	99.0 ± 0.4	98.3 ± 0.5	94.0 ± 3.9	99.0 ± 0.4	99.5 ± 0.1
6	GB1	97.2 ± 1.3	99.0 ± 0.0	92.6 ± 4.7	99.2 ± 0.1	99.3 ± 0.2
	GB2	98.6 ± 0.3	99.0 ± 0.0	94.2 ± 3.7	98.8 ± 0.2	99.4 ± 0.2
7	GB1	98.4 ± 0.4	98.9 ± 0.0	89.6 ± 0.9	98.4 ± 0.3	93.6 ± 0.5
	GB2	98.5 ± 0.3	98.9 ± 0.0	89.2 ± 4.7	98.4 ± 0.3	95.8 ± 1.7
8	GB1	98.7 ± 0.4	99.3 ± 0.3	97.5 ± 0.8	96.6 ± 1.4	98.7 ± 0.4
	GB2	99.3 ± 0.1	99.2 ± 0.0	97.4 ± 1.4	99.1 ± 0.1	99.3 ± 0.1
9	GB1	99.0 ± 0.2	97.4 ± 0.7	87.9 ± 0.2	98.3 ± 1.2	87.5 ± 1.5
	GB2	97.9 ± 0.1	97.8 ± 0.9	94.6 ± 4.7	99.0 ± 0.7	87.9 ± 0.8
10	GB1	99.6 ± 0.0	98.0 ± 1.3	97.4 ± 2.2	99.8 ± 0.0	94.2 ± 2.6
	GB2	98.6 ± 0.7	99.4 ± 0.3	97.8 ± 0.5	99.8 ± 0.0	98.5 ± 0.6
11	GB1	99.3 ± 0.0	99.2 ± 0.0	94.1 ± 1.5	99.1 ± 0.0	96.2 ± 1.5
	GB2	99.3 ± 0.0	99.2 ± 0.2	94.1 ± 2.8	99.1 ± 0.0	98.1 ± 0.1
12	GB1	99.4 ± 0.1	99.5 ± 0.0	97.0 ± 0.0	99.0 ± 0.3	97.0 ± 1.8
	GB2	99.5 ± 0.0	99.5 ± 0.0	97.2 ± 0.6	99.1 ± 0.2	98.1 ± 1.0
Mean value		98.8 ± 0.8	98.9 ± 0.6	94.6 ± 3.3	98.8 ± 0.7	96.4 ± 3.9

Results are presented as removal (%) ± STD (n = 3). GB1 and GB2: duplicate GAC biofilters. SMX, sulfamethoxazole; TMP: trimethoprim; AMOX: amoxicillin; OTC: oxytetracycline; CTM: clarithromycin.

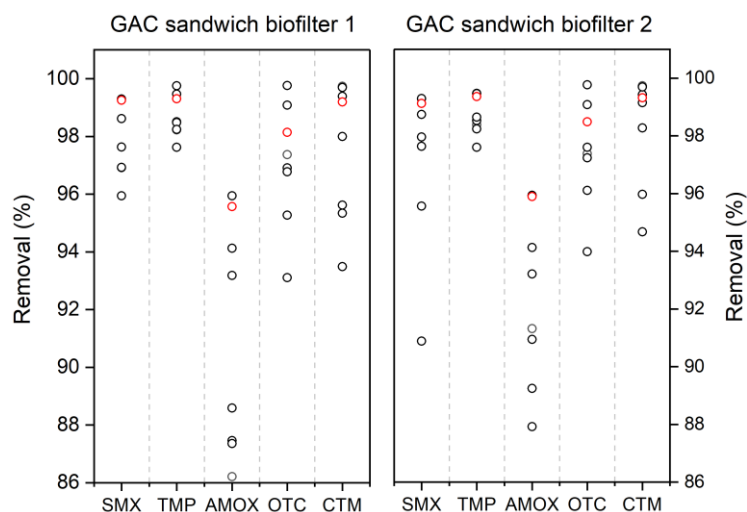


Figure 5.5 Removal efficiencies of antibiotics by GAC sandwich biofilter 1 and 2. Red dots indicate the removal after backwashing/cleaning process. SMX, sulfamethoxazole; TMP: trimethoprim; AMOX: amoxicillin; OTC: oxytetracycline; CTM: clarithromycin.

Table 5.4 Removal of antibiotics by GAC sandwich biofilters.

Week	Biofilter	SMX	TMP	AMOX	OTC	CTM
5	GSB1	95.9 ± 1.6	98.2 ± 0.6	86.2 ± 3.0	97.4 ± 0.8	99.7 ± 0.0
	GSB2	95.6 ± 2.0	98.4 ± 0.7	91.3 ± 0.7	98.4 ± 0.5	99.7 ± 0.0
6	GSB1	96.9 ± 1.1	98.5 ± 0.9	87.5 ± 1.7	96.9 ± 1.1	99.4 ± 0.0
	GSB2	90.9 ± 5.4	98.9 ± 0.7	89.2 ± 1.0	97.6 ± 0.2	99.4 ± 0.0
7	GSB1	98.6 ± 0.1	99.5 ± 0.0	88.6 ± 3.1	95.3 ± 2.0	95.6 ± 0.8
	GSB2	98.7 ± 0.1	98.6 ± 1.0	90.9 ± 2.6	96.1 ± 1.4	96.0 ± 0.4
8	GSB1	99.3 ± 0.3	99.8 ± 0.0	93.2 ± 3.4	93.1 ± 3.4	98.0 ± 0.1
	GSB2	98.6 ± 0.1	99.5 ± 0.1	92.2 ± 4.2	94.0 ± 0.8	99.1 ± 0.2
9	GSB1	96.9 ± 0.5	98.6 ± 0.4	87.4 ± 1.8	96.8 ± 1.5	93.5 ± 0.8
	GSB2	98.0 ± 0.3	97.6 ± 0.8	87.9 ± 0.4	97.2 ± 0.9	94.7 ± 0.4
10	GSB1	97.6 ± 1.3	98.5 ± 0.2	96.0 ± 0.0	99.5 ± 0.0	95.3 ± 0.8
	GSB2	97.6 ± 1.3	99.5 ± 0.0	94.8 ± 0.7	99.5 ± 0.0	98.3 ± 0.5
11	GSB1	99.3 ± 0.7	98.7 ± 0.8	94.1 ± 1.3	99.1 ± 0.0	99.7 ± 0.0
	GSB2	99.3 ± 0.7	98.2 ± 0.1	91.1 ± 2.8	99.1 ± 0.0	99.7 ± 0.0
12	GSB1	99.3 ± 0.0	99.1 ± 0.3	95.6 ± 1.0	98.1 ± 0.7	99.2 ± 0.4
	GSB2	99.1 ± 0.2	99.2 ± 0.0	95.9 ± 0.7	98.5 ± 0.1	99.3 ± 0.1
Mean value		97.6 ± 2.2	98.7 ± 0.7	91.7 ± 3.5	97.3 ± 1.9	97.9 ± 2.1

Results are presented as removal (%) ± STD (n = 3). GSB1 and GSB2: duplicate GAC sandwich biofilters. SMX, sulfamethoxazole; TMP: trimethoprim; AMOX: amoxicillin; OTC: oxytetracycline; CTM: clarithromycin.

5.1.5 Removal mechanism by GAC adsorption

Both dosage and contact time play important roles when using activated carbon as adsorptive media. Higher activated carbon dosage can increase the adsorbable area, and increasing contact time can result in a more complete adsorption equilibrium [185].

5.1.5.1 Role of contact time in adsorption removal

Kinetic modelling of the adsorption removal of antibiotics onto GAC was carried out using Lagergren pseudo-first-order and pseudo-second-order equations. The pseudo-first-order model, according to Lagergren [278], assumes that the adsorption rate is proportional to the difference of adsorbate adsorbed at equilibrium (q_e) and at time (q_t) shown by Eq. (1) (k_1 : pseudo-first-order kinetic rate constant).

$$\frac{dq_t}{dt} = k_1 (q_e - q_t) \quad (1)$$

Which can be rearranged to Eq. (2):

$$\ln(q_e - q_t) = \ln q_e - k_1 t \quad (2)$$

To fit the data to Eq. (2), $\ln (q_e - q_t)$ was plotted against time which gives a slope of $-k_1$ and intercept of $\ln q_e$, R^2 indicating the applicability of pseudo-first-order model can be obtained. The pseudo-second-order model [279] is shown by Eq. (3) (k_2 : pseudo-second-order kinetic rate constant)

$$\frac{dq_t}{dt} = k_2 (q_e - q_t)^2 \quad (3)$$

Which can be rearranged to Eq. (4):

$$\frac{t}{q_t} = \frac{1}{k_2 q_e^2} + \left(\frac{1}{q_t}\right) t \quad (4)$$

To fit the data to Eq. (4), t/q_t was plotted against time and from which q_e and k_2 can be calculated. R^2 indicating the applicability of pseudo-second-order model can be obtained. Figure 5.6 shows the adsorption of the five antibiotics by GAC in surface water samples. The optimal contact time was 48 h in surface water, when each antibiotic had reached an equilibrium concentration and > 90% removal was achieved. From Figure 5.6, experimental adsorption capacity (q_e) of the five antibiotics in surface water was about 0.0099, 0.0099, 0.0091, 0.0097, and 0.0096 mg/g for SMX, TMP, AMOX, OTC and CTM, respectively.

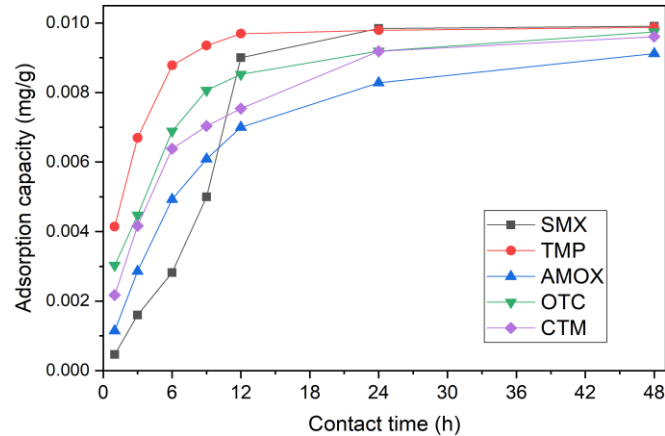


Figure 5.6 Effect of contact time on the adsorption removal of antibiotics in surface water (spiked at 5 $\mu\text{g/L}$). SMX, sulfamethoxazole; TMP: trimethoprim; AMOX: amoxicillin; OTC: oxytetracycline; CTM: clarithromycin.

Table 5.5 below lists the results of the rate constants for different antibiotics, and a higher value of R^2 indicates a better fit. The result suggested that for TMP, AMOX, OTC and CTM, the pseudo-second-order adsorption mechanism was predominant, and that the rate of the adsorption process appeared to be controlled by the adsorption reaction at the liquid/solid interface in the GAC (chemisorption process) [279, 280]. SMX fitted better with pseudo-first-order model, suggesting that the adsorption is a diffusion-controlled process [281].

Table 5.5 Comparison of the pseudo-first-order and pseudo-second-order adsorption rate constants.

Antibiotic	Pseudo-first order kinetic model				Pseudo-second order kinetic model		
	$q_{e,exp}$ (mg/g)	$q_{e,cal}$ (mg/g)	k_1 (1/h)	R^2	$q_{e,cal}$ (mg/g)	k_2 (g/mg h)	R^2
SMX	0.0099	0.0191	0.0038	0.9845	0.0891	0.0011	0.0603
TMP	0.0099	0.0040	0.0031	0.8761	0.0104	1.2050	0.9985
AMOX	0.0091	0.0079	0.0016	0.9833	0.0114	0.1761	0.9933
OTC	0.0097	0.0060	0.0018	0.9285	0.0104	0.5369	0.9954
CTM	0.0096	0.0078	0.0020	0.9908	0.0108	0.3466	0.9967

$q_{e,exp}$: experimental adsorption capacity; $q_{e,cal}$: calculated adsorption capacity; k_1 : pseudo-first-order constant; k_2 : pseudo-second-order constant. SMX, sulfamethoxazole; TMP: trimethoprim; AMOX: amoxicillin; OTC: oxytetracycline; CTM: clarithromycin.

5.1.5.2 Role of GAC dosage in adsorption

The impact of GAC dosage on antibiotics removal is shown in Figure 5.7. Data from the batch experiments were fitted to the Freundlich and Langmuir isotherm models to evaluate the adsorption characteristics of the five antibiotics on GAC. The adsorption uptake at equilibrium (q_e : concentration of antibiotics on the surface of the adsorbent GAC) can be calculated from the initial solution concentration (C_0) at $t = 0$, solution concentration after 24 h of contact time (C_e : final concentration of solution in equilibrium), and the material (GAC) loading concentration (C_{solid}) as Eq. (1) demonstrates [282].

$$q_e = \frac{C_0 - C_e}{C_{solid}} \quad (1)$$

The Freundlich model can be represented by Eq. (2) which shows the empirical relationship between C_e and q_e with two specific Freundlich constants, K_F (indicates adsorption capacity) and $1/n$ (indicates adsorption intensity), that are dependent on the adsorbate and adsorbent [282].

$$q_e = K_F C_e^{1/n} \quad (2)$$

Which can be rearranged to Eq. (3):

$$\log q_e = \log K_F + \frac{1}{n} \log C_e \quad (3)$$

The Langmuir model shows the relationship between C_e and q_e with two constants, K_L (Langmuir constant in $L \text{ mg}^{-1}$) and q_m (maximum/saturation adsorption capacity in mg g^{-1}) [283] (shown by Eq. (4)).

$$q_e = \frac{K_L C_e q_m}{1 + K_L C_e} \quad (4)$$

Which can be rearranged to Eq. (5):

$$\frac{C_e}{q_e} = \frac{1}{K_L q_m} + \frac{C_e}{q_m} \quad (5)$$

Isotherm parameters are summarised in Table 5.6. Real data fitted better with the Langmuir model ($R^2 > 0.9099$) than the Freundlich model, especially for AMOX and CTM. Based on the results of the fitting to the Langmuir isotherm, GAC has q_m values (maximum/saturation adsorption capacity) ranging from 0.0072 mg/g for CTM to 0.0269 mg/g

for TMP. This could be explained by the hydrophobicity of CTM as the difference in adsorption capacities is related to the hydrophobicity of a compound [185]. Considering the antibiotic spike concentration (2 and 5 $\mu\text{g/L}$) and the amount of GAC loaded (approximately 50 g in sandwich filter), theoretically, it would take approximately 2 years until the GAC sandwich filter reaches its service life end (surface sand cleaning is required every 1 ~ 2 months). This is consistent with practice in drinking water treatment works, as it typically requires years of operation until GAC sorption capacity becomes exhausted.

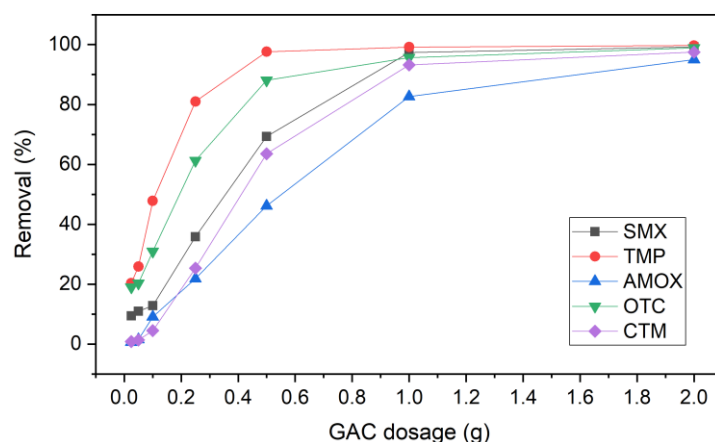


Figure 5.7 Effect of GAC dosage on the adsorption removal of antibiotics. Contact time: 24 h; 5 $\mu\text{g/L}$ antibiotics in surface water. SMX, sulfamethoxazole; TMP: trimethoprim; AMOX: amoxicillin; OTC: oxytetracycline; CTM: clarithromycin.

Table 5.6 Comparison of the Freundlich and Langmuir isotherm.

Antibiotic	Freundlich isotherm			Langmuir isotherm		
	K_F (mg g^{-1})/(mg L^{-1}) ^{1/n}	1/n	R^2	K_L L mg^{-1}	q_m mg g^{-1}	R^2
SMX	0.0544	0.2822	0.8656	3801	0.0090	0.9099
TMP	0.2647	0.3995	0.9634	3642	0.0269	0.9861
AMOX	0.0134	0.1602	0.1362	2487	0.0080	0.9672
OTC	0.2343	0.4603	0.9850	1927	0.0171	0.9850
CTM	0.0021	-0.081	0.0438	8516	0.0072	0.9885

K_F : Freundlich constant, indicating adsorption capacity; 1/n: Freundlich constant, indicating adsorption intensity. K_L : Langmuir constant, indicating the binding energy; q_m : maximum/saturation adsorption capacity. SMX, sulfamethoxazole; TMP: trimethoprim; AMOX: amoxicillin; OTC: oxytetracycline; CTM: clarithromycin.

5.2 Biofiltration experiment 2 – different types of GAC sandwich biofilters

5.2.1 The occurrence of antibiotic in River Thames

Trimethoprim (TMP) and clarithromycin (CTM) were present in raw water samples, ranging from 60.8 ± 28.7 ng/L for TMP and 33.8 ± 31.4 ng/L for CTM (Table A5.3). Five out of eight batch samples detected TMP and CTM. In general, the concentration and frequency of detection of antibiotics are within the same range as the mean river concentration (17–74 ng/L) reported by Singer *et al.* [206], with CTM (max = 292 ng/L) yielding the highest single measure in the River Thames catchment samples. These results suggested the prevalence of antibiotic residues in the River Thames. In addition, various ARGs were also detected in the River Thames [284], and the co-occurrence of antibiotics and ARGs in the river environments have given rise to concerns over possible links between antibiotic usage and antibiotic resistance [285]. Although two of the target antibiotics were present in raw water, when serving as the biofilter feedwater, they were diluted with dechlorinated tap water each time and the resulting concentration was approximately 500-1000 times lower than the spike concentration (10 µg/L) in Set A.

5.2.2 The removal of antibiotics

Testing for antibiotic removal began in week 4, allowing an initial 3-week maturation period for the biofilm to establish within the top layer sand. During the experimental period, all sandwich biofilters achieved 90% antibiotic removal, which is consistent with the observations in the previous study using lake water as biofilter feed (Section 5.1.4). Overall mean removal of antibiotics is summarised in Table 5.7.

Table 5.7 Overall mean removal of antibiotics (%) by GAC sandwich biofilters.

Antibiotics	GSB 1	GSB 2	GSB 3	GSB 4
SMX	99.3 ± 0.6	99.2 ± 0.7	99.4 ± 0.5	99.3 ± 0.7
TMP	99.4 ± 0.6	99.4 ± 0.6	99.4 ± 0.6	99.3 ± 0.7
AMOX	95.9 ± 3.1	95.7 ± 2.1	95.5 ± 2.0	94.7 ± 1.8
OTC	99.2 ± 0.6	98.7 ± 0.8	98.4 ± 0.9	98.6 ± 0.6
CTM	99.4 ± 0.8	99.5 ± 0.8	99.3 ± 0.9	99.5 ± 0.7
Mean value	98.6 ± 1.6	98.5 ± 1.6	98.4 ± 1.7	98.3 ± 2.0

Results are presented as removal (%) ± STD. STD was calculated based on the removals from all 8 batch samples. SMX, sulfamethoxazole; TMP: trimethoprim; AMOX: amoxicillin; OTC: oxytetracycline; CTM: clarithromycin.

No difference in removal was found between biofilters with different GAC thickness (9 cm or 4 cm GAC), or between biofilters with 4 cm of GAC at different depths ($p > 0.05$). In addition, the removal was not affected by biofilter cleaning, which could be attributed to the superior adsorption capacity of GAC. The relatively low concentration of antibiotics added to the feed and the complete removal by GAC adsorption resulted in difficulties in detection of the target compounds in the effluent due to restrictions in the analytical method. AMOX was only detected occasionally in the effluent due to the poor recovery (Table A5.4). Therefore, the values below the limit of quantification (LOQ) in the filtered water were taken as half of the LOQ according to Zuccato *et al.* [55]. Details of the recovery rates, LOQ and matrix effect are provided in Table A5.4 and A5.5.

5.3 Summary

- The mean removals of the five antibiotics during the first biofiltration experiment were 20.3% by sand biofilter, 97.4% by GAC biofilter, 96.6% by GAC sandwich biofilter, and 17.7% by anthracite-sand dual biofilter.
- For the non-adsorptive media, trimethoprim was biodegraded more effectively in the sand biofilter (55.5%) than that in the anthracite-sand biofilter (12.9%). By

contrast, oxytetracycline was removed more effectively by anthracite-sand (33.1%) than sand media (20.0%).

- The GAC sandwich biofilters exhibited considerably superior performance in eliminating all of the five antibiotics (> 90%), indicating the applicability of GAC sandwich biofiltration to reduce the risk associated with antibiotics in drinking water.
- No difference in antibiotic removal was found between biofilters with different GAC thicknesses (9 cm or 4 cm GAC), or between biofilters with 4 cm of GAC at different depths.

Chapter 6

ANTIBIOTICS RESISTANCE GENES AND BACTERIAL COMMUNITY

6 ANTIBIOTICS RESISTANCE GENES AND BACTERIAL COMMUNITY

Influent, effluent and media (biofilm) samples were collected on a regular basis and subjected to genomic DNA extraction. Both normal qPCR and high-throughput qPCR (HT-qPCR) were conducted for the quantification of ARGs in aqueous or biofilm samples. In addition, the bacterial community was also analysed on the selected biofilm samples. This chapter presents 1) the results of ARGs in all types of samples; 2) the bacterial community structures in biofilms; and 3) the correlations between ARGs and bacterial communities.

6.1 Biofiltration experiment 1 – different types of filter media

6.1.1 ARGs in the biofilm samples

6.1.1.1 Overall behaviour of *16S rRNA* gene, ARGs and integron genes

An overview of the absolute abundance of *16S rRNA* gene, ARGs and integrons in all biofilm samples is shown in Figure 6.1. Biofilm samples were collected from different sampling sites at 4 weeks (before antibiotics spike) and 11 weeks (before backwashing/cleaning) of the biofilter run. For a better understanding of the sampling positions, M0, M8, M17 and M20 referred to media samples collected at 0 cm, 8 cm, 17 cm, and 20 cm along the column, respectively. Surface sand showed the highest absolute abundance of *16S rRNA* gene, followed by GAC and anthracite, which is in accordance with DNA yields obtained (Table A6.1). This observation is consistent with Zhang *et al.*, whom reported that at a depth of 5 cm in biofilter bed, the amount of biomass attached to quartz sand was the greatest followed by the amounts attached to GAC and anthracite [258]. The abundance of *16S rRNA* gene in sand and GAC decreased more drastically from surface (0 cm) to deeper layers (8-20 cm) than anthracite. The total concentration of ARGs among all of the media samples was between 10^4 ~ 10^7 copies/g media. Among all biofilm samples, positive correlations in absolute abundance were found between the ARGs and *16S rRNA* gene and the integrons (Figure 6.2), suggesting that the biofilm biomass drives the absolute abundance of ARG.

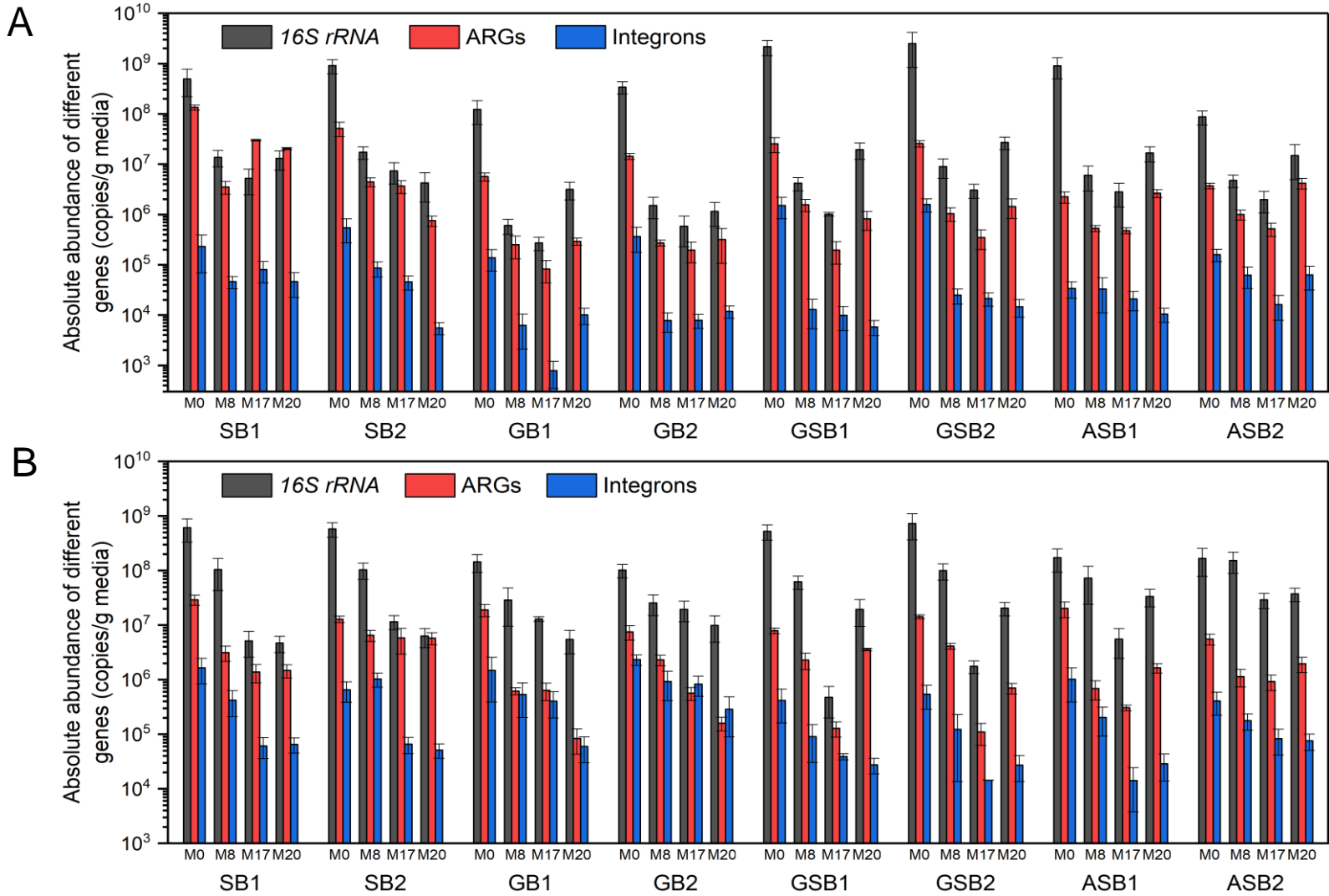


Figure 6.1 Absolute abundance of 16S rRNA gene, ARGs and integrons (copies/g) in media samples at A) 4-weeks and B) 11-weeks of system run. Samples M0, M8, M17 and M20 refer to media (biofilm) samples collected at different sampling sites (0, 8, 17, and 20 cm). The error bars represent STD from the mean value of qPCR replicates (n = 3).

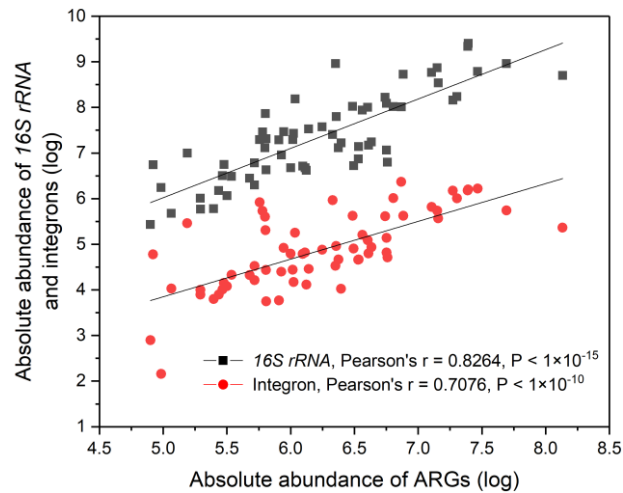


Figure 6.2 The correlations between the absolute abundance (copies/g media, log transformed) of ARGs and the corresponding *16S rRNA* gene and integrons in all biofilm samples.

6.1.1.2 Behaviour of ARGs and integron in individual biofilter type

Figure 6.3 – 6.6 show an overview of the variation of ARGs and integrons in biofilms from all biofilters. The absolute abundance of individual genes is provided in the appendix (Figure A6.1-A6.4). No statistical differences ($p > 0.05$) in total ARG abundance were found between duplicate columns or between 4-week and 11-week biofilm samples.

In SB biofilms, the total ARG abundance decreased with increasing depth and *sul 1*, *tetX* and *bla_{CTX-M}* present in all 16 biofilm sample (Figure A6.1). Among the ARGs present, *sul 1* was the most abundant resistance gene (4.73×10^7 copies/g), followed by *bla_{TEM}* (3.39×10^7 copies/g) and *sul 2* (6.07×10^6 copies/g). The trimethoprim resistance gene *dfrA12* had the lowest abundance (3.79×10^3 copies/g). *Int1 1* showed 5-fold higher gene abundance (on average) than *int1 2*. Data in Figure 6.3 B show the relative abundance of ARG category and integron in SB biofilm samples. Among the ARGs present, the normalised copy number of ARGs was up to 0.60 copies per bacterial cell, meaning that out of every five bacterial cells, three could carry ARG fragments. ARGs varied greatly in biofilms collected at different positions. For instance, the relative abundance of sulfonamide resistance genes increased significantly ($p < 0.01$) with increasing depth while the absolute concentration decreased. These observations are consistent with Wan *et al.*'s study on sand biofilm, where the relative abundance of ARGs increased with depth in all sand filters [193].

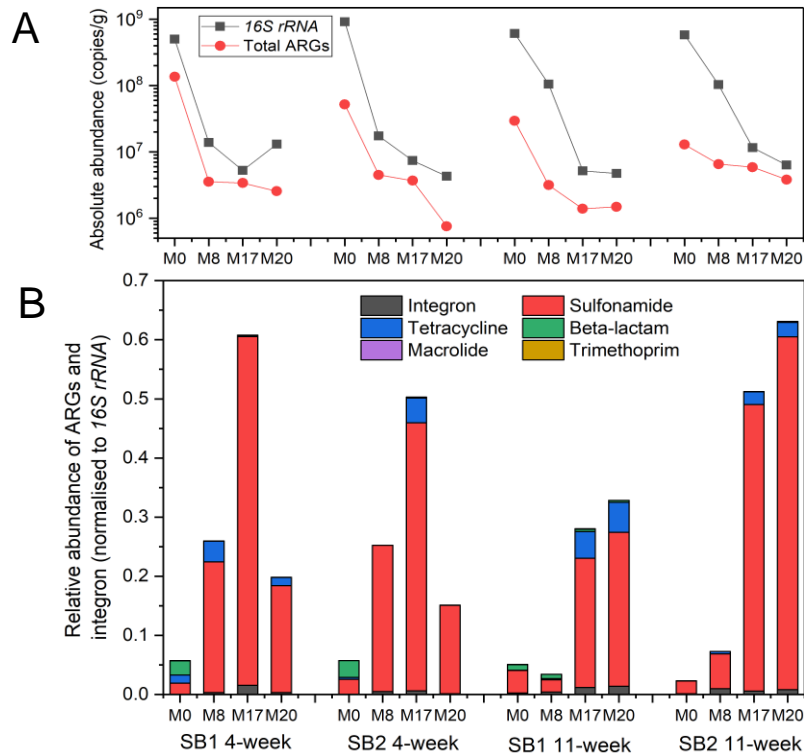


Figure 6.3 A): Absolute abundance of *16S rRNA* gene and total ARGs; **B):** Relative abundance of ARG categories and integron at each sampling site of sand biofilter (SB). Sample M0-M20 refer to biofilm collected at different sampling sites (0, 8, 17, and 20 cm).

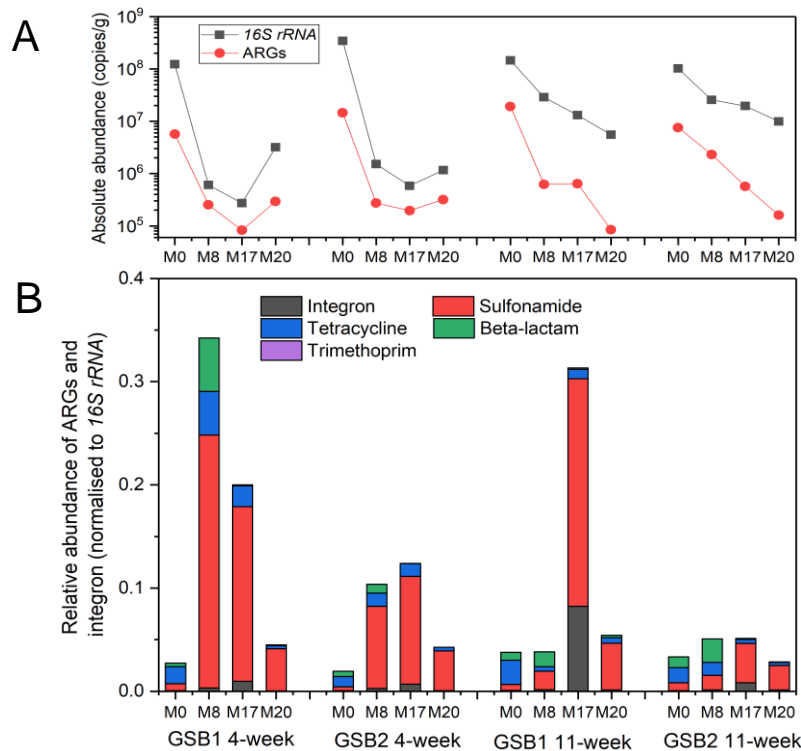


Figure 6.4 A): Absolute abundance of *16S rRNA* gene and total ARGs; **B):** Relative abundance of ARG categories and integron at each sampling site of GAC biofilter (GB). Sample M0-M20 refer to biofilm collected at different sampling sites (0, 8, 17, and 20 cm).

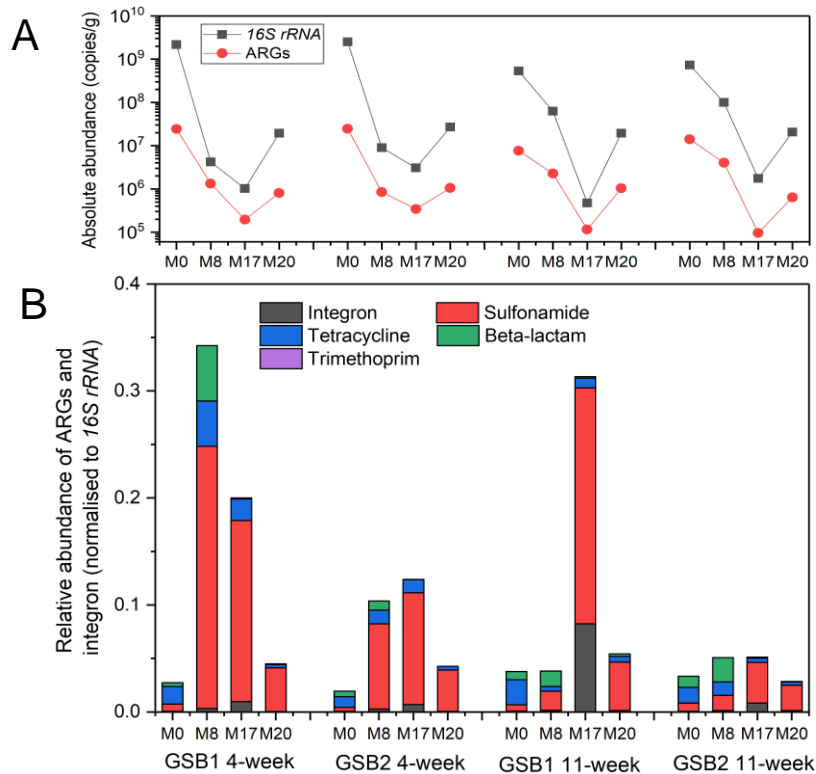


Figure 6.5 A): Absolute abundance of *16S rRNA* gene and total ARGs; **B):** Relative abundance of ARG categories and integron at each sampling site of GAC sandwich biofilter (GSB). Sample M0-M20 refer to biofilm collected at different sampling sites (0, 8, 17, and 20 cm).

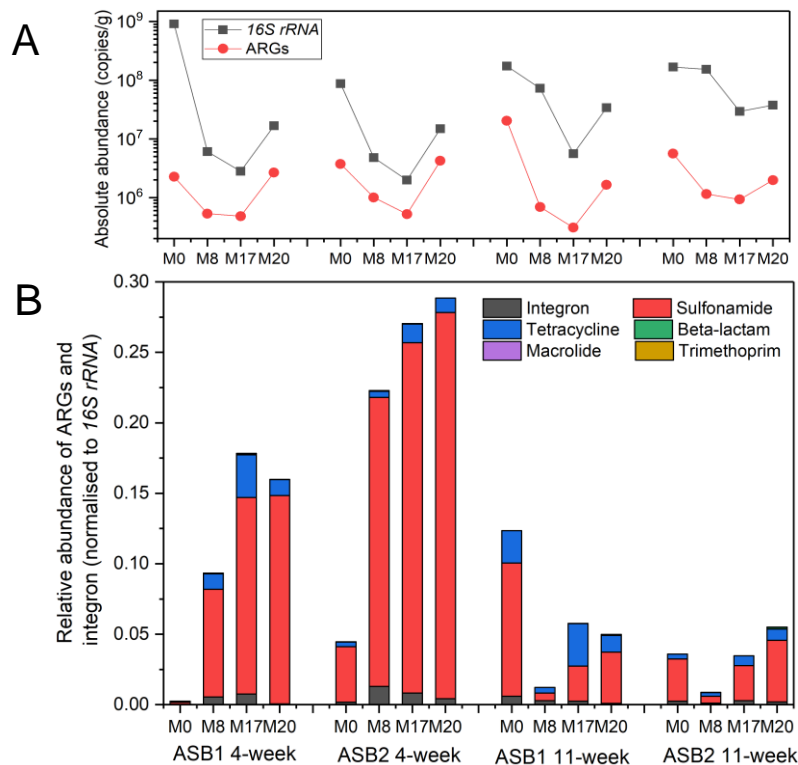


Figure 6.6 A): Absolute abundance of *16S rRNA* gene and total ARGs; **B):** Relative abundance of ARG categories and integron at each sampling site of anthracite-sand dual biofilter (ASB). Sample M0-M20 refer to biofilm collected at different sampling sites (0, 8, 17, and 20 cm).

Data in Figure 6.4 B show the relative abundance of ARG category and integron in GB biofilm samples. The copy numbers of *16S rRNA* gene in the lower layers (8-20 cm) of media biofilm samples collected in 11-week was significantly higher ($p < 0.01$) than that in 4-week samples (Figure 6.4 A). Similarly, the total ARGs abundance also increased over time, albeit not significantly. The overall ARG concentrations ranged between 5.65×10^6 and 1.87×10^7 copies/g in surface biofilm samples and between 7.94×10^4 to 2.13×10^6 copies/g in the lower layers. *Sul1*, *tetA*, *tetX* and *bla_{CTX-M}* were persistent in all GAC biofilm samples (Figure A6.2). After the addition of antibiotics, the relative abundance of integron genes increased significantly ($p < 0.01$) in both surface and lower layer biofilms, raising the mean concentration from 6.91×10^4 in week 4 samples to 8.27×10^5 copies/g in week 11 samples. Although no reference of ARGs variation within the GAC biofilm over time is available, research focused on ARG prevalence in drinking water treatment works has shown that the biofilm on a GAC filter influenced ARG profiles in the filtered water and the diversity of ARGs in water increased after GAC filtration [192]. This is also confirmed by another case study, where the number of detected ARGs raised significantly from 76 to 150 after GAC treatment [75]. The enhanced ARG and integron levels in GAC biofilm observed in this study suggest that they might pose a potential impact on the ARG profile in the filtered water.

For the sandwich filters, biofilm collected at 17 cm depth (M17) was GAC media and at 8 cm and 20 cm depth (M8 and M20) were sand media. Figure A6.3 shows the variation of individual ARG abundance in GSB biofilms. The concentration of *16S rRNA* gene in GAC biofilm was 1.17 log lower than that in sand. A similar trend was also found in ARG variations. Figure 6.5 B summarises the relative abundance of ARGs categories in biofilm samples. Despite the lower levels of *16S rRNA* gene and ARGs abundance observed, the relative abundance of ARGs in the GAC biofilm was the highest compared to sand in week 11 samples. This may be due to the adsorption capacity of GAC on antibiotics which could exert a selective pressure for the resistant bacteria in the biofilm, contributing to an enhanced relative abundance. The slightly increased levels of integrons in the GAC biofilm from 1.57×10^4

copies/g at week 4 to 2.68×10^4 copies/g at week 11 may also contribute to ARG transfer within the bacterial community developed in the GAC layer.

For the ASB, M8 and M17 represented anthracite biofilms, and M20 was a sand biofilm. Anthracite biofilms showed decreased *16S rRNA* gene and ARGs abundance with increasing depth (Figure 6.6 A and A6.4). The lower sand (20 cm) had higher surface microbial attached per gram of media than did the anthracite collected at 17 cm, and the abundance of *16S rRNA* gene (on average) was 9.90×10^6 and 2.57×10^7 copies/g in anthracite (M17) and sand (M20) biofilms, respectively. *Sul 1*, *sul 2*, *tet A* and *tetX* were present in all 16 biofilm samples. No difference of the relative abundance of ARGs was found between the two non-adsorptive media (Figure 6.6 B).

6.1.1.3 Comparison of ARGs behaviour between different biofilters

Due to the different types of biofilters used in this study, only relative abundance of ARGs was compared. No statistical difference was found between all duplicate biofilters. Figure 6.7 shows the total relative abundance of ARGs in surface (0 cm) and lower layer (8-20 cm) biofilms from different biofilters. It should be noted that the surface biofilms, which were affected directly from the feed and had the most abundant ARGs, revealed the lowest ARGs per bacterial cell ($p < 0.01$) compared to the deeper layer biofilms. This indicates that the proportion of ARGs-carrying bacteria was greater in the lower position. Little research has been conducted on the behavioural mechanisms of ARGs in different depths of filter columns, nor has this been investigated in the context of the impact of different types of media on ARG variation. Wan *et al.* have found a similar trend of an increasing ARG relative abundance in the lower depths of sand biofilms [193]. They concluded three possible reasons for the variation of antibiotic resistome with depth: 1) the consumption of organic carbon in the filter column may result in an increased diversity of resistant bacteria in the biofilm; 2) the oligotrophic environment is conducive to the survival of resistant bacteria; and 3) the fitness cost of bacterial antibiotic resistance is directly affected by the carbon source. Although organic carbon concentration was not monitored at different depths in the present study,

similar influent DOC level and DOC removal were observed compared to Wan *et al.*'s study [193], which could explain to a certain extent the variation of ARGs with depth in the biofilters.

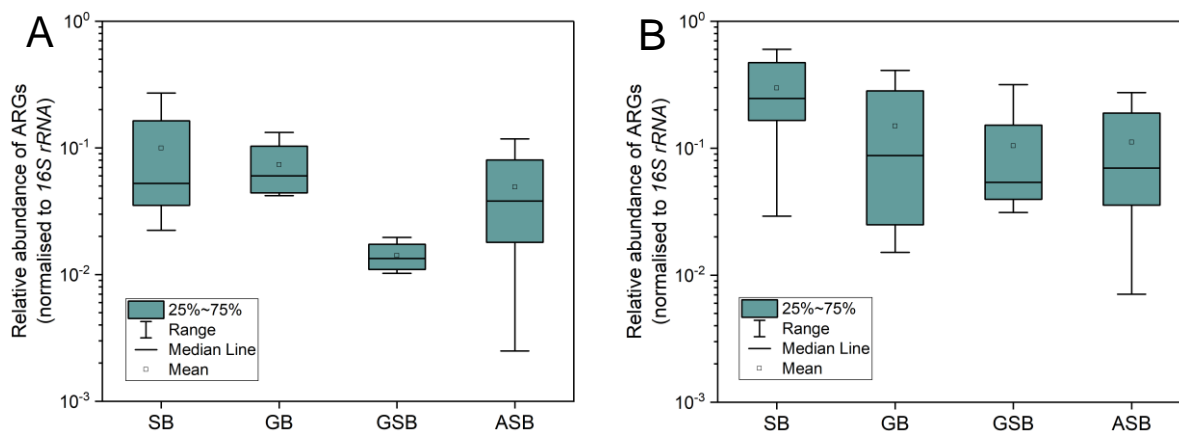


Figure 6.7 Relative abundance of ARGs (normalised to 16S rRNA gene) in **A): surface biofilms;** and **B): lower position biofilms from different biofilters.** SB: sand biofilter; GB: GAC biofilter; GSB: GAC sandwich biofilter; ASB: anthracite-sand dual biofilter.

Due to the differences in surface characteristics, media substrate could affect the behaviour of ARGs. Carbon-based media showed similar total relative abundance of ARGs, with anthracite biofilm varying the most. The two surface sand biofilms showed different relative abundance of ARGs, and this discrepancy may relate to the indigenous microbial community attached. Unlike media samples collected from the lower depth, surface biofilm samples consisted of a mixture of filter media and the slimy layer formed on top of the media (Figure A6.5). Once matured, the composition of this layer was dynamically balanced and affected directly by feedwater quality and indirectly by the possible sloughed biomass from the water inlet tubing, although this was minimised by replacing the tubing frequently. Therefore, in addition to the media type, the biofilm formed inside the smooth surface of water inlet tubing could also contribute to the differences seen in ARG profiles. For the biofilms obtained from the lower depth (Figure 6.7 B), SB showed significantly higher ($p < 0.05$) relative abundance of ARGs than the other three types of biofilters. Only a slight change in the ARGs' total relative abundance was observed between the two GAC-associated biofilters.

6.1.1.4 Lower layer sand biofilm comparison

Replacing sand with 9 cm of GAC in the middle of sand column or with 18 cm of anthracite affected bacterial activity in the underlying sand biofilm. For the biofilm samples collected at the same sampling site (20 cm), GSB-sand and ASB-sand had significantly higher ($p < 0.01$) abundance of *16S rRNA* gene than the SB-sand biofilm (Figure 6.8). However, this is not the case for the behaviour of ARGs and integrons. Higher levels of the relative abundance of ARGs and integrons were observed in SB-sand, while GSB-sand showed the lowest abundance. This could be attributed to two reasons: 1) the nutrients and DO concentration became limiting factors in the lower portion of the GSB column due to the strong adsorption capacity of middle layer GAC [258], these conditions may not be conducive to the growth of resistant bacteria; and 2) the sand microbial community in the lower depth of SB/ASB columns was continuously exposed to higher levels of antibiotics in the liquid phase than in the GSB, which may give rise to more resistant bacteria containing various ARGs in sand biofilm.

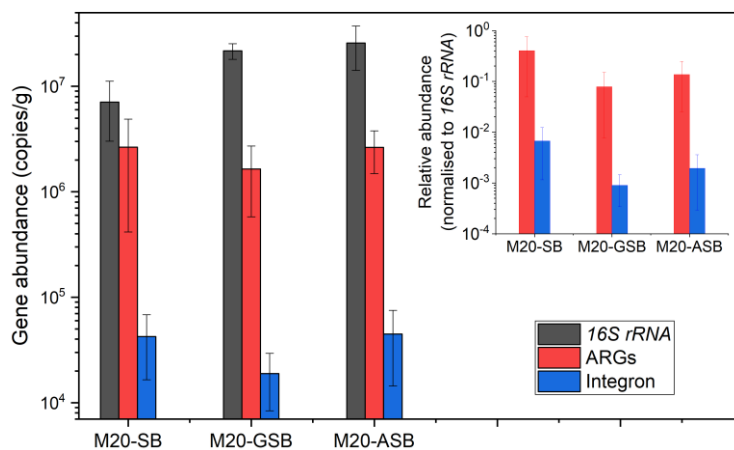


Figure 6.8 Comparison of sand biofilms collected at 20 cm (M20) in sand (SB), GAC sandwich (GSB) and anthracite-sand (ASB) biofilters. The error bars represent STD from the mean value of duplicate biofilm samples ($n = 2$).

6.1.2 ARGs in the aqueous samples

A total of five batches of influent and effluent samples were collected throughout this study, including the week after the addition of antibiotics (batch 1) and then every two weeks afterwards (batch 2-4). Samples were also collected after the backwashing/cleaning of

biofilters (batch 5). Raw water samples were included to investigate the pollution of ARGs in surface water and to provide background information on the ARGs profile.

6.1.2.1 ARGs in lake water samples

The concentrations of *16S rRNA* gene, individual ARG, and integrons, in Regent's Park Pond raw water samples are provided in Figure A6.6. Among all of the five batch samples, the copy numbers of ARGs ranged from 1.44×10^2 copies/L for *dfrA12* to 4.43×10^7 copies/L for *sul 1*. The levels of ARGs/integron abundance fluctuated over time, and 10 out of 15 target genes were present in all batch samples, including *intl 1* and *intl 2* which represent the ARGs transfer potential. In addition to the research of ARGs in London's surface water [284], the above findings further confirmed the wide spread of ARGs and integrons in the pond water in Regent's Park.

6.1.2.2 ARGs in the influent and effluent samples

Figure 6.9 shows an overview of the ARGs abundance in the influent and effluent samples. No statistical differences were found between the duplicate columns. Positive correlations in absolute abundance were found between the ARGs and *16S rRNA* gene and the integrons in water samples (Figure 6.10). The overall ARG concentration ranged from 2.96×10^6 to 1.86×10^8 copies/L in the influents and from 1.73×10^5 to 7.36×10^7 copies/L in the effluents. After filtration, 0.76-log, 0.66-log, 1.29-log and 1.15-log reduction in ARGs copy numbers were observed for SB, GB, GSB and ASB, respectively. Although the absolute abundance of ARGs in the effluent samples decreased for all biofilters, the ARGs' normalised copy number showed an increasing trend in the filtered water. *Intl 1* also showed a trend of increasing in relative abundance, although this trend fluctuated for duplicate biofilters. The significant positive correlations between ARGs and integron in both media biofilm and water samples indicated that horizontal gene transfer might occur not only in the biofilm community but also in bacteria in planktonic phase flowing near the biofilm [75], contributing to the increased levels of ARGs per bacterial cell in the filtered water. These findings are consistent with the findings in drinking water treatment works, where the relative abundance of ARGs increased after sand or GAC biofiltration [75, 140, 192].

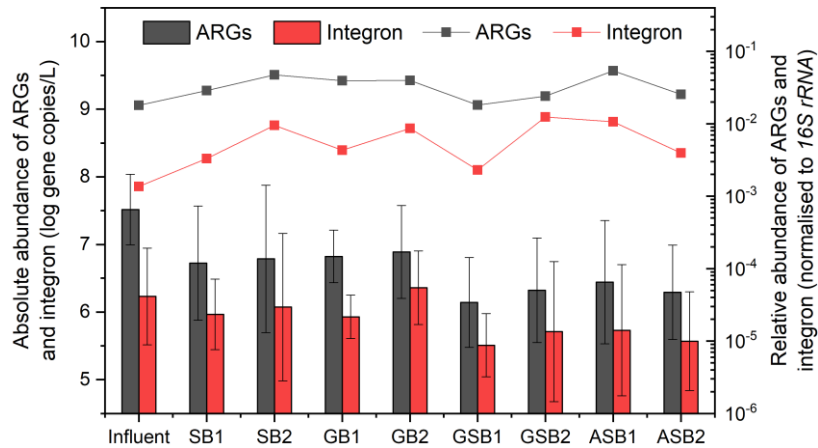


Figure 6.9 Absolute abundance (bar chart, left Y-axis) and relative abundance (line and symbol, right Y-axis) of ARGs and integrons in the influent and effluent samples. The error bars represent STD from the mean value of all batch samples ($n = 5$). SB: sand biofilter; GB: GAC biofilter; GSB: GAC sandwich biofilter; ASB: anthracite-sand dual biofilter.

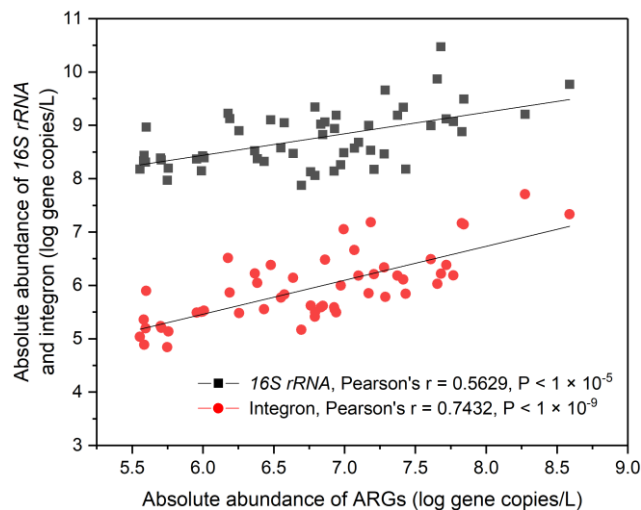


Figure 6.10 The correlations between the absolute abundance (copies/L, log transformed) of ARGs and the corresponding 16S rRNA gene and integron in influent and effluent samples.

The variation of individual ARGs and integron in the influents and effluents of all biofilters from batch 1 to 5 is shown in Figure A6.7. To reduce the impact of influent ARGs, log reductions of ARGs copy numbers in the effluents over time were compared (Figure 6.11). In general, the trends for the reduction of ARGs in GAC-associated biofilters (GB and GSB) were more stable than those in the biofilters using non-adsorptive media (SB and ASB). The sandwich biofilters showed the highest removal of ARGs in all batch samples. After the addition of antibiotics, the reduction of ARGs fluctuated greatly in batch 1 and 2 samples and

remained relatively stable in batch 3 and 4 samples. Backwashing and cleaning of biofilters did not affect the removal of ARGs significantly (Batch 5), especially for the GAC biofilter. No reference information on the impact of backwashing/cleaning on ARG behaviour is available, however, Kim *et al.* found that backwashing had no significant effect on the bacterial population and diversity in GAC biofilms [175], which might allow the GAC biofilter to function in a stable manner in terms of ARG reduction.

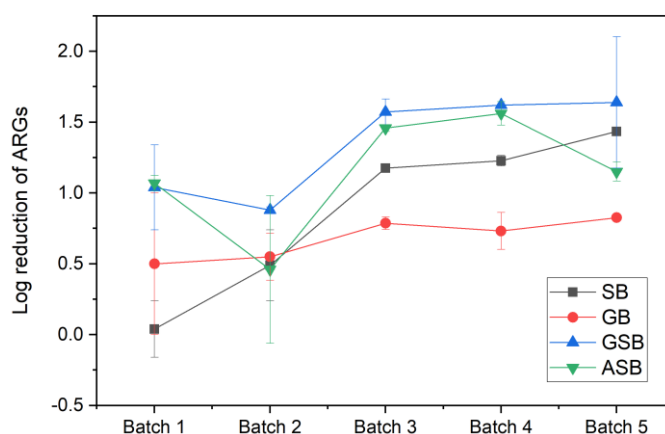


Figure 6.11 The reduction of the copy numbers of ARGs (log transformed) in all biofilters. The error bars represent STD from the mean value of duplicate biofilters (n = 2). SB: sand biofilter; GB: GAC biofilter; GSB: GAC sandwich biofilter; ASB: anthracite-sand dual biofilter.

6.1.3 Comparison of ARGs profiles in biofilm and aqueous samples

Pearson correlation analysis was conducted to study the correlations among the various types of ARGs and integron genes in both biofilm and aqueous samples (Table A6.2 and A6.3). Significant positive correlations were identified between the integrons and different classes of ARGs in all samples.

In biofilm samples, *intl 1* displayed significant correlations with the total concentrations of two classes of ARGs ($\sum sul$ and $\sum tet$) ($r = 0.60$ and 0.44 , respectively, $P < 0.01$). And in aqueous samples, *intl 1* was found to significantly relate to the total concentrations of three classes of ARGs ($\sum sul$, $\sum tet$ and $\sum bla$) ($r = 0.50$, 0.35 and 0.91 , respectively, $P < 0.05$). In addition, *intl 2* had strong and significant relationships with *dfrA1* and *dfrA12* ($r = 0.43$ and 0.53 , respectively, $P < 0.05$) in aqueous samples, as well as with all ARGs ($r = 0.64$, $P < 0.01$). Integron genes have been intensively detected in DWTPs and the association between

integrons and ARGs contributed to the persistence and spread of ARGs in drinking water distribution systems [75, 99]. Shi *et al.* have found that the gene cassettes carried on the integrons contain miscellaneous ARGs encoding resistance to all major antibiotic categories, including β -Lactam, aminoglycoside, sulfonamides, trimethoprim, tetracycline, streptomycin and chloramphenicol in the drinking water by metagenomic analysis [99]. The significant correlations observed between integron genes with ARGs indicated that class 1 and class 2 integrons play important roles in the dissemination of ARGs in the biofilms and filtered water through horizontal gene transfer.

Significant positive correlations ($P < 0.05$) were found between all types of samples (Table 6.1), indicating that the distributions of ARGs in the filtered water were affected by both raw water and biofilms formed in the filter column. Relative abundance of ARGs which was indicative of the proportion of bacteria carrying ARGs was compared for biofilm and aqueous samples. A heatmap showing the distinct patterns of the relative abundance of ARGs (normalised to *16S rRNA* gene) in raw water, influent, effluent, surface biofilm, and low layer biofilm samples is shown in Figure 6.12. Biofilm samples represented a higher risk of ARG levels per bacterial cell (6.61×10^{-3} on average) than in the aqueous samples (2.12×10^{-3} on average). Among the ARGs present, *sul 1* was the most persistent resistance gene in all types of samples. It should be noted that the β -lactam resistance genes (*bla*) accumulated considerably more (20-fold) in biofilms than in the aqueous samples, probably due to the continuous exposure of the biofilm microbial community to higher concentration of amoxicillin.

Table 6.1 The correlation of the relative abundance of ARGs between raw water, influent, effluent, surface biofilm and lower layer biofilm samples.

Sample type	Surface biofilm	Lower layer biofilm	Raw water	Influent	Effluent
Lower layer biofilm	0.895				
Raw water	0.524*	0.801			
Influent	0.614*	0.900	0.912		
Effluent	0.783	0.944	0.808	0.908	

* $P < 0.05$; All other P values < 0.001 .

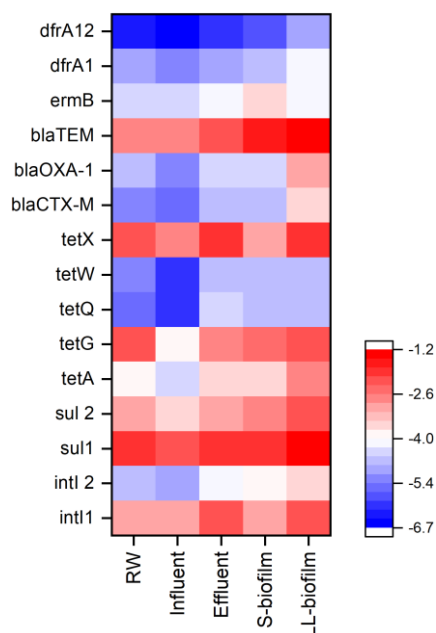


Figure 6.12 A heatmap showing the distinct patterns of the relative abundance of ARGs (normalised to *16S rRNA* gene) in raw water (RW), influent, effluent, S-biofilm (surface biofilm), and LL-biofilm (low layer biofilm) samples.

6.1.4 Bacterial community in filter biofilm

Few previous studies have investigated the composition of bacterial communities in the surface biofilm formed on different media types, while many researchers focused on a single medium used in biofiltration [173, 193, 286]. This study investigated the bacterial community structure in surface biofilms formed on sand, GAC and anthracite by high-throughput sequencing of the *16S rRNA* gene. A total of 1,069,777 tags with an average of 116,226 high quality tags per sample were obtained. These sequences were clustered into 3313 OTUs at the 97% similarity level. The dominant phyla in all samples were *Proteobacteria* (51.9%), *Actinobacteria* (13.5%), *Bacteroidetes* (8.5%), *Firmicutes* (7.6%), and *Acidobacteria* (5.2%), accounting 87% of the total bacterial communities (Figure 6.13). No statistical differences were found between duplicate biofilters at the phylum level. Further analysis has shown that at class level, *Alphaproteobacteria* and *Betaproteobacteria* were more predominant in GAC than sand and anthracite (Figure A6.8). As the second most abundant phylum, *Actinobacteria* was more abundant in sand biofilm communities (SB and GSB).

Bacteroidetes was the third most abundant phylum in surface biofilms, which was attributed to its member classes *Sphingobacteriia* and *Cytophagia*. The *Firmicutes* were primarily composed of class *Clostridia*, which occupied 5.7%, 4.4% and 3.1% in sand, GAC and anthracite biofilms, respectively. Previous research has also reported similarities in microbial taxa in biofilters [192, 287, 288], but the corresponding percentage differed by filter type (e.g., relative abundance of *Proteobacteria*: GAC > sand > anthracite).

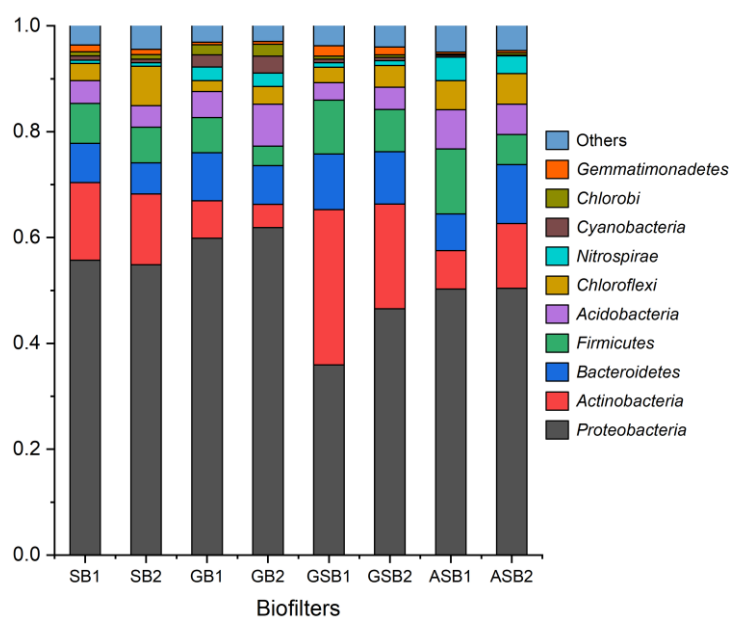


Figure 6.13 Structure of surface biofilm microbial community at phylum level. SB: sand biofilter, GB: GAC biofilter; GSB: GAC sandwich biofilter; and ASB: anthracite-sand biofilter.

At genus level, *Sulfuritalea* and *Sphingobium*, which belong to the *Proteobacteria*, were the dominant genus in sand and GAC surface biofilms, respectively (Figure 6.14). *Bacillus*, within the *Firmicutes*, was the most abundant genus in anthracite. Typical genera associated with opportunistic human pathogens were observed in this study. The genera *Bacillus*, *Legionella*, *Mycobacterium*, and *Pseudomonas* were present in all biofilm samples, and their relative abundance was up to 8.6% (Table 6.2).

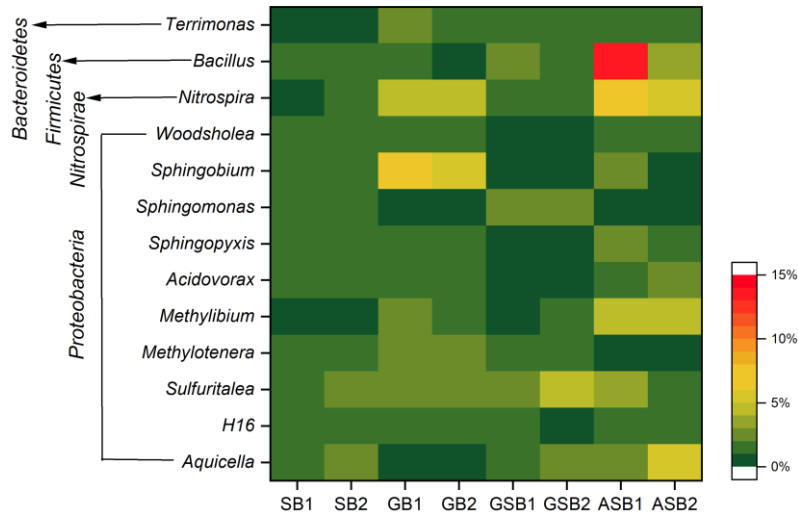


Figure 6.14 Relative abundance of each taxonomic genus (>1 % in any sample) in the surface biofilm samples of sand biofilter (SB), GB (GAC biofilter), GSB (GAC sandwich biofilter), and ASB (anthracite-sand biofilter). The colour intensity in each panel shows the percentage of each genus in one sample.

Table 6.2 The percentage relative abundance of genera associated with opportunistic human pathogens.

Genera	SB1	SB2	GB1	GB2	GSB1	GSB2	ASB1	ASB2
<i>Acinetobacter</i>	1.280	0.258	0.033	0.035	0.161	0.154	0.066	0.069
<i>Aeromonas</i>	0.544	0.101	0.017	0.020	0.016	0.020	0.032	0.004
<i>Bacillus</i>	1.293	0.989	0.649	0.499	1.893	1.145	8.589	2.060
<i>Clostridium</i>	0.140	0.056	0.015	0.016	0.183	0.017	0.008	0.011
<i>Escherichia</i>	0.023	0.078	0.004	0.018	0.018	0.372	0.001	0.039
<i>Legionella</i>	1.009	0.795	0.369	0.311	0.081	0.134	0.239	0.252
<i>Mycobacterium</i>	0.255	0.301	0.477	0.554	0.199	0.358	0.845	1.288
<i>Pseudomonas</i>	0.079	0.075	0.095	0.076	0.409	0.547	2.003	1.138
<i>Streptococcus</i>	0.003	0.013	0.003	0.006	0.018	0.045	0.079	0.013

SB: sand biofilter, GB: GAC biofilter; GSB: GAC sandwich biofilter; and ASB: anthracite-sand biofilter.

Based on the Bray-Curtis distance, PCoA showed that the duplicate biofilters were clustered together and separated from other biofilter types (Figure 6.15), indicating that the filter substrate plays an important role in determining bacterial community composition. The first two PCs explained a total of 84.5% variance in the bacterial community, with PC1

explaining 60.7% and PC2 explaining 23.8% of the variance. The distant positioning of SB and GSB in the PCoA plots suggests differences in bacterial community structure between the two surface sand biofilms, and this may be due to the long-term effect of the inherent microflora in the feedwater bottles. In addition to the filter substrate, biofilm formation rate could also affect community structure as different microorganisms thrive in the filters depending on the overall biological activity [272].

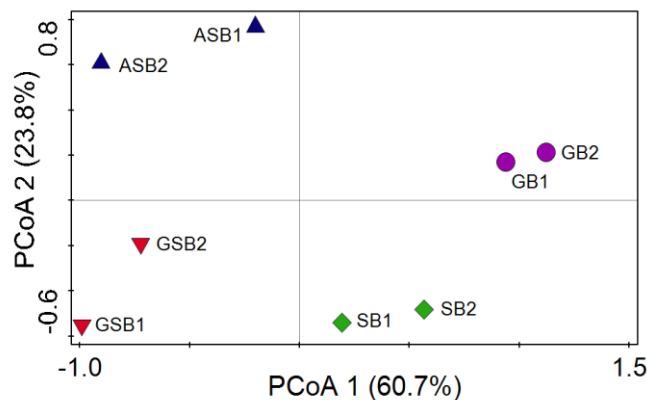


Figure 6.15 Principal coordinate analysis (PCoA) based on the Bray-Curtis distance showing the overall distribution of bacterial communities in surface biofilm samples. SB: sand biofilter, GB: GAC biofilter; GSB: GAC sandwich biofilter; and ASB: anthracite-sand biofilter.

6.1.5 Relationship between water quality, antibiotics, ARGs and bacterial community

6.1.5.1 Water quality parameters, antibiotics and ARGs

Potential links between the environmental conditions and the relative abundance of ARGs in effluent samples were explored by RDA, using the water quality parameters as an explanatory matrix. Results showed that most chosen ARGs were associated with the nutrient levels (DOC, nitrate and phosphate) in effluent samples (Figure 6.16A). However, Pearson correlation analysis showed no significant correlation between them (Table A6.4). The lack of correlations was further confirmed by VPA, where the environmental factors only contributed 15.7% on the change of ARGs (Figure 6.16B). The contribution of *intl 1* (3.3%) was similar to their joint effects (5.9%). As discussed above in section 4.4.3.3, the ARG profiles in the effluent were likely affected by both raw water, influent and biofilm according to the Pearson correlation analysis. The relative stability of raw water may limit the impact of environmental factors on

ARG. The lake water used as biofilter feed only exposes to natural conditions and limited human activities, therefore, the lack of environmental stresses such as antibiotics, heavy metals, or oxidative stresses [223] may limit the proliferation of ARGs in the raw water.

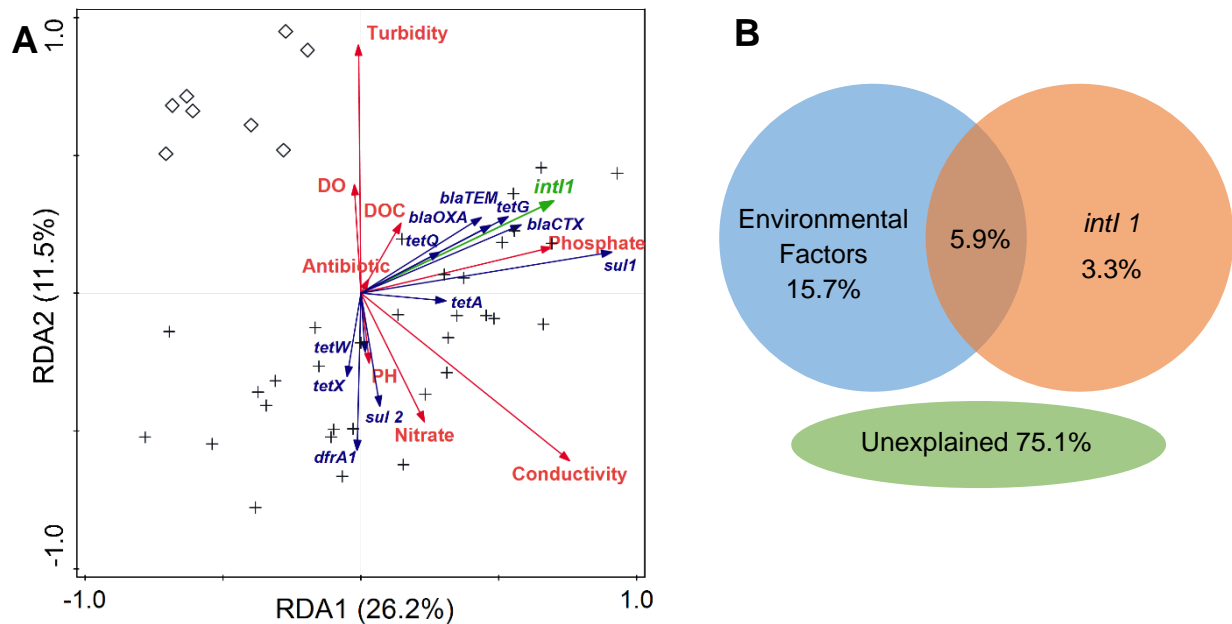


Figure 6.16 Redundancy analysis (RDA) of the correlation between ARGs/*intl 1* and environmental variables (A) and variation partitioning analysis (VPA) differentiating effects of environmental factors and *intl 1* on the ARGs variation (B) in effluent samples. The lengths of the arrows reveal the strength of the relationship and the angles between arrows indicate the correlation between different variables. Cross scatters: a total of 32 effluent samples after the addition of antibiotics; diamond scatters: 8 effluent samples after biofilter backwashing/cleaning. *Intl 2* and *ermB* were excluded from the analysis due to the low detection frequencies.

Although *intl 1* was significantly and strongly correlated to most of the ARGs, the low contribution of *intl 1* indicated that other HGT vehicles (e.g. transposons) may also contribute to the propagation of ARGs in the effluent. These results implied that environmental factors and *intl 1* were not the dominant mechanisms driving ARG variation in the filtered water. Environmental variables, such as temperature, heavy metals, nutrients, oxygen depletion, chemical residues and pH can affect functional gene distribution by altering the bacterial community [191, 193, 209, 223]. As a result, the bacterial community is generally considered a major factor in shaping the resistome in a specific environmental matrix. For instance, Zheng *et al.* reported a 3.77% contribution of MGEs and 50.44% of bacterial community to the change

in the resistome in samples collected from a drinking water biological GAC filtration process [192]. Furthermore, bacterial communities (57.22% contribution) and MGEs (16.63%) were found to drive the resistome in drinking water chlorination [223]. A study on mariculture discovered that nutrients and the bacterial community could explain a total of 45.5% of variance in the ARGs [209]. These studies suggest that bacterial communities may also play important roles in altering ARGs profiles in the effluent in the present study. This is further discussed in the context of the surface biofilms samples in the following section.

It should be noted that all target ARGs were not significantly correlated to antibiotics in the effluent. Although ARG abundance was higher in both the biofilm and effluent samples after the addition of antibiotics, no statistical difference was found before and after the antibiotics spike. This may be due to the lack of detectable antibiotics in the raw water, or because the amount of antibiotics spiked to the feed (2 and 5 µg/L) was not sufficient to exert a selective pressure for genotypic resistance. Lundström reported a possible minimal selective concentration (MSC) range for tetracycline for the selection of a set of *tet* genes, including *tetA* and *tetG*, estimated to be around 1-10 µg/L in aquaria biofilm samples [122]. Much higher MSCs ranging from 2 to 125 µg/L were reported by Bengtsson-Palme and Larsson in order to select phenotypically resistant bacteria to the five target antibiotics [289]. These findings could explain the negligible effect of antibiotics to ARG variation in this study. However, to date, no studies can be found investigating the effect of antibiotics on the behaviour of ARGs in the biofiltration process. Previous research is generally based on simplified competition situations without the presence of much more complex bacterial communities with a large diversity of ARGs. The roles antibiotics and the bacterial community play in the variation of ARGs during biofiltration need further clarification.

6.1.5.2 Bacterial community, ARGs and integrons

Bacterial phyla were considered as the environmental factors affecting ARG variation in RDA. The analysis explained that 90.6% of the variance in ARGs could be explained by the selected variables with the first two axes (Figure 6.17). Most chosen ARGs correlated to *Proteobacteria*, *Acidobacteria* and *Nitrospirae*, which accounted for 51.9%, 5.2% and 2.0% of

the bacterial phyla in biofilm communities, respectively. In contrast, the variations of β -lactam resistance genes were correlated to *Actinobacteria* and *Bacteroidetes*. Huerta *et al* found that the bla_{TEM} is associated with *Actinobacteria* in water samples collected from man-made reservoirs, which is consistent with the observations in study [290]. In literature, β -lactamases genes have also been found in the members of phylum *Actinobacteria*, such as *Leucobacter komagatae* (bla_{TEM}) isolated from drinking water and *Acidothermus* (bla_{TEM} and bla_{CTX}) isolated from soil samples [291]. Liu *et al.* have reported that the phylum *Bacteroidetes* harbours 37 ARGs, including *tetA* and *tetX*, *sul 2*, and bla_{OXA} , in activated sludge samples [292]. *Bacteroides*, member of phylum *Bacteroidetes*, harbour a variety of transmissible elements that are involved in the dissemination of ARGs [293]. Previous study has found a strong correlation between bla_{TEM} and *Bacteroides* in hospital effluent [130]. *Sphingobacterium*, a genus belongs to phylum *Bacteroidetes*, showed significant positive correlation with bla_{TEM} and bla_{CTX} in aquaculture pond samples [291]. These observations indicated that phylum *Actinobacteria* and *Bacteroidetes* may be the host for β -lactam resistance genes.

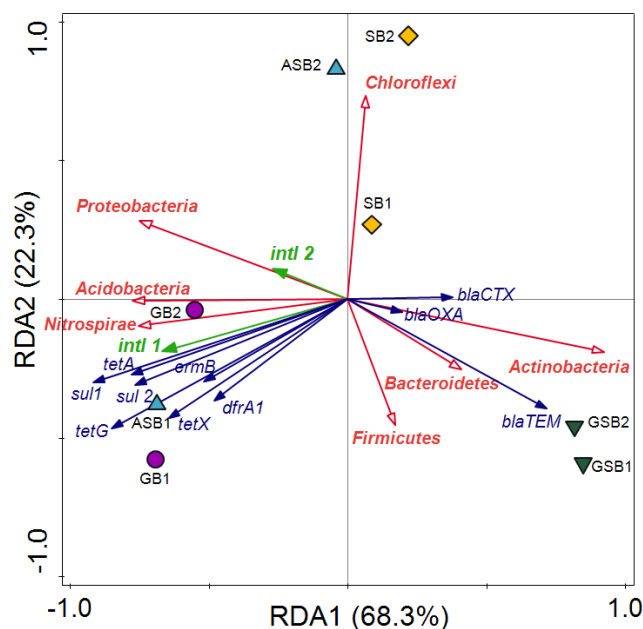


Figure 6.17 Redundancy analysis (RDA) of the correlation between major phyla (1% in any samples) and target ARGs and integron genes (*intl 1* and *intl 2*) in surface biofilm samples. The lengths of the arrows reveal the strength of the relationship and the angles between arrows indicate the correlation between specific genes and major phyla. *TetQ* and *tetW* were excluded from the analysis due to the low detection frequencies.

Int1 was associated with *Nitrospirae* in biofilm samples. Notably, previous studies have described *Nitrospirae*-related *intl* genes. *Nitrospirae* strains isolated from acid mine drainage biofilm have shown to carry both integrase and ARGs (e.g. beta-lactamase) on chromosomes [294], and an *intl* gene cassette was carried by the *Nitrospirae* phylum isolated from the sediment of a metal-rich stream [295]. Although *Nitrospirae* was found to correlate with most chosen ARGs, it is unclear whether *Nitrospirae*-related *intl* genes have contributed to ARG transfer in biofilms. It should be noted that GAC media were more closely related to *intl 1* than other biofilters, suggesting a greater extent of integron-mediated ARGs exchange in GB. The superior adsorption capacity of GAC may lead to an accumulation of antibiotics within the biofilm and consequently exert a selective potential. For example, research in DWTPs has reported enhanced ARGs diversity and abundance in GAC biofilms and filtered water [75, 192]. Pearson correlations between the relative abundance of ARGs and major bacterial phyla are summarised in Table A6.5. To differentiate the effects of the bacterial community and integrons on the change of ARG composition in surface biofilms, VPA showed that a total of 77.7% variance of ARGs could be explained by selected variables in the biofilm samples (Figure 6.18). Bacterial community explained the largest variation (55.3%), which is similar to the contributions of 50.44% and 57.22% observed in previous drinking water-related research [192, 223]. The integron explained 7.9% of the variation of ARGs, and the joint effect of bacterial community and integron contributed 14.5% on the ARG variation.

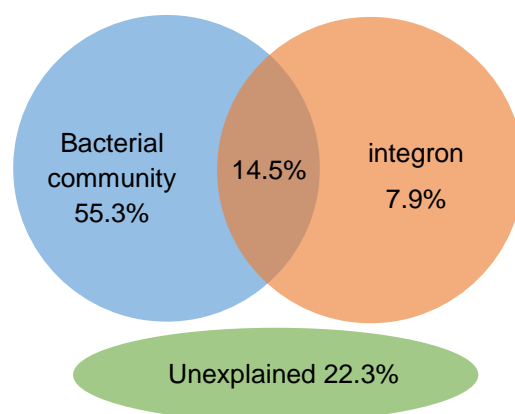


Figure 6.18 Variation partitioning analysis (VPA) differentiating effects of microbial community and integron on the ARGs variation in surface biofilm samples. *TetQ* and *tetW* were excluded from the analysis due to the low detection frequencies.

In the context of microbial risk, it is essential to investigate the microbial composition in the filter media as they dictate the microbiological quality of the filtered water and shape the bacterial community structure in the drinking water microbiome [272, 286]. Previous studies observed some pathogenic species (e.g. *Klebsiella pneumoniae* and *Aeromonas hydrophila*) in GAC media and they were released to the effluent by shedding from the biofilters [296]. The opportunistic human pathogens (e.g. *Pseudomonas spp.*, *Acinetobacter spp.*, and *Legionella spp.*) found in surface biofilms in this study may be unintentionally released to the filtered water and pose potential risks to distribution waters.

6.1.6 Summary

- Results showed that although the absolute abundance of ARGs decreased (0.97-log reduction on average), the ARGs' normalised copy number showed an increasing trend in the filtered water. In fact, according to the higher relative abundance of *intl 1* in the effluent, the biofiltration process seemed to increase the resistance gene transfer potential in the treated water.
- Biofilm samples represented higher risk of ARG pollution than in the aqueous samples; Surface biofilms revealed the lowest relative abundance of ARGs compared to the deeper layer biofilms, indicating that the proportion of ARGs-carrying bacteria was greater in the lower position.
- General water quality parameters and *intl 1* were not the dominant mechanisms driving ARG variation in the filtered water.
- ARGs were correlated to *Proteobacteria*, *Acidobacteria* and *Nitrospirae* in biofilms. Redundancy analysis implied that the bacterial community and presence of integrons contributed a total of 77.7% of variance in ARGs in the surface biofilm samples.

6.2 Biofiltration experiment 2 – different types of GAC sandwich biofilters

Surface biofilms, GAC biofilms was collected from all biofilters before the addition of antibiotics and at the end of the system run. Paired influent and effluent were taken every two weeks for qPCR analysis. To further explore the behaviour of ARGs in surface biofilms, the *schmutzdecke* layer and top layer of sand (hereafter referred to as B-*schm* and B-sand, respectively) collected at the end were separated for DNA extraction and qPCR analysis.

6.2.1 The occurrence of ARGs in the River Thames

The presence and abundance of the target genes in the River Thames did not show much variation over the experimental period (Figure 6.19). A decreasing trend in *16S rRNA* abundance was observed over time, lowering from 8.45×10^9 copies/L in July to 2.88×10^9 copies/L in September. All ARGs were present in raw water samples, among which *tetG* had the highest abundance (2.53×10^7 copies/L on average), followed by *sul1* (6.08×10^6 copies/L on average) and *bla_{OXA-1}* (4.19×10^6 copies/L on average). *DfrA12* was less prevalent in raw water. The levels are within the same range of ARG concentrations as in a previous survey conducted in 2017 [284], indicating the ubiquitous presence of ARGs in London's surface water. Therefore, the inherent ARGs and integron genes in raw water likely act as the source for the biofiltration system.

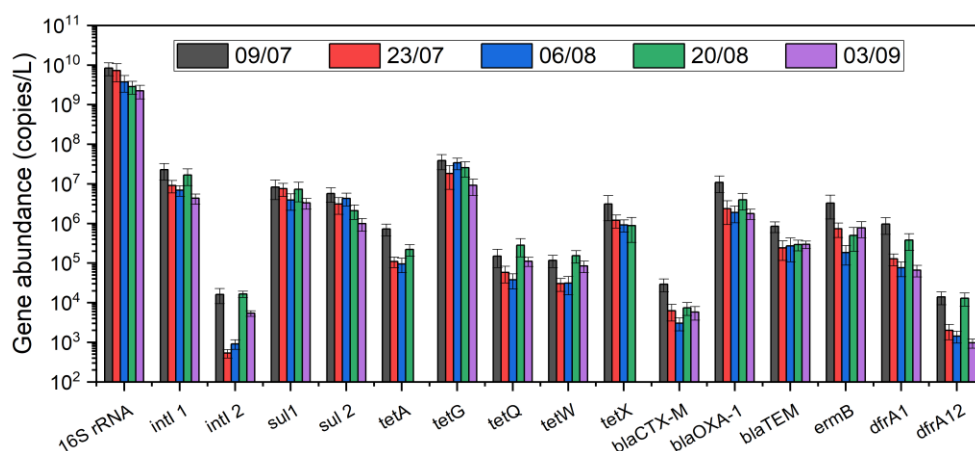


Figure 6.19 The concentration of *16S rRNA*, ARGs and integron genes in raw water samples over time. The error bars represent STD from the mean value of qPCR replicates ($n = 3$).

6.2.2 ARGs in biofilm samples

6.2.2.1 Conventional qPCR

1) ARGs richness

The number of ARGs detected in all biofilm samples is summarised in Table 6.3. In general, biofilms within the *schmutzdecke* layer (B-*schm*) showed highest ARG richness in 11-week's samples, followed by GAC (B-GAC) and sand (B-sand). Comparing the numbers in 3-week and 11-week samples, the number of detected ARGs increased from 52 to 72 in B-sand and from 62 to 86 in B-GAC, respectively. Despite their presence in raw water, *tetQ*, *tetW*, and *ermB* were either absent or present in only one biofilm sample before the spike of antibiotics. It should be mentioned that the detection frequency of *dfrA1* and *dfrA12* genes was consistently higher in B-GAC (71.9% on average) than in B-sand (28.1% on average), indicating that the *dfrA* carrying bacteria was more competitive within the GAC biofilm communities. Interestingly, the number of detected ARGs also increased in the control system (Set B) without the addition of antibiotics to the feed, although to a lesser extent compared to Set A. In addition to the antibiotics and ARGs found in the raw water, Set B may also be exposed to other classes of antibiotics or antibiotic-like environmental pollutants (e.g. heavy metals and disinfectants), which are important contributors to the spread of antibiotic resistance in aquatic environments [99, 106]. More ARGs were detected in Set A, indicating the spike of the target antibiotics may impose a selective pressure for antibiotic resistance in microbial communities during filtration.

Table 6.3 Richness of ARGs in biofilm samples.

Samples	3-week			11-week		
	Set A (antibiotic -)	Set B (antibiotic -)	Total	Set A (antibiotic +)	Set B (antibiotic -)	Total
B-sand	27	25	52	40	32	72
B- <i>schm</i>	n.a.	n.a.	n.a.	50	46	96
B-GAC	29	33	62	42	44	86
Total	56	58	-	132	122	-

B-sand: biofilms collected from surface sand; B-*schm*: biofilms collected from *schmutzdecke* layer; B-GAC: biofilms collected from GAC layer.

2) Behaviour of ARGs in 3-weeks' biofilm samples

After three weeks of operation, eight surface sand biofilm replicates showed similar levels of both absolute and relative abundance of ARGs and *intl 1* (Figure 6.20 A) as expected. Total ARGs abundance ranged from 1.54×10^6 copies/g to 6.08×10^6 copies/g in surface sand, and the relative abundance ranged from 1.90×10^{-2} to 3.97×10^{-2} . For GAC biofilms, the concentration of ARGs decreased with increasing depth (Figure 6.20 B). Data of individual ARG are provided in Figure A6.9 in the appendix. In general, duplicate biofilters showed similar trends with respect to the behaviour of ARGs and *intl 1*, which reduce bias in assessing the effect of antibiotic on the variation of ARGs and microbial community structure in the following experimental stage.

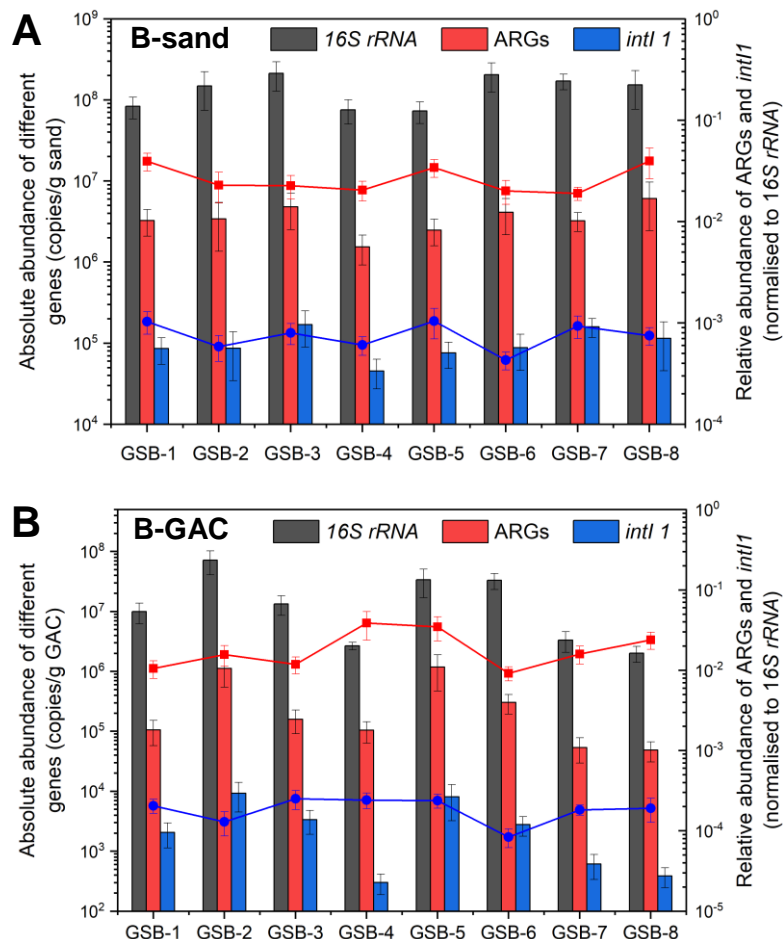


Figure 6.20 The absolute (bars) and relative (lines) abundance of ARGs and *intl 1* in **A: surface sand biofilm (B-sand)** and **B: GAC layer biofilm (B-GAC)** samples. The error bars represent STD from the mean value of qPCR replicates (n = 3).

3) Behaviour of ARGs in 11-weeks' biofilm samples

When all of the biofilters reached maturation, target antibiotics were added to Set A at 10 µg/L continuously for 8 weeks. Results showed that higher values of ARGs and *intl 1* (both the absolute and relative abundance) were consistently found in Set A than the control system (Figure 6.21 and 6.22), indicating an effect of the antibiotic selective pressure on microbial activity. Similar levels of the absolute abundance of ARGs were found in all GAC biofilms. This may indicate a homogeneous distribution of resistant bacteria within the GAC layer in different positions. The biofilms of 4-cm GAC layer loaded at upper and middle of filter bed represented similar level of ARGs risks in terms of the relative abundance (0.071 at upper layer and 0.066 at middle layer, respectively), where lower position GAC layer showed the least ARG risks (0.046). Similar trend was also observed for the variation of *intl 1*.

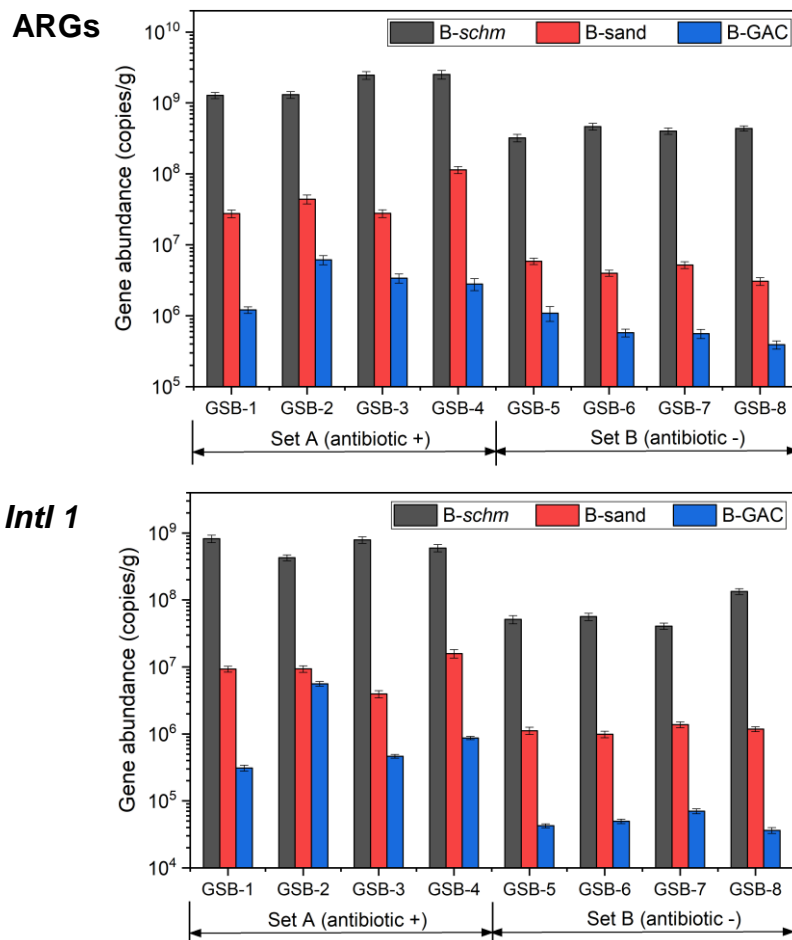


Figure 6.21 Absolute abundance of ARGs and *intl 1* in *schmutzdecke* (B-*schm*), sand (B-*sand*) and GAC (B-*GAC*) biofilm samples collected at 11-week. The error bars represent STD from the mean value of qPCR replicates (n = 3).

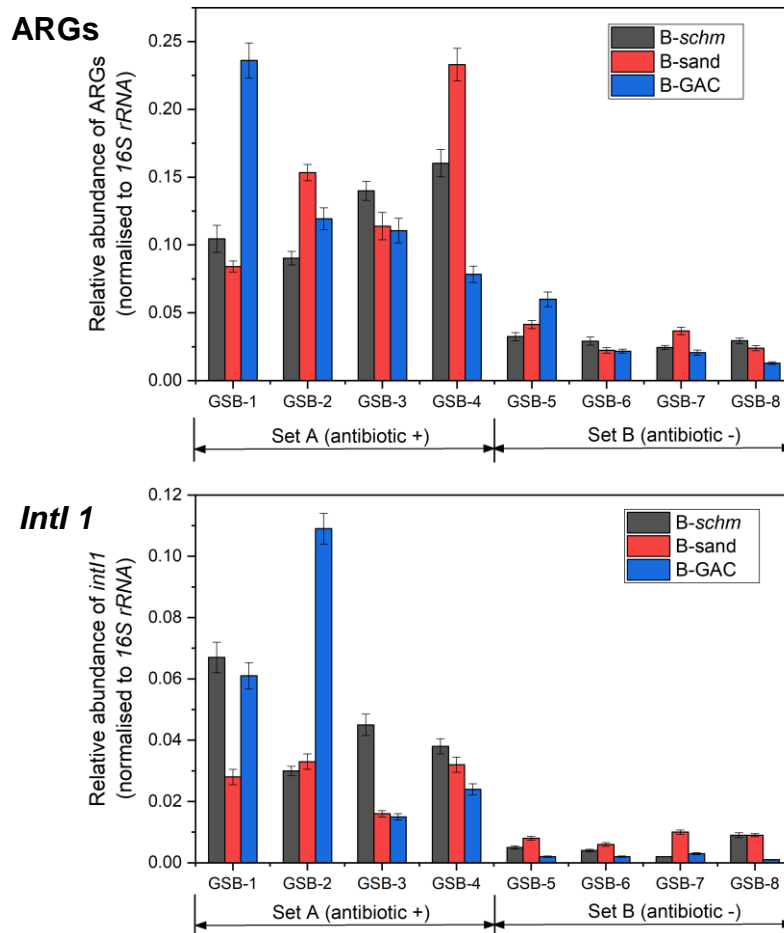


Figure 6.22 Relative abundance of ARGs and *int1* (normalised to *16S rRNA*) in *schmutzdecke* (B-schm), sand (B-sand) and GAC (B-GAC) biofilm samples collected at 11-week. The error bars represent STD from the mean value of qPCR replicates (n = 3).

The absolute abundance of individual genes in B-sand, B-schm, and B-GAC is summarised in the appendix (Figure A6.10 – A6.12). Despite the increase of the overall abundance of ARGs in Set A, variations in individual ARG enrichment were observed in different types of biofilms. For instance, *tetX* enriched 104-fold, 5-fold and 29-fold in B-sand, B-schm and B-GAC, respectively, when exposed to antibiotics compared to the control biofilms. By contrast, *sul1* showed consistent enrichment in Set A ranging from 4-fold in B-schm to 7-fold in B-GAC. *Int1* increased significantly ($p < 0.01$) in GAC biofilms (37-fold) compared to surface biofilms (9-fold), indicating a higher potential of horizontal gene transfer within the GAC microbial community under the selective pressure. The discrepancies mentioned above may relate to the specific bacterial communities developed on the media

surface. In addition, the difference of ARGs and *intl 1* levels in biofilms before and after exposure of antibiotics suggests that the target antibiotics affect the behaviour of ARGs during biofiltration.

6.2.2.2 High-throughput qPCR (HT-qPCR)

1) Richness and diversity of ARGs

In addition to the conventional qPCR assays, biofilm DNA of the eight *schmutzdecke* and eight GAC media collected at the end of system operation were also sent for HT-qPCR analysis. Results of HT-qPCR indicated that a total of 155 and 141 ARGs were detected in the B-*schm* and the B-GAC, respectively. These ARGs can confer resistance to almost all the major classes of antibiotics commonly administered to humans, including aminoglycoside, beta-lactams, FCA (fluoroquinolone, quinolone, florfenicol, chloramphenicol and amphenicol), MLSB (Macrolide-Lincosamide-Streptogramin B), multidrug, sulfonamide, tetracycline, and vancomycin. The richness of detected ARGs was generally identical in the B-*schm* replicates in each Set, ranging from 125 to 134 in Set A and from 104 to 116 in Set B, respectively (Figure 6.23 A). Specifically, the richness and Shannon diversity of ARGs were higher in Set A compared to the control system, which is consistent with the trend observed by conventional qPCR analysis (as shown in Table 6.3). Beta-lactamase resistance genes contributed the most (from 86 to 110 in total) to the increased richness in the B-*schm* in Set A, probably due to continuous exposure to amoxicillin during the experimental period. The number of detected ARGs classified based on the mechanism of resistance is shown in appendix (Figure A6.13). Antibiotic deactivation and efflux pump were the two dominant resistance mechanisms, accounting for 81.9% of all ARG subtypes. The number of detected ARGs classified as encoding antibiotic deactivation was slightly higher when exposed to antibiotics, and accordingly, the percentage of efflux pump mechanism was higher in the control biofilms. In particular, numbers of detected efflux pump ARGs became predominant (43.7%) in B-GAC in Set B, mainly due to the contribution of *tet* genes.

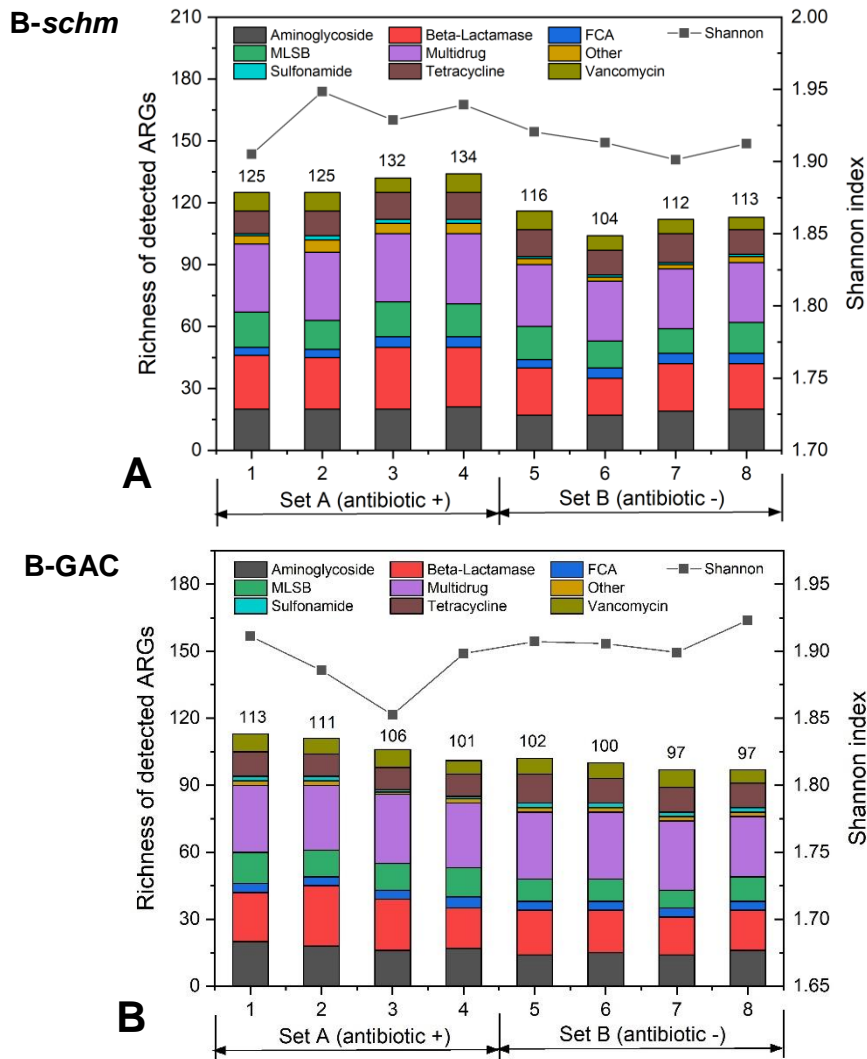


Figure 6.23 Richness of detected ARGs and Shannon index indicating diversity of detected ARGs in A: *schmutzdecke* biofilms (B-*schm*) and B: GAC biofilms (B-GAC). 1-8 indicate the eight biofilters. MLSB = Macrolide-Lincosamide-Streptogramin B resistance genes; FCA = fluoroquinolone, quinolone, florfenicol, chloramphenicol and amphenicol resistance genes.

Although fewer numbers of ARGs were detected in GAC biofilms, they hosted a similar diversity of ARGs profiles compared to B-*schm* (Shannon index on average: B-GAC = 1.90 and B-*schm* = 1.92), suggesting that all ARG categories decreased in richness along the filter. This is also confirmed by the decreasing numbers of ARGs detected in lower position B-GAC (Figure 6.23 B). Interestingly, unlike B-*schm*, an opposite trend of higher ARGs diversity was found in B-GAC in Set B. A possible explanation is that the bacterial community within the *schmutzdecke* layer was only exposed to lower concentration of antibiotics in the planktonic phase when water flowed, where above 90% of antibiotics can be adsorbed by GAC.

Consequently, the antibiotics accumulated within the GAC layer may reach the minimum inhibitory concentration for the growth of some specific bacterial communities, contributing to a lower ARGs diversity in GAC biofilms in Set A. The correlation between the ARGs diversity and the bacterial community is discussed in detail later in this chapter.

2) Relative abundance of ARGs

Data in Figure 6.24 show the relative abundance of ARG category (normalised to 16S *rRNA*) of each sample in order to minimise the variations caused by the background bacterial population. Multidrug resistance genes were predominant in all samples. B-*schm* exposed to antibiotics represented the highest risks of ARGs pollution (biofilters 1-4). Compared to the control system, aminoglycoside, MLSB, sulfonamide and vancomycin resistance genes were significantly enriched ($p < 0.01$) when exposed to antibiotics, among which *ereA* and *ermF*, two macrolide resistance genes achieved the highest enrichment (112-fold and 44-fold, respectively). *aadA-01* was the most enriched (37-fold) aminoglycoside resistance gene in B-*schm* in Set A.

It should be noted that the co-selection of aminoglycoside and vancomycin resistance gene (*van*) was observed in B-*schm*, with their relative abundance enriched significantly ($p < 0.001$) in Set A. *Van* gene has been widely detected in water-related matrix such as dairy farm water, municipal wastewater, surface water, and drinking water biofilms [79]. The cluster of genes encoding high-level resistance to vancomycin are typically located on transposons of the Tn1546 type [297] and *vanA* can be transferred together with MLSB resistance genes *ermB* and *vatE* [298]. The co-transfer of vancomycin- and MLSB- resistance genes may occur at the same time in B-*schm* under selective pressure from clarithromycin. Furthermore, a significant positive correlation of the relative abundance of ARGs was found between vancomycin and MLSB ($r = 0.89$, $P < 0.0001$) in B-*schm*. As vancomycin is recognised as a 'last-resort' life-saving antibiotic [299], the enhanced relative abundance of this gene category in the biofilms of drinking water biofilters may pose a risk to human health.

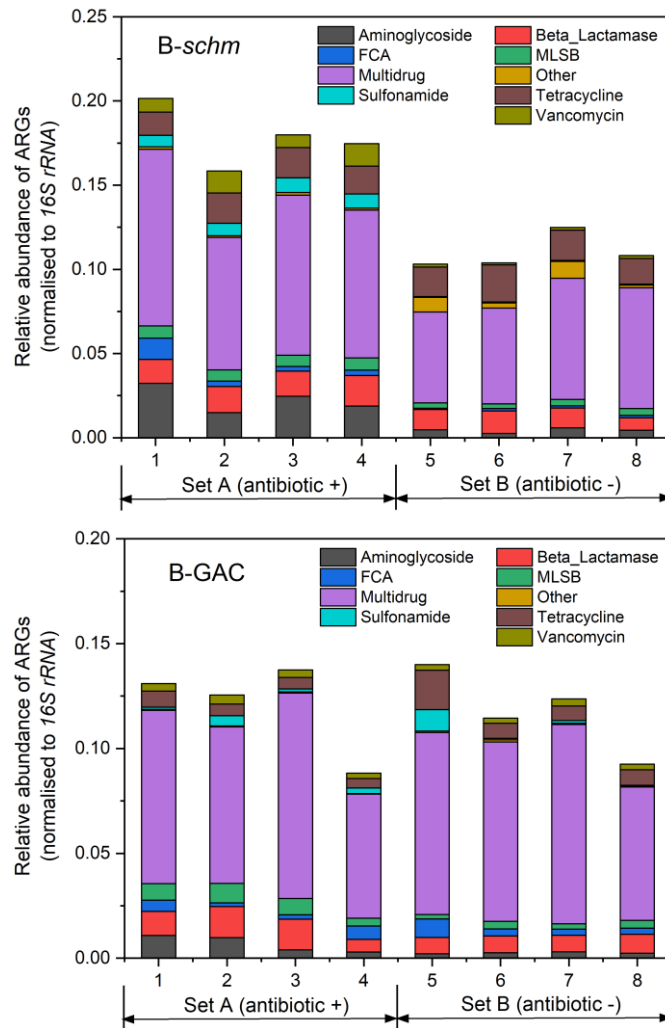


Figure 6.24 Relative abundance of ARGs in B-schm (*schmutzdecke* layer) and B-GAC samples. MLSB = Macrolide-Lincosamide-Streptogramin B resistance genes; FCA = fluoroquinolone, quinolone, florfenicol, chloramphenicol and amphenicol resistance genes.

GAC biofilm at the lowest position represented the least risks of ARGs pollution. In general, no statistical difference in the relative abundance of ARGs was found between B-GAC. GAC biofilms exposed to antibiotics presented higher abundance of aminoglycoside, beta-lactamase and MLSB resistance genes but was less abundant in tetracycline resistance genes compared with the control biofilms. The behaviour of tetracycline resistance genes observed in this study is conflicting with the previous research as OTC exposure has generally been associated with an increased occurrence and diversity of *tet* genes in environmental water or soil samples [139, 300, 301]. This could be explained in two ways: 1) the host bacterial community of *tet* may be a strong competitor within biofilms unexposed to OTC; and 2) the

effects of OTC on biofilm communities in the *schmutzdecke* and GAC biofilms occurred to various extents. A limited amount of OTC can be biodegraded in the *schmutzdecke* layer while the majority was adsorbed by the GAC, resulting in an accumulation of OTC in GAC biofilms which may consequently inhibit the growth of specific bacterial hosts for *tet* genes. Although the variations of *tet* are inconsistent with the conventional qPCR analysis, overall, both qPCR results suggested that the GAC biofilm reveals a similar level of relative abundance of ARGs compared to the *schmutzdecke* layer, which is generally considered as the most biologically active layer in slow sand filters.

Although higher levels of antibiotic concentrations were used throughout this study, the accumulation of these compounds may occur in the natural environment, especially those close to WWTPs. Insufficient removal of antibiotics by WWTPs results in detectable concentrations ranging from ng/L to µg/L in treated effluents [302]. Furthermore, much higher concentrations have been detected in treated wastewater from antibiotic-production facilities, in the mg/L range [4]. Considering that selective effects of antibiotics on the resistome occurred at 10 µg/L in this study, there are clearly environments where pollution with antibiotics poses a risk of promoting horizontal transfer of antibiotic resistance. In particular, those genes (e.g. aminoglycoside and vancomycin ARGs) enriched without the exposure of the antibiotic to which they confer resistance complicates their dissemination in the environment.

3) ARG sources in *schmutzdecke* and GAC biofilms

The relationships between the biofilm samples were further explored using the PCoA approach (Bray-Curtis distance) according to the relative abundance of resistance types (Figure 6.25). The structures of ARGs in Set A (biofilter 1-4) or Set B (biofilter 5-8) were clustered together. The *schmutzdecke* biofilms exposed to target antibiotics were clearly distinct from those in the control biofilms. In contrast, GAC biofilms in Set A and B were grouped close to each other due to the similarity of their antibiotic resistance profiles.

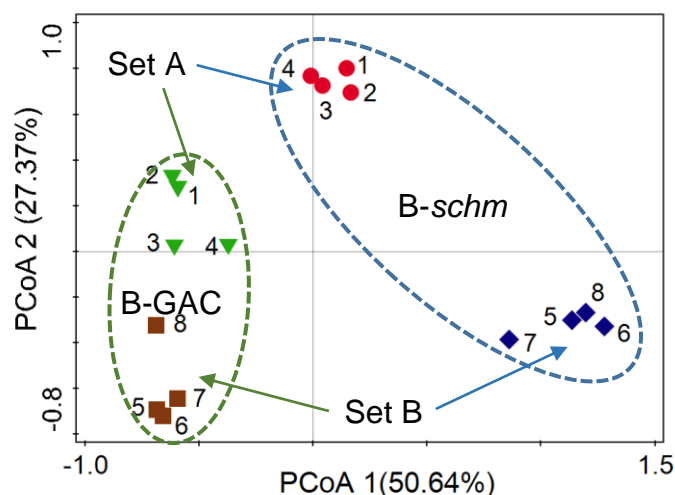


Figure 6.25 Principal coordinate analysis (PCoA) of ARGs in B-schm (*schmutzdecke* layer) and B-GAC biofilm samples based on Bray-Curtis distance. Number 1-8 indicate the eight biofilters.

Set A: biofilter 1-4; Set B: biofilter 5-8.

The number of detected ARGs in *schmutzdecke* and GAC biofilms samples was compared to ascertain the variation in sources of ARGs. A total of 98 ARGs were core ARGs that persisted in all biofilm samples, accounting for 60.5% and 71.6% of the total number of detected ARGs in Set A and Set B, respectively (Figure 6.26). In total, 20 and 11 unique ARGs were detected in B-schm and B-GAC in Set A, respectively, where only one ARG was unique in both biofilms in Set B. As all ARGs present in biofilms originated from the same source water, considering no other potential sources, target antibiotics spiked to the system were the main driving factors for the selection of ARGs during biofiltration. This is further supported by the evidence that among all of the 42 unique ARGs detected in Set A, the top three ARG categories were beta-lactams, MLSB, and tetracycline which contain the target antibiotics of AMOX, CTM and OTC, respectively. Venn diagrams comparing the number of detected ARGs in B-schm and B-GAC in individual biofilters are summarised in the appendix (Figure A6.14 and A6.15).

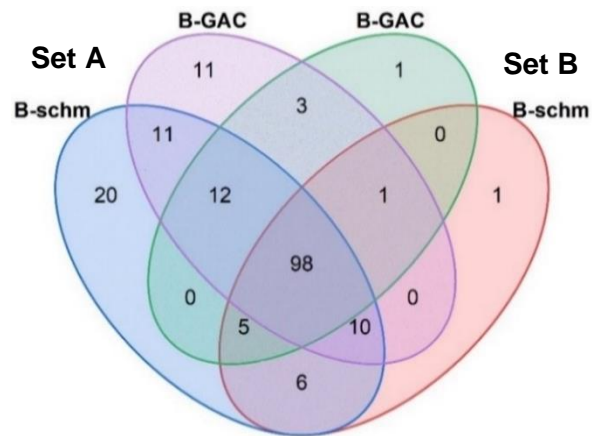


Figure 6.26 Venn diagram showing the number of detected ARGs among *B-schm* (*schmutzdecke* layer) and B-GAC biofilm samples. Left two circles are samples from Set A (antibiotic +), and right two are from Set B (antibiotic -).

6.2.3 ARGs in influent and effluent

Paired influent and effluent samples were collected throughout this study, including the week before and after the addition of antibiotics (batches 1 & 2) and then every two weeks afterwards (batches 3 – 5). Samples were also collected after biofilter cleaning (batch 6). Figure 6.27 shows an overview of the abundance of ARGs in the influents and effluents. The levels of ARGs in the effluents varied in accordance with the influent, as significant positive correlations ($r = 0.87$, $P < 0.001$) were found between them. The overall ARG concentration ranged from 1.37×10^7 copies/L to 6.97×10^8 copies/L in the influent and from 5.06×10^6 copies/L to 3.73×10^8 copies/L in the effluent, respectively. Positive correlations in absolute abundance were found between the ARGs and *16S rRNA* and the integrin in aqueous samples (Figure 6.28). The addition of the target antibiotics affected the behaviour of ARGs considerably in the filtered water. A significant difference ($p < 0.01$) in both the absolute and relative abundance of ARGs was found between the effluents from Set A and Set B, while the influents showed no difference. This is probably due to two reasons: 1) bacteria in the planktonic phase acquired ARGs from the biofilm community through horizontal gene transfer when water flowed and 2) the detachment of biofilm from the media surface. Biofilms undergo shedding over time when they become thick, releasing ARGs into planktonic phase again. As discussed above, higher levels of ARGs and *intl 1* in biofilms were consistently observed after

the addition of antibiotics, consequently increasing the ARG levels in the effluent of Set A. The control Set B biofilters revealed better performance in reducing resistance-related risks, as both the absolute and relative abundance of ARGs and *intl 1* decreased after filtration.

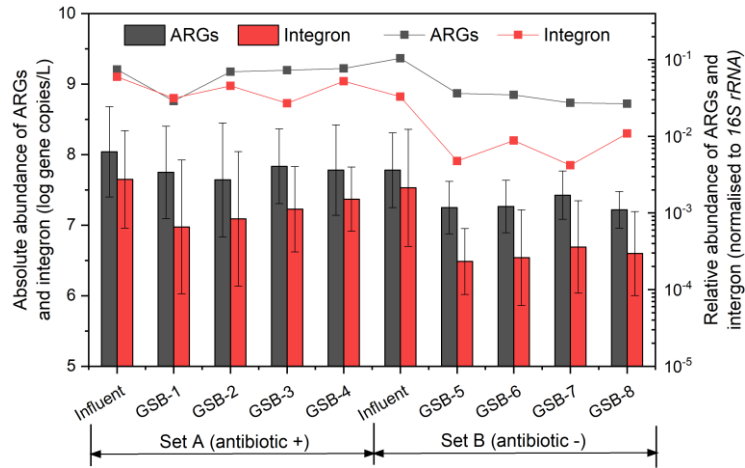


Figure 6.27 Behaviour of ARGs and integron in the influent and effluent samples. Absolute abundance shown as bars, relative as lines. The error bars represent STD from the mean value of all batch samples ($n = 6$).

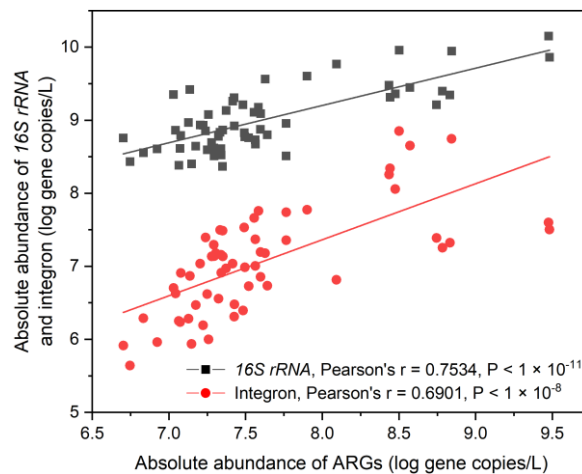


Figure 6.28 The correlations between the absolute abundance (copies/L, log transformed) of ARGs and the corresponding 16S rRNA and integron in influent and effluent samples.

The variation of individual ARG and integron in the influent and effluent of all sandwich biofilters from batch 1 to 6 is shown in appendix (Figure A6.16). Figure 6.29 shows the log reductions of ARGs copy numbers in the effluents over time. No obvious trend was found between biofilters with different GAC thickness or position as the reduction varied significantly over time. All ARGs reduction was less than 1.0-log, which is lower than the value (1.29-log) observed by sandwich biofilters in the previous study (Section 6.1.2.2). In short, GAC

sandwich biofiltration showed limited effect in reducing resistance-related risks from the influent. When exposed to antibiotic, no reduction was observed in normalised ARG copy numbers in the filtered water. Cleaning significantly lowered ARGs reduction, meaning that the *schmutzdecke* played an important role in holding ARG-related microorganisms from the feed. However, this is inconsistent with the observation in the previous biofiltration experiment, where the cleaning process showed limited effect on the behaviour of ARGs in the filtered water. This may be attributed to the composition of bacterial communities within the *schmutzdecke* as different source waters were used.

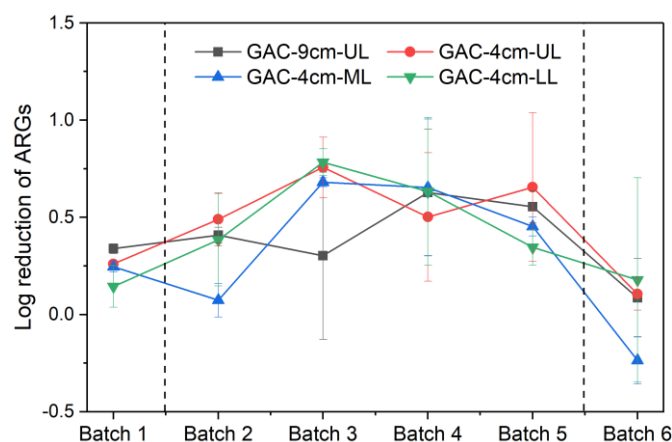


Figure 6.29 The reduction of the concentration of ARGs (log transformed) in all GAC sandwich biofilters. The error bars represent STD from the mean value of duplicate biofilters ($n = 2$). GAC-9cm-UL: 9 cm of GAC in upper layer; GAC-4cm-UL: 4 cm of GAC in upper layer; GAC-4cm-ML: 4 cm of GAC in middle layer; GAC-4cm-LL: 4 cm of GAC in lower layer.

6.2.4 Comparison of ARGs profiles in biofilm and aqueous sample

For the consistency of data analysis, only the relative abundance of target genes obtained from conventional qPCR were compared for all types of samples. Significant positive correlations ($P < 0.001$) were found between all types of samples (Table A6.6). A heatmap illustrating the distinct patterns of the relative abundance of ARGs in B-*schm*, B-sand, B-GAC, raw water, influent and effluent samples is shown in Figure 6.30. Similar levels of ARG were found between samples from the same biofilter Set. It is interesting to find that the GAC layers harboured same levels of resistance genes compared to surface biofilms, which are generally considered as the most biologically active layer in sand filters. In addition to the *schmutzdecke*

layer, the lower layer biological activity is also important affecting the stability of biological processes [271]. Among the ARGs present, *sul1*, *tetG* and *bla_{OXA-1}* were the most prevalent genes among the sulfonamide, tetracycline and beta-lactams resistance genes, respectively. The efflux protein gene *tetA* was significantly affected by the biofiltration process, with the relative abundance increasing 76-fold in biofilms and 95-fold in effluents of the duplicate columns compared to the source water. This suggests that the concentration of oxytetracycline (10 µg/L) spiked is likely sufficient to select for *tetA*. The relative abundance of *sul* genes also increased 20-fold when exposed to antibiotics.

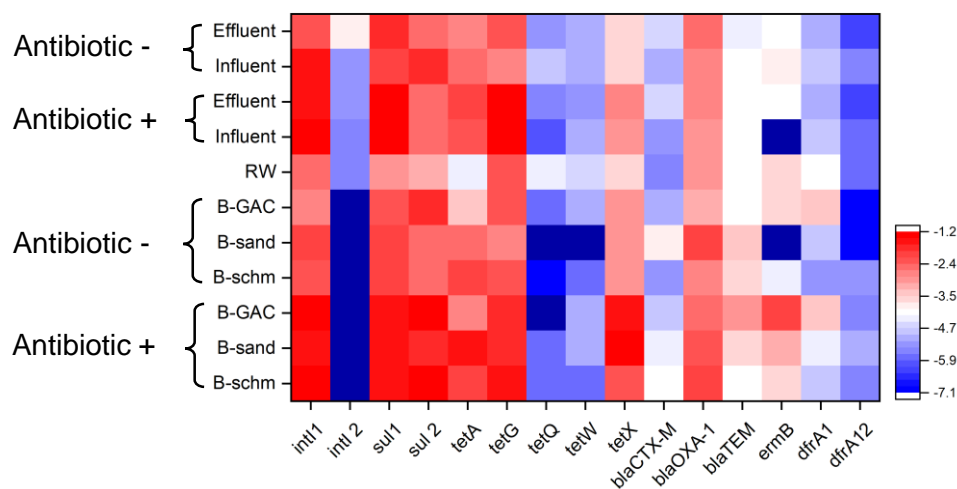


Figure 6.30 A heatmap showing the distinct patterns of the relative abundance of ARGs and integron genes in B-*schm* (*schmutzdecke* layer), B-sand (surface sand biofilm), B-GAC (GAC layer biofilm), raw water (RW), influent and effluent samples.

6.2.5 Bacterial community in *schmutzdecke* and GAC biofilms

Metagenomic DNA from *schmutzdecke* and GAC biofilms was sent for 16S *rRNA* gene amplicon sequencing to further explore the compositions of bacterial communities. A total of 1,763,413 tags with average of 123,177 and 71,317 high quality tags per B-*schm* and B-GAC sample were obtained, respectively (Table A6.7). The top 10 largest taxonomic phyla in B-*schm* and B-GAC are shown in Figure 6.31. Seeded from the River Thames, biofilms harboured a large diversity of bacterial phyla with an average of 38 ± 3 and 40 ± 2 phyla detected in *schmutzdecke* and GAC biofilms, respectively. *Proteobacteria* (62.1%) was dominant in all 16 biofilm samples, followed by *Firmicutes* (11.0%), *Actinobacteria* (7.0%), *Acidobacteria* (4.4%) and *Bacteroidetes* (4.2%), accounting 88.7% of the total bacterial

communities. At the class level, bacterial community differences became more divergent (Figure 6.32). For instance, *Betaproteobacteria* was most abundant in GAC biofilms exposed to antibiotics, while in control GAC biofilms, the most abundant class shifted to *Alphaproteobacteria*.

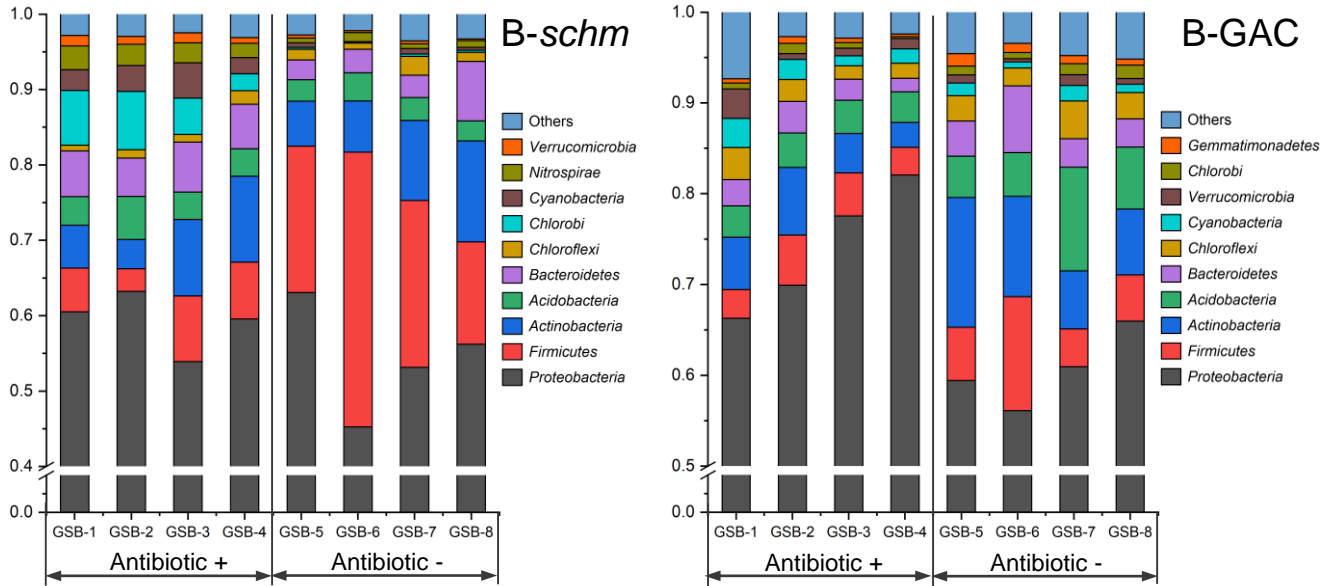


Figure 6.31 Bacterial community composition B-schm (*schmutzdecke* biofilm) and B-GAC (GAC biofilm) samples based on the average percentage of the top 10 largest taxonomic phyla.

GSB 1-4: biofilters exposed to antibiotics; GSB 5-8: biofilters without the addition of antibiotic.

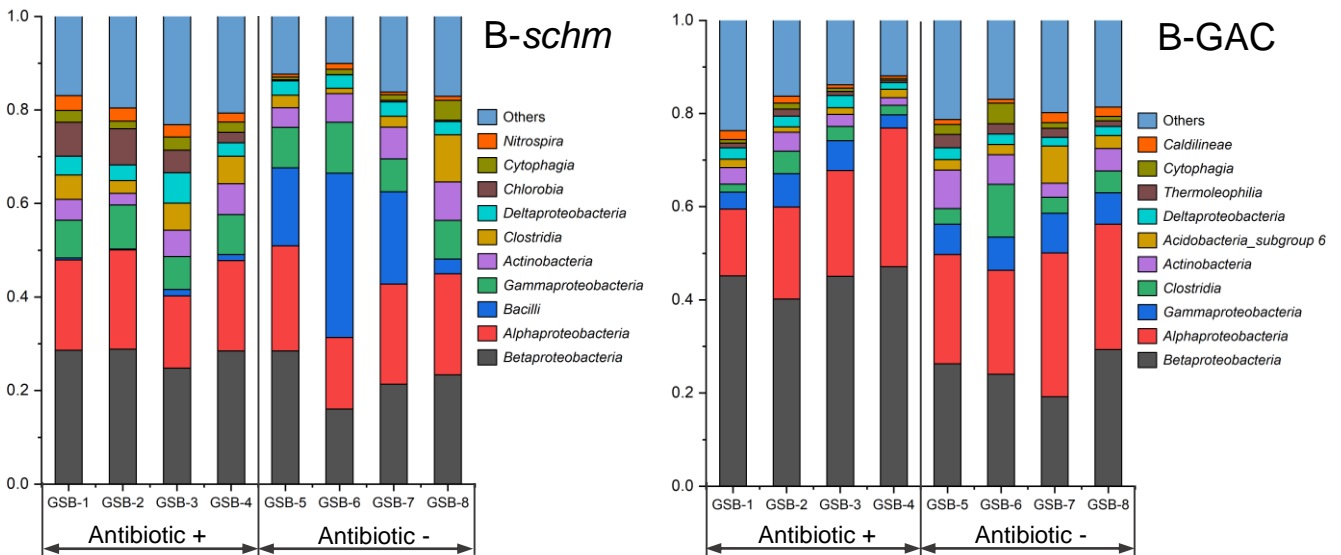


Figure 6.32 Bacterial community composition in B-schm (*schmutzdecke* biofilm) and B-GAC (GAC biofilm) samples based on the average percentage of the top 10 largest taxonomic class.

GSB 1-4: biofilters exposed to antibiotics; GSB 5-8: biofilters without the addition of antibiotic.

The microbial community profile in the *schmutzdecke* biofilm was significantly ($P < 0.01$) correlated to the underlying GAC biofilm. As replicate samples, B-*schm* in Set A or Set B showed similar distributions of bacterial community, as evidenced by principal coordinates analysis (PCoA, Figure 6.33). The distribution of B-*schm* in Set A and B clearly indicated the effect of antibiotic exposure. Under the selective pressure of antibiotics, the proportion of *Firmicutes* in *schmutzdecke* biofilms was significantly reduced ($p < 0.01$) from $22.89\% \pm 9.72\%$ in Set B to $6.27\% \pm 2.18\%$ in Set A, respectively, and consequently affected its proportion in the underlying GAC biofilms, albeit not significantly. On the contrary, B-*schm* biofilms collected from Set A were more abundant in the phylum *Chlorobi* ($6.61\% \pm 1.55\%$) compared with Set B ($0.23\% \pm 0.13\%$). Further analysis at class level showed that *Bacilli* (0.8% in Set A and 18.7% in Set B) and *Chlorobia* (5.5% in Set A and 0.2% in Set B) contributed the most to the variation in abundance of phyla *Firmicutes* and *Chlorobi* in B-*schm* samples, respectively.

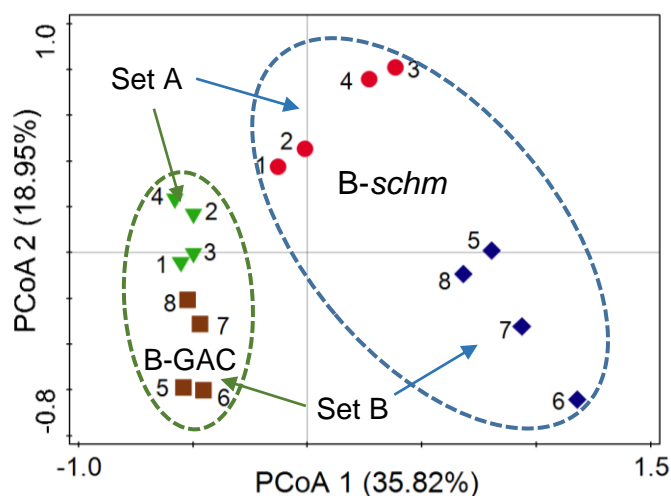


Figure 6.33 Principal coordinate analysis (PCoA) based on Bray-Curtis distance showing the overall distribution of bacterial communities in B-*schm* (*schmutzdecke* layer) and B-GAC biofilm samples. 1-8 refer to biofilm samples collected from different sandwich biofilters.

To establish a more detailed view on the bacterial community, Figure 6.34 depicts the abundance of 80 major genera ($> 0.5\%$ in at least one sample). *Sulfuritalea* (7.3% on average) and *Bacillus* (5.2% on average) were the most abundant genera. *Sulfuritalea* was more abundant in biofilms exposed to antibiotics, especially within the GAC biofilm. Previously, *Sulfuritalea* species were found to be a major component of the planktonic bacterial

community in nitrate-depleted hypoxic water [303]. The consistent lower concentrations of nitrate in the influent spiked with antibiotics and the lack of oxygen in the GAC layer may have favoured the growth of *Sulfuritalea* within the GAC biofilms. *Bacillus* (belonging to *Firmicutes*) showed a much higher relative abundance (18.4%) in the control *schmutzdecke* biofilms.

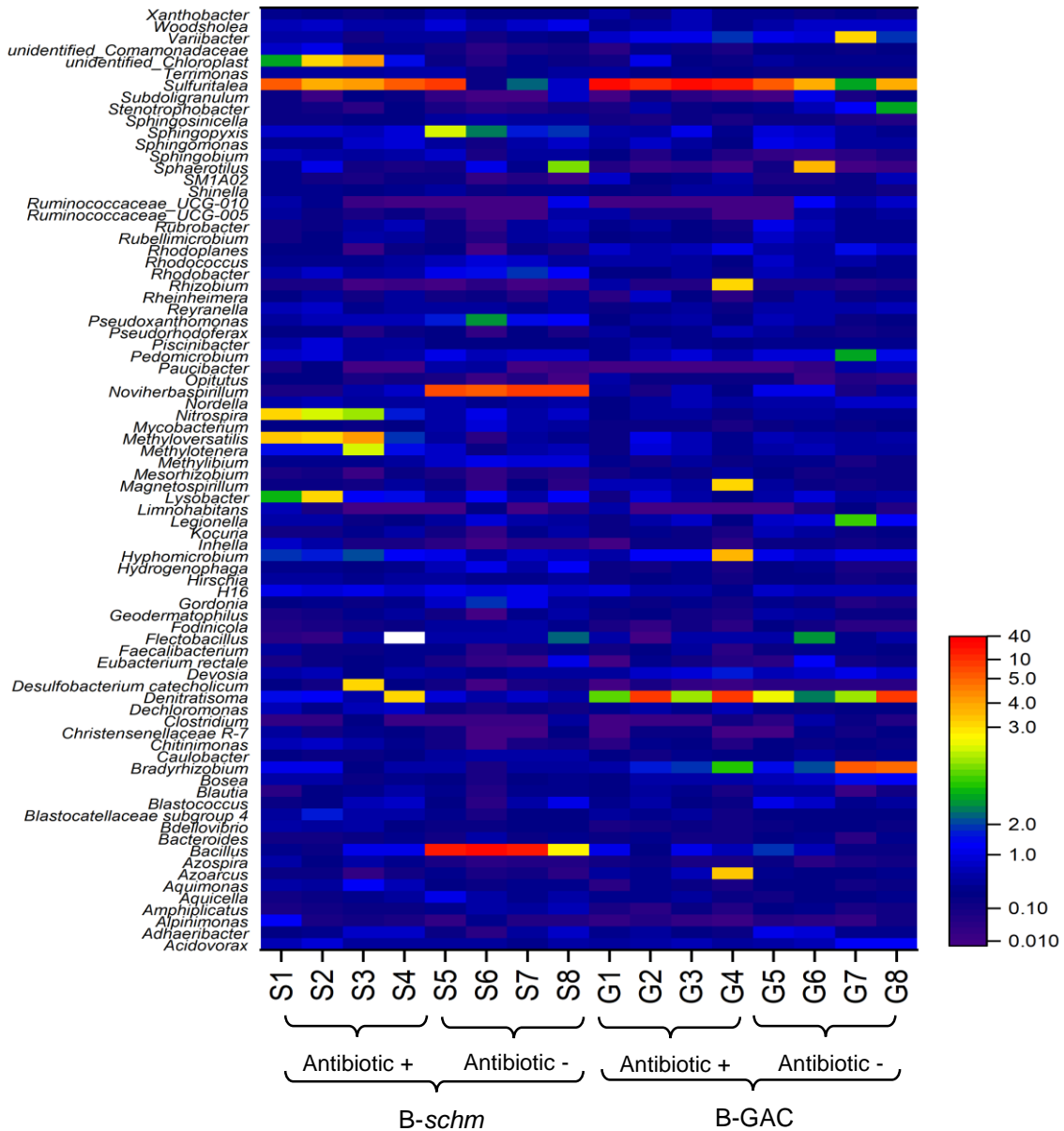


Figure 6.34 Heatmap showing the distribution of major genera (relative abundance > 0.5% in at least one sample) in B-schm: *schmutzdecke* biofilms; and B-GAC: GAC layer biofilms.

Genera associated with the nitrogen cycle present in biofilms. For instance, *Bradyrhizobium*, a well-known nitrogen fixer, showed a slightly higher percentage in GAC biofilms. *Nitrospira* is a globally distributed group of nitrite oxidisers and usually exist in the

interiors of biofilms and flocs [304, 305]. The higher percentage of *Nitrospira* in surface biofilms indicated a greater extent of nitrification. On the contrary, *Denitratisoma*, which is related to denitrification and is involved in nitrate reduction [306], was found to be more abundant in GAC biofilms. *Noviherbaspirillum*, another genus associated with denitrification [307], was sensitive under exposure to antibiotics and more prone to inhabit the surface biofilm (7.0%) than GAC (0.7%). These results could be responsible for the variations of nitrate observed in the effluents. In particular, the results provided evidence for the observed higher reduction of nitrate after cleaning, when nitrifiers/denitrifiers were removed along with the *schmutzdecke* layer and microbes within GAC biofilms dominated in denitrification. High abundance of genera *Hyphomicrobium*, *Nitrospira*, and *Bradyrhizobium* has also been found in drinking water or in GAC biofilters [175, 219, 308, 309], indicating that they may be common inhabitants in biofiltration systems. The listed genera in Figure 6.34 exhibit a variety of metabolic capabilities such as nitrogen fixation, nitrification, denitrification, photosynthesis, degradation of carbon compounds, etc., indicating the potential functional diversity of the sandwich biofilters. Furthermore, this also implies that the functional redundancy within the community may make up for the loss of sensitive bacteria under antibiotic pressure. Typical genera associated with opportunistic human pathogens were observed in this study. The genera of *Bacillus*, *Legionella*, *Mycobacterium*, and *Pseudomonas* were present in all biofilm samples, and *Bacillus* showed the highest abundance (up to 34.9%) in one of the *schmutzdecke* biofilm samples (Table A6.8 and A6.9).

6.2.6 Relationship among the water quality parameters and ARGs

Pearson correlation and redundancy analysis (RDA) were conducted to identify the association between the distribution characteristics of ARGs and various operational parameters in effluent samples. RDA showed that the water quality parameters explained 34.6% of the variability of the relative abundance of ARGs (Figure 6.35 A). Turbidity, DOC exhibited a positive relationship with the relative abundance of most ARGs in effluents, while the nitrate on the other hand was negatively correlated with *bla*_{TEM}. Additionally, pH and conductivity

exhibited no significant correlation with ARGs. Turbidity exhibited the strongest effect on the relative abundance of *intl 1*, *sul1* and *tet* (Pearson's $r = 0.39 - 0.71$, $P < 0.05$, Table A6.10). This may be due to the attachment of microorganisms to the surface of turbidity causing materials (e.g. natural organic matter, inorganic particles and biological particles) [310]; or the detachment of microorganisms from filter beds as GAC can be heavily colonised by heterotrophic microorganisms [296]. Nutrient levels (i.e. DOC, nitrate and phosphate) showed limited effects on the distribution characteristics of ARGs in the effluents, among which organic carbon showed significant correlations with *sul1*, *tetA* and *tetX* (Pearson's $r = 0.36 - 0.44$, $P < 0.05$). Paired Pearson's correlations also showed significance between *intl 1* and *sul1*, *sul2*, *tetQ* and *dfrA1* (Table A6.11). Further VPA showed the environmental factors, *intl 1* and their joint effects contributed 22.7%, 3.5% and 5.0% on the change of ARGs, respectively (Figure 6.35B).

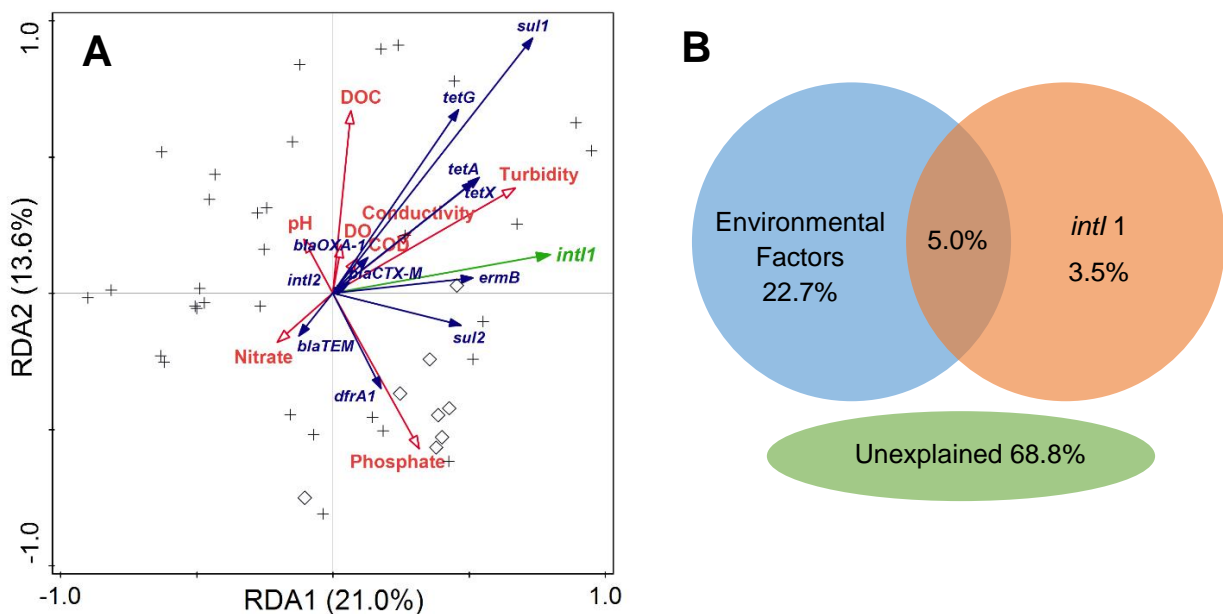


Figure 6.35 Redundancy analysis (RDA) of the correlation between ARGs/*intl 1* and environmental variables (A) and variation partitioning analysis (VPA) differentiating effects of environmental factors and *intl 1* on the ARGs variation (B) in effluent samples.

The lengths of the arrows reveal the strength of the relationship and the angles between arrows indicate correlation between different variables. Cross scatters: a total of 32 effluent samples after the addition of antibiotics; diamond scatters: 8 effluent samples after biofilter backwashing/cleaning. *Intl 1*, *tetQ*, *tetW* and *dfrA12* were excluded from the analysis due to the low detection frequencies.

Although the environmental factors contributed greater than in the previous experiment (5.8%), the high unexplained percentage (68.8%) suggested that the bacterial community may still be a major factor affecting ARGs profiles in the effluents. These results could not be compared with literature, since the behaviour of ARGs was not generally monitored along with water quality in both lab-scale and pilot-scale biofiltration systems. However, investigations on the occurrence of ARGs in river water suggested that the environmental factors (pH, conductivity, turbidity, dissolved oxygen and total phosphorus) are not associated with the presence/absence of ARGs [311]. Similarly, Su *et al.* also reported that no correlation is observed between 14 ARGs (including *tet* and *sul*) and water quality parameters in shrimp aquaculture [312]. Only COD was reported to be correlated with *tetM* in water samples collected from six water supply reservoirs [313]. All of these results suggested that the water quality constitutes have no significant impact on the behaviour of ARGs in natural aquatic environments.

Unlike water sample, Wan *et al.* have identified that the organic carbon shapes the ARG profile in sand filter biofilms [193]. In the present study, there were no significant variations of organic carbon levels or ARGs in raw water over the sampling period. The biodegradation and adsorption processes involved in the sandwich biofiltration may have complicated the mechanisms underlying ARG variation in the effluents. GAC biofilm is believed to have a complex and dynamic microbial community [175], and hence, it was speculated that the interactions between bacteria in the planktonic phase and biofilm developed on media surface may contribute to the dynamic changes of ARGs in the effluent. This is also supported by the significant positive correlations of the relative abundance of ARGs among the biofilms and aqueous samples (raw water, influent and effluent) (Table A6.6).

6.2.7 Correlation between bacterial community and antibiotic resistome

Bacterial genera were considered as the environmental factors affecting the ARG variation in RDA. Result of HT-qPCR was used for RDA as it provides a more comprehensive picture of the ARG profiles within the *schmutzdecke* and GAC biofilms. RDA showed that a

total of 70.09% of the difference in the relative abundance of ARG types in biofilm samples could be explained by variations in the bacterial community (Figure 6.36). It is clear that the variations of biofilm resistome in the *schmutzdecke* or GAC, or when exposed to antibiotics, are associated with different bacterial communities. More specifically, the genera *Methyloversatilis*, *Hyphomicrobium*, *Nitrospira*, and *Lysobacter* significantly ($P < 0.05$) contributed to the relative abundance of ARGs in B-*schm* (antibiotic +), while the genera *Bacillus*, *Noviherbaspirillum* and *Sphingopyxis* were significantly ($P < 0.05$) correlated to the ARG abundance in B-*schm* (antibiotics -). Genera *Denitratisoma* and *Bradyrhizobium* were significantly ($P < 0.05$) correlated with ARGs in GAC biofilms.

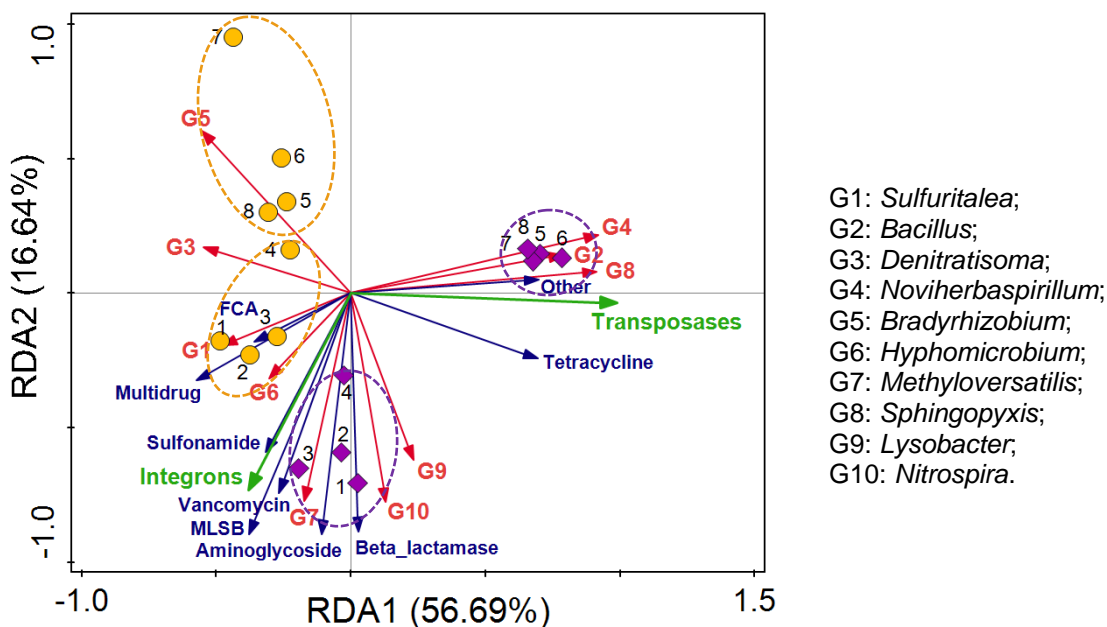


Figure 6.36 Redundancy analysis (RDA) of the correlation between major genera (top 10) and relative abundance of ARGs types in biofilm samples. MLSB = Macrolide-Lincosamide-Streptogramin B resistance genes; FCA = fluoroquinolone, quinolone, florfenicol, chloramphenicol and amphenicol resistance genes. Purple and diamond scatters 1-4: *schmutzdecke* biofilms exposed to antibiotics; 5-8: *schmutzdecke* biofilms unexposed to antibiotics; Yellow and circle scatters 1-4: GAC biofilms exposed to antibiotics; 5-8: GAC biofilms unexposed to antibiotics.

In this study, the spike of antibiotics to the biofilter feed directly affected the bacterial community structure in the *schmutzdecke* and GAC biofilms and indirectly affected the antibiotic resistome. Eight out of ten most abundant genera were significantly correlated with the relative abundance of ARGs (Table A6.12). Aminoglycoside, beta-lactamase, MLSB,

sulfonamide and vancomycin resistance genes were significantly correlated ($P < 0.05$) to the main genera in the *schmutzdecke* biofilms when exposed to the target antibiotics. By contrast, tetracycline resistance genes (*tet*) were related to the genera *Bacillus*, *Noviherbaspirillum* and *Sphingopyxis* in the control *schmutzdecke* biofilms. This could explain the unchanged relative abundance of *tet* in the experimental and control *schmutzdecke* biofilms. Genus *Bacillus*, which was a strong competitor (accounting for 18.4%) within the B-*schm* (antibiotic -), was likely to be one of the main hosts for *tet*-carrying resistant bacteria and contributed to the persistence of *tet* in the absence of antibiotic selective pressure. Previous studies have found that members of *Firmicutes* were potential hosts of ARGs; among which genus *Bacillus* was found to be associated with *tetW* during manure composting [215].

The enhanced levels of the relative abundance of aminoglycoside and vancomycin (*van*) resistance genes without exposure to the corresponding antibiotic indicated the co-occurrence of these two ARG types with specific ARGs and microorganisms. Both aminoglycoside and vancomycin ARGs were strongly and significantly correlated to beta-lactamase, MLSB, and sulfonamide (Pearson's $r = 0.62 - 0.72$, $P < 0.05$), and with *Methyloversatilis*, *Nitrospira*, and *Lysobacter* (Pearson's $r = 0.66 - 0.83$, $P < 0.01$) (Table A6.12 and A6.13). Ma *et al.* have identified *Methyloversatilis* as one of the main genus hosts of multidrug resistance genes in tap water samples based on a large scale survey across 25 cities in seven countries and regions [219]. The genera *Nitrospira* and *Lysobacter* have also been identified as the major hosts of ARGs in surface water [222]. Moreover, many strains of *Lysobacter* are producers of antibiotics and confer high levels of intrinsic resistance to kanamycin, ampicillin, streptomycin, tetracycline, and rifampicin through the mechanisms of enzymatic inactivation and alteration of antibiotic targets [314, 315]. Overall, the observations in this study are in accordance with the previous studies, suggesting that the differences in bacterial community structure were correlated with the changes in the resistome in drinking water-related samples [192, 193, 223]. RDA showing similar distribution patterns of ARG types with top 10 bacterial phyla is provided in the appendix (Figure A6.17).

Although the RDA suggested a positive association between integrons and the five ARG types, paired Pearson's correlations only showed significance ($P < 0.001$) between integrons and MLSB resistance genes (Table A6.13). By contrast, the transposase gene was positively correlated to tetracycline resistance genes. To differentiate the effects of bacterial communities and MGEs, including transposases and integrons, on the variation of antibiotic resistome in biofilms, the VPA showed that a total of 72.9% of the variance of ARGs could be explained by the selected variables in biofilm samples (Figure 6.37). Bacterial community and MGEs explained 45.1% and 8.5% difference in ARGs patterns, respectively. 19.3% of the variation could be attributed to the interactions between bacterial communities and MGEs. These results indicated that the bacterial community was the main factor driving changes in ARG profiles in biofilms.

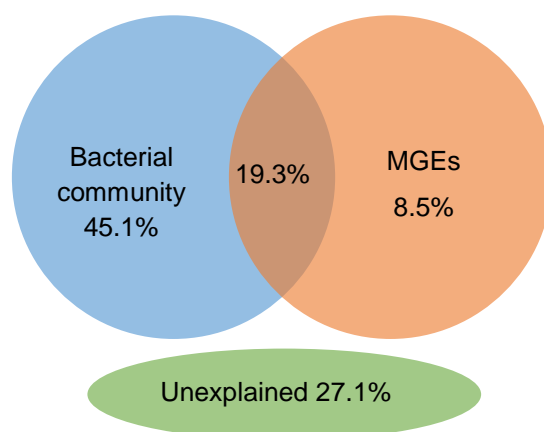


Figure 6.37 Variation partitioning analysis (VPA) differentiating effects of bacterial community and MGEs (mobile genetic elements) on the variations of ARGs in biofilm samples. VPA was conducted based on the major genus and the relative abundance of MGEs, including transposases and integrons

To further visualize the connections between the bacterial community and ARGs, a co-occurrence network was constructed between the bacterial taxa (at the genus level) and ARGs. Among the 295 ARGs tested, only ARGs that occurred in all 16 biofilm samples (77 ARGs in total) were used to construct the network. This preliminary data process could remove those poorly represented ARG subtypes in order to reduce the artificial association bias [201, 208]. The top 20 most abundant microorganism populations at the genus level were selected for network construction. The network analysis is based on the hypothesis that the non-random

co-occurrence patterns between ARGs and bacterial taxa could be used to provide new insights into ARGs and their possible hosts if the ARGs and the co-existing bacterial taxa possessed a strong and significantly positive correlation (Pearson's $r > 0.8$, $P < 0.01$) [208, 219]. After construction, the entire network consisted of 48 nodes and 272 edges. Figure 6.38 showed the co-occurrence patterns among ARG subtypes, MGEs and bacterial taxa, among which ten bacterial genera could be possible ARG hosts. It can be seen that more ARG subtypes belonging to multidrug resistance (20 edges in total) were carried by the identified bacterial genera. Genus *Nitrospira* had the most edges (15) with the ARGs, followed by *Methyloversatilis* (14) and *Methylothermobacter* (12). *Bacillus* and *Sphingopyxis* were possible hosts for the tetracycline resistance gene *tetPB-01* (Figure 6.39). *Lysobacter* was observed to be the host of *vanYD-01* (vancomycin) and *cmx(A)* (FCA). *Noviherbaspirillum* only carried *oleC* (MLSB), whereas *Nitrospira* and *Methyloversatilis* carried more diverse ARGs, including genes encoding resistance to all ARG types.

The network analysis further confirmed that the co-occurrence patterns among aminoglycoside or vancomycin ARGs with other ARG subtypes and bacterial taxa could explain their enhanced abundance under exposure to the target antibiotics. Most of the aminoglycoside or vancomycin ARGs were found carried by *Methyloversatilis* and *Nitrospira*, both showed a higher proportion in surface biofilms when exposed to the target antibiotics. In particular, *vanYD-01* was frequently associated with five different genera. Aminoglycoside and vancomycin ARGs were also found closely correlated to multidrug, beta-lactamase and MLSB, where their relative abundance all increased when exposed to antibiotics. Network analysis showing the co-occurrence among ARG subtypes and MGEs is provided in appendix (Figure A6.18). MGEs co-occurred with multidrug, beta-lactamase, MLSB and tetracycline resistance genes. Similar co-occurrence among MGEs and ARGs subtypes was also reported in various environmental samples, including lettuce [208], natural waterbodies [191], farmed fish [316], soil [74], and drinking water [75], indicating that the dissemination of those ARGs groups was associated with transposons and integrons. In particular, *tnpA-02*, *tnpA-04* and *intl 1* showed more frequent co-occurrence with ARGs in various environmental matrix.

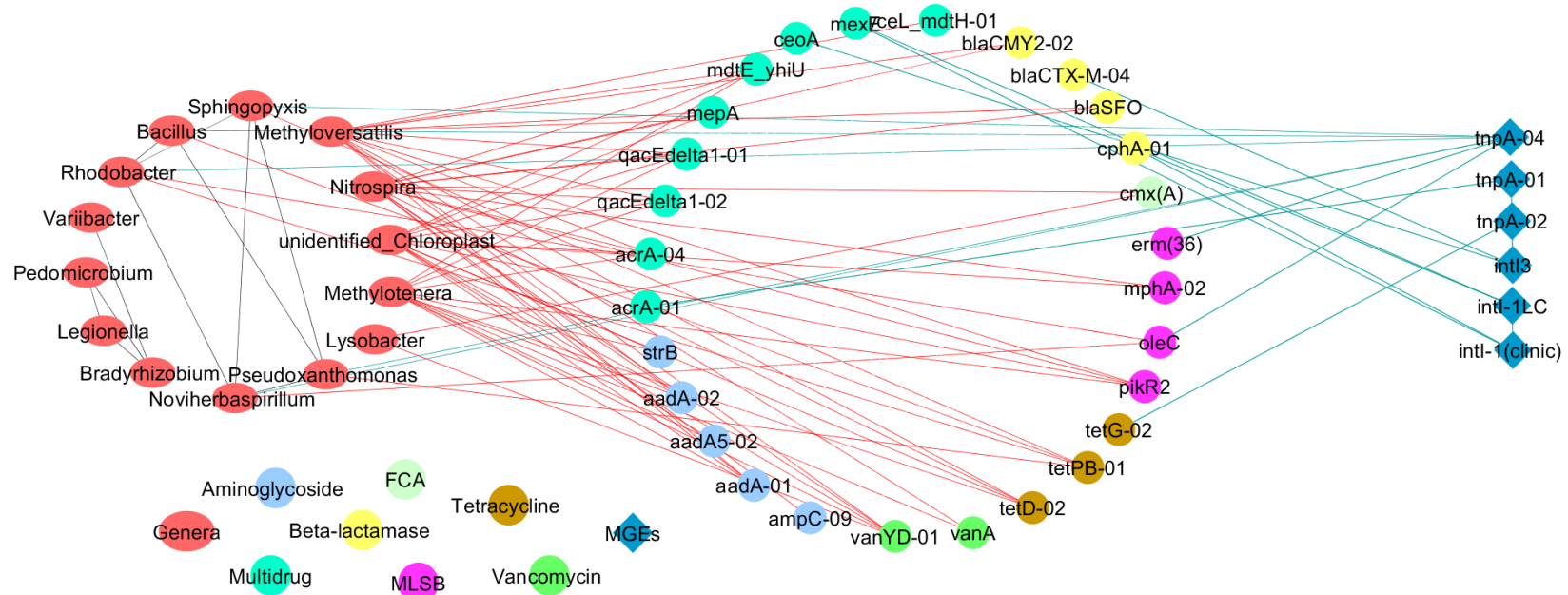


Figure 6.38 Network analysis revealing the co-occurrence patterns between ARG subtypes, MGEs and bacterial taxa (genus level). The nodes were coloured according to ARGs types. The connection between ARGs and bacterial taxa represents a strong (Pearson's $r > 0.8$) and significant ($P < 0.01$) correlation. Red edges indicate the connection between bacterial genus and ARG subtypes; black edges are the connections among bacterial genus; and green edges indicate the connection between MGEs and ARG subtypes/bacterial genus. MLSB = Macrolide-Lincosamide-Streptogramin B resistance genes; FCA = fluoroquinolone, quinolone, florfenicol, chloramphenicol and amphenicol resistance genes. MGEs: mobile genetic elements, including transposons and integrons.

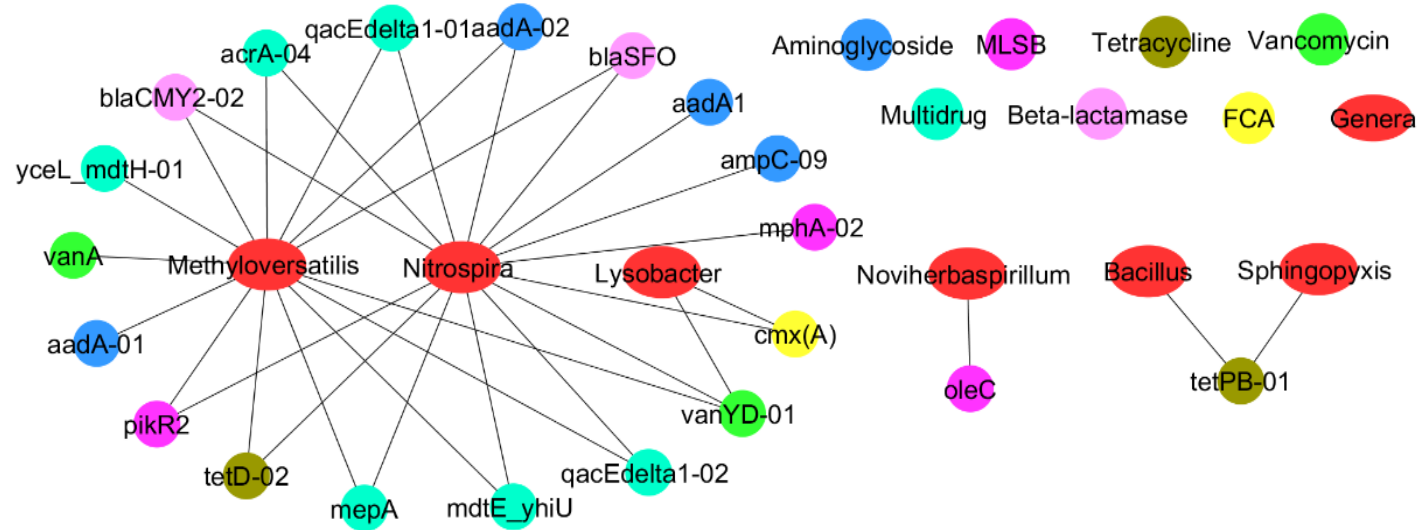


Figure 6.39 Network analysis revealing the co-occurrence patterns between ARG subtypes and top taxonomic genera. The nodes were coloured according to ARGs types. The connection between ARGs and bacterial taxa represents a strong (Pearson's $r > 0.8$) and significant ($P < 0.01$) correlation.

MLSB = Macrolide-Lincosamide-Streptogramin B resistance genes; FCA = fluoroquinolone, quinolone, florfenicol, chloramphenicol and amphenicol resistance genes.

6.2.8 Summary

- Conventional qPCR and HT-qPCR showed that the diversity and abundance of ARGs in the *schmutzdecke* biofilms were clearly affected by the addition of the target antibiotics. In particular, the relative abundance of aminoglycoside, MLSB (Macrolide-Lincosamide-Streptogramin B), sulfonamide and vancomycin resistance genes was significantly enriched in the *schmutzdecke* biofilms when exposed to antibiotics.
- GAC media represented a similar level of risk of ARGs pollution (richness, absolute and relative abundance) compared with the *schmutzdecke* layer in the control biofilters.
- Among all bacterial phyla identified, *Firmicutes* and *Chlorobi* were significantly affected by antibiotics. Further analysis at class level revealed that *Bacilli* and *Chlorobia* contributed the most to the observed differences.
- The differences in bacterial community structure were correlated with the changes in the resistome. RDA and VPA showed that the bacterial community, mobile genetic elements and their joint effects were the dominant mechanisms governing the variability of the distribution characteristics of ARGs in the *schmutzdecke* and GAC biofilms. Further network analysis showing the co-occurrence patterns between ARGs and bacterial taxa suggested that 10 taxonomic genera were implicated as possible ARG hosts.

Chapter 7

IMPACT OF BIOFILTRATION ON PLASMID CONJUGATIVE TRANSFER

7 IMPACT OF BIOFILTRATION ON PLASMID CONJUGATIVE TRANSFER

A small scale biofiltration system was setup at bench-scale and *E. coli* strains J53 (harbouring the RP1 plasmid) and HB101 were used to establish the conjugative transfer model. Changes in the conjugative transfer frequency and the underlying mechanisms during biofiltration experiment are discussed in this chapter according to the observations in different batch samples.

7.1 Conjugative transfer model construction

7.1.1 Antibiotic susceptibility testing

The results for the antibiotic susceptibility testing are shown in Figure 7.1. Comparing the zone of inhibition for each antibiotic to the reference zone of inhibition according to the EUCAST standard, *E. coli* J53 possessing the RP1 plasmid was confirmed to be resistant to ampicillin, tetracycline and kanamycin and susceptible to streptomycin; while *E. coli* HB101 showed an opposite behaviour. Therefore, LB plates supplemented with ampicillin, tetracycline and kanamycin or streptomycin can be used to distinguish the donor and recipient, respectively.

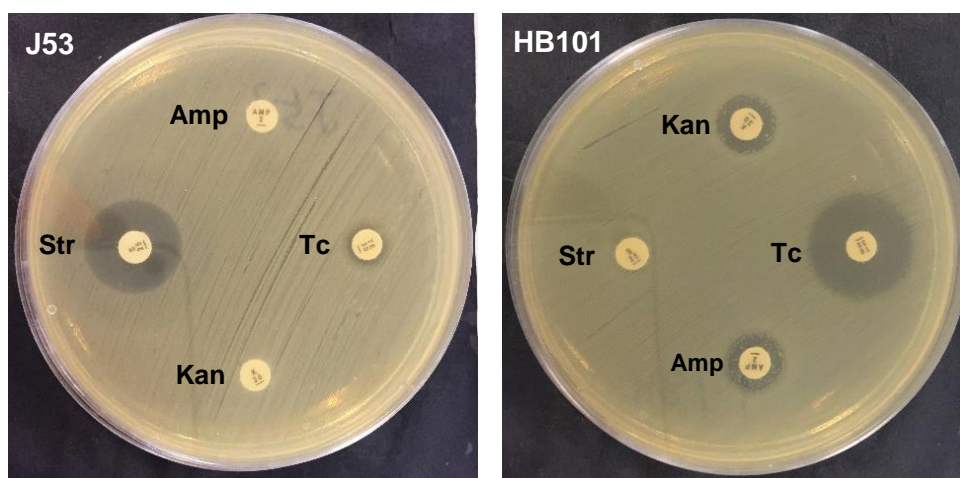


Figure 7.1 Petri dishes showing different zone of inhibition. Amp: ampicillin (2 µg); Tc: tetracycline (30 µg); Kan: kanamycin (30 µg); and Str: streptomycin (25 µg). *E. coli* J53: donor strain harbouring the RP1 plasmid; *E. coli* HB101: recipient strain.

7.1.2 Transfer frequency of RP1 plasmid in pure *E. coli* cultures

The transferability of RP1 to *E. coli* HB101 was tested in agar and broth mating system, respectively. The conjugative transfer frequency was calculated based on the numbers of transconjugants per recipient cell. Results are shown in Table 7.1. In general, the RP1 plasmid exhibited high rates of transferability to the recipient strain with transfer frequencies ranging from -0.4 to -0.2 log units transconjugants per recipient in agar mating system and -3.2 to -3.7 in broth mating system, respectively. This confirms that conjugation occurs at higher frequencies within biofilm communities than when in a planktonic state [95]. In broth mating system, results also showed that a high bacterial density was conducive for close contact between cells, facilitating plasmid transfer [317].

Table 7.1 RP1 plasmid conjugative transfer frequency in agar and broth mating systems.

	Agar mating	Broth mating	
	OD ₆₀₀ = 0.1	OD ₆₀₀ = 0.1	OD ₆₀₀ = 0.5
Initial cell density	OD ₆₀₀ = 0.1	OD ₆₀₀ = 0.1	OD ₆₀₀ = 0.5
Transfer frequency	$5.5 \pm 1.4 \times 10^{-1}$	$2.3 \pm 0.5 \times 10^{-4}$	$4.1 \pm 1.9 \times 10^{-4}$

OD₆₀₀: absorbance at 600 nm wavelength. Results are presented as mean value \pm STD, n = 3.

7.1.3 Transconjugants identification

Possible transconjugants were randomly chosen and screened for the presence of four ARGs: *bla*_{CTX-M}, *bla*_{OXA-1}, *bla*_{TEM} and *tetA*, to determine the antibiotic resistance genotype and transfer of the RP1 plasmid. Figure 7.2 shows the amplification plots of transconjugant colony PCR and electrophoresis bands. All of the transconjugants were confirmed to have *bla*_{TEM} (516 bp) and *tetA* (210 bp), encoding resistance to ampicillin and tetracycline, respectively. No false-positive colonies were identified by colony PCR. To further confirm the occurrence of RP1 plasmid transfer, PCR products with the expected sizes were sent for sequencing. Sequence alignment results showed that the PCR products had 100% sequence identity with *bla*_{TEM} and *tetA* gene, indicating that all colonies acquired the RP1 plasmid. In addition, natural transformation from naked RP1 plasmid DNA to the recipients was not observed in this study. These result indicated that the construction of conjugative transfer model was successful.

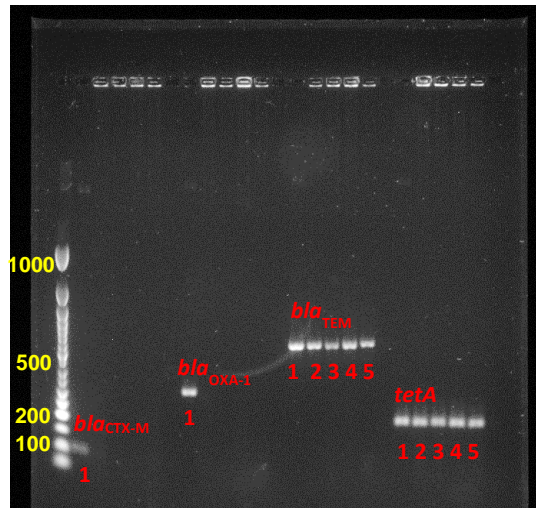


Figure 7.2 Transconjugants colony PCR amplification plots and electrophoresis bands.

Lane 1: PCR positive control; Lane 2 and 3: transconjugants from agar mating; Lane 4 and 5: Transconjugants from broth mating.

7.2 Plasmid conjugative transfer in biofilter

7.2.1 Plasmid conjugative transfer in media (biofilm) samples

Due to the difference in surface structures, sand, GAC and anthracite represented different habitat environments for the donor and recipient cells. The biofilm formed on the media surface was a relatively complex and competitive environment where donor and recipient were likely to make physical contact, attach, and then conjugate during the biofiltration process. The impact of biofiltration on the RP1 plasmid conjugative transfer are discussed below.

7.2.1.1 Sand Biofiltration

The numbers of recipient and donor in sand media remained stable over time, with recipient colonies (4.58×10^9 CFU/g on average) consistently higher than donors (3.22×10^8 CFU/g on average) despite of the same inoculation concentration in the feed. The RP1 plasmid conjugative transfer frequency increased steadily from 4.41×10^{-8} on day 1 to 6.04×10^{-6} on day 5, then plateaued between 10^{-6} to 10^{-5} after a week (Figure 7.3), indicating the bacterial attachment and detachment remained dynamically balanced in the biofilm. After backwashing was conducted on day 14, the transfer frequency dropped down to 1.14×10^{-6} and 7.16×10^{-7} in Set A and B, respectively. In fact, 1.80-log, 2.45-log and 2.46-log reductions

were observed for the recipient, donor and transconjugant cells after backwashing, respectively. Although the cell numbers were reduced, the transfer frequency was still 30 times higher than the initial frequency found on day 1, indicating that the backwash was not efficient in reducing the plasmid transfer rate. The number of transconjugants was significantly correlated to the number of donors ($r = 0.952$, $P < 1 \times 10^{-5}$) and transfer frequency ($r = 0.905$, $P < 0.001$) in sand samples. No correlation was found between transconjugants and recipients. In addition to the factors that might affect conjugative transfer, for instance nutrient level, temperature, residence time etc., the results indicated that the transfer frequencies in sand media were mainly determined by the numbers of donor cells, with a higher donor density providing more transferable plasmids and a greater chance of physical interaction with recipient cells.

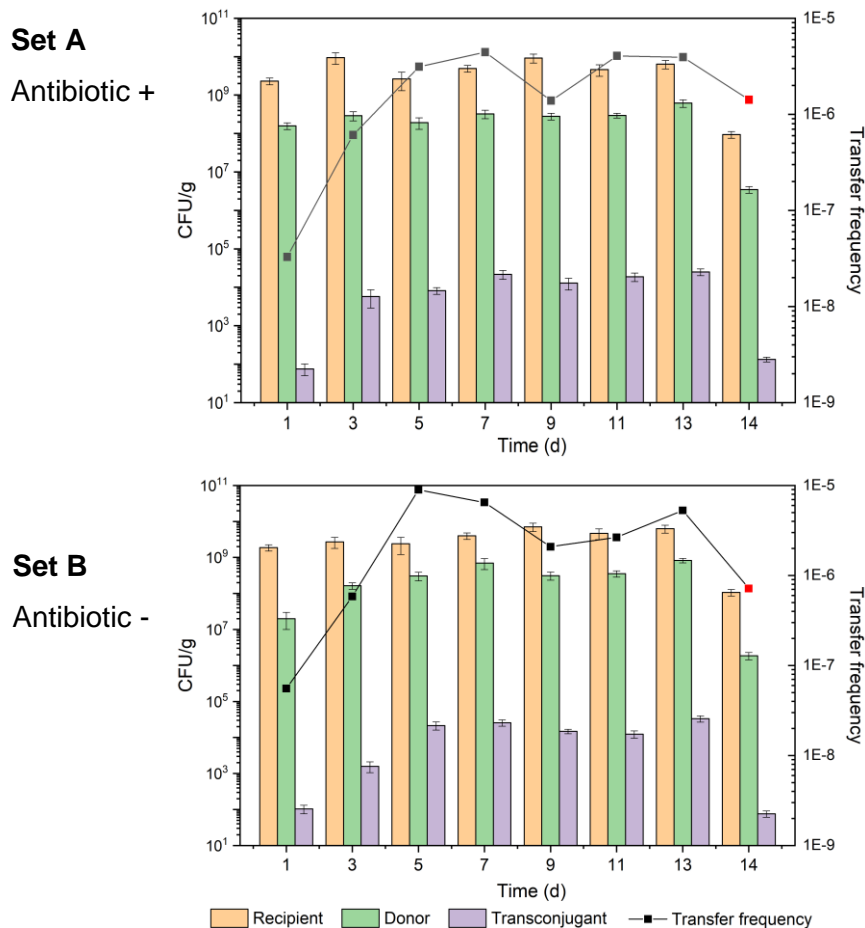


Figure 7.3 Impact of sand biofiltration on the frequency of RP1 plasmid conjugative transfer.

Bars: Numbers of *E. coli*; Lines: Transfer frequency. Backwash was conducted on day 14. The error bars represent STD from the mean value of triplicate samples ($n = 3$).

7.2.1.2 GAC Biofiltration

Unlike sand, where the numbers of donor and recipient slightly fluctuated during the experimental period, steady increase trends for both strains were observed in GAC media samples from day 1 to day 13 (Figure 7.4). A 1.87-log and 2.34-log increase was observed for recipient and donor cells, respectively. It is worth noting that the number of transconjugants remained at similar levels (3.92×10^4 CFU/g on average) over time, resulting in a reduced transfer frequency from 5.40×10^{-5} on day 3 to 1.05×10^{-5} on day 13. No transfer was observed on day 1.

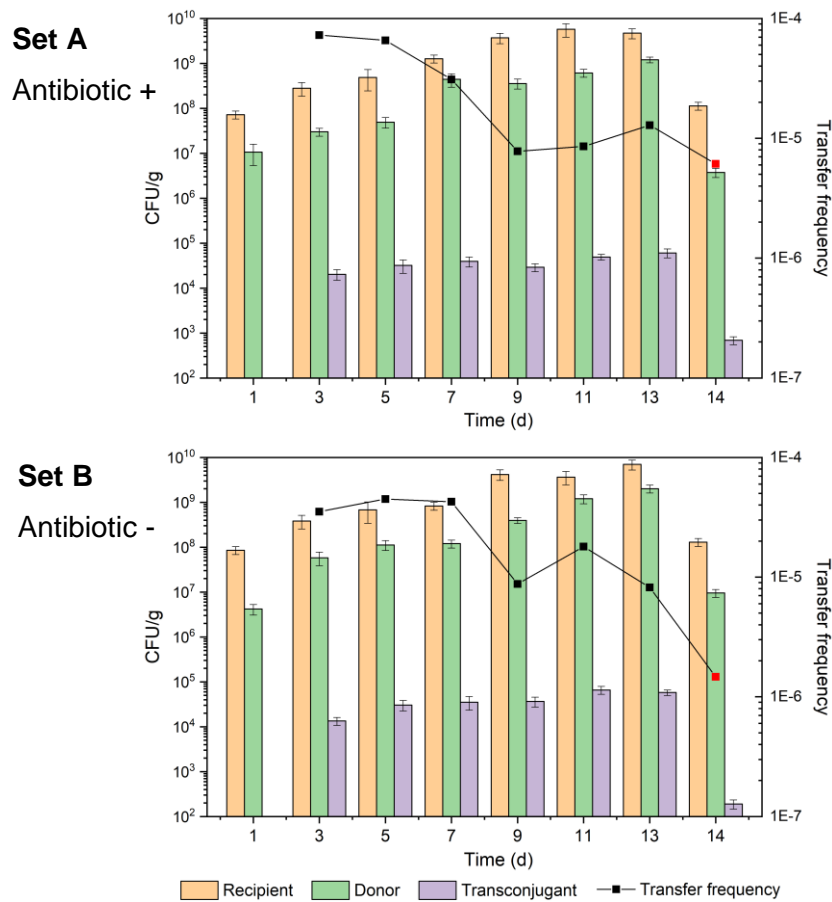


Figure 7.4 Impact of GAC biofiltration on the frequency of RP1 plasmid conjugative transfer.

Bars: Numbers of *E. coli*; Lines: Transfer frequency. Backwash was conducted on day 14. The error bars represent STD from the mean value of triplicate samples ($n = 3$).

After backwashing (day 14), the number of recipient and donor cells was reduced from 5.88×10^9 and 1.61×10^9 CFU/g to 1.22×10^8 and 6.65×10^6 CFU/g, respectively, with the transfer frequency lowered 4-fold compared to day 13. The number of transconjugants was

significantly correlated to both the donor ($r = 0.897$, $P < 0.001$) and recipient cells ($r = 0.875$, $P < 0.01$) in GAC media samples, indicating that the occurrence of conjugative transfer in GAC was affected by both the donor and recipient cell densities.

7.2.1.3 Anthracite Biofiltration

The donor and recipient cell densities in anthracite media samples in both Set A and B increased gradually over time (Figure 7.5), similar to the trend observed in GAC samples, indicating that the *E. coli* cells accumulated on the carbon-rich/based media surface. Compared to GAC, anthracite had a slightly lower *E. coli* cell load, with 0.53-log and 0.27-log fewer donor and recipient cells, respectively, probably due to the non-porous structure of anthracite. The number of transconjugants increased gradually from 8.58×10^2 CFU/g on day 3 to 1.85×10^4 CFU/g on day 13. No transconjugant colonies were found on day 14. The number of transconjugants increased gradually from 8.58×10^2 CFU/g on day 3 to 1.85×10^4 CFU/g on day 13. No transconjugant colonies were found on day 14.

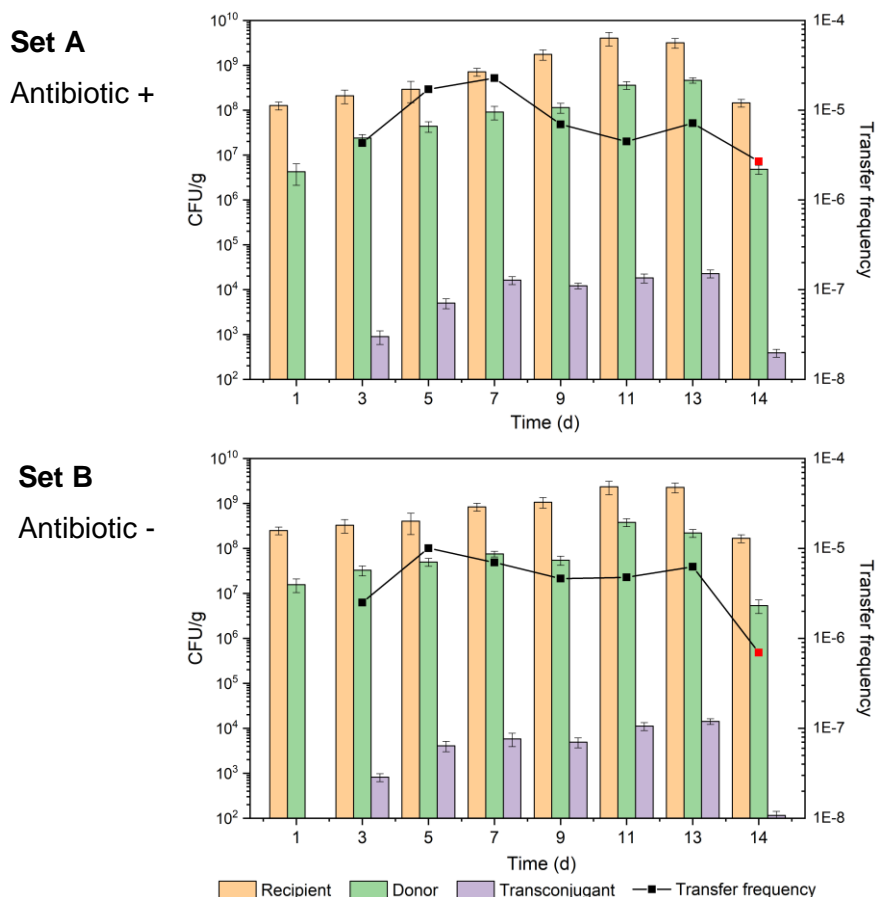


Figure 7.5 Impact of anthracite biofiltration on the frequency of RP1 plasmid conjugative transfer. Bars: Numbers of *E. coli*; Lines: Transfer frequency. Backwash was conducted on day 14.

The error bars represent STD from the mean value of triplicate samples ($n = 3$).

Due to the simultaneous growth of both recipients and transconjugants, transfer frequency remained at around 10^{-5} over time from day 3 to day 13, and dropped down to 2.69×10^{-6} and 6.93×10^{-7} in Set A and B, respectively, after backwashing (day 14). The number of transconjugants was significantly correlated to both the donor ($r = 0.916$, $P < 0.001$) and recipient cells ($r = 0.922$, $P < 0.01$) in anthracite media samples.

7.2.1.4 Comparisons between different media

Transconjugants were firstly found in sand samples on day 1, probably due to the fine size of sand could retain more bacterial cells and increase the incidence of the physical contact of donor and recipient. Figure 7.6 shows that the GAC media had the highest RP1 plasmid conjugative transfer frequency (2.60×10^{-5} on average), followed by anthracite (5.31×10^{-6} on average) and sand (2.47×10^{-6} on average). The high surface area and unique pore structure of GAC may induce bacterial collision and attachment, contributing to a more frequent conjugation. Anthracite showed a fluctuating but relatively stable transfer frequency compared to sand and GAC. Transfer frequencies reduced significantly ($p < 0.01$) in all of the media samples after backwashing was conducted on day 14.

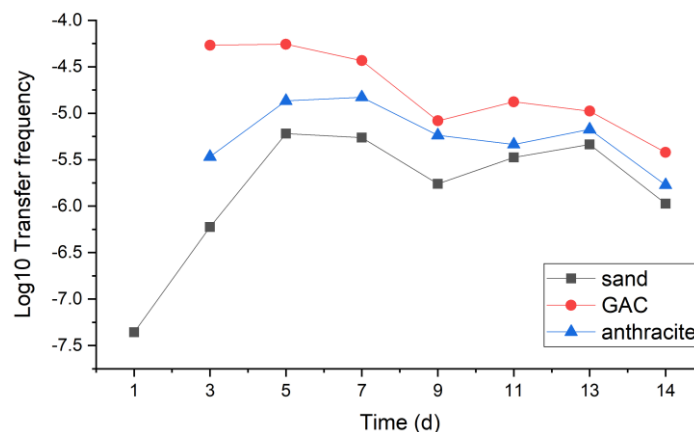


Figure 7.6 Dynamic changes of RP1 plasmid transfer frequency in media samples over time.

7.2.1.5 Impact of antibiotic spike

Biofilters were exposed to $2 \mu\text{g/L}$ of antibiotic mixture in Set A, while Set B was only fed with 1% LB without antibiotics addition. The average conjugative transfer frequency in media samples in Set A and B are shown in Figure 7.7. Although slightly higher transfer rates were observed in GAC and anthracite media samples when exposed to antibiotics, no

statistical difference ($p > 0.05$) was found between the Set A and B. This is possibly due to the antibiotic spike concentration was not sufficient to exhibit a selective pressure on *E. coli* strains to induce the conjugative transfer. Lundström *et al.* reported that 1 µg/L tetracycline selects for *tetA* gene in freshwater biofilms, and a higher level of 10 µg/L is sufficient to select for resistant bacteria [122]. The minimal selective concentration for resistant bacteria was predicted at 2 µg/L for amoxicillin and clarithromycin; 4 µg/L for oxytetracycline; 8 µg/L for trimethoprim; and 125 µg/L for sulfamethoxazole [289]. The concentration of 2 µg/L used throughout this study was likely to be too low for the selection of resistant recipients. However, in real drinking water treatment conditions, microbes are generally exposed not only to trace levels of antibiotics, but also to other micropollutant residues such as disinfection by-products and heavy metals, which can co-select for MGEs carrying multiple resistant genes, contributing to the spread of resistance in both biofilm and water samples [106, 108, 318].

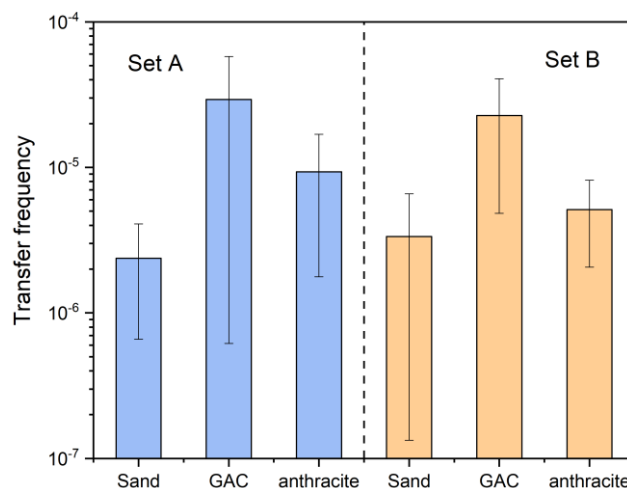


Figure 7.7 Comparisons of RP1 plasmid conjugative transfer frequency in Set A: biofilters exposed to 2 µg/L of antibiotic mixture; and Set B: biofilters without antibiotics exposure.

The error bars represent STD from the mean value of all batch samples ($n = 8$).

7.2.2 Plasmid conjugative transfer in biofilter aqueous samples

7.2.2.1 Influent samples

The system was fed with approximately 10^7 CFU/mL donor and recipient cells through this study. Figure 7.8 shows the actual number of donor and recipient colonies in Set A and B influent samples. No statistical difference ($p = 0.816$) was found between the donor and

recipient in biofilter feed. Although the biofilm developed on the media surface was seeded from the same feed, recipient colonies found in the media samples were significantly higher ($p < 1.0 \times 10^{-7}$) than donors. This indicated that the recipient *E. coli* HB101 strain has a stronger biofilm-forming ability on the media surface, which is crucial for the occurrence of conjugative transfer. The influent samples on day 14 were collected from each biofilter top after backwashing was conducted, therefore, the numbers indicated the donor and recipient in the backwashed water instead of freshly prepared feed. Bacterial cells were washed off from the media surface (stationary phase) by physical scouring and entered into the feed (planktonic phase) again. Not surprisingly, higher numbers of recipient cells were found in the backwashed water, similar to the trend found in media samples.

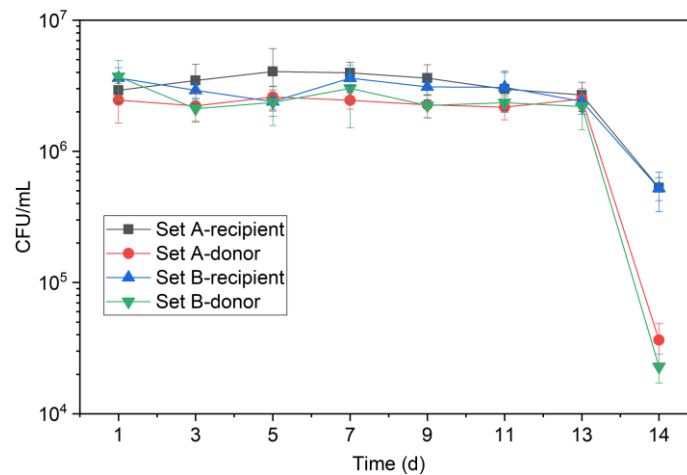


Figure 7.8 Number of donor and recipient cells (CFU/mL) in the influent samples. The error bars represent STD from the mean value of triplicate samples ($n = 3$).

7.2.2.2 The removal of *E. coli* strains

The average removal of *E. coli* strains was 55.1% by the biofilters during the two-week's operation. Although no significant difference was found between the removal of the recipient and donor ($p > 0.05$), it should be noted that sand filter preferably reduced the number of donors, while GAC and anthracite had higher removal of the recipients (Figure 7.9). This might be related to the differences in characteristics of the filter media. The numbers of *E. coli* strains in the filtered water were positively correlated to the numbers in the influent ($r > 0.89$, $P < 0.01$) and independent to the numbers found in the corresponding media samples ($P >$

0.40), suggesting that the donor and recipient behaved differently in stationary phase (media surface) and planktonic phase (influent and effluent), which could consequently affect the conjugative transfer.

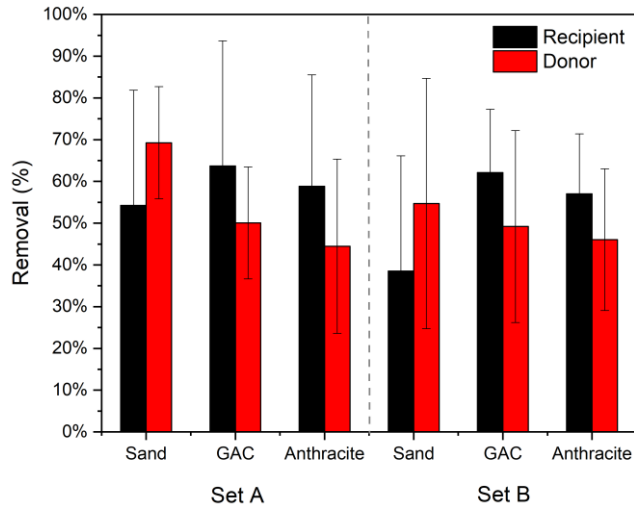


Figure 7.9 The removal of donor and recipient by biofilters. **Set A: biofilters exposed to 2 µg/L of antibiotic mixture; Set B: biofilters without antibiotics exposure.** The error bars represent STD from the mean value of all batch samples (n = 8).

7.2.2.3 Conjugative transfer occurred in aqueous samples

Table 7.2 summarises the transfer frequency of the RP1 plasmid in the influent and effluent samples. Numbers of transconjugants ranged from 10 CFU/mL to 50 CFU/mL, with an average transfer frequency of 3.17×10^{-6} in the influent and 1.86×10^{-5} in the effluent samples during days 1 to 13. Apart from the spontaneous occurrence of conjugation, the enhanced transfer rate in the filtered water was probably due to the 'escape' of transconjugants from the media surface. During days 1 to 13, transconjugants were found in 57.1% of the Set A influent sample, while only 14.3% were detected in Set B. No transconjugants were found in the sand biofilter effluent samples. Interestingly, on day 1, transconjugants were absent in GAC media while present in one of the GAC filtered water samples, and an opposite trend was found in the sand biofilters. This further confirmed that the conjugative transfers in stationary phase (media surface) and planktonic phase (influent and effluent) were different. After backwashing was conducted on day 14, transconjugants were found in 67% of the effluent samples.

Table 7.2 The transfer frequency of RP1 plasmid in the influent and effluent samples.

Time (d)	Influent		Effluent - Set A			Effluent – Set B		
	Set A	Set B	Sand	GAC	Anthracite	Sand	GAC	Anthracite
1	3.42×10^{-7}	n.a.	n.a.	n.a.	n.a.	n.a.	2.40×10^{-6}	n.a.
3	n.a.	n.a.	n.a.	n.a.	n.a.	n.a.	n.a.	4.48×10^{-5}
5	4.93×10^{-6}	n.a.	n.a.	1.56×10^{-5}	n.a.	n.a.	n.a.	n.a.
7	n.a.	n.a.	n.a.	n.a.	1.72×10^{-5}	n.a.	n.a.	6.58×10^{-6}
9	n.a.	n.a.	n.a.	n.a.	2.16×10^{-5}	n.a.	n.a.	n.a.
11	3.36×10^{-6}	3.25×10^{-6}	n.a.	n.a.	n.a.	n.a.	n.a.	n.a.
13	3.72×10^{-6}	n.a.	n.a.	n.a.	n.a.	n.a.	1.47×10^{-5}	n.a.
*14	1.90×10^{-5}	1.92×10^{-5}	1.60×10^{-5}	4.55×10^{-5}	3.07×10^{-5}	n.a.	n.a.	1.66×10^{-5}

Set A: biofilters exposed to 2 µg/L of antibiotic mixture; Set B: biofilters without antibiotics exposure.

*14: backwash was conducted for the system. Colours indicate the levels of transfer frequency.

7.3 Overall discussion

7.3.1 Mechanisms underlying the RP1 plasmid conjugative transfer

To rule out spontaneous mutation of recipient strains during biofiltration and to confirm the transfer of RP1 plasmid, one to three colonies were randomly chosen from the plates on which transconjugants grew for all batch samples. No false-positive colony was identified by PCR (Figure A7.1). All of the transconjugants were confirmed to have *bla*_{TEM} and *tetA*. The result indicated that all colonies have acquired RP1 plasmids. No spontaneous mutation of recipient strains was observed throughout the study.

The donor and recipient have the ability to attach, form and integrate into a biofilm on the media surface, providing a stationary phase in a continuous feed (planktonic phase) allowing for a longer contact time between the donor and recipient cells. Based on the findings of this study, we inferred that RP1 plasmid conjugative transfer might occur in three different contexts (Figure 7.10): 1) stationary phase, where the transfer takes place either on the surface or inside the media (e.g. GAC micropores). In the biofilm, the relative spatial stability and the close contact of donor and recipient numbers prompted the plasmid conjugative transfer; 2) stationary-planktonic phase, where the transfer occurs between the bacteria

retained in the biofilm and the bacteria in the feed water flowing through the media. A relatively lower HLR was used throughout this study, allowing the microbes in the feedwater to have the opportunity to interact with microbes in the biofilm, resulting in conjugative transfer of RP1; and 3) planktonic phase, where the transfer might occur in the feed (before filtration), during filtration, or in the effluent (after filtration). The frequency of transfer in the planktonic phase is expected to be much lower than that in other two forms. For conjugative transfer of a plasmid in liquid environments, donor and recipient cells must make physical contact, attach, and then conjugate before detachment occurs [92]. Theoretically, it is not possible to distinguish between the three contexts. Bacteria can be mobilised between the biofilm and water (e.g. biofilm detachment) during the biofiltration. In this study, we assumed that the occurrence of plasmid conjugative transfer in stationary phase affected the results obtained from media samples, and the other two phases affected the results in effluent samples.

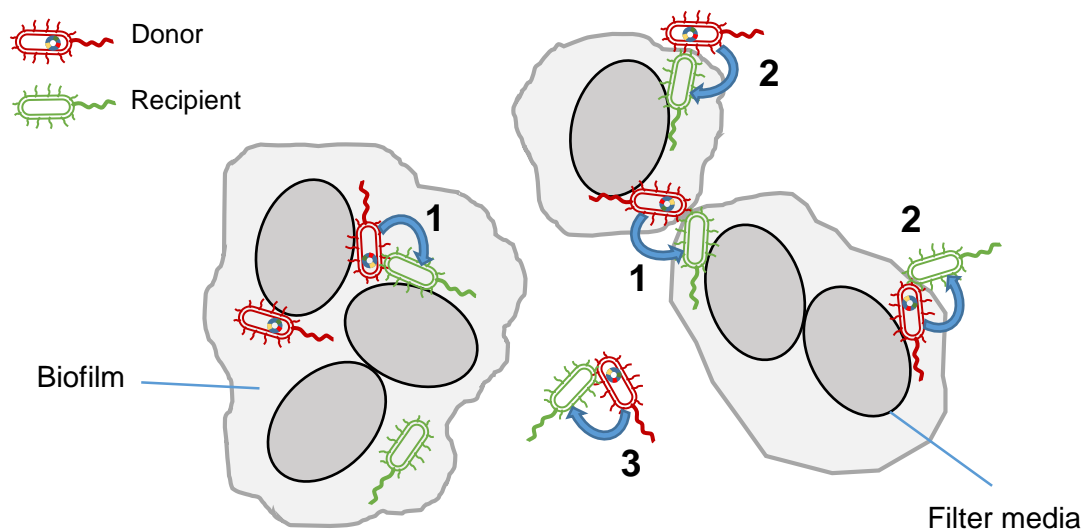


Figure 7.10 Conjugative transfer of RP1 plasmid within stationary phase (1); between stationary and planktonic phase (2); and in planktonic phase (3).

7.3.2 Reduction of conjugative transfer in drinking water treatment process

Conventional water disinfection processes can generally minimise the risks of conjugative transfer by reducing the numbers of viable donor cells containing transferable plasmids. Lin *et al.* confirmed that UV irradiation and chlorination could reduce the rate of conjugative plasmid transfer and the inhibitory effect on transferability increased with

increasing doses of chlorine [317]. The researchers were also concerned that the bacteria, post-UV irradiation, may still transfer plasmids to the surrounding communities by entering a viable but not culturable state. In fact, even if the resistant bacteria are fully inactivated after the disinfection process, intact DNA residues contained within the resulting cell debris could still confer resistance genotypes to downstream bacterial populations by natural transformation and/or transduction, which do not require live donor cells [103, 256].

7.3.3 Environmental implications

Conjugative transfer during the biofiltration process in this study was achieved with higher bacterial cell densities than the real ones in drinking water conditions and only limited to exposure to five antibiotics, although a similar nutrient concentration (TOC = 6 mg/L) was used throughout the study. However, the results can be extended to drinking water environment to a certain degree. For example, after backwashing, high densities of donors and transconjugants with transferable plasmids were removed from the media surface and entered into the planktonic phase again, rendering the backwashed 'waste' (mixture of surface media and water) a new environmental hot spot for the release of resistance genes. Furthermore, different media exhibited different levels of conjugative transfer potential, which could be used in assessing risk and can provide a useful reference for researchers.

Because the donor strain and recipient strain used in this study were both *E. coli* strains which belong to the *Enterobacteriaceae* family, the high transfer frequency of the RP1 plasmid in media sample reflects the rapid spread of these plasmid-mediated ARGs among *Enterobacteriaceae* family in the biofilm environment [97]. This family also includes many classic waterborne pathogens such as *Salmonella* spp. and *Shigella* spp., which are widely distributed in natural water bodies and are important vehicles of antibiotic resistance, namely in drinking water [319-321]. The horizontal transfer of the conjugative plasmids that occurs during biofiltration may lead to the emergence of multi-drug resistant human pathogens in the treated water, which requires a more rigorous disinfection strategy prior to entering the distribution systems.

7.4 Summary

Overall, this study has found that the transferability of the RP1 plasmid to the recipient *E. coli* HB101 is affected by the biofiltration process. Listed below are the main findings in the present study:

- RP1 transfer occurred more frequently in biofilm samples than influent and effluent samples;
- GAC media samples had the highest conjugative transfer frequency, followed by anthracite and sand;
- The spike of 2 µg/L antibiotic mixture to biofilter feed did not affect the transferability of RP1 plasmid during biofiltration. The transfer frequency was 1.5×10^{-5} in the biofilms exposed to antibiotics and 1.2×10^{-5} in the control biofilms.
- Backwash can reduce the transferability of RP1 plasmid significantly in biofilms but introduces more transconjugants into the planktonic phase.

Chapter 8

CONCLUSION AND FUTURE WORK

8 CONCLUSION AND FUTURE WORK

8.1 Summary and Conclusions

This study thoroughly investigated the drinking water biofiltration systems for the attenuation of five antibiotics (amoxicillin, clarithromycin, oxytetracycline, sulfamethoxazole, and trimethoprim), 13 ARGs (*bla_{CTX-M}*, *bla_{OXA-1}*, *bla_{TEM}*, *ermB*, *tetA*, *tetG*, *tetQ*, *tetW*, *tetX*, *sul 1*, *sul 2*, *dfrA1* and *dfrA12*) and integrons (*intl 1* and *intl 2*). As a starting point, all methodologies used for the analysis of general water quality parameters, antibiotics and the target genes were developed prior to the set-up of biofilters. Then, sand, GAC and anthracite were selected as the filter media and three biofiltration experiments were performed at bench-scale. Over a period of 3 months, the overall performance, removal of antibiotics and behaviour of ARGs were explored during the first and second biofiltration experiments, where different types of biofilter columns were established. Finally, the impact of filter media on the transfer of resistance genes was also evaluated based on the last biofiltration experiment. A schematic summarising the overall structure and main findings of the biofiltration research is given in Figure 8.1. Overall, the results of this study may provide insights into the mechanism of persistent bacterial antibiotic resistance in drinking water treatment. The most significant conclusions related to different aspects of this study are summarised below.

8.1.1 Biofilter performance

- GAC-associated biofilters exhibited superior performance in reducing organic carbon from the feed compared to the non-adsorptive sand and anthracite biofilters.
- The addition of antibiotics (at 10 µg/L) to the feed has the potential to interrupt microbial nitrification/denitrification processes.
- GAC sandwich biofilters with the GAC layer loaded in the middle of filter bed showed a better removal of organic carbons than those with the GAC layer in the upper or lower position.

- Biofilter backwashing/cleaning had a considerable impact on pH, conductivity, DO, turbidity, nitrate, total coliforms and *E. coli*, while organic carbon-related parameters were not sensitive to backwashing/cleaning, allowing conventional performance parameters to be optimised without compromising DOC removal.

8.1.2 Removal of antibiotics by biofiltration

- Drinking water biofiltration has the potential to be an effective process for the control of trace level antibiotic contaminations. The target antibiotics were substantially removed (> 90%) by GAC-associated biofilters and partially removed (< 20%) by sand and anthracite-sand dual media biofilters.
- For the non-adsorptive media, trimethoprim was biodegraded more effectively in the sand biofilter (55.5%) than that in the anthracite-sand biofilter (12.9%). By contrast, oxytetracycline was removed more effectively by anthracite-sand (33.1%) than sand media (20.0%).
- The GAC sandwich biofilter represents a more promising process for drinking water treatment in order to reduce the risk associated with antibiotics in drinking water.
- No difference in antibiotic removal was found between biofilters with different GAC thicknesses (9 cm or 4 cm GAC), or between biofilters with 4 cm of GAC at different depths.
- Except for trimethoprim, biofilter backwashing/cleaning process did not exert a noticeable effect on the removal of the amoxicillin, clarithromycin, oxytetracycline and sulfamethoxazole.
- Adsorption kinetics showed that sulfamethoxazole fitted with pseudo-first-order adsorption model, while trimethoprim, amoxicillin, oxytetracycline and clarithromycin fitted the pseudo-second-order model. All antibiotics fitted with Langmuir model according to the isotherm experiment.

8.1.3 Behaviour of ARGs during biofiltration

- Positive correlations in absolute abundance were found between the ARGs and the *16S rRNA* gene and the integrons in all biofilm and water samples.
- Among the ARGs present, *sul 1* was the most abundant resistance gene in all types of samples. *TetG* and *tetX* were more abundant among the tetracycline resistance genes; while *bla_{TEM}* and *bla_{OXA-1}* were more prevalent among β -lactam resistance genes. Trimethoprim resistance genes (*dfrA*) showed the least abundance.
- The absolute abundance of ARGs decreased (1.0-log reduction on average) after biofiltration, while the ARGs' normalised copy number remained unchanged or showed an increasing trend in the filtered water, especially when exposed to the target antibiotics.
- Biofilm samples represented higher risk of ARG pollution than in the aqueous samples; and for the same types of media, the proportion of ARGs-carrying bacteria was greater in the deeper layer biofilms compared to the surface biofilms.
- General water quality parameters showed limited effects (16%~23%) on the distribution characteristics of ARGs in the effluents.

8.1.4 Association of ARGs with bacterial community in biofilms

- Bacterial community and mobile genetic elements explained 50.2% (on average) and 8.2% (on average) difference in ARG patterns in biofilms, respectively, and 16.9% (on average) of the variation could be attributed to the interactions between bacterial communities and MGEs.
- The exposure to the target antibiotics at 10 $\mu\text{g/L}$ affected the bacterial community in biofilm samples and the differences in bacterial community structure were correlated with the changes in the resistome.
- Network analysis showing the co-occurrence patterns between ARGs and bacterial taxa suggested that 10 taxonomic genera (*Nitrospira*, *Methyloversatilis*, *Methylotenera*,

Bacillus, *Sphingopyxis*, *Lysobacter*, *Noviherbaspirillum*, *Nitrospira*, *Methyloversatilis*, *Rhodobacter*) were implicated as possible ARG hosts.

8.1.5 Horizontal gene transfer during biofiltration

- Compared to sand and anthracite, GAC media is more conducive to the horizontal conjugative transfer of ARGs in biofilms.
- Conjugative plasmid transfer occurred more frequently in biofilms than in the influents and effluents.
- The spike of 2 µg/L antibiotic mixture to biofilter feed did not affect the transferability of RP1 plasmid during biofiltration. The transfer frequency was 1.5×10^{-5} in the biofilms exposed to antibiotics and 1.2×10^{-5} in the control biofilms.
- Backwashing can reduce the transferability of RP1 plasmid significantly in biofilms but introduces more transconjugants into the planktonic phase.

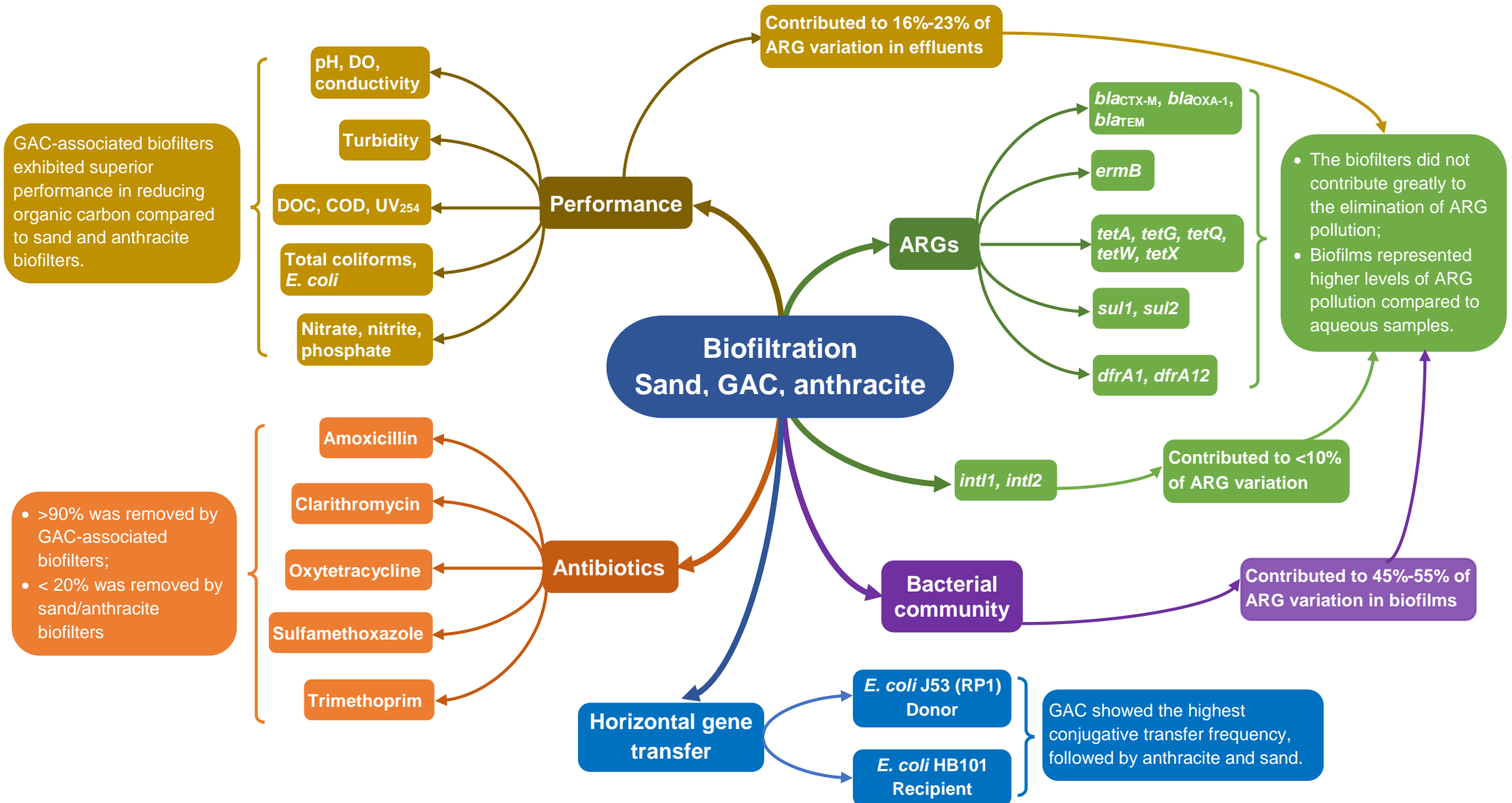


Figure 8.1 Mind map showing the overall structure of the biofiltration experiment.

GAC: granular activated carbon; DO: dissolved oxygen; DOC: dissolved organic carbon; COD: chemical oxygen demand; UV₂₅₄: specific ultraviolet absorbance (254 nm).

8.2 Limitations and suggestions for future research

As with the majority of studies, the design of the current study is subject to limitations. Based on the experimental work from the bench-scale biofilters, the potential limitations are identified and discussed below.

Although natural surface water is generally used as a drinking water source and was also used throughout this study, the quality of raw water was expected to be less complex than the feedwater used in real drinking water biofilters. Prior to biofiltration, various treatment strategies were employed in DWTPs, such as coagulation/flocculation together with sedimentation to remove particles from the source water and pre-ozonation to reduce the production of disinfection by-products as well as to increase the biodegradability of organic compounds [42, 62]. These pre-treatments could increase the complexity of the feedwater for biofilters. Nevertheless, the interactions observed between the naturally occurring organic matter and the antibiotics, and between the indigenous microbial community and ARGs/integrans in this study could provide a useful reference for researchers and can also be extended to the real drinking water treatment environment to a certain degree.

For the elimination of the target antibiotics, the present research only investigated the antibiotics in their original form. Biodegradation pathways and metabolites could be further studied to understand the antibiotic degradation mechanisms. This can be difficult due to the typically low concentration of antibiotic residues in the feed and high background organic matter which could interfere with product identification and quantification [156]. Additional research is needed to identify the dominant antibiotic biodegradation by-products and clarify the relevant pathways in drinking water biofilters.

Previous research and the first biofiltration experiment considered the mixture of surface filter medium and the upper slimy layer as the surface biofilm samples, however, they may represent different levels of risk of ARG pollution. As the surface biofilm shapes the bacterial community in the drinking water microbiome [286], it is important to understand which part of the biofilm exerts higher risks in ARG proliferation during biofiltration. This could further provide

an insight into biofilter management strategies and appropriate ways for the disposal of used media. For instance, considering the persistence of ARGs during biofiltration process, land application of drinking water waste products may act as an environmental exposure route for trace level ARGs and introduce a reservoir and source for diffuse pollution in previously unexposed regions.

The bacterial community in the filtered water was not targeted in this study. Previous research has reported that the bacterial community within surface GAC biofilms in GAC-sand biofilter shapes the drinking water microbiome in DWTP and water quality parameters were related to different bacterial groups in the filtered water [286]. Therefore, this provides an operational option to control the bacterial community structure by altering water quality parameters and consequently affecting ARG profiles as they significantly correlate to the bacterial community during biofiltration. This may help to reduce ARG-related risks from the source water without compromising the superior operational performance of the GAC sandwich biofilter.

Previous studies have confirmed that network analysis can be used to provide new insights into ARGs and their possible hosts in complex environmental scenarios (e.g. surface water, soil and vegetables) [191, 208, 211]. The network analysis used in this study was based on correlation analysis, therefore, the correlation between the two nodes (ARG subtype and bacterial taxa) merely depends on their presence and abundance. Metagenomic analysis, on the other hand, is a powerful tool which can be used to explore the entire antibiotic resistome and therefore could improve the robustness of the network analysis in predicting ARG hosts, especially in complex environmental microbial communities [201, 207, 221]. In addition to the benefits of metagenomics for broad observation of the taxonomic and functional genes from an entire community, metatranscriptomics could further provide a functional profile by analysing which ARGs are actively being expressed by the community [322]. The advancement of messenger RNA (mRNA) extraction from environmental samples enables metatranscriptomics the potential to become the main method for the detection of functional resistance genes [216]. For future work, the combination of metagenomics and metatranscriptomics can be utilised to

specifically link ARGs to their transcripts and genetic context, providing a comprehensive insight into the abundance, diversity, expression and hosts of ARGs in various environmental samples. Two recent studies are cited here. By using metagenomic and metatranscriptomic approaches, Liu *et al.* reported that 65.8% of the identified ARGs in activated sludge samples are being expressed and plasmid-associated ARGs are more likely to be expressed, which further enhance the understanding of the prevalence of ARGs in WWTPs and benefit environmental risk assessment and management of ARGs [292]. Another case study conducted by Rowe *et al.* has found that ARGs in hospital effluents are expressed at significant levels and are possibly related to the level of antibiotic usage at the effluent source [323]. Metaproteomic sequencing involves random sequencing of the amino acid sequences that represent the protein material in a microbial community. The primary advantage of metaproteomics is the ability to identify proteins (e.g. proteins related to antibiotic resistance) that have not only been expressed as mRNA but have also been folded and have potentially formed active proteins in a cell [322]. A very recent study applying both metagenomics and metaproteomics has revealed the significant co-occurrence patterns among bacteria, ARGs and transposase gene during aerobic composting. This indicates the applicability of the combination of metagenomic and metaproteomic approaches in the field of AMR [324]. So far, metagenomics, metatranscriptomics, metaproteomics or the combination of them have not been applied on ARG research in drinking water biofiltration treatment. Considering the complexity of surface biofilms, the application of these techniques could help to further explain how the microbiome react to antibiotic stress within biofilms and how the expression of ARGs relate to antibiotic selection pressure during the biofiltration process.

Further experiments are needed to explore the impact of biofiltration variables on plasmid conjugative transfer. For example, flow rate is a critical operational factor that could affect the performance of biofilters; the antibiotic spike concentration plays an important role in selecting both phenotypic and genotypic resistance. Genotypic analysis could be included in a future study as the trace level of antibiotics may induce genotypic resistance but may not be sufficient to induce phenotypic resistance due to the lack of gene expression.

References

References

1. Wright, G.D., The antibiotic resistome: the nexus of chemical and genetic diversity. *Nature Reviews Microbiology*, 2007. **5**(3): p. 175-186.
2. Coates, A.R.M., Halls, G., and Hu, Y.M., Novel classes of antibiotics or more of the same? *British Journal of Pharmacology*, 2011. **163**(1): p. 184-194.
3. Powers, J.H., Antimicrobial drug development - the past, the present, and the future. *Clinical Microbiology and Infection*, 2004. **10**: p. 23-31.
4. Kummerer, K., Antibiotics in the aquatic environment - A review - Part I. *Chemosphere*, 2009. **75**(4): p. 417-434.
5. Finberg, R.W., *et al.*, The importance of bactericidal drugs: Future directions in infectious disease. *Clinical Infectious Diseases*, 2004. **39**(9): p. 1314-1320.
6. Wong, W.R., Oliver, A.G., and Linington, R.G., Development of antibiotic activity profile screening for the classification and discovery of natural product antibiotics. *Chemistry & Biology*, 2012. **19**(11): p. 1483-1495.
7. Acar, J.F., Classification of antibiotics. *Revue Du Praticien*, 1977. **27**(43): p. 2757-2759.
8. Burch, D., Problems of antibiotic resistance in pigs in the UK. *In Practice*, 2005. **27**(1): p. 37-43.
9. Kemper, N., Veterinary antibiotics in the aquatic and terrestrial environment. *Ecological Indicators*, 2008. **8**(1): p. 1-13.
10. Martinez, J.L., Environmental pollution by antibiotics and by antibiotic resistance determinants. *Environmental Pollution*, 2009. **157**(11): p. 2893-2902.
11. Aarestrup, F.M., Veterinary drug usage and antimicrobial resistance in bacteria of animal origin. *Basic & Clinical Pharmacology & Toxicology*, 2005. **96**(4): p. 271-281.
12. Landers, T.F., *et al.*, A review of antibiotic use in food animals: perspective, policy, and potential. *Public Health Reports*, 2012. **127**(1): p. 4-22.

13. Klein, E.Y., *et al.*, Global increase and geographic convergence in antibiotic consumption between 2000 and 2015. *Proceedings of the National Academy of Sciences*, 2018. **115**(15): p. E3463-E3470.
14. Van Boeckel, T.P., *et al.*, Global antibiotic consumption 2000 to 2010: an analysis of national pharmaceutical sales data. *The Lancet Infectious Diseases*, 2014. **14**(8): p. 742-750.
15. Aarestrup, F., Get pigs off antibiotics. *Nature*, 2012. **486**(7404): p. 465-466.
16. ECDC, The bacterial challenge: time to react. 2009: *ECDC/EMEA Joint Technical Report*. p. 13-42.
17. Antibiotic resistance threats in the United States, 2013. US Centers for Disease Control and Prevention.
18. O'Neill, J., Antimicrobial resistance: tackling a crisis for the health and wealth of nations. *Review on Antimicrobial Resistance*, 2014. **20**: p. 1-16.
19. Veterinary Medicines Directorate, UK One Health Report - Joint report on antibiotic use and antibiotic resistance, 2013–2017. 2019.
20. Public Health England, English surveillance programme for antimicrobial utilisation and resistance (ESPAUR), 2018.
21. Veterinary Medicines Directorate, Veterinary Antimicrobial Resistance and Sales Surveillance 2017, 2017.
22. Kummerer, K., Significance of antibiotics in the environment. *Journal of Antimicrobial Chemotherapy*, 2003. **52**(1): p. 5-7.
23. Boleda, M.R., Galceran, M.T., and Ventura, F., Validation and uncertainty estimation of a multiresidue method for pharmaceuticals in surface and treated waters by liquid chromatography-tandem mass spectrometry. *Journal of Chromatography A*, 2013. **1286**: p. 146-58.
24. Tran, N.H., *et al.*, Occurrence and removal of multiple classes of antibiotics and antimicrobial agents in biological wastewater treatment processes. *Water Research*, 2016. **104**: p. 461-472.

25. Le-Minh, N., *et al.*, Fate of antibiotics during municipal water recycling treatment processes. *Water Research*, 2010. **44**(15): p. 4295-4323.
26. Hao, H.H., *et al.*, Benefits and risks of antimicrobial use in food-producing animals. *Frontiers in Microbiology*, 2014. **5**.
27. Larsson, D.G.J., de Pedro, C., and Paxeus, N., Effluent from drug manufactures contains extremely high levels of pharmaceuticals. *Journal of Hazardous Materials*, 2007. **148**(3): p. 751-755.
28. Chang, X.S., *et al.*, Determination of antibiotics in sewage from hospitals, nursery and slaughter house, wastewater treatment plant and source water in Chongqing region of Three Gorge Reservoir in China. *Environmental Pollution*, 2010. **158**(5): p. 1444-1450.
29. Yan, C.X., *et al.*, Antibiotics in the surface water of the Yangtze Estuary: Occurrence, distribution and risk assessment. *Environmental Pollution*, 2013. **175**: p. 22-29.
30. Xu, J., *et al.*, Occurrence of antibiotics and antibiotic resistance genes in a sewage treatment plant and its effluent-receiving river. *Chemosphere*, 2015. **119**: p. 1379-1385.
31. Boleda, M.R., *et al.*, Survey of the occurrence of pharmaceuticals in Spanish finished drinking waters. *Environmental Science and Pollution Research*, 2014. **21**(18): p. 10917-10939.
32. Jiang, L., *et al.*, Occurrence, distribution and seasonal variation of antibiotics in the Huangpu River, Shanghai, China. *Chemosphere*, 2011. **82**(6): p. 822-828.
33. Watkinson, A.J., *et al.*, The occurrence of antibiotics in an urban watershed: from wastewater to drinking water. *Science of the Total Environment*, 2009. **407**(8): p. 2711-23.
34. Benotti, M.J., *et al.*, Pharmaceuticals and endocrine disrupting compounds in US drinking water. *Environmental Science & Technology*, 2009. **43**(3): p. 597-603.
35. Leung, H.W., *et al.*, Pharmaceuticals in tap water: human health risk assessment and proposed monitoring framework in China. *Environmental Health Perspectives*, 2013. **121**(7): p. 839-846.
36. WHO, Pharmaceuticals in drinking-water. 2012.

37. Boleda, M.R., Galceran, M.T., and Ventura, F., Behavior of pharmaceuticals and drugs of abuse in a drinking water treatment plant (DWTP) using combined conventional and ultrafiltration and reverse osmosis (UF/RO) treatments. *Environmental Pollution*, 2011. **159**(6): p. 1584-1591.
38. Simazaki, D., *et al.*, Occurrence of selected pharmaceuticals at drinking water purification plants in Japan and implications for human health. *Water Research*, 2015. **76**: p. 187-200.
39. Ye, Z.Q., Weinberg, H.S., and Meyer, M.T., Trace analysis of trimethoprim and sulfonamide, macrolide, quinolone, and tetracycline antibiotics in chlorinated drinking water using liquid chromatography electrospray tandem mass spectrometry. *Analytical Chemistry*, 2007. **79**(3): p. 1135-1144.
40. Dantas, G., *et al.*, Bacteria subsisting on antibiotics. *Science*, 2008. **320**(5872): p. 100-103.
41. Reungoat, J., *et al.*, Biofiltration of wastewater treatment plant effluent: Effective removal of pharmaceuticals and personal care products and reduction of toxicity. *Water Research*, 2011. **45**(9): p. 2751-2762.
42. Reungoat, J., *et al.*, Removal of micropollutants and reduction of biological activity in a full scale reclamation plant using ozonation and activated carbon filtration. *Water Research*, 2010. **44**(2): p. 625-37.
43. Liu, J.G., *et al.*, Removal of typical antibiotics in the advanced treatment process of productive drinking water. *Desalination and Water Treatment*, 2016. **57**(24): p. 11386-11391.
44. Ternes, T.A., *et al.*, Removal of pharmaceuticals during drinking water treatment. *Environmental Science & Technology*, 2002. **36**(17): p. 3855-3863.
45. Paredes, L., *et al.*, Understanding the fate of organic micropollutants in sand and granular activated carbon biofiltration systems. *Science of the Total Environment*, 2016. **551-552**: p. 640-648.

46. Luo, Y., *et al.*, A review on the occurrence of micropollutants in the aquatic environment and their fate and removal during wastewater treatment. *Science of the Total Environment*, 2014. **473–474**: p. 619-641.
47. Githinji, L.J.M., Musey, M.K., and Ankumah, R.O., Evaluation of the fate of ciprofloxacin and amoxicillin in domestic wastewater. *Water Air and Soil Pollution*, 2011. **219**(1-4): p. 191-201.
48. Andreozzi, R., *et al.*, Antibiotics in the environment: occurrence in Italian STPs, fate, and preliminary assessment on algal toxicity of amoxicillin. *Environmental Science & Technology*, 2004. **38**(24): p. 6832-6838.
49. Castiglioni, S., *et al.*, A multiresidue analytical method using solid-phase extraction and high-pressure liquid chromatography tandem mass spectrometry to measure pharmaceuticals of different therapeutic classes in urban wastewaters. *Journal of Chromatography A*, 2005. **1092**(2): p. 206-15.
50. Ankley, G.T., *et al.*, Repeating history: Pharmaceuticals in the environment. *Environmental Science & Technology*, 2007. **41**(24): p. 8211-8217.
51. Baumann, M., *et al.*, Aquatic toxicity of the macrolide antibiotic clarithromycin and its metabolites. *Chemosphere*, 2015. **120**: p. 192-198.
52. European Union, Commission implementing decision establishing a watch list of substances for Union-wide monitoring in the field of water policy pursuant to Directive 2008/105/EC of the European Parliament and of the Council. 2015.
53. Barbosa, M.O., *et al.*, Occurrence and removal of organic micropollutants: An overview of the watch list of EU Decision 2015/495. *Water Research*, 2016. **94**: p. 257-279.
54. Feitosa-Felizzola, J. and Chiron, S., Occurrence and distribution of selected antibiotics in a small Mediterranean stream (Arc River, Southern France). *Journal of Hydrology*, 2009. **364**(1-2): p. 50-57.
55. Zuccato, E., *et al.*, Source, occurrence and fate of antibiotics in the Italian aquatic environment. *Journal of Hazardous Materials*, 2010. **179**(1-3): p. 1042-1048.

56. Tasho, R.P. and Cho, J.Y., Veterinary antibiotics in animal waste, its distribution in soil and uptake by plants: A review. *Science of the Total Environment*, 2016. **563-564**: p. 366-376.
57. Kim, K.R., *et al.*, Occurrence and environmental fate of veterinary antibiotics in the terrestrial environment. *Water Air and Soil Pollution*, 2011. **214**(1-4): p. 163-174.
58. De Liguoro, M., *et al.*, Use of oxytetracycline and tylosin in intensive calf farming: evaluation of transfer to manure and soil. *Chemosphere*, 2003. **52**(1): p. 203-212.
59. Liu, Y., *et al.*, The effect of aging on sequestration and bioaccessibility of oxytetracycline in soils. *Environmental Science and Pollution Research*, 2015. **22**(14): p. 10425-10433.
60. Sebastine, I.M. and Wakeman, R.J., Consumption and environmental hazards of pharmaceutical substances in the UK. *Process Safety and Environmental Protection*, 2003. **81**(B4): p. 229-235.
61. Qiting, J. and Z. Xiheng, Combination process of anaerobic digestion and ozonization technology for treating wastewater from antibiotics production. *Water Treatment*, 1988. **3**: p. 285-291.
62. Li, K.X., *et al.*, Ozonation of oxytetracycline and toxicological assessment of its oxidation by-products. *Chemosphere*, 2008. **72**(3): p. 473-478.
63. Seydel, J.K., *et al.*, Kinetics and mechanisms of action of trimethoprim and sulfonamides, alone or in combination, upon *Escherichia coli* (Part 1 of 2). *Chemotherapy*, 1972. **17**(4): p. 217-237.
64. Gao, S., *et al.*, Oxidation of sulfamethoxazole (SMX) by chlorine, ozone and permanganate--a comparative study. *Journal of Hazardous Materials*, 2014. **274**: p. 258-69.
65. Hilton, M., Thomas, K., and Ashton, D., Targeted monitoring programme for pharmaceuticals in the aquatic environment. 2003: *Environment agency Bristol*, UK.
66. Monteiro, S.C. and Boxall, A.B.A., Occurrence and fate of human pharmaceuticals in the environment, *Reviews of Environmental Contamination and Toxicology*. 2010. p. 53-154.

67. Carattoli, A., Plasmid-mediated antimicrobial resistance in *Salmonella enterica*. *Current Issues in Molecular Biology*, 2003. **5**: p. 113-122.
68. WHO, Antimicrobial resistance: global report on surveillance 2014.
69. Tenover, F.C., Mechanisms of antimicrobial resistance in bacteria. *American Journal of Medicine*, 2006. **119**(6): p. S3-S10.
70. Levy, S.B. and Marshall, B., Antibacterial resistance worldwide: causes, challenges and responses. *Nature Medicine*, 2004. **10**(12 Suppl): p. S122-9.
71. Taubes, G., The bacteria fight back. *Science*, 2008. **321**(5887): p. 356-361.
72. D'Costa, V.M., *et al.*, Antibiotic resistance is ancient. *Nature*, 2011. **477**(7365): p. 457-461.
73. Fernando, D.M., *et al.*, Detection of antibiotic resistance genes in source and drinking water samples from a First Nations community in Canada. *Applied and Environmental Microbiology*, 2016. **82**(15): p. 4767-4775.
74. Wang, F.H., *et al.*, High throughput profiling of antibiotic resistance genes in urban park soils with reclaimed water irrigation. *Environmental Science & Technology*, 2014. **48**(16): p. 9079-9085.
75. Xu, L., *et al.*, High-throughput profiling of antibiotic resistance genes in drinking water treatment plants and distribution systems. *Environment Pollution*, 2016. **213**: p. 119-126.
76. Chen, B., *et al.*, Metagenomic analysis revealing antibiotic resistance genes (ARGs) and their genetic compartments in the Tibetan environment. *Environmental Science & Technology*, 2016.
77. Gao, P., *et al.*, Occurrence of sulfonamide and tetracycline-resistant bacteria and resistance genes in aquaculture environment. *Water Research*, 2012. **46**(7): p. 2355-2364.
78. Agerso, Y. and Sandvang, D., Class 1 integrons and tetracycline resistance genes in *Alcaligenes*, *Arthrobacter*, and *Pseudomonas* spp. isolated from pigsties and manured soil. *Applied and Environmental Microbiology*, 2005. **71**(12): p. 7941-7.
79. Zhang, X.X., Zhang, T., and Fang, H., Antibiotic resistance genes in water environment. *Applied Microbiology and Biotechnology*, 2009. **82**(3): p. 397-414.

80. Czekalski, N., Diez, E.G., and Burgmann, H., Wastewater as a point source of antibiotic-resistance genes in the sediment of a freshwater lake. *The ISME Journal*, 2014. **8**(7): p. 1381-1390.
81. Rizzo, L., *et al.*, Urban wastewater treatment plants as hotspots for antibiotic resistant bacteria and genes spread into the environment: A review. *Science of the Total Environment*, 2013. **447**: p. 345-360.
82. Yang, Y., *et al.*, Fate of antibiotic resistance genes in sewage treatment plant revealed by metagenomic approach. *Water Research*, 2014. **62**: p. 97-106.
83. Marti, E., Variatza, E., and Balcazar, J.L., The role of aquatic ecosystems as reservoirs of antibiotic resistance. *Trends in Microbiology*, 2014. **22**(1): p. 36-41.
84. Cheng, W., *et al.*, Abundance and persistence of antibiotic resistance genes in livestock farms: a comprehensive investigation in eastern China. *Environment International*, 2013. **61**: p. 1-7.
85. Jones, O.A., Lester, J.N., and Voulvoulis, N., Pharmaceuticals: a threat to drinking water? *Trends in Biotechnology*, 2005. **23**(4): p. 163-7.
86. Cox, G. and Wright, G.D., Intrinsic antibiotic resistance: Mechanisms, origins, challenges and solutions. *International Journal of Medical Microbiology*, 2013. **303**(6): p. 287-292.
87. Alekshun, M.N. and Levy, S.B., Molecular mechanisms of antibacterial multidrug resistance. *Cell*, 2007. **128**(6): p. 1037-1050.
88. Poole, K., Mechanisms of bacterial biocide and antibiotic resistance. *Journal of Applied Microbiology*, 2002. **92**: p. 55S-64S.
89. Roberts, M.C., Update on acquired tetracycline resistance genes. *FEMS Microbiology Letters*, 2005. **245**(2): p. 195-203.
90. de la Cruz, F. and Davies, J., Horizontal gene transfer and the origin of species: lessons from bacteria. *Trends in Microbiology*, 2000. **8**(3): p. 128-133.
91. Gyles, C. and Boerlin, P., Horizontally transferred genetic elements and their role in pathogenesis of bacterial disease. *Veterinary Pathology*, 2014. **51**(2): p. 328-340.

92. Zhong, X., *et al.*, Accounting for mating pair formation in plasmid population dynamics. *Journal of Theoretical Biology*, 2010. **262**(4): p. 711-719.
93. Davies, J. and Davies, D., Origins and evolution of antibiotic resistance. *Microbiology and Molecular Biology Reviews*, 2010. **74**(3): p. 417-+.
94. Sørensen, S.J., *et al.*, Studying plasmid horizontal transfer in situ: a critical review. *Nature Reviews Microbiology*, 2005. **3**(9): p. 700-710.
95. Madsen, J.S., *et al.*, The interconnection between biofilm formation and horizontal gene transfer. *FEMS Immunology and Medical Microbiology*, 2012. **65**(2): p. 183-195.
96. Alcaide, E. and Garay, E., R-plasmid transfer in *Salmonella* spp. isolated from wastewater and sewage-contaminated surface waters. *Applied and Environmental Microbiology*, 1984. **48**(2): p. 435-438.
97. Dang, B., *et al.*, Conjugative multi-resistant plasmids in Haihe River and their impacts on the abundance and spatial distribution of antibiotic resistance genes. *Water Research*, 2016.
98. Bennett, P.M., Plasmid encoded antibiotic resistance: acquisition and transfer of antibiotic resistance genes in bacteria. *British Journal of Pharmacology*, 2008. **153**: p. S347-S357.
99. Shi, P., *et al.*, Metagenomic insights into chlorination effects on microbial antibiotic resistance in drinking water. *Water Research*, 2013. **47**(1): p. 111-120.
100. Miller, R.V., Environmental bacteriophage-host interactions: factors contribution to natural transduction. *Antonie Van Leeuwenhoek*, 2001. **79**(2): p. 141-147.
101. Colomer-Lluch, M., Jofre, J., and Muniesa, M., Antibiotic resistance genes in the bacteriophage DNA fraction of environmental samples. *Plos One*, 2011. **6**(3).
102. Parsley, L.C., *et al.*, Identification of diverse antimicrobial resistance determinants carried on bacterial, plasmid, or viral metagenomes from an activated sludge microbial assemblage. *Applied and Environmental Microbiology*, 2010. **76**(11): p. 3753-3757.
103. Dodd, M.C., Potential impacts of disinfection processes on elimination and deactivation of antibiotic resistance genes during water and wastewater treatment. *Journal of Environmental Monitoring*, 2012. **14**(7): p. 1754-1771.

104. Barbe, V., *et al.*, Unique features revealed by the genome sequence of *Acinetobacter* sp. ADP1, a versatile and naturally transformation competent bacterium. *Nucleic Acids Research*, 2004. **32**(19): p. 5766-5779.
105. Lorenz, M.G. and Wackernagel, W., Bacterial gene transfer by natural genetic transformation in the environment. *Microbiology and Molecular Biology Reviews*, 1994. **58**(3): p. 563-602.
106. Li, D., *et al.*, Water disinfection byproducts induce antibiotic resistance-role of environmental pollutants in resistance phenomena. *Environmental Science & Technology*, 2016. **50**(6): p. 3193-3201.
107. Seiler, C. and Berendonk, T.U., Heavy metal driven co-selection of antibiotic resistance in soil and water bodies impacted by agriculture and aquaculture. *Frontiers in Microbiology*, 2012. **3**: p. 399.
108. Baker-Austin, C., *et al.*, Co-selection of antibiotic and metal resistance. *Trends in Microbiology*, 2006. **14**(4): p. 176-182.
109. Ghigo, J.-M., Natural conjugative plasmids induce bacterial biofilm development. *Nature*, 2001. **412**(6845): p. 442-445.
110. Schlüter, A., *et al.*, Genomics of IncP-1 antibiotic resistance plasmids isolated from wastewater treatment plants provides evidence for a widely accessible drug resistance gene pool. *FEMS Microbiology Reviews*, 2007. **31**(4): p. 449-477.
111. Schwartz, T., *et al.*, Detection of antibiotic-resistant bacteria and their resistance genes in wastewater, surface water, and drinking water biofilms. *FEMS Microbiology Ecology*, 2003. **43**(3): p. 325-335.
112. Farkas, A., *et al.*, Microbiological contamination and resistance genes in biofilms occurring during the drinking water treatment process. *Science of the Total Environment*, 2013. **443**: p. 932-938.
113. Zhang, W., *et al.*, Accumulation of tetracycline resistance genes in aquatic biofilms due to periodic waste loadings from swine lagoons. *Environmental Science & Technology*, 2009. **43**(20): p. 7643-7650.

114. Berendonk, T.U., *et al.*, Tackling antibiotic resistance: the environmental framework. *Nature Reviews Microbiology*, 2015. **13**: p. 310.
115. Poole, K., Resistance to β -lactam antibiotics. *Cellular and Molecular Life Sciences CMLS*, 2004. **61**(17): p. 2200-2223.
116. Monstein, H.J., *et al.*, Multiplex PCR amplification assay for the detection of (SHV)-S-*bla*, (TEM)-T-*bla* and (CTX)-C-*bla*-M genes in *Enterobacteriaceae*. *Apmis*, 2007. **115**(12): p. 1400-1408.
117. Singh, N.S., Singhal, N., and Viridi, J.S., Genetic environment of *bla*_{TEM-1}, *bla*_{CTX-M-15}, *bla*_{CMY-42} and characterization of integrons of *Escherichia coli* isolated from an Indian urban aquatic environment. *Frontiers in Microbiology*, 2018. **9**: p. 382.
118. Tennstedt, T., *et al.*, Occurrence of integron-associated resistance gene cassettes located on antibiotic resistance plasmids isolated from a wastewater treatment plant. *FEMS Microbiology Ecology*, 2003. **45**(3): p. 239-252.
119. Wei, D.-D., *et al.*, Characterization of extended-spectrum beta-lactamase, carbapenemase, and plasmid quinolone determinants in *Klebsiella pneumoniae* isolates carrying distinct types of 16S rRNA methylase genes, and their association with mobile genetic elements. *Microbial Drug Resistance*, 2014. **21**(2): p. 186-193.
120. Canton, R., Antibiotic resistance genes from the environment: a perspective through newly identified antibiotic resistance mechanisms in the clinical setting. *Clinical Microbiology and Infection*, 2009. **15**: p. 20-25.
121. De Leener, E., *et al.*, Distribution of the *erm* (B) Gene, tetracycline resistance genes, and *Tn1545*-like transposons in macrolide- and lincosamide-resistant enterococci from pigs and humans. *Microbial Drug Resistance*, 2004. **10**(4): p. 341-345.
122. Lundström, S.V., *et al.*, Minimal selective concentrations of tetracycline in complex aquatic bacterial biofilms. *Science of the Total Environment*, 2016. **553**: p. 587-595.
123. Gillings, M.R., *et al.*, Using the class 1 integron-integrase gene as a proxy for anthropogenic pollution. *The ISME Journal*, 2015. **9**(6): p. 1269-1279.

124. Leng, Z., *et al.*, Distribution and mobility of the tetracycline resistance determinant *tetQ*. *Journal of Antimicrobial Chemotherapy*, 1997. **40**(4): p. 551-559.
125. Gao, P., Munir, M., and Xagorarakis, I., Correlation of tetracycline and sulfonamide antibiotics with corresponding resistance genes and resistant bacteria in a conventional municipal wastewater treatment plant. *Science of the Total Environment*, 2012. **421**: p. 173-183.
126. Speer, B.S., Bedzyk, L., and Salyers, A.A., Evidence that a novel tetracycline resistance gene found on two *Bacteroides* transposons encodes an NADP-requiring oxidoreductase. *Journal of Bacteriology*, 1991. **173**(1): p. 176-183.
127. Akiba, T., *et al.*, On the mechanism of the development of multidrug resistant clones of *Shigella*. *Japanese journal of microbiology*, 1960. **4**(2): p. 219-227.
128. Singh, R., *et al.*, Identification of antimicrobial resistance and class 1 integrons in Shiga toxin-producing *Escherichia coli* recovered from humans and food animals. *Journal of Antimicrobial Chemotherapy*, 2005. **56**(1): p. 216-219.
129. Blair, J.M.A., *et al.*, Molecular mechanisms of antibiotic resistance. *Nature Reviews Microbiology*, 2015. **13**(1): p. 42-51.
130. Narciso-da-Rocha, C., *et al.*, *bla*(TEM) and *vanA* as indicator genes of antibiotic resistance contamination in a hospital-urban wastewater treatment plant system. *Journal of Global Antimicrobial Resistance*, 2014. **2**(4): p. 309-315.
131. Tao, C.W., *et al.*, Evaluation of five antibiotic resistance genes in wastewater treatment systems of swine farms by real-time PCR. *Science of the Total Environment*, 2014. **496**: p. 116-121.
132. Amos, G.C.A., *et al.*, Functional metagenomic analysis reveals rivers are a reservoir for diverse antibiotic resistance genes. *Veterinary Microbiology*, 2014. **171**(3-4): p. 441-447.
133. Lachmayr, K.L., *et al.*, Quantifying nonspecific TEM β -lactamase (*bla*TEM) genes in a wastewater stream. *Applied and Environmental Microbiology*, 2009. **75**(1): p. 203-211.

134. Liu, Y.-F., *et al.*, Presence of plasmid pA15 correlates with prevalence of constitutive MLSB resistance in group A Streptococci isolates at a university hospital in southern Taiwan. *Journal of Antimicrobial Chemotherapy*, 2007. **59**(6): p. 1167-1170.
135. Bockelmann, U., *et al.*, Quantitative PCR monitoring of antibiotic resistance genes and bacterial pathogens in three European artificial groundwater recharge systems. *Applied and Environmental Microbiology*, 2009. **75**(1): p. 154-163.
136. Okitsu, N., *et al.*, Characterization of *ermB* gene transposition by *Tn1545* and *Tn917* in macrolide-resistant *Streptococcus pneumoniae* isolates. *Journal of Clinical Microbiology*, 2005. **43**(1): p. 168-173.
137. Chen, L., *et al.*, Relationship between *ermB* gene and transposons *Tn1545* and *Tn917* in *Enterococcus faecalis*. *Chinese Journal of Nosocomiology*, 2010. **20**(6): p. 763-766.
138. Chen, J., *et al.*, Development and application of real-time PCR assays for quantification of *erm* genes conferring resistance to macrolides-lincosamides-streptogramin B in livestock manure and manure management systems. *Applied and Environmental Microbiology*, 2007. **73**(14): p. 4407-4416.
139. Liu, M.M., *et al.*, Abundance and distribution of tetracycline resistance genes and mobile elements in an oxytetracycline production wastewater treatment system. *Environmental Science & Technology*, 2012. **46**(14): p. 7551-7557.
140. Guo, X.P., *et al.*, Prevalence of sulfonamide and tetracycline resistance genes in drinking water treatment plants in the Yangtze River Delta, China. *Science of the Total Environment*, 2014. **493**: p. 626-631.
141. Peak, N., *et al.*, Abundance of six tetracycline resistance genes in wastewater lagoons at cattle feedlots with different antibiotic use strategies. *Environmental Microbiology*, 2007. **9**(1): p. 143-151.
142. Harnisz, M., *et al.*, *tet* genes as indicators of changes in the water environment: Relationships between culture-dependent and culture-independent approaches. *Science of the Total Environment*, 2015. **505**: p. 704-711.

143. Akinbowale, O.L., Peng, H., and Barton, M., Diversity of tetracycline resistance genes in bacteria from aquaculture sources in Australia. *Journal of Applied Microbiology*, 2007. **103**(5): p. 2016-2025.
144. Sköld, O., Sulfonamide resistance: mechanisms and trends. *Drug Resistance Updates*, 2000. **3**(3): p. 155-160.
145. Akiba, T., *et al.*, On the mechanism of the development of multiple drug-resistant clones of *Shigella*. *Japanese Journal of Microbiology*, 1960. **4**(2): p. 219-227.
146. Sköld, O., Resistance to trimethoprim and sulfonamides. *Veterinary Research*, 2001. **32**(3-4): p. 261-273.
147. Shah, S.Q.A., *et al.*, Prevalence of antibiotic resistance genes in the bacterial flora of integrated fish farming environments of Pakistan and Tanzania. *Environmental Science & Technology*, 2012. **46**(16): p. 8672-8679.
148. Blahna, M.T., *et al.*, The role of horizontal gene transfer in the spread of trimethoprim-sulfamethoxazole resistance among uropathogenic *Escherichia coli* in Europe and Canada. *Journal of Antimicrobial Chemotherapy*, 2006. **57**(4): p. 666-72.
149. Antunes, P., Machado, J., and Peixe, L., Characterization of antimicrobial resistance and class 1 and 2 integrons in *Salmonella enterica* isolates from different sources in Portugal. *Journal of Antimicrobial Chemotherapy*, 2006. **58**(2): p. 297-304.
150. Gillings, M., *et al.*, The evolution of class 1 integrons and the rise of antibiotic resistance. *Journal of Bacteriology*, 2008. **190**(14): p. 5095-100.
151. Deng, Y., *et al.*, Resistance integrons: class 1, 2 and 3 integrons. *Annals of Clinical Microbiology and Antimicrobials*, 2015. **14**: p. 45-45.
152. Zearley, T.L. and Summers, R.S., Removal of trace organic micropollutants by drinking water biological filters. *Environmental Science & Technology*, 2012. **46**(17): p. 9412-9419.
153. Zhu, I.X. and Bates, B.J., Conventional media filtration with biological activities. *Water Treatment*, 2013.
154. Haig, S.J., *et al.*, Biological aspects of slow sand filtration: past, present and future. *Water Supply*, 2011. **11**(4): p. 468-472.

-
155. Campos, L.C., *et al.*, Biomass development in slow sand filters. *Water Research*, 2002. **36**(18): p. 4543-4551.
 156. Ma, B., Arnold, W.A., and Hozalski, R.M., The relative roles of sorption and biodegradation in the removal of contaminants of emerging concern (CECs) in GAC-sand biofilters. *Water Research*, 2018. **146**: p. 67-76.
 157. Huisman, L. and Wood, W.E., Slow Sand Filtration. World Health Organization, Geneva. 1974.
 158. Kennedy, A.M., *et al.*, Full- and pilot-scale GAC adsorption of organic micropollutants. *Water Research*, 2015. **68**: p. 238-248.
 159. Gerrity, D., *et al.*, Pilot-scale evaluation of ozone and biological activated carbon for trace organic contaminant mitigation and disinfection. *Water Research*, 2011. **45**(5): p. 2155-65.
 160. Gibert, O., *et al.*, Fractionation and removal of dissolved organic carbon in a full-scale granular activated carbon filter used for drinking water production. *Water Research*, 2013. **47**(8): p. 2821-2829.
 161. Baraee, I., *et al.*, Performance of biofilters in GAC-sand and anthracite-sand dual-media filters in a water treatment plant in Abadan, Iran. *Desalination and Water Treatment*, 2016. **57**(42): p. 19655-19664.
 162. Bauer, M., *et al.*, GAC/slow sand filter sandwich--from concept to commissioning. *Water supply: the review journal of the International Water Supply Association*, 1996.
 163. Li, J.A., Zhou, Q.Z., and Campos, L.C., The application of GAC sandwich slow sand filtration to remove pharmaceutical and personal care products. *Science of the Total Environment*, 2018. **635**: p. 1182-1190.
 164. Ratnayaka, D.D., Brandt, M.J., and Johnson, K.M., CHAPTER 8 - Water Filtration Granular Media Filtration, in *Water Supply (Sixth Edition)*, 2009. p. 315-350.
 165. Jenkins, M.W., Tiwari, S.K., and Darby, J., Bacterial, viral and turbidity removal by intermittent slow sand filtration for household use in developing countries: Experimental investigation and modeling. *Water Research*, 2011. **45**(18): p. 6227-6239.

166. Sharma, D., Taylor-Edmonds, L., and Andrews, R.C., Comparative assessment of ceramic media for drinking water biofiltration. *Water Research*, 2018. **128**: p. 1-9.
167. Kitis, M., *et al.*, Adsorption of natural organic matter from waters by iron coated pumice. *Chemosphere*, 2007. **66**(1): p. 130-138.
168. Valdes, J.R. and Liang, S.-H., Stress-controlled filtration with compressible particles. *Journal of Geotechnical and Geoenvironmental Engineering*, 2006. **132**(7): p. 861-868.
169. Soyer, E., *et al.*, On the use of crushed recycled glass instead of silica sand in dual-media filters. *Clean – Soil, Air, Water*, 2013. **41**(4): p. 325-332.
170. Sánchez, L.D., *et al.*, Multi-stage filtration. *Thematic overview paper*, 2006. **15**.
171. Letterman, R.D., Filtration strategies to meet the surface water treatment rule. 1991, American Water Works Association.
172. Zhang, S. and Huck, P.M., Parameter estimation for biofilm processes in biological water treatment. *Water Research*, 1996. **30**: p. 456-464.
173. Liao, X.B., *et al.*, Changes of biomass and bacterial communities in biological activated carbon filters for drinking water treatment. *Process Biochemistry*, 2013. **48**(2): p. 312-316.
174. Luddeke, F., *et al.*, Removal of total and antibiotic resistant bacteria in advanced wastewater treatment by ozonation in combination with different filtering techniques. *Water Research*, 2015. **69**: p. 243-251.
175. Kim, T.G., *et al.*, Effects of water temperature and backwashing on bacterial population and community in a biological activated carbon process at a water treatment plant. *Applied Microbiology and Biotechnology*, 2014. **98**(3): p. 1417-1427.
176. Hollender, J., *et al.*, Elimination of organic micropollutants in a municipal wastewater treatment plant upgraded with a full-scale post-ozonation followed by sand filtration. *Environmental Science & Technology*, 2009. **43**(20): p. 7862-7869.
177. Zuehlke, S., Duennbier, U., and Heberer, T., Investigation of the behavior and metabolism of pharmaceutical residues during purification of contaminated ground water used for drinking water supply. *Chemosphere*, 2007. **69**(11): p. 1673-1680.

-
178. Wang, H.X., *et al.*, Discriminating and assessing adsorption and biodegradation removal mechanisms during granular activated carbon filtration of microcystin toxins. *Water Research*, 2007. **41**(18): p. 4262-4270.
179. Rooklidge, S.J., *et al.*, Antimicrobial contaminant removal by multistage slow sand filtration. *Journal American Water Works Association*, 2005. **97**(12): p. 92-+.
180. Baumgarten, B., *et al.*, Long term laboratory column experiments to simulate bank filtration: Factors controlling removal of sulfamethoxazole. *Water Research*, 2011. **45**(1): p. 211-220.
181. Nakada, N., *et al.*, Removal of selected pharmaceuticals and personal care products (PPCPs) and endocrine-disrupting chemicals (EDCs) during sand filtration and ozonation at a municipal sewage treatment plant. *Water Research*, 2007. **41**(19): p. 4373-4382.
182. Zhang, S.Y., *et al.*, Biologically active filters - An advanced water treatment process for contaminants of emerging concern. *Water Research*, 2017. **114**: p. 31-41.
183. Zhang, S.Y., *et al.*, A pilot plant study using conventional and advanced water treatment processes Evaluating removal efficiency of indicator compounds representative of pharmaceuticals and personal care products. *Water Research*, 2016. **105**: p. 85-96.
184. Justo, A., *et al.*, BAC filtration to mitigate micropollutants and EfOM content in reclamation reverse osmosis brines. *Chemical Engineering Journal*, 2015. **279**: p. 589-596.
185. Nam, S.W., *et al.*, Adsorption characteristics of selected hydrophilic and hydrophobic micropollutants in water using activated carbon. *Journal of Hazardous Materials*, 2014. **270**: p. 144-152.
186. Taheran, M., *et al.*, Membrane processes for removal of pharmaceutically active compounds (PhACs) from water and wastewaters. *Science of the Total Environment*, 2016. **547**: p. 60-77.
187. Hai, F.I., *et al.*, Removal of micropollutants by membrane bioreactor under temperature variation. *Journal of Membrane Science*, 2011. **383**(1-2): p. 144-151.

188. Xi, C.W., *et al.*, Prevalence of antibiotic resistance in drinking water treatment and distribution systems. *Applied and Environmental Microbiology*, 2009. **75**(17): p. 5714-5718.
189. Luprano, M.L., *et al.*, Antibiotic resistance genes fate and removal by a technological treatment solution for water reuse in agriculture. *Science of the Total Environment*, 2016. **571**: p. 809-818
190. Farkas, A., *et al.*, Microbiological contamination and resistance genes in biofilms occurring during the drinking water treatment process. *Science of the Total Environment*, 2013. **443**: p. 932-938.
191. Liu, L.M., *et al.*, Large-scale biogeographical patterns of bacterial antibiotic resistome in the waterbodies of China. *Environment International*, 2018. **117**: p. 292-299.
192. Zheng, J., Chen, T., and Chen, H., Antibiotic resistome promotion in drinking water during biological activated carbon treatment: Is it influenced by quorum sensing? *Science of the Total Environment*, 2018. **612**: p. 1-8.
193. Wan, K., *et al.*, Organic carbon: An overlooked factor that determines the antibiotic resistome in drinking water sand filter biofilm. *Environment International*, 2019. **125**: p. 117-124.
194. Moreno-Bondi, M.C., *et al.*, An overview of sample preparation procedures for LC-MS multiclass antibiotic determination in environmental and food samples. *Analytical and Bioanalytical Chemistry*, 2009. **395**(4): p. 921-946.
195. Batt, A.L. and Aga, D.S., Simultaneous analysis of multiple classes of antibiotics by ion trap LC/MS/MS for assessing surface water and groundwater contamination. *Analytical Chemistry*, 2005. **77**(9): p. 2940-2947.
196. European Union Decision 2002/657/EC. *Official Journal of the European Communities*, 2002.
197. Fatta, D., *et al.*, Analytical methods for tracing pharmaceutical residues in water and wastewater. *Trac-Trends in Analytical Chemistry*, 2007. **26**(6): p. 515-533.

198. Hong, Y., *et al.*, Fast-target analysis and hourly variation of 60 pharmaceuticals in wastewater using UPLC-high resolution mass spectrometry. *Archives of Environmental Contamination and Toxicology*, 2015. **69**(4): p. 525-534.
199. Grujic, S., Vasiljevic, T., and Lausevic, M., Determination of multiple pharmaceutical classes in surface and ground waters by liquid chromatography-ion trap-tandem mass spectrometry. *Journal of Chromatography A*, 2009. **1216**(25): p. 4989-5000.
200. McNeece, G., *et al.*, Array based detection of antibiotic resistance genes in Gram negative bacteria isolated from retail poultry meat in the UK and Ireland. *International Journal of Food Microbiology*, 2014. **179**: p. 24-32.
201. Li, B., *et al.*, Metagenomic and network analysis reveal wide distribution and co-occurrence of environmental antibiotic resistance genes. *The ISME Journal*, 2015. **9**(11): p. 2490-2502.
202. Xu, Y., *et al.*, Occurrence and distribution of antibiotics, antibiotic resistance genes in the urban rivers in Beijing, China. *Environmental Pollution*, 2016. **213**: p. 833-840.
203. Cheng, W., *et al.*, Behavior of antibiotics and antibiotic resistance genes in eco-agricultural system: A case study. *Journal of Hazardous Materials*, 2016. **304**: p. 18-25.
204. Allen, H.K., Antibiotic resistance gene discovery in food-producing animals. *Current Opinion in Microbiology*, 2014. **19**: p. 25-29.
205. World Health Organization. Antibiotic resistance. 2018; Available from: <http://www.who.int/news-room/fact-sheets/detail/antibiotic-resistance>.
206. Luby, E., *et al.*, Molecular methods for assessment of antibiotic resistance in agricultural ecosystems: Prospects and challenges. *Journal of Environmental Quality*, 2016. **45**(2): p. 441-453.
207. Su, J.-Q., *et al.*, Application of genomic technologies to measure and monitor antibiotic resistance in animals. *Annals of the New York Academy of Sciences*, 2017. **1388**(1): p. 121-135.

-
208. Zhu, B., *et al.*, Does organically produced lettuce harbor higher abundance of antibiotic resistance genes than conventionally produced? *Environment International*, 2017. **98**: p. 152-159.
209. Zhao, Z., *et al.*, Nutrients, heavy metals and microbial communities co-driven distribution of antibiotic resistance genes in adjacent environment of mariculture. *Environmental Pollutin*, 2016.
210. Hu, H.W., *et al.*, Temporal changes of antibiotic-resistance genes and bacterial communities in two contrasting soils treated with cattle manure. *FEMS Microbiology Ecology*, 2016. **92**(2).
211. Han, X.M., *et al.*, Impacts of reclaimed water irrigation on soil antibiotic resistome in urban parks of Victoria, Australia. *Environmental Pollution*, 2016. **211**: p. 48-57.
212. Claesson, M.J., *et al.*, Comparison of two next-generation sequencing technologies for resolving highly complex microbiota composition using tandem variable 16S rRNA gene regions. *Nucleic Acids Research*, 2010. **38**(22).
213. Zhang, H., *et al.*, Abundance of antibiotic resistance genes and their association with bacterial communities in activated sludge of wastewater treatment plants: Geographical distribution and network analysis. *Journal of Environmental Sciences*, 2019. **82**: p. 24-38.
214. Wu, H., *et al.*, Biofilm bacterial communities in urban drinking water distribution systems transporting waters with different purification strategies. *Applied Microbiology and Biotechnology*, 2015. **99**(4): p. 1947-55.
215. Duan, M., *et al.*, Changes in antibiotic resistance genes and mobile genetic elements during cattle manure composting after inoculation with *Bacillus subtilis*. *Bioresource Technology*, 2019. **292**: p. 122011.
216. Schmieder, R. and Edwards, R., Insights into antibiotic resistance through metagenomic approaches. *Future Microbiology*, 2012. **7**(1): p. 73-89.
217. Allen, H.K., *et al.*, Functional metagenomics reveals diverse β -lactamases in a remote Alaskan soil. *The ISME Journal*, 2009. **3**(2): p. 243-251.

-
218. Diaz-Torres, M., *et al.*, Novel tetracycline resistance determinant from the oral metagenome. *Antimicrobial agents and chemotherapy*, 2003. **47**(4): p. 1430-1432.
219. Ma, L., *et al.*, Catalogue of antibiotic resistome and hosttracking in drinking water deciphered by a large scale survey. *Microbiome*, 2017. **5**(1): p. 154.
220. Chen, Q., *et al.*, Long-term field application of sewage sludge increases the abundance of antibiotic resistance genes in soil. *Environment International*, 2016. **92-93**: p. 1-10.
221. Fogler, K., *et al.*, Microbiota and antibiotic resistome of lettuce leaves and radishes grown in soils receiving manure-based amendments derived from antibiotic-treated cows. *Frontiers in Sustainable Food Systems*, 2019. **3**(22).
222. Chen, H.Y., *et al.*, A metagenomic analysis framework for characterization of antibiotic resistomes in river environment: Application to an urban river in Beijing. *Environmental Pollution*, 2019. **245**: p. 398-407.
223. Jia, S., *et al.*, Bacterial community shift drives antibiotic resistance promotion during drinking water chlorination. *Environment Science & Technology*, 2015. **49**(20): p. 12271-9.
224. Tian, Z., *et al.*, Changes of resistome, mobilome and potential hosts of antibiotic resistance genes during the transformation of anaerobic digestion from mesophilic to thermophilic. *Water Research*, 2016. **98**: p. 261-9.
225. D'Alessio, M., *et al.*, Pharmaceutically active compounds: Their removal during slow sand filtration and their impact on slow sand filtration bacterial removal. *Science of the Total Environment*, 2015. **524**: p. 124-135.
226. Liu, B., *et al.*, Dissolved organic nitrogen (DON) profile during backwashing cycle of drinking water biofiltration. *Science of the Total Environment*, 2012. **414**: p. 508-514.
227. Baird, R.B., *et al.*, Standard methods for the examination of water and wastewater. 2012. American public health association.
228. International Organization for Standardization., ISO 7027-1:2016 — Water quality — Determination of turbidity — Part 1: Quantitative methods. 2016.

229. International Organization for Standardization., ISO 9308-1:2014 — Water quality — Enumeration of *Escherichia coli* and coliform bacteria — Part 1: Membrane filtration method for waters with low bacterial background flora. 2014.
230. Kasprzyk-Hordern, B., Dinsdale, R.M., and Guwy, A.J., Multiresidue methods for the analysis of pharmaceuticals, personal care products and illicit drugs in surface water and wastewater by solid-phase extraction and ultra performance liquid chromatography-electrospray tandem mass spectrometry. *Analytical and Bioanalytical Chemistry*, 2008. **391**(4): p. 1293-308.
231. Huerta-Fontela, M., Galceran, M.T., and Ventura, F., Fast liquid chromatography quadrupole-linear ion trap mass spectrometry for the analysis of pharmaceuticals and hormones in water resources. *Journal of Chromatography A*, 2010. **1217**(25): p. 4212-4222.
232. Ben, W.W., *et al.*, Simultaneous determination of sulfonamides, tetracyclines and tiamulin in swine wastewater by solid-phase extraction and liquid chromatography-mass spectrometry. *Journal of Chromatography A*, 2008. **1202**(2): p. 173-180.
233. Gbylik-Sikorska, M., *et al.*, Liquid chromatography-tandem mass spectrometry multiclass method for the determination of antibiotics residues in water samples from water supply systems in food-producing animal farms. *Chemosphere*, 2015. **119**: p. 8-15.
234. Gros, M., Rodriguez-Mozaz, S., and Barcelo, D., Fast and comprehensive multi-residue analysis of a broad range of human and veterinary pharmaceuticals and some of their metabolites in surface and treated waters by ultra-high-performance liquid chromatography coupled to quadrupole-linear ion trap tandem mass spectrometry. *Journal of Chromatography A*, 2012. **1248**: p. 104-121.
235. Ibanez, M., *et al.*, Screening of antibiotics in surface and wastewater samples by ultra-high-pressure liquid chromatography coupled to hybrid quadrupole time-of-flight mass spectrometry. *Journal of Chromatography A*, 2009. **1216**(12): p. 2529-2539.

-
236. Martinez-Carballo, E., *et al.*, Environmental monitoring study of selected veterinary antibiotics in animal manure and soils in Austria. *Environmental Pollution*, 2007. **148**(2): p. 570-579.
237. Conley, J.M., *et al.*, Rapid liquid chromatography–tandem mass spectrometry method for the determination of a broad mixture of pharmaceuticals in surface water. *Journal of Chromatography A*, 2008. **1185**(2): p. 206-215.
238. Luo, Y., *et al.*, Occurrence and transport of tetracycline, sulfonamide, quinolone, and macrolide antibiotics in the Haihe River basin, China. *Environmental Science & Technology*, 2011. **45**(5): p. 1827-1833.
239. Koesukwiwat, U., Jayanta, S., and Leepipatpiboon, N., Validation of a liquid chromatography–mass spectrometry multi-residue method for the simultaneous determination of sulfonamides, tetracyclines, and pyrimethamine in milk. *Journal of Chromatography A*, 2007. **1140**(1–2): p. 147-156.
240. Matuszewski, B.K., Constanzer, M.L., and Chavez-Eng, C.M., Strategies for the assessment of matrix effect in quantitative bioanalytical methods based on HPLC–MS/MS. *Analytical Chemistry*, 2003. **75**(13): p. 3019-3030.
241. Hirsch, R., *et al.*, Occurrence of antibiotics in the aquatic environment. *Science of the Total Environment*, 1999. **225**(1-2): p. 109-118.
242. Buesing, N. and Gessner, M.O., Comparison of detachment procedures for direct counts of bacteria associated with sediment particles, plant litter and epiphytic biofilms. *Aquatic Microbial Ecology*, 2002. **27**(1): p. 29-36.
243. Marti, E., Jofre, J., and Balcazar, J.L., Prevalence of antibiotic resistance genes and bacterial community composition in a river influenced by a wastewater treatment plant. *Plos One*, 2013. **8**(10).
244. Tennstedt, T., *et al.*, Sequence of the 68,869 bp *IncP-1* alpha plasmid *pTB11* from a waste-water treatment plant reveals a highly conserved backbone, a *Tn402*-like integron and other transposable elements. *Plasmid*, 2005. **53**(3): p. 218-238.

-
245. Mabilat, C. and Courvalin, P., Development of oligotyping for characterization and molecular epidemiology of tem beta-lactamases in members of the family *Enterobacteriaceae*. *Antimicrobial Agents and Chemotherapy*, 1990. **34**(11): p. 2210-2216.
246. Ng, L.K., *et al.*, Multiplex PCR for the detection of tetracycline resistant genes. *Molecular and Cellular Probes*, 2001. **15**(4): p. 209-215.
247. Aminov, R.I., Garrigues-Jeanjean, N., and Mackie, R.I., Molecular ecology of tetracycline resistance: Development and validation of primers for detection of tetracycline resistance genes encoding ribosomal protection proteins. *Applied and Environmental Microbiology*, 2001. **67**(1): p. 22-32.
248. Luo, Y., *et al.*, Trends in antibiotic resistance genes occurrence in the Haihe River, China. *Environmental Science & Technology*, 2010. **44**(19): p. 7220-7225.
249. Grape, M., *et al.*, Standard and real-time multiplex PCR methods for detection of trimethoprim resistance *dfr* genes in large collections of bacteria. *Clinical Microbiology and Infection*, 2007. **13**(11): p. 1112-1118.
250. Goldstein, C., *et al.*, Incidence of class 1 and 2 integrases in clinical and commensal bacteria from livestock, companion animals, and exotics. *Antimicrobial Agents and Chemotherapy*, 2001. **45**(3): p. 723-726.
251. Gaze, W.H., *et al.*, Impacts of anthropogenic activity on the ecology of class 1 integrons and integron-associated genes in the environment. *The ISME Journal*, 2011. **5**(8): p. 1253-1261.
252. Zhang, T., *et al.*, Tetracycline resistance genes and tetracycline resistant lactose-fermenting enterobacteriaceae in activated sludge of sewage treatment plants. *Environmental Science & Technology*, 2009. **43**(10): p. 3455-3460.
253. Calero-Caceres, W., *et al.*, Sludge as a potential important source of antibiotic resistance genes in both the bacterial and bacteriophage fractions. *Environmental Science & Technology*, 2014. **48**(13): p. 7602-7611.

254. European Committee on Antimicrobial Susceptibility Testing, Antimicrobial susceptibility testing EUCAST disk diffusion method - Version 7.0. 2019.
255. Wang, Q., Mao, D., and Luo, Y., Ionic Liquid Facilitates the Conjugative Transfer of Antibiotic Resistance Genes Mediated by Plasmid RP4. *Environmental Science & Technology*, 2015. **49**(14): p. 8731-40.
256. Overballe-Petersen, S., *et al.*, Bacterial natural transformation by highly fragmented and damaged DNA. *Proceedings of the National Academy of Sciences*, 2013. **110**(49): p. 19860-19865.
257. Pompei, C.M.E., *et al.*, Influence of PPCPs on the performance of intermittently operated slow sand filters for household water purification. *Science of the Total Environment*, 2017. **581-582**: p. 174-185.
258. Zhang, H.N., *et al.*, Variations in dissolved organic nitrogen concentration in biofilters with different media during drinking water treatment. *Chemosphere*, 2015. **139**: p. 652-658.
259. O'Melia, C.R. and Crapps, D.K., Some Chemical Aspects of Rapid Sand Filtration. *Journal American Water Works Association*, 1964. **56**(10): p. 1326-1344.
260. Pacini, V.A., Ingallinella, A.M., and Sanguinetti, G., Removal of iron and manganese using biological roughing up flow filtration technology. *Water Research*, 2005. **39**(18): p. 4463-4475.
261. Weishaar, J.L., *et al.*, Evaluation of specific ultraviolet absorbance as an indicator of the chemical composition and reactivity of dissolved organic carbon. *Environmental Science & Technology*, 2003. **37**(20): p. 4702-4708.
262. Hozalski, R.M., Goel, S., and Bouwer, E.J., TOC Removal in Biological Filters. *Journal American Water Works Association*, 1995. **87**(12): p. 40-54.
263. Linlin, W., Xuan, Z., and Meng, Z., Removal of dissolved organic matter in municipal effluent with ozonation, slow sand filtration and nanofiltration as high quality pre-treatment option for artificial groundwater recharge. *Chemosphere*, 2011. **83**(5): p. 693-699.
264. Emelko, M.B., *et al.*, Effects of media, backwash, and temperature on full scale biological filtration. *Journal American Water Works Association*, 2006. **98**(12): p. 61-73.

-
265. Yu, X., *et al.*, Nitrogen loss and oxygen paradox in full-scale biofiltration for drinking water treatment. *Water Research*, 2007. **41**(7): p. 1455-1464.
266. Brown, L.C. and Barnwell, T.O., The enhanced stream water quality models QUAL2E and QUAL2E-UNCAS: Documentation and user manual. 1987. US Environmental Protection Agency.
267. Slow Sand Filtration. 2000, National Drinking Water Clearinghouse (U.S.).
268. Costanzo, S.D., Murby, J., and Bates, J., Ecosystem response to antibiotics entering the aquatic environment. *Marine Pollution Bulletin*, 2005. **51**(1-4): p. 218-223.
269. Klaver, A.L. and Matthews, R.A., Effects of oxytetracycline on nitrification in a model aquatic system. *Aquaculture*, 1994. **123**(3-4): p. 237-247.
270. Halling-Sorensen, B., Inhibition of aerobic growth and nitrification of bacteria in sewage sludge by antibacterial agents. *Archives of Environmental Contamination and Toxicology*, 2001. **40**(4): p. 451-460.
271. Nakhla, G. and Farooq, S., Simultaneous nitrification–denitrification in slow sand filters. *Journal of Hazardous Materials*, 2003. **96**(2): p. 291-303.
272. de Vera, G.A., *et al.*, Impact of upstream chlorination on filter performance and microbial community structure of GAC and anthracite biofilters. *Environmental Science-Water Research & Technology*, 2018. **4**(8): p. 1133-1144.
273. Lee, C.O., Howe, K.J., and Thomson, B.M., Ozone and biofiltration as an alternative to reverse osmosis for removing PPCPs and micropollutants from treated wastewater. *Water Research*, 2012. **46**(4): p. 1005-1014.
274. Unger, M. and Collins, M.R., Assessing *Escherichia coli* removal in the schmutzdecke of slow-rate biofilters. *Journal American Water Works Association*, 2008. **100**(12): p. 60-73.
275. Dalahmeh, S., *et al.*, Potential of biochar filters for onsite sewage treatment: Adsorption and biological degradation of pharmaceuticals in laboratory filters with active, inactive and no biofilm. *Science of the Total Environment*, 2018. **612**: p. 192-201.

276. Maeng, S.K., *et al.*, Role of biodegradation in the removal of pharmaceutically active compounds with different bulk organic matter characteristics through managed aquifer recharge: Batch and column studies. *Water Research*, 2011. **45**(16): p. 4722-4736.
277. Gruenheid, S., Huebner, U., and Jekel, M., Impact of temperature on biodegradation of bulk and trace organics during soil passage in an indirect reuse system. *Water Science and Technology*, 2008. **57**(7): p. 987-994.
278. Lagergren, S.K., About the theory of so-called adsorption of soluble substances. *Kungliga Svenska Vetenskapsakademiens Handlingar*, 1898. **24**: p. 1-39.
279. Ho, Y.-S. and McKay, G., Pseudo-second order model for sorption processes. *Process biochemistry*, 1999. **34**(5): p. 451-465.
280. Hameed, B. and Rahman, A., Removal of phenol from aqueous solutions by adsorption onto activated carbon prepared from biomass material. *Journal of Hazardous Materials*, 2008. **160**(2-3): p. 576-581.
281. Simonin, J.P., On the comparison of pseudo-first order and pseudo-second order rate laws in the modeling of adsorption kinetics. *Chemical Engineering Journal*, 2016. **300**: p. 254-263.
282. Kumar, A., Prasad, B., and Mishra, I., Adsorptive removal of acrylonitrile by commercial grade activated carbon: kinetics, equilibrium and thermodynamics. *Journal of Hazardous Materials*, 2008. **152**(2): p. 589-600.
283. Li, Z., *et al.*, Degradation of metaldehyde in water by nanoparticle catalysts and powdered activated carbon. *Environmental Science and Pollution Research*, 2017. **24**(21): p. 17861-17873.
284. Xu, L., *et al.*, Use of synthesized double-stranded gene fragments as qPCR standards for the quantification of antibiotic resistance genes. *Journal of Microbiological Methods*, 2019. **164**: p. 105670.
285. Johnson, A.C., *et al.*, Linking changes in antibiotic effluent concentrations to flow, removal and consumption in four different UK sewage treatment plants over four years. *Environmental Pollution*, 2017. **220**: p. 919-926.

286. Pinto, A.J., Xi, C.W., and Raskin, L., Bacterial community structure in the drinking water microbiome is governed by filtration processes. *Environmental Science & Technology*, 2012. **46**(16): p. 8851-8859.
287. Li, J., *et al.*, Physico-chemical and biological aspects of a serially connected lab-scale constructed wetland-stabilization tank-GAC slow sand filtration system during removal of selected PPCPs. *Chemical Engineering Journal*, 2019. **369**: p. 1109-1118.
288. Haig, S.J., *et al.*, Replicating the microbial community and water quality performance of full-scale slow sand filters in laboratory-scale filters. *Water Research*, 2014. **61**: p. 141-151.
289. Bengtsson-Palme, J. and Larsson, D.G.J., Concentrations of antibiotics predicted to select for resistant bacteria: Proposed limits for environmental regulation. *Environment International*, 2016. **86**: p. 140-149.
290. Huerta, B., *et al.*, Exploring the links between antibiotic occurrence, antibiotic resistance, and bacterial communities in water supply reservoirs. *Science of the Total Environment*, 2013. **456**: p. 161-170.
291. Zhou, Q., *et al.*, Dissemination of resistance genes in duck/fish polyculture ponds in Guangdong Province: correlations between Cu and Zn and antibiotic resistance genes. *Environmental Science and Pollution Research*, 2019. **26**(8): p. 8182-8193.
292. Liu, Z., *et al.*, Metagenomic and metatranscriptomic analyses reveal activity and hosts of antibiotic resistance genes in activated sludge. *Environment International*, 2019. **129**: p. 208-220.
293. Whittle, G., Shoemaker, N.B., and Salyers, A.A., The role of *Bacteroides* conjugative transposons in the dissemination of antibiotic resistance genes. *Cellular and Molecular Life Sciences CMLS*, 2002. **59**(12): p. 2044-2054.
294. Goltsman, D.S.A., *et al.*, Community genomic and proteomic analyses of chemoautotrophic iron-oxidizing "*Leptospirillum rubarum*" (Group II) and "*Leptospirillum ferrodiazotrophum*" (Group III) bacteria in acid mine drainage biofilms. *Applied and Environmental Microbiology*, 2009. **75**(13): p. 4599.

-
295. Oliveira-Pinto, C., *et al.*, Diversity of gene cassettes and the abundance of the class 1 integron-integrase gene in sediment polluted by metals. *Extremophiles*, 2016. **20**(3): p. 283-289.
296. Camper, A.K., *et al.*, Bacteria associated with granular activated carbon particles in drinking water. *Applied and Environmental Microbiology*, 1986. **52**(3): p. 434-438.
297. Aarestrup, F.M., Butaye, P., and Witte, W., Nonhuman reservoirs of Enterococci, in *The Enterococci*. 2002, American Society of Microbiology.
298. Lester, C.H., *et al.*, In vivo transfer of the *vanA* resistance gene from an *Enterococcus faecium* isolate of animal origin to an *E. faecium* isolate of human origin in the intestines of human volunteers. *Antimicrobial Agents and Chemotherapy*, 2006. **50**(2): p. 596-599.
299. Ziglam, H.M. and Finch, R.G., Limitations of presently available glycopeptides in the treatment of Gram-positive infection. *Clinical Microbiology and Infection*, 2001. **7**: p. 53-65.
300. Seyfried, E.E., *et al.*, Occurrence of tetracycline resistance genes in aquaculture facilities with varying use of oxytetracycline. *Microbial Ecology*, 2010. **59**(4): p. 799-807.
301. Ma, J., *et al.*, Soil oxytetracycline exposure alters the microbial community and enhances the abundance of antibiotic resistance genes in the gut of *Enchytraeus crypticus*. *Science of the Total Environment*, 2019. **673**: p. 357-366.
302. Michael, I., *et al.*, Urban wastewater treatment plants as hotspots for the release of antibiotics in the environment: A review. *Water Research*, 2013. **47**(3): p. 957-995.
303. Watanabe, T., *et al.*, Dominance of *Sulfuritalea* species in nitrate-depleted water of a stratified freshwater lake and arsenate respiration ability within the genus. *Environmental Microbiology Reports*, 2017. **9**(5): p. 522-527.
304. Daims, H., *et al.*, Complete nitrification by *Nitrospira* bacteria. *Nature*, 2015. **528**: p. 504.
305. Ushiki, N., *et al.*, Nitrite oxidation kinetics of two *Nitrospira* strains: the quest for competition and ecological niche differentiation. *Journal of Bioscience and Bioengineering*, 2017. **123**(5): p. 581-589.

306. Sheng, S., *et al.*, Effects of different carbon sources and C/N ratios on the simultaneous anammox and denitrification process. *International Biodeterioration & Biodegradation*, 2018. **127**: p. 26-34.
307. Ishii, S., *et al.*, *Noviherbaspirillum denitrificans* sp. nov., a denitrifying bacterium isolated from rice paddy soil and *Noviherbaspirillum autotrophicum* sp. nov., a denitrifying, facultatively autotrophic bacterium isolated from rice paddy soil and proposal to reclassify *Herbaspirillum massiliense* as *Noviherbaspirillum massiliense* comb. nov. *International Journal of Systematic and Evolutionary Microbiology*, 2017. **67**(6): p. 1841-1848.
308. White, C.P., DeBry, R.W., and Lytle, D.A., Microbial survey of a full-scale, biologically active filter for treatment of drinking water. *Applied and Environmental Microbiology*, 2012. **78**(17): p. 6390-6394.
309. Liao, X.B., *et al.*, Operational performance, biomass and microbial community structure: impacts of backwashing on drinking water biofilter. *Environmental Science and Pollution Research*, 2015. **22**(1): p. 546-554.
310. Farrell, C., *et al.*, Turbidity composition and the relationship with microbial attachment and UV inactivation efficacy. *Science of the Total Environment*, 2018. **624**: p. 638-647.
311. Barker-Reid, F., Fox, E.M., and Faggian, R., Occurrence of antibiotic resistance genes in reclaimed water and river water in the Werribee Basin, Australia. *Journal of Water and Health*, 2010. **8**(3): p. 521-531.
312. Su, H., *et al.*, Occurrence and temporal variation of antibiotic resistance genes (ARGs) in shrimp aquaculture: ARGs dissemination from farming source to reared organisms. *Science of the Total Environment*, 2017. **607-608**: p. 357-366.
313. Zhang, K., *et al.*, Occurrence and distribution of antibiotic resistance genes in water supply reservoirs in Jingjinji area, China. *Ecotoxicology*, 2017. **26**(9): p. 1284-1292.
314. Reichenbach, H., The genus *Lysobacter*. *The Prokaryotes: Volume 6: Proteobacteria: Gamma Subclass*, 2006: p. 939-957.

-
315. Yu, M. and Zhao, Y., Comparative resistomic analyses of *Lysobacter* species with high intrinsic multidrug resistance. *Journal of Global Antimicrobial Resistance*, 2019. **19**: p. 320-327
316. Muziasari, W.I., *et al.*, The resistome of farmed fish feces contributes to the enrichment of antibiotic resistance genes in sediments below Baltic Sea fish farms. *Frontiers in Microbiology*, 2017. **7**: p. 2137.
317. Lin, W.F., *et al.*, Reduction in horizontal transfer of conjugative plasmid by UV irradiation and low-level chlorination. *Water Research*, 2016. **91**: p. 331-338.
318. Lv, L., *et al.*, Exposure to mutagenic disinfection byproducts leads to increase of antibiotic resistance in *Pseudomonas aeruginosa*. *Environmental Science & Technology*, 2014. **48**(14): p. 8188-8195.
319. Falkinham, J.O., Pruden, A., and Edwards, M., Opportunistic premise plumbing pathogens: Increasingly important pathogens in drinking water. *Pathogens*, 2015. **4**(2): p. 373-86.
320. Karkey, A., *et al.*, The ecological dynamics of fecal contamination and *Salmonella typhi* and *Salmonella paratyphi A* in municipal Kathmandu drinking water. *PLoS Neglected Tropical Diseases*, 2016. **10**(1): p. e0004346.
321. Figueira, V., *et al.*, Comparison of ubiquitous antibiotic-resistant *Enterobacteriaceae* populations isolated from wastewaters, surface waters and drinking waters. *Journal of Water and Health*, 2012. **10**(1): p. 1-10.
322. Kelley, S.T. and Gilbert, J.A., Studying the microbiology of the indoor environment. *Genome biology*, 2013. **14**(2): p. 202.
323. Rowe, W.P.M., *et al.*, Overexpression of antibiotic resistance genes in hospital effluents over time. *Journal of Antimicrobial Chemotherapy*, 2017. **72**(6): p. 1617-1623.
324. Zhang, L., *et al.*, Aerobic composting as an effective cow manure management strategy for reducing the dissemination of antibiotic resistance genes: An integrated meta-omics study. *Journal of Hazardous Materials*, 2020. **386**: p. 121895.

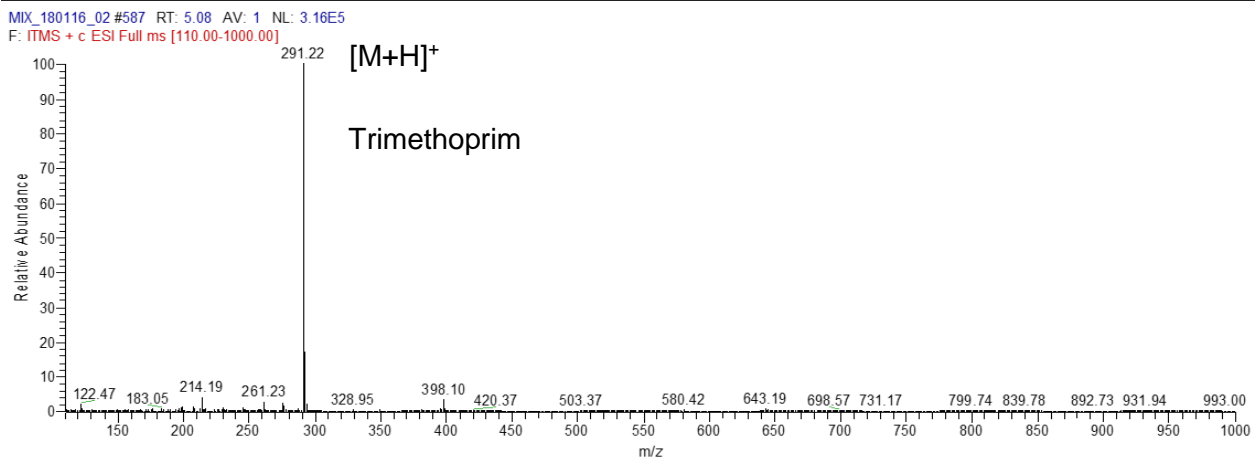
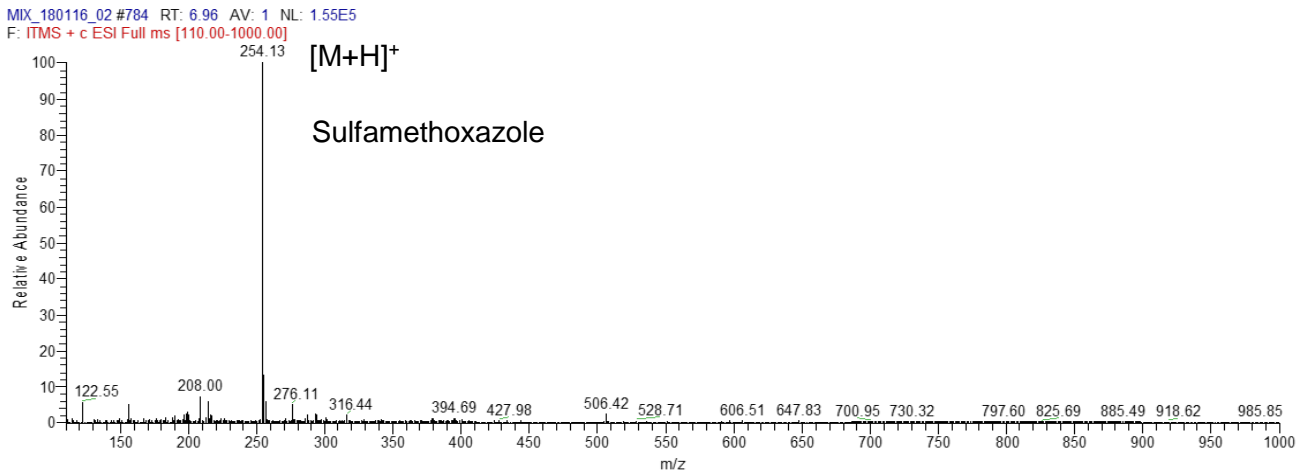
Appendix

Appendix – Chapter 3

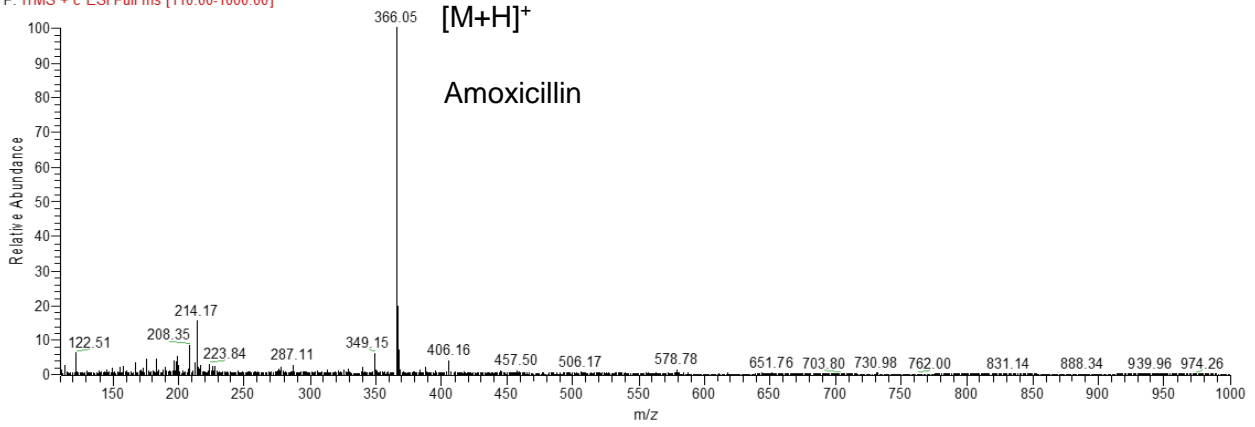
Table A3.1 Specifications of tubing used for biofilter system setup.

Usage	Material	Bore size (mm)	Supplier (Cat #)
peristaltic pump	PVC	NA	Agilent (3710047000)
Water inlet	PVC	3.0	Altec (01-94-1518)
Water outlet	silicone	3.1	Masterflex (96400-16)
Overflow	PVC	6.0	Altec (01-94-1523)
Sampling port - sand	silicone	3.1	Masterflex (96400-16)
Sampling port - GAC/anthracite	silicone	3.1	Masterflex (96400-16)

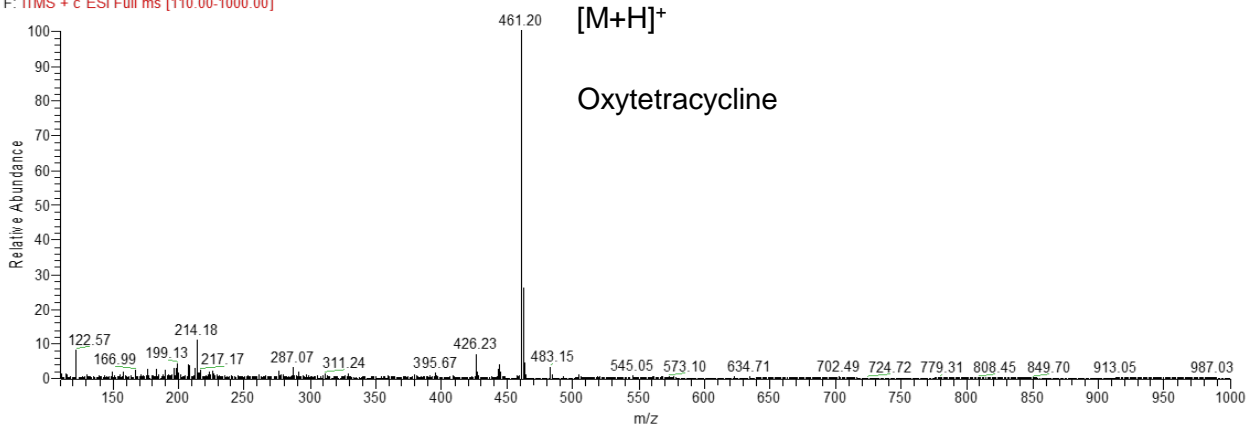
PVC: Polyvinyl chloride.



MIX_180116_02 #209 RT: 1.62 AV: 1 NL: 1.27E5
 F: ITMS + c ESI Full ms [110.00-1000.00]



MIX_180116_02 #607 RT: 5.25 AV: 1 NL: 1.05E5
 F: ITMS + c ESI Full ms [110.00-1000.00]



MIX_180116_02 #1036 RT: 9.21 AV: 1 NL: 7.33E5
 F: ITMS + c ESI Full ms [110.00-1000.00]

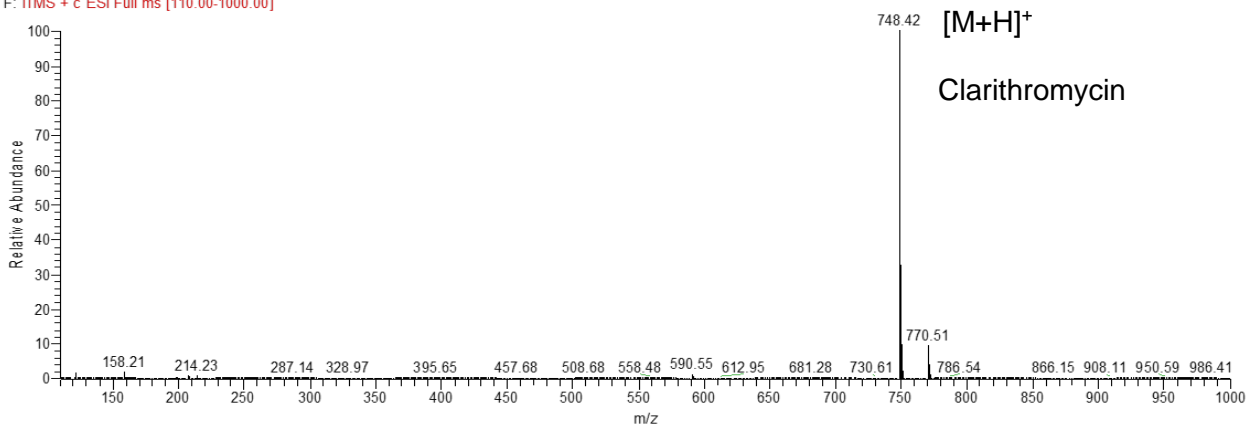


Figure A3.1 Mass chromatogram of precursor ion (m/z).

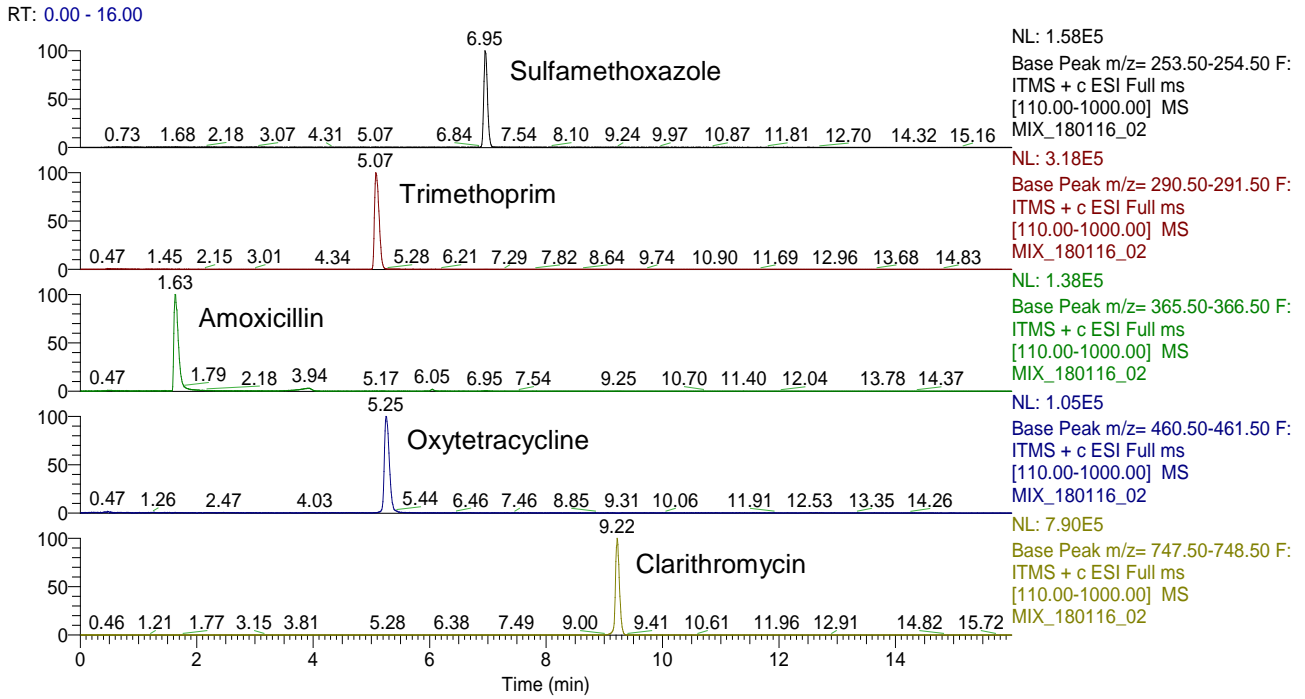


Figure A3.2 Chromatographic separation of target antibiotics.

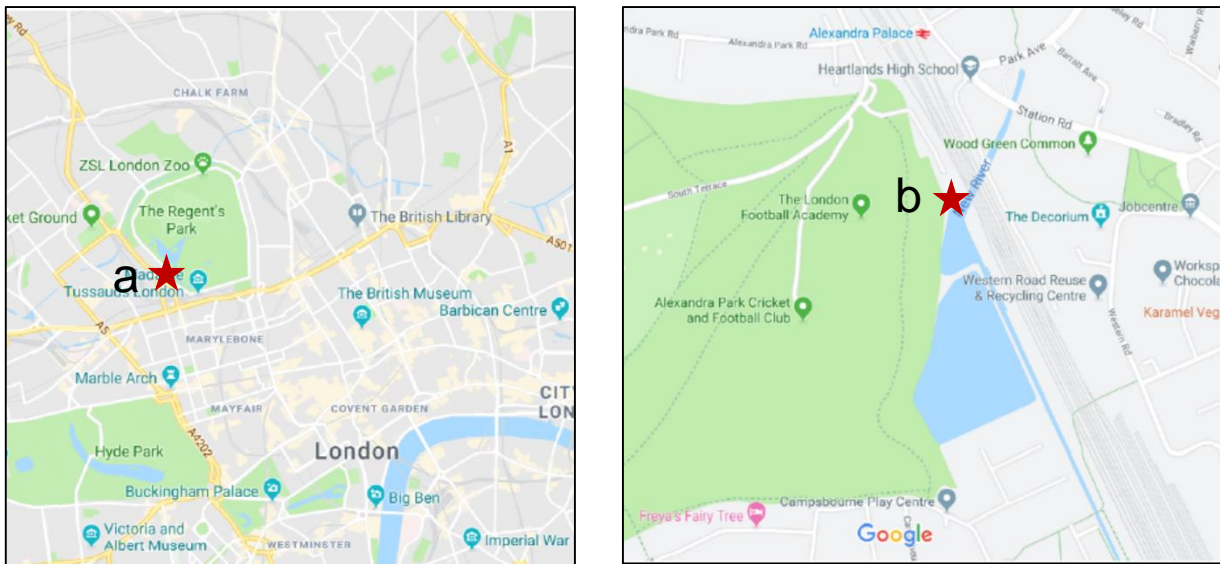


Figure A3.3 Geographic locations of sampling site a: Regent's Park; b: New River.

Map data ©2019 Google.

Table A3.2 Antibiotic Resistance Genes (ARGs) Oligonucleotides Used in This Study

Gene	Amplicon Size (bp)	GeneBank Accession No.	Sequence used in this study
<i>bla_{CTX-M}</i>	103	KT867021.1	CTATGGCACCACCAACGATATCGCGGTGATCTGGCCAAAAGATCGTGCCCGCTGATTCTGGTCA CTTACTTCACCCAGCCTCAACCTAAGGCAGAAAGCCGT
<i>bla_{TEM}</i>	516	KT867019.1	CCCCGAAGAACGTTTTCCAATGATGAGCACTTTAAAGTTCTGCTATGTGGTGGCGGTATTATCCCCTGTTGACGCCGGGCAAGCAACTCGGTGCGCGCATACACTATTCTCAG AATGACTTGGTTGAGTACTCACCAGTACAGAAAAGCATCTTACGGATGGCATGACAGTAAGAGAATTATGCAGTCTGCCATAACCATGAGTGATAAACAAGTCTGCCAACTTAC TTCTGACAACGATCGGAGGACCGAAGGAGCTAACCCTTTTTTGCACAACATGGGGGATCATGTAACCTCGCCTTGATCGTTGGGAACCGGAGCTGAATGAAGCCATACCAAACG ACGAGCGTGACACCACGATGCCTGCAGCAATGGCAACAACGTTGCGCAAACTATTAACCTGGCGAACTACTTACTCTAGCTTCCCAGCAAACTAATAGACTGGATGGAGGCGG ATAAAGTTGCAGGCACTTCTGCGCTCGGCCCTTCCGGCTGGCTGTTTTATTGCTGAT
<i>bla_{OXA-1}</i>	325	KR338947.1	ACCAAAGACGTGGATGCAATTTCTGTTGTTGGGTTTCGCAAGAAATAACCCAAAAAATTGGATTAATAAAAAAACAAGAATTATCTCAAAGATTTTATTGAAATCAAGACTTC TCTGGAGATAAAGAAAAGAAACAACGGATTAACAGAAGCATGGCTCGAAAAGTAGCTTAAAAAATTCACCAGAAGAACAATCAATTCCTGCGTAAAATTTAATCACAATCTCCCA GTTAAAAAAGTCAAGCATAGAAAACACCATAGAGAACATGTATCTACAAGATCTGGATAATAGTACAAAACTGTATGGGAAAAGTGGTGCA
<i>ermB</i>	412	EU595407.1	ACGACGAAACTGGCTAAAATAAGTAAACAGGTAACGTCTATTGAAATTAGACAGTCACTCTATTCACCTTATCGTCAGAAAAAATTAAGAACTGAATACTCGTGTCACTTTAATTCACAA GATATTCTACAGTTTCAATTCCTAACAAACAGAGGTATAAAAATTGTTGGGAATATTCTTACCATTTAAGCACACAAATTTAAAAAAGTGGTTTTTGAAGCCATGCGTCTGACA TCTATCTGATTGTTGAAGAAGGATTCTACAAGCGTACCTTGGATATTCACCGAACAAGTGGGTTGCTTTCACACTCAAGTCTCGATTGCAATGCTTAAAGCTGCCAGCGGAA TGCTTTTCACTAAACAAAAGTAAACAGTGTCTTAATAAACTTACCCGCCATACCACAG
<i>tetA</i>	210	KF240812.1	GCTACATCCTGCTTGCCTTCGCGACACGGGGATGGATGGCGTTCCCGATCATGGTCTGCTTGCCTCGGGTGGCATCGGAATGCCGGCGCTGCAAGCAATGTTGTCCAGGCAG GTGGATGAGGAACGTCAGGGGCAGCTGCAAGGCTCACTGGCGGCGCTCACCAGCCTGACCTCGATCGTGGACCCCTCCTCTTACGGCGATCTATG
<i>tetG</i>	468	KJ603219.1	GCTCGGTGGTATCTCTGCTCATGCCCGTTTATCGCCGCCGCCCTTCTCAACGGGTTCCGCTTCCGCTTGCCTGCATTTTCTCAAGGAGACTCATCACAGCCATGGCGGGAC CGGAAAGCCGGTTCGCATCAAACTTCCGTTCTGTTACGGCTGGATGATGCATTGCGCGGGCTAGGTGCGCTTTTCGAGTTTTTCTTCACTGATCGGCCAAGTGCCT GCAGCCATATGGTCAATATGGCGAGGACCGTTTTCAAGTGAACACCGCCGTTTGTGCTCGCGGCTTTGGGGCAACACATGCGATCTTCAAGCGTTTTGTTACC GGCCCGCTTTCAAGCCGGCTTGAGAGCGGGCGCACGCTGCTGTTTGGCATGGCTGCGGATGCGACTGGCTTCTGTTCTTCTGCTTTTGCACGCGAGGGATGGTGGTTC CATTCTGTTGCT
<i>tetQ</i>	169	KX034803.1	AGAATCTGCTGTTTGGCAGTGGAGCAACGGAAAAGTGGCGCCGTGTGGATAATGGTGACACCATAACGGACTCTATGGATATAGAGAAAACGTAGAGGAATTACTGTCCGGGCTT CTACGACTCTATTATCTGGAATGGAGTGAATGCAATATCATTGACACTCCG
<i>tetW</i>	168	EF489472.1	GAGAGCCTGCTATATGCCAGCGGAGCCATTTAGAAACCGGGAGCGTCGAAAAAGGGACAACGAGGACGGACACCATGTTTTGGAGCGGCAGCGTGGGATTACCATTCAAGC GGCAGTCACTTCTTCCAGTGGCACAGATGTAAGTTAACATTGTGGATACGCC
<i>tetX</i>	468	KF905572.1	CAATAATTGGTGGTGGACCCGTTGGACTGACTATGGCAAAATTTATACAGCAAAACGGCATAGACGTTTTCAGTTTACGAAAGAGACAACGACCGAGAGGCAAGAATTTTTGGTGG AACCCTTGACCTACACAAGGTTCAAGGTGAGGAAGCAATGAAAAAGCGGATTGTTACAACTTATTATGACTTAGCCTTACCAATGGGTGTAATATTGCTGATGAAAAAGGCA ATATTTTATCCACAAAAATGTAAGCCCGGAAAAATCGATTTGACAACTCTGAAATAAACAGAAATGACTTAAGGGCTATCTTGTGAAATAGTTAGAAAAACGACACGGTTATTTGG ATAGAAAACTTGTATGCTTGAACCTGGTAAGAAGAAGTGGACACTAACTTTTTGAGAATAAACCGAGTAAACAGCAGATTTGTTATTCTTGCCTTGGCCGATGTTCAAGGTA AGAA
<i>sul I</i>	158	KJ801663.1	CACCGGAAACATCGCTGCACGTGCTGTGCAACCTTCAAAGCTGAAGTCGGCGTTGGGGCTTCCGCTATTGGTCTCGGTGTCGGGAAATCCTTCTTGGGCGCCACCGTTGGC CTTCTGTAAAGGATCTGGGTCCAGCGAGCCTTGCAGCGGAACTT
<i>sul II</i>	190	KC898873.1	CTCCGATGGAGGCCGTTACTGGCGCAGACGCGCAGCTTGGCAGGGCGTAAAGCTGATGGCCGAGGGGGCAGATGTGATCGACCTCGGTCCGGCATCCAGCAATCCCGA CGCCGCGCTGTTTCTCGACACAGAAAATCGCGCTATCGCGCCGGTCTGAGCGCGCTCAAGGCAGATGGCATTCCC
<i>dfrA1</i>	425	KC862256.1	TGGTAGCTATATCGAAGAATGGAGTTATCGGGAATGGCCCTGATATTCATGGAGTGCCAAAGGTGAACAGCTCCTGTTTAAAGCTATTACCTATAACCAATGGCTGTTGGTTGG ACGCAAGACTTTTGAATCAATGGGAGCATTACCAACCGAAAAGTATCGGGTCGTAACACGTTCAAGTTTTACATCTGACAATGAGACGTAGTGATCTTCCATCAATTAAGATG CTTTAAACCAACCTAAAGAAAATAACGGATCATGTCATTGTTTACGGTGGTGGGGAGATATACAAAAGCCTGATCGATCAAGTAGATACACTACATATATCTACAATAGACATCGAG CCGAAAGGTGATGTTACTTTCTGAAATCCCAGCAATTTAGGCCAGTTTTTACCAAGACTTCGCCTTAACATA
<i>dfrA12</i>	155	GU944735.1	GAGCTGAGATATACACTCTGGCACTACCTCACGCCACGGCGTGTTCATCTGAGGTGACATCAAACCTTCCAGGGTGACGCTTCTTCCCAATGCTCAACGAAACAGAATTCGA GCTTGTCTCAACCGAAACATTCAAGCTGTAATCCGTAC
<i>intl 1</i>	280	JN837682.1	CCTCCCGCACGATGATCGTGCCTGATCGAAATCCAGATCCTTGACCCGCAAGTTGCAAAACCTCACTGATCCGATGCCGTTCCATACAGAAGCTGGGCGAACAAACGATGCT CGCCTTCCAGAAAACCGAGGATGCAACCACTTCAATCCGGGTCACGACCACCGGCAAGCGCCGCGACGGCCGAGGTCTCCGATCTCCTGAAGCCAGGGCAGATCCGTGCA CAGCACCCTGGCTAGAAGAACAGCAAGGCGCCAAATGCGGATGACGATGCGTGA
<i>intl 2</i>	233	FJ785524.1	TTATTGCTGGGATTAGCGCGTGGGCGTAGGCTGTTTCTGCTTTTCCACCCTTACCGTATGCACAGTGTGACGCCATTATCAAAATCAAAATCTTTAACCCGCAACCGCAA GCATTCATTAATGCGCAACCTGCACCATACAGCAGCGTAAAAATAAATTGGTTGCGAGTATCCATAACCTGCAAAATGCGTTGCACCTCATTTGCAGAGATAACAGAGGGTAGC CGT

A3.1 PCR Procedures

A 25 μL PCR reaction system was performed for all genes. The reaction mixture consisted of 12.5 μL BioMixTM Red (BIOLINE, UK), 1 μL of each primer (10 μM), 1 μL of DNA template, and 9.5 μL of PCR grade water. The PCR programme used was as follows: 95 $^{\circ}\text{C}$ for 3 min, followed by 35 cycles consisting of 95 $^{\circ}\text{C}$ for 15 s, 55 $^{\circ}\text{C}$ for 30 s, 75 $^{\circ}\text{C}$ for 30 s, and a final extension step at 72 $^{\circ}\text{C}$ for 7 min. PCR grade water was used as the negative control in every run.

A3.2 qPCR Method validation

Different types of environmental samples were used to validate the qPCR assays. Water samples were collected from the River Thames, ponds in Regent's Park and Hyde Park in London; soil and duck faeces samples were collected from Regent's Park. The geographical location of sampling sites is provided in Figure S3.4. DNA extraction from water samples followed the methods described in section 3.4.1. For soil and faeces samples, DNA was extracted directly from 0.5 g (wet) of the raw samples. The quality and concentration of the extracted DNA were determined by NanoDrop and 1.5% agarose gel electrophoresis and stored at -20 $^{\circ}\text{C}$ until further analysis. qPCR settings for environmental DNA samples were the same as for qPCR standards as described above.



Figure A3.4 Geographic map of sampling sites. 1: Regent's Park; 2: Hyde Park; 3: River Thames.

Map data ©2019 Google.

An overview of the absolute abundance of ARGs and integron genes *intl 1* and *intl 2* in different environmental samples is shown in Figure 3.7. The concentration of ARGs among all the samples was between $10^3 \sim 10^8$ copies/L, with the detection frequencies ranging from 71.42% to 100%. All of the 13 selected ARGs were detected in River Thames water samples. In general, the overall abundance of ARGs in the River Thames was two to three orders of magnitude higher than in the parks' water samples. The order of the average gene copies from low to high was: RP-F (3.86×10^4 copies/g), RP-S (7.28×10^4 copies/g), RP-W (7.97×10^4 copies/L), HP (9.91×10^4 copies/L), and RT (3.37×10^7 copies/L).

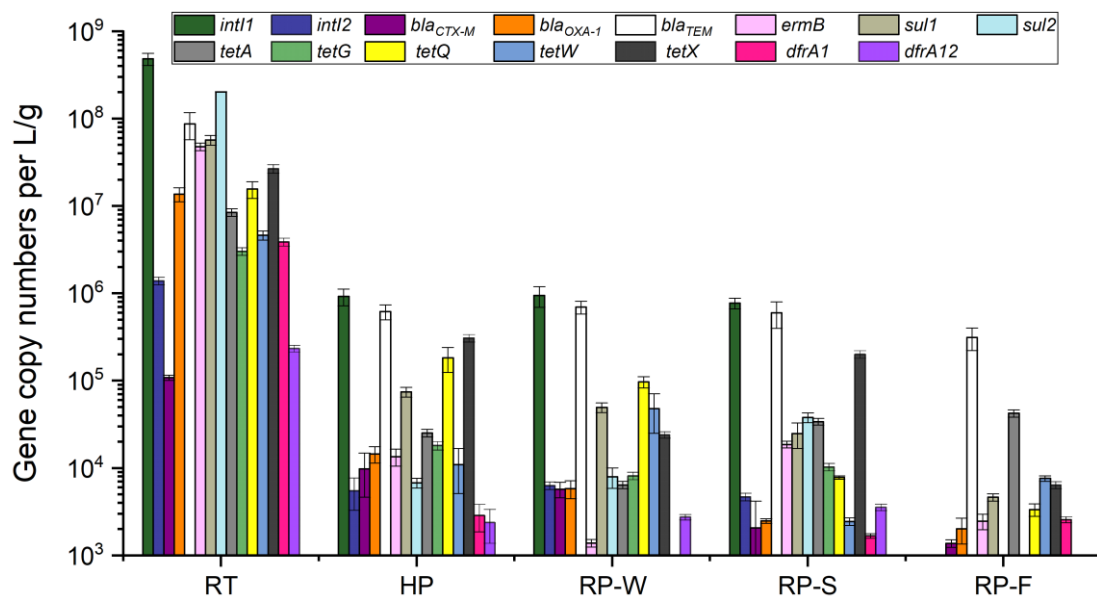


Figure A3.5 Concentrations of ARGs and integron genes in environmental samples. RT: River Thames; HP: Hyde Park; RP-W: Regent's Park water; RP-S: Regent's Park; RP-F: Regent's Park faeces sample. The error bars represent STD from the mean value of triplicate samples ($n = 3$).

Table A3.3 Primers and gene classifications of all genes from high-throughput qPCR (HT-qPCR).

Gene Name	Forward Primer	Reverse Primer	Gene Classification	Resistance Mechanism
<i>16S rRNA</i>	GGGTTGCGCTCGTTGC	ATGGYTGTGCTCAGCTCGTG		
<i>aac</i>	CCCTGCGTTGTGGCTATGT	TTGGCCACGCCAATCC	Aminoglycoside	deactivate
<i>aac(6')I1</i>	GACCGGATTAAGGCCGATG	CTTGCCTTGATATTCAGTTTTTATAACCA	Aminoglycoside	deactivate
<i>aac(6')-Ib(aka aacA4)-01</i>	GTTTGAGAGGCAAGGTACCGTAA	GAATGCCTGGCGTGTGTTGA	Aminoglycoside	deactivate
<i>aac(6')-Ib(aka aacA4)-02</i>	CGTCGCCGAGCAACTTG	CGGTACCTTGCCCTCTCAAACC	Aminoglycoside	deactivate
<i>aac(6')-Ib(aka aacA4)-03</i>	AGAAGCACGCCGACACTT	GCTCTCCATTGAGCATTGCA	Aminoglycoside	deactivate
<i>aac(6')-II</i>	CGACCCGACTCCGAACAA	GCACGAATCCTGCCTTCTCA	Aminoglycoside	deactivate
<i>aac(6')-Iy</i>	GCTTTGCGGATGCCTCAAT	GGAGAACAATAATACCTTCAAGGAAA	Aminoglycoside	deactivate
<i>aacA_aphD</i>	AGAGCCTTGGGAAGATGAAGTTT	TTGATCCATACCATAGACTATCTCATCA	Aminoglycoside	deactivate
<i>aacC</i>	CGTCACCTTATTCGATGCCCTTAC	GTCGGGCGCGGCATA	Aminoglycoside	deactivate
<i>aacC1</i>	GGTCGTGAGTTCGGAGACGTA	GCAAGTTCGCGAGGTAATCG	Aminoglycoside	deactivate
<i>aacC2</i>	ACGGCATTCTCGATTGCTTT	CCGAGCTTCACGTAAGCATT	Aminoglycoside	deactivate
<i>aacC4</i>	CGGCGTGGGACACGAT	AGGGAACCTTTGCCATCAACT	Aminoglycoside	deactivate
<i>aadA-01</i>	GTTGTGCACGACGACATCATT	GGCTCGAAGATACCTGCAAGAA	Aminoglycoside	deactivate
<i>aadA-02</i>	CGAGATTCTCCGCGCTGTA	GCTGCCATTCTCCAAATTGC	Aminoglycoside	deactivate
<i>aadA1</i>	AGCTAAGCGGAACTGCAAT	TGGCTCGAAGATACCTGCAA	Aminoglycoside	deactivate
<i>aadA-1-01</i>	AAAAGCCCGAAGAGGAACTTG	CATCTTTCACAAAGATGTTGCTGTCT	Aminoglycoside	deactivate
<i>aadA-1-02</i>	CGGAATTGAAAAACTGATCGAA	ATACCGGCTGTCCGTCATTT	Aminoglycoside	deactivate
<i>aadA2-01</i>	ACGGCTCCGCGAGTGGAT	GGCCACAGTAACCAACAAATCA	Aminoglycoside	deactivate
<i>aadA2-02</i>	CTTGTCGTGCATGACGACATC	TCGAAGATACCCGCAAGAATG	Aminoglycoside	deactivate
<i>aadA2-03</i>	CAATGACATTCTTGGGGTATC	GACCTACCAAGGCAACGCTATG	Aminoglycoside	deactivate
<i>aadA5-01</i>	ATCACGATCTTGCGATTTTGCT	CTGCGGATGGGCCTAGAAG	Aminoglycoside	deactivate
<i>aadA5-02</i>	GTTCTTGCTCTTGCTCGCATT	GATGCTCGGCAGGCAAAC	Aminoglycoside	deactivate
<i>aadA9-01</i>	CGCGGCAAGCCTATCTTG	CAAATCAGCGACCGCAGACT	Aminoglycoside	deactivate
<i>aadA9-02</i>	GGATGCACGCTTGGATGAA	CCTCTAGCGGCCGGAGTATT	Aminoglycoside	deactivate
<i>aadD</i>	CCGACAACATTTCTACCATCCTT	ACCGAAGCGCTCGTCGTATA	Aminoglycoside	deactivate
<i>aadE</i>	TACCTTATTGCCCTTGAAGAGTTA	GGAAGTATGTCCCTTTTAATTCTACAATCT	Aminoglycoside	deactivate
<i>acrA-01</i>	CAACGATCGGACGGGTTTC	TGGCGATGCCACCGTACT	FCA	efflux

<i>acrA-02</i>	GGTCTATCACCTACGCGTATC	GCGCGCACGAACATACC	FCA	efflux
<i>acrA-03</i>	CAGACCCGCATCGCATATT	CGACAATTTGCGGCTCATG	FCA	efflux
<i>acrA-04</i>	TACTTTGCGCGCCATCTTC	CGTGCGCGAACGAACAT	FCA	efflux
<i>acrA-05</i>	CGTGCGCGAACGAACA	ACTTTGCGCGCCATCTTC	FCA	efflux
<i>acrB-01</i>	AGTCGGTGTTCGCGTAAAC	CAAGGAAACGAACGCAATACC	FCA	efflux
<i>acrF</i>	GCGGCCAGGCACAAAA	TACGCTCTTCCCACGGTTTC	FCA	efflux
<i>acrR-01</i>	GCGCTGGAGACACGACAAC	GCCTTGCTGCGAGAACAAA	other/efflux	efflux
<i>acrR-02</i>	GATGATACCCCCTGCTGTGAGA	ACCAAACAAGAAGCGCAAGAA	other/efflux	efflux
<i>adeA</i>	CAGTTCGAGCGCTATTTCTG	CGCCCTGACCGACCAAT	FCA	efflux
<i>ampC_blaDHA</i>	TGGCCGCAGCAGAAAAGA	CCGTTTTATGCACCCAGGAA	Beta Lactams	deactivate
<i>ampC-01</i>	TGGCGTATCGGGTCAATGT	CTCCACGGGCCAGTTGAG	Beta Lactams	deactivate
<i>ampC-02</i>	GCAGCACGCCCCGTAA	TGTACCCATGATGCGGCTACT	Beta Lactams	deactivate
<i>ampC-04</i>	TCCGGTGACGCGACAGA	CAGCACGCCGGTGAAGT	Beta Lactams	deactivate
<i>ampC-05</i>	CTGTTCGAGCTGGTTCTATAAGTAAA	CAGTATCTGGTCAACGGATCGT	Beta Lactams	deactivate
<i>ampC-06</i>	CCGCTCAAGCTGGACCATAC	CCATATCCTGCACGTTGGTTT	Beta Lactams	deactivate
<i>ampC-07</i>	CCGCCCAGAGCAAGGACTA	GCTCGACTTCACGCCGTAAG	Beta Lactams	deactivate
<i>ampC-09</i>	CAGCCGCTGATGAAAAAATATG	CAGCGAGCCCACTTCGA	Beta Lactams	deactivate
<i>aph</i>	TTTCAGCAAGTGGATCATGTTAAAAT	CCAAGCTGTTTCCACTGTTTTTC	Aminoglycoside	deactivate
<i>aph(2')-Id-01</i>	TGAGCAGTATCATAAGTTGAGTGAAAAG	GACAGAACAATCAATCTCTATGGAATG	Aminoglycoside	deactivate
<i>aph(2')-Id-02</i>	TAAGGATATACCGACAGTTTTGGAAA	TTTAATCCCTCTTCATACCAATCCATA	Aminoglycoside	deactivate
<i>aph6ia</i>	CCCATCCCATGTGTAAGGAAA	GCCACCGCTTCTGCTGTAC	Aminoglycoside	deactivate
<i>aphA1(aka kanR)</i>	TGAACAAGTCTGGAAAGAAATGCA	CCTATTAATTTCCCTCGTCAAAAA	Aminoglycoside	deactivate
<i>bacA-01</i>	CGGCTTCGTGACCTCGTT	ACAATGCGATACCAGGCAAAT	other/efflux	deactivate
<i>bacA-02</i>	TTCCACGACACGATTAAGTCATTG	CGGCTCTTTGCGCTTCAG	other/efflux	deactivate
<i>bla1</i>	GCAAGTTGAAGCGAAAAGAAAAGA	TACCAGTATCAATCGCATATACACCTAA	Beta Lactams	deactivate
<i>bla-ACC-1</i>	CACACAGCTGATGGCTTATCTAAAA	AATAAACGCGATGGGTTCCA	Beta Lactams	deactivate
<i>blaCMY</i>	CCGCGGCGAAAATTAAGC	GCCACTGTTTGCCTGTCAGTT	Beta Lactams	deactivate
<i>blaCMY2-01</i>	AAAGCCTCATGGGTGCATAAA	ATAGCTTTTGTGGCCAGCATCA	Beta Lactams	deactivate
<i>blaCMY2-02</i>	GCGAGCAGCCTGAAGCA	CGGATGGGCTTGTCTCTT	Beta Lactams	deactivate
<i>blaCTX-M-01</i>	GGAGGCGTGACGGCTTTT	TTCAGTGCGATCCAGACGAA	Beta Lactams	deactivate
<i>blaCTX-M-02</i>	GCCGCGGTGCTGAAGA	ATCGGATTATAGTTAACCAGGTCAGATTT	Beta Lactams	deactivate

<i>blaCTX-M-03</i>	CGATACCACCACGCCGTTA	GCATTGCCCAACGTCAGATT	Beta Lactams	deactivate
<i>blaCTX-M-04</i>	CTTGGCGTTGCGCTGAT	CGTTCATCGGCACGGTAGA	Beta Lactams	deactivate
<i>blaCTX-M-05</i>	GCGATAACGTGGCGATGAAT	GTTCGAGACGGAACGTTTCGT	Beta Lactams	deactivate
<i>blaCTX-M-06</i>	CACAGTTGGTGACGTGGCTTAA	CTCCGCTGCCGGTTTTATC	Beta Lactams	deactivate
<i>blaGES</i>	GCAATGTGCTCAACGTTCAAG	GTGCCTGAGTCAATTCTTTCAAAG	Beta Lactams	deactivate
<i>blaIMP-01</i>	AACACGGTTTGGTGGTTCTTGTA	GCGCTCCACAAACCAATTG	Beta Lactams	deactivate
<i>blaIMP-02</i>	AAGGCAGCATTTCTCTCATTTT	GGATAGATCGAGAATTAAGCCACTCT	Beta Lactams	deactivate
<i>bla-L1</i>	CACCGGGTTACCAGCTGAAG	GCGAAGCTGCGCTTGTAGTC	Beta Lactams	deactivate
<i>blaMOX_blaCMY</i>	CTATGTCAATGTGCCGAAGCA	GGCTTGTCTCTTTTGAATAGC	Beta Lactams	deactivate
<i>blaOCH</i>	GGCGACTTGCGCCGTAT	TTTTCTGCTCGGCCATGAG	Beta Lactams	deactivate
<i>blaOKP</i>	GCCGCCATCACCATGAG	GGTGACGTTGTACCCGATCTG	Beta Lactams	deactivate
<i>blaOXA1_blaOXA30</i>	CGGATGGTTTGAAGGGTTTATTAT	TCTTGGCTTTTTATGCTTGATGTTAA	Beta Lactams	deactivate
<i>blaOXA10-01</i>	CGCAATTATCGGCCTAGAAACT	TTGGCTTTCCGTCCCATT	Beta Lactams	deactivate
<i>blaOXA10-02</i>	CGCAATTATCGGCCTAGAAACT	TTGGCTTTCCGTCCCATT	Beta Lactams	deactivate
<i>blaOXY</i>	CGTTCAGGCGGCAGGTT	GCCGCGATATAAGATTTGAGAATT	Beta Lactams	deactivate
<i>blaPAO</i>	CGCCGTACAACCGGTGAT	GAAGTAATGCGGTTCTCCTTTCA	Beta Lactams	deactivate
<i>blaPER</i>	TGCTGGTTGCTGTTTTGTGA	CCTGCGCAATGATAGCTTCAT	Beta Lactams	deactivate
<i>blaPSE</i>	TTGTGACCTATCCCCTGTAATAGAA	TGCGAAGCACGCATCATC	Beta Lactams	deactivate
<i>blaROB</i>	GCAAAGGCATGACGATTGC	CGCGCTGTTGTCGCTAAA	Beta Lactams	deactivate
<i>blaSFO</i>	CCGCCGCCATCCAGTA	GGGCCGCCAAGATGCT	Beta Lactams	deactivate
<i>blaSHV-01</i>	TCCCATGATGAGCACCTTTAAA	TTCGTACCCGGCATCCA	Beta Lactams	deactivate
<i>blaSHV-02</i>	CTTTCCCATGATGAGCACCTTT	TCCTGCTGGCGATAGTGGAT	Beta Lactams	deactivate
<i>blaTEM</i>	AGCATCTTACGGATGGCATGA	TCCTCCGATCGTTGTCAGAAGT	Beta Lactams	deactivate
<i>blaTLA</i>	ACACTTTGCCATTGCTGTTTATGT	TGCAAATTTGCGCAATAATCTTT	Beta Lactams	deactivate
<i>blaVEB</i>	CCCGATGCAAAGCGTTATG	GAAAGATTCCTTTATCTATCTCAGACAA	Beta Lactams	deactivate
<i>blaVIM</i>	GCACTTCTCGCGGAGATTG	CGACGGTGATGCGTACGTT	Beta Lactams	deactivate
<i>blaZ</i>	GGAGATAAAGTAACAAATCCAGTTAGATATGA	TGCTTAATTTTCCATTTGCGATAAG	Beta Lactams	deactivate
<i>carB</i>	GGAGTGAGGCTGACCGTAGAAG	ATCGGCGAAACGCACAAA	MLSB	efflux
<i>catA1</i>	GGGTGAGTTTACCAGTTTTGATT	CACCTTGTGCGCTTTCGTATA	FCA	deactivate
<i>catB3</i>	GCACTCGATGCCTTCCAAAA	AGAGCCGATCCAAACGTCAT	FCA	deactivate
<i>catB8</i>	CACTCGACGCCCTTCCAAAG	CCGAGCCTATCCAGACATCATT	other/efflux	deactivate

<i>ceoA</i>	ATCAACACGGACCAGGACAAG	GGAAAGTCCGCTCACGATGA	other/efflux	efflux
<i>cepA</i>	AGTTGCGCAGAACAGTCCTCTT	TCGTATCTTGCCCCGTCGATAAT	Beta Lactams	deactivate
<i>cfiA</i>	GCAGCGTTGCTGGACACA	GTTCCGGGATAAACGTGGTGACT	Beta Lactams	deactivate
<i>cfr</i>	GCAAAATTCAGAGCAAGTTACGAA	AAAATGACTCCCAACCTGCTTTAT	FCA	deactivate
<i>cfxA</i>	TCATTCCCTCGTTCAAGTTTTTCAGA	TGCAGCACCAAGAGGAGATGT	Beta Lactams	deactivate
<i>clnI1-1(class1)</i>	GGCATCCAAGCAGCAAG	AAGCAGACTTGACCTGA	integron	integron
<i>cmeA</i>	GCAGCAAAGAAGAAGCACCAA	AGCAGGGTAAGTAAACTAAGTGGTAAATCT	FCA	efflux
<i>cmlA1-01</i>	TAGGAAGCATCGGAACGTTGAT	CAGACCGAGCACGACTGTTG	FCA	efflux
<i>cmlA1-02</i>	AGGAAGCATCGGAACGTTGA	ACAGACCGAGCACGACTGTTG	FCA	efflux
<i>cmr</i>	CGGCATCGTCAGTGGAATT	CGGTTCCGAAAAAGATGGAA	other/efflux	efflux
<i>cmx(A)</i>	GCGATCGCCATCCTCTGT	TCGACACGGAGCCTTGGT	FCA	efflux
<i>cphA-01</i>	GCGAGCTGCACAAGCTGAT	CGGCCAGTCGCTCTTC	Beta Lactams	deactivate
<i>cphA-02</i>	GTGCTGATGGCGAGTTTCTG	GGTGTGGTAGTTGGTGTGATCAC	Beta Lactams	deactivate
<i>dfrA1</i>	GGAATGGCCCTGATATTCCA	AGTCTTGCGTCCAACCAACAG	other/efflux	deactivate
<i>dfrA12</i>	CCTCTACCGAACCGTCACACA	GCGACAGCGTTGAAACAACACTAC	other/efflux	deactivate
<i>emrD</i>	CTCAGCAGTATGGTGGTAAGCATT	ACCAGGCGCCGAAGAAC	other/efflux	efflux
<i>ereA</i>	CCTGTGGTACGGAGAATTCATGT	ACCGCATTGCTTTGCTT	MLSB	deactivate
<i>ereB</i>	GCTTTATTTACAGGAGCGGAAT	TTTTAAATGCCACAGCACAGAATC	other/efflux	deactivate
<i>erm(34)</i>	GCGCGTTGACGACGATT	TGGTCATACTCGACGGCTAGAAC	MLSB	protection
<i>erm(35)</i>	TTGAAAACGATGTTGCATTAAGTCA	TCTATAATCACAACCTAACCATTGAACGT	MLSB	protection
<i>erm(36)</i>	GGCGGACCGACTTGCCAT	TCTGCGTTGACGACGGTTAC	MLSB	protection
<i>ermA</i>	TTGAGAAGGGATTTGCGAAAAG	ATATCCATCTCCACCATTAATAGTAAACC	MLSB	protection
<i>ermA_ermTR</i>	ACATTTTACCAAGGAACCTTGTTGAA	GTGGCATGACATAAACCTTCATCA	MLSB	protection
<i>ermB</i>	TAAAGGGCATTTAACGACGAAACT	TTTATACCTCTGTTTGTAGGGAATTGAA	MLSB	protection
<i>ermC</i>	TTTGAAATCGGCTCAGGAAAA	ATGGTCTATTTCAATGGCAGTTACG	MLSB	protection
<i>ermF</i>	CAGCTTTGGTTGAACATTTACGAA	AAATTCCTAAAATCACAACCGACAA	MLSB	protection
<i>ermJ_ermD</i>	GGACTCGGCAATGGTCAGAA	CCCCGAAACGCAATATAATGTT	MLSB	protection
<i>ermK-01</i>	GTTTGATATTGGCATTGTCAGAGAAA	ACCATTGCCGAGTCCACTTT	MLSB	protection
<i>ermK-02</i>	GAGCCGCAAGCCCCTTT	GTGTTTCATTTGACGCGGAGTAA	MLSB	protection
<i>ermT-01</i>	GTTCACTAGCACTATTTTTAATGACAGAAGT	GAAGGGTGTCTTTTTAATACAATTAACGA	MLSB	protection
<i>ermT-02</i>	GTAAAATCCCTAGAGAATACTTTTCATCCA	TGAGTGATATTTTTGAAGGGTGTCTT	MLSB	protection

<i>ermX</i>	GCTCAGTGGTCCCCATGGT	ATCCCCCGTCAACGTTT	MLSB	protection
<i>ermY</i>	TTGTCTTTGAAAGTGAAGCAACAGT	TAACGCTAGAGAACGATTTGTATTGAG	MLSB	protection
<i>fabK</i>	TTTCAGCTCAGCACTTTGGTCAT	AAGGCATCTTTTTCAGCCAGTTC	other/efflux	deactivate
<i>floR</i>	ATTGTCTTCACGGTGTCCGTTA	CCGCGATGTCGTCGAACT	FCA	efflux
<i>folA</i>	CGAGCAGTTCCTGCCAAAG	CCCAGTCATCCGGTTCATAATC	other/efflux	deactivate
<i>fosB</i>	TCACTGTAACATAATGAAGCATTAGACCAT	CCATCTGGATCTGTAAAGTAAAGAGATC	other/efflux	deactivate
<i>fosX</i>	GATTAAGCCATATCACTTTAATTGTGAAAG	TCTCCTCCATAATGCAAATCCA	other/efflux	deactivate
<i>fox5</i>	GGTTTGCCGCTGCAGTTC	GCGGCCAGGTGACCAA	Beta Lactams	deactivate
<i>imiR</i>	CCGGACTAGAGCTTCATGTAAGC	CCCACGCGGTACTCTTGTAAG	other/efflux	unknown
<i>intl-1(clinic)</i>	CGAACGAGTGGCGGAGGGTG	TACCCGAGAGCTTGGCACCCA	integron	integron
<i>IS613</i>	AGGTTCCGACTCAATGCAACA	TTCAGCACATACCGCCTTGAT	IS613	transposase
<i>lmrA-01</i>	TCGACGTGACCGTAGTGAACA	CGTGACTACCCAGGTGAGTTGA	MLSB	efflux
<i>lnuA-01</i>	TGACGCTCAACACACTCAAAAA	TTCATGCTTAAGTTCCATACGTGAA	MLSB	deactivate
<i>lnuB-01</i>	TGAACATAATCCCCTCGTTTAAAGAT	TAATTGCCCTGTTTCATCGTAAATAA	MLSB	deactivate
<i>lnuB-02</i>	AAAGGAGAAGGTGACCAATACTCTGA	GGAGCTACGTCAAACAACCAGTT	MLSB	deactivate
<i>lnuC</i>	TGGTCAATATAACAGATGTAAACCAGATTT	CACCCAGCCACCATCAA	MLSB	deactivate
<i>marR-01</i>	GCGGCGTACTGGTGAAGCTA	TGCCCTGGTTCGTTGATGA	other/efflux	efflux
<i>matA_mel</i>	TAGTAGGCAAGCTCGGTGTTGA	CCTGTGCTATTTTAAAGCCTTGTTCT	MLSB	efflux
<i>mdet1</i>	ATACAGCAGTGATATTGGTTAATTGT	TGCATAAGGTGAATGTTCCATGA	other/efflux	efflux
<i>mdtA</i>	CCTAACGGGCGTGACTTCA	TTCACCTGTTTCAAGGGTCAAA	MLSB	efflux
<i>mdtE_yhiU</i>	CGTCGGCGCACTCGTT	TCCAGACGTTGTACGGTAACCA	other/efflux	efflux
<i>mecA</i>	GGTTACGGACAAGGTGAAATACTGAT	TGTCTTTTAAATAAGTGAGGTGCGTTAATA	Beta Lactams	protection
<i>mefA</i>	CCGTAGCATTGGAACAGCTTTT	AAACGGAGTATAAGAGTGCTGCAA	MLSB	efflux
<i>mepA</i>	ATCGGTGCTCTTCGTTTAC	ATAAATAGGATCGAGCTGCTGGAT	other/efflux	efflux
<i>mexA</i>	AGGACAACGCTATGCAACGAA	CCGGAAGGGCCGAAAT	FCA	efflux
<i>mexD</i>	TTGCCACTGGCTTTCATGAG	CACTGCGGAGAACTGTCTGTAGA	FCA	efflux
<i>mexE</i>	GGTCAGCACCGACAAGGTCTAC	AGCTCGACGTAATTGAGGAACAC	FCA	efflux
<i>mexF</i>	CCGCGAGAAGGCCAAGA	TTGAGTTCGGCGGTGATGA	FCA	efflux
<i>mphA-01</i>	CTGACGCGCTCCGTGTT	GGTGGTGCATGGCGATCT	MLSB	deactivate
<i>mphA-02</i>	TGATGACCCTGCCATCGA	TTCGCGAGCCCCTCTTC	MLSB	deactivate
<i>mphB</i>	CGCAGCGCTTGATCTTGAG	TACTGCATCCATACGCTGCTT	MLSB	deactivate

<i>mphC</i>	CGTTTGAAGTACCGAATTGGAAA	GCTGCGGGTTTGCCTGTA	MLSB	deactivate
<i>msrA-01</i>	CTGCTAACACAAGTACGATTCCAAAT	TCAAGTAAAGTTGTCTTACCTACACCATT	MLSB	efflux
<i>msrC-01</i>	TCAGACCGGATCGGTTGTC	CCTATTTTTTGGAGTCTTCTCTCTAATGTT	MLSB	efflux
<i>mtrC-01</i>	GGACGGGAAGATGGTCCAA	CGTAGCGTTCCGGTTCGAT	other/efflux	efflux
<i>mtrC-02</i>	CGGAGTCCATCGACCATTTG	ATCGTCGGCAAGGAGAATCA	other/efflux	efflux
<i>mtrD-02</i>	GGTCGGCACGCTCTTGTC	TGAAGAATTTGCGCACCCTAC	other/efflux	efflux
<i>mtrD-03</i>	CCGCCAAGCCGATATAGACA	GGCCGGGTTGCCAAA	other/efflux	efflux
<i>ndm-1</i>	ATTAGCCGCTGCATTGAT	CATGTGCGAGATAGGAAGTG	Beta Lactams	unknown
<i>nimE</i>	CGATGTGTCGTTTTGGAAGGT	CCTGCACCATGATTCCTCAATA	other/efflux	unknown
<i>nisB</i>	GGGAGAGTTGCCGATGTTGTA	AGCCACTCGTTAAAGGGCAAT	other/efflux	unknown
<i>oleC</i>	CCCGGAGTCGATGTTCGA	GCCGAAGACGTACACGAACAG	MLSB	efflux
<i>oprD</i>	ATGAAGTGGAGCGCCATTG	GGCCACGGCGAACTGA	other/efflux	efflux
<i>oprJ</i>	ACGAGAGTGGCGTCGACAA	AAGGCGATCTCGTTGAGGAA	FCA	efflux
<i>pbp</i>	CCGGTGCCATTGGTTTAGA	AAAATAGCCGCCCAAGATT	Beta Lactams	protection
<i>pbp2x</i>	TTTCATAAGTATCTGGACATGGAAGAA	CCAAAGGAAACTTGCTTGAGATTAG	Beta Lactams	protection
<i>pbp5</i>	GGCGAACTTCTAATTAATCCTATCCA	CGCCGATGACATTCTTCTTATCTT	Beta Lactams	protection
<i>penA</i>	AGACGGTAACGTATAACTTTTTGAAAGA	GCGTGTAGCCGGCAATG	Beta Lactams	protection
<i>pikR1</i>	TCGACATGCGTGACGAGATT	CCGCGAATTAGGCCAGAA	MLSB	protection
<i>pikR2</i>	TCGTGGGCCAGGTGAAGA	TTCCCCTTGCCGGTGAA	MLSB	protection
<i>pmrA</i>	TTTGCAGTTTTTGTTCCTAATGC	GCAGAGCCTGATTTCTCCTTTG	FCA	efflux
<i>pncA</i>	GCAATCGAGGCGGTGTTT	TTGCCGCAGCCAATTCA	other/efflux	unknown
<i>putitive multidrug</i>	AATTTTGCCGATTATTGCTGAAA	GATTGTGTCATTCGTTTATCACCAA	other/efflux	efflux
<i>qac</i>	CAATAATAACCGAAATAATAGGGACAAGTT	AATAAGTGTTCTAGTGTGGCCATAG	other/efflux	efflux
<i>qacA</i>	TGGCAATAGGAGCTATGGTGTTT	AAGGTAACACTATTTTCCGGTCCAAATC	other/efflux	efflux
<i>qacA_qacB</i>	TTTAGGCAGCCTCGCTTCA	CCGAATCCAAATAAAACCCAATAA	other/efflux	efflux
<i>qacEdelta1-01</i>	TCGCAACATCCGCATTAATAA	ATGGATTTTCCAGAACAGAGAAAGAAA	other/efflux	efflux
<i>qacEdelta1-02</i>	CCCCTTCCGCCGTTGT	CGACCAGACTGCATAAGCAACA	other/efflux	efflux
<i>qacH-01</i>	GTGGCAGCTATCGCTTGGAT	CCAACGAACGCCACAA	other/efflux	efflux
<i>qacH-02</i>	CATCGTGCTTGTGGCAGCTA	TGAACGCCCAGAAGTCTAGTTTT	other/efflux	efflux
<i>qnrA</i>	AGGATTTCTCACGCCAGGATT	CCGCTTTCAATGAAACTGCAA	FCA	unknown
<i>rarD-02</i>	TGACGCATCGCGTGATCT	AAATTTTCTGTGGCGTCTGAATC	other/efflux	efflux

<i>sat4</i>	GAATGGGCAAAGCATAAAAACTTG	CCGATTTTGAACCACAATTATGATA	other/efflux	deactivate
<i>sdeB</i>	CACTACCGCTTCCGCACTTAA	TGAAAAACGGGAAAAAGTCCAT	other/efflux	efflux
<i>spcN-01</i>	AAAAGTTCGATGAAACACGCCTAT	TCCAGTGGTAGTCCCCGAATC	Aminoglycoside	deactivate
<i>spcN-02</i>	CAGAATCTTCCTGAAAAGTTTGATGAA	CGCAGACACGCCGAATC	Aminoglycoside	deactivate
<i>speA</i>	GCAAGAGGTATTTGCTCAACAAGA	CAGGGTCACCCCTATAAAGAAAA	other/efflux	unknown
<i>str</i>	AATGAGTTTTGGAGTGTCTCAACGTA	AATCAAACCCCTATTAAGCCAAT	Aminoglycoside	deactivate
<i>strA</i>	CCGGTGGCATTGAGAAAAA	GTGGCTCAACCTGCGAAAAAG	Aminoglycoside	deactivate
<i>strB</i>	GCTCGGTCGTGAGAACAATCT	CAATTCGGTCGCCTGGTAGT	Aminoglycoside	deactivate
<i>sul1</i>	CAGCGCTATGCGCTCAAG	ATCCCCTGCGCTGAGT	Sulfonamide	protection
<i>sul2</i>	TCATCTGCCAACTCGTCGTGA	GTCAAAGAACGCCGCAATGT	Sulfonamide	protection
<i>sulA-foIP-01</i>	CAGGCTCGTAAATTGATAGCAGAAG	CTTTCCTTGCGAATCGCTTT	Sulfonamide	protection
<i>sulA-foIP-03</i>	GCGATTGCAAGGAAAGTGA	CACATGGGCCATTTTTTCATC	Sulfonamide	protection
<i>tet(32)</i>	CCATTACTTCGACAACGGTAGA	CAATCTCTGTGAGGGCATTAAACA	Tetracycline	protection
<i>tet(34)</i>	CTTAGCGCAAACAGCAATCAGT	CGGTGATACAGCGCGTAAACT	Tetracycline	unknown
<i>tet(35)</i>	ACCCCATGACGTACCTGTAGAGA	CAACCCACACTGGCTACCAGTT	Tetracycline	unknown
<i>tet(36)-01</i>	AGAATACTCAGCAGAGGTCAGTTCCT	TGGTAGGTCGATAACCCGAAAAT	Tetracycline	protection
<i>tet(36)-02</i>	TGCAGGAAAGACCTCCATTACAG	CTTTGTCCACACTTCCACGTACTATG	Tetracycline	protection
<i>tet(37)</i>	GAGAACGTTGAAAAGGTGGTGAA	AACCAAGCCTGGATCAGTCTCA	Tetracycline	unknown
<i>tetA-01</i>	GCTGTTTGTCTGCCGAAA	GGTTAAGTTCCTTGAACGCAAAC	Tetracycline	efflux
<i>tetA-02</i>	CTCACCAGCCTGACCTCGAT	CACGTTGTTATAGAAGCCGCATAG	Tetracycline	efflux
<i>tetB-01</i>	AGTGCGCTTTGGATGCTGTA	AGCCCCAGTAGCTCCTGTGA	Tetracycline	efflux
<i>tetB-02</i>	GCCCAGTGCTGTTGTTGTCAT	TGAAAGCAAACGGCCTAAATACA	Tetracycline	efflux
<i>tetC-01</i>	CATATCGCAATACATGCGAAAAA	AAAGCCGCGGTAAATAGCAA	Tetracycline	efflux
<i>tetC-02</i>	ACTGGTAAGGTAAACGCCATTGTC	ATGCATAAACCCAGCCATTGAGTAAG	Tetracycline	efflux
<i>tetD-01</i>	TGCCGCGTTTGATTACACA	CACCAGTGATCCCGGAGATAA	Tetracycline	efflux
<i>tetD-02</i>	TGTCATCGCGCTGGTGATT	CATCCGCTTCCGGGAGAT	Tetracycline	efflux
<i>tetE</i>	TTGGCGCTGTATGCAATGAT	CGACGACCTATGCGATCTGA	Tetracycline	efflux
<i>tetG-01</i>	TCAACCATTGCCGATTGCGA	TGGCCCGGCAATCATG	Tetracycline	efflux
<i>tetG-02</i>	CATCAGCGCCGGTCTTATG	CCCCATGTAGCCGAACCA	Tetracycline	efflux
<i>tetH</i>	TTTGGGTCATCTTACCAGCATTA	TTGCGCATTATCATCGACAGA	Tetracycline	efflux
<i>tetJ</i>	GGGTGCCGCATTAGATTACCT	TCGTCCAATGTAGAGCATCCATA	Tetracycline	efflux

<i>tetK</i>	CAGCAGTCATTGGAAAATTATCTGATTATA	CCTTGTACTAACCTACCAAAAATCAAATA	Tetracycline	efflux
<i>tetL-01</i>	AGCCCCGATTTATCAAGGAATTG	CAAATGCTTTCCCCCTGTTCT	Tetracycline	efflux
<i>tetL-02</i>	ATGGTTGTAGTTGCGCGCTATAT	ATCGCTGGACCGACTCCTT	Tetracycline	efflux
<i>tetM-01</i>	CATCATAGACACGCCAGGACATAT	CGCCATCTTTTGCAGAAATCA	Tetracycline	protection
<i>tetM-02</i>	TAATATTGGAGTTTTAGCTCATGTTGATG	CCTCTCTGACGTTCTAAAAGCGTATTAT	Tetracycline	protection
<i>tetO-01</i>	ATGTGGATACTACAACGCATGAGATT	TGCCTCCACATGATATTTTTCT	Tetracycline	protection
<i>tetPA</i>	AGTTGCAGATGTGTATAGTCGTAAACTATCTATT	TGCTACAAGTACGAAAACAAAAGTAGAA	Tetracycline	protection
<i>tetPB-01</i>	ACACCTGGACACGCTGATTTT	ACCGTCTAGAACGCGGAATG	Tetracycline	efflux
<i>tetPB-02</i>	TGATACACCTGGACACGCTGAT	CGTCCAAAACGCGGAATG	Tetracycline	protection
<i>tetPB-03</i>	TGGGCGACAGTAGGCTTAGAA	TGACCCTACTGAAACATTAGAAATATACCT	Tetracycline	protection
<i>tetPB-04</i>	AGTGGTGCAAATACTGAAAAAGTTGT	TTTGTTCCTTCGTTTTGGACAGA	Tetracycline	protection
<i>tetPB-05</i>	CTGAAGTGGAGCGATCATTCC	CCCTCAACGGCAGAAAATAACTAA	Tetracycline	protection
<i>tetQ</i>	CGCCTCAGAAGTAAGTTCATACACTAAG	TCGTTTCATGCGGATATTATCAGAAT	Tetracycline	protection
<i>tetR-02</i>	CGCGATAGACGCCCTTCGA	TCCTGACAACGAGCCTCCTT	Tetracycline	efflux
<i>tetR-03</i>	CGCGATGGAGCAAAAAGTACAT	AGTGAAAAACCTTGTTGGCATAAAA	Tetracycline	efflux
<i>tetS</i>	TTAAGGACAACTTTCTGACGACATC	TGTCTCCATTGTTCTGGTTCA	Tetracycline	protection
<i>tetT</i>	CCATATAGAGGTTCCACCAAATCC	TGACCCTATTGGTAGTGTTCTATTG	Tetracycline	protection
<i>tetU-01</i>	GTGGCAAAGCAACGGATTG	TGCGGGCTTGCAAACTATC	Tetracycline	unknown
<i>tetV</i>	GCGGGAACGACGATGTATATC	CCGCTATCTCACGACCATGAT	Tetracycline	efflux
<i>tetX</i>	AAATTTGTTACCGACACGGAAGTT	CATAGCTGAAAAAATCCAGGACAGTT	Tetracycline	unknown
<i>tnpA-01</i>	CATCATCGGACGGACAGAATT	GTCGGAGATGTGGGTGTAGAAAGT	IS21 Group	transposase
<i>tnpA-02</i>	GGGCGGGTCGATTGAAA	GTGGGCGGGATCTGCTT	IS4 Group	transposase
<i>tnpA-03</i>	AATTGATGCGGACGGCTTAA	TCACCAAAGTGTATGGAGTCGTT	IS6 Group	transposase
<i>tnpA-04</i>	CCGATCACGGAAAAGCTCAAG	GGCTCGCATGACTTCGAATC	IS6 Group	transposase
<i>tnpA-05</i>	GCCGCACTGTGATTTTTATC	GCGGGATCTGCCACTTCTT	IS6 Group	transposase
<i>tnpA-07</i>	GAAACCGATGCTACAATATCCAATTT	CAGCACCGTTTTGCAGTGTAAG	ISEcp1B	transposase
<i>tolC-01</i>	GGCCGAGAACCCTGATGCA	AGACTTACGCAATTCCGGGTTA	other/efflux	efflux
<i>tolC-02</i>	CAGGCAGAGAACCCTGATGCA	CGCAATTCCGGGTTGCT	other/efflux	efflux
<i>tolC-03</i>	GCCAGGCAGAGAACCCTGATG	CGCAATTCCGGGTTGCT	other/efflux	efflux
<i>Tp614</i>	GGAAATCAACGGCATCCAGTT	CATCCATGCGCTTTTGTCTCT	Tp614	transposase
<i>ttgA</i>	ACGCCAATGCCAAACGATT	GTCACGGCGCAGCTTGA	other/efflux	efflux

<i>ttgB</i>	TCGCCCTGGATGTACACCT	ACCATTGCCGACATCAACAAC	other/efflux	efflux
<i>vanA</i>	AAAAGGCTCTGAAAACGCAGTTAT	CGGCCGTTATCTTGTA AAAACAT	Vancomycin	protection
<i>vanB-01</i>	TTGTCGGCGAAGTGGATCA	AGCCTTTTTCCGGCTCGTT	Vancomycin	protection
<i>vanB-02</i>	CCGGTCGAGGAACGAAATC	TCCTCCTGCAAAAAAAGATCAAC	Vancomycin	protection
<i>vanC-01</i>	ACAGGGATTGGCTATGAACCAT	TGACTGGCGATGATTTGACTATG	Vancomycin	protection
<i>vanC-03</i>	AAATCAATACTATGCCGGGCTTT	CCGACCGCTGCCATCA	Vancomycin	protection
<i>vanC1</i>	AGGCGATAGCGGGTATTGAA	CAATCGTCAATTGCTCATTTCC	Vancomycin	protection
<i>vanC2_vanC3</i>	TTTGACTGTCGGTGCTTGTGA	TCAATCGTTTCAGGCAATGG	Vancomycin	protection
<i>vanG</i>	ATTTGAATTGGCAGGTATACAGGTTA	TGATTTGTCTTTGTCCATACATAATGC	Vancomycin	protection
<i>vanHB</i>	GAGGTTTCCGAGGCGACAA	CTCTCGGCGGCAGTCGTAT	Vancomycin	protection
<i>vanHD</i>	GTGGCCGATTATACCGTCATG	CGCAGGTCATTGAGGCAAT	Vancomycin	protection
<i>vanRA-01</i>	CCCTTACTCCCACCGAGTTTT	TTCGTGCCCCATATCTCAT	Vancomycin	protection
<i>vanRA-02</i>	CCACTCCGGCCTTGTGATT	GCTAACACATTCCCCTTGTTTT	Vancomycin	protection
<i>vanRB</i>	GCCCTGTGCGATGACGAA	TTACATAGTCGTCTGCCTCTGCAT	Vancomycin	protection
<i>vanRC</i>	TGCGGGAAAACTGAACGA	CCCCCATAACGGTTTTGATTA	Vancomycin	protection
<i>vanRC4</i>	AGTGCTTTGGCTTATCTCGAAAA	TCCGGCAGCATCACATCTAA	Vancomycin	protection
<i>vanRD</i>	TTATAATGGCAAGGATGCACTAAAGT	CGTCTACATCCGGAAGCATGA	Vancomycin	protection
<i>vanSA</i>	CGCGTCATGCTTTCAAATTC	TCCGCAGAAAGCTCAATTTGTT	Vancomycin	protection
<i>vanSB</i>	GCGCGCAAATGACAAC	TTTGCCATTTTATTCGCACTGT	Vancomycin	protection
<i>vanSC-02</i>	GCCATCAGCGAGTCTGATGA	CAGCTGGGATCGTTTTTCCTT	Vancomycin	protection
<i>vanSE</i>	TGGCCGAAGAAGCAGGAA	CAATAACTCGTCAAAGGAGTTCTCA	Vancomycin	protection
<i>vanTC-01</i>	CACACGCATTTTTTCCCATCTAG	CAGCCAACAGATCATCAAAACAA	Vancomycin	protection
<i>vanTC-02</i>	ACAGTTGCCGCTGGTGAAG	CGTGGCTGGTCGATCAAAA	Vancomycin	protection
<i>vanTE</i>	GTGGTGCCAAGGAAGTTGCT	CGTAGCCACCGCAAAAAAAT	Vancomycin	protection
<i>vanTG</i>	CGTGTAGCCGTTCCGTTCTT	CGGCATTACAGGTATATCTGGAAA	Vancomycin	protection
<i>vanWB</i>	CGGACAAAGATACCCCTATAAAG	AAATAGTAAATTGCTCATCTGGCACAT	Vancomycin	protection
<i>vanWG</i>	ACATTTTCATTTTGGCAGCTTGTAC	CCGCCATAAGAGCCTACAATCT	Vancomycin	protection
<i>vanXA</i>	CGCTAAATATGCCACTTGGGATA	TCAAAGCGATTGAGCCAAT	Vancomycin	protection
<i>vanXB</i>	AGGCACAAAATCGAAGATGCTT	GGGTATGGCTCATCAATCAACTT	Vancomycin	protection
<i>vanXD</i>	TAAACCGTGTTATGGGAACGAA	GCGATAGCCGTCCATAAGA	Vancomycin	protection
<i>vanYB</i>	GGCTAAAGCGGAAGCAGAAA	GATATCCACAGCAAGACCAAGCT	Vancomycin	protection

<i>vanYD-01</i>	AAGGCGATACCCTGACTGTCA	ATTGCCGGACGGAAGCA	Vancomycin	protection
<i>vanYD-02</i>	CAAACGGAAGAGAGGTCACTTACA	CGGACGGTAATAGGGACTGTTC	Vancomycin	protection
<i>vatB-01</i>	GGAAAAAGCAACTCCATCTCTTGA	TCCTGGCATAACAGTAACATTCTGA	MLSB	deactivate
<i>vatB-02</i>	TTGGGAAAAAGCAACTCCATCT	CAATCCACACATCATTTCACA	MLSB	deactivate
<i>vatC-01</i>	CGGAAATTGGGAACGATGTT	GCAATAATAGCCCCGTTTCTA	MLSB	deactivate
<i>vatC-02</i>	CGATGTTTGGATTGGACGAGAT	GCTGCAATAATAGCCCCGTTT	MLSB	deactivate
<i>vatE-01</i>	GGTGCCATTATCGGAGCAAAT	TTGGATTGCCACCGACAAT	MLSB	deactivate
<i>vatE-02</i>	GACCGTCCTACCAGGCGTAA	TTGGATTGCCACCGACAATT	MLSB	deactivate
<i>vgaA-01</i>	CGAGTATTGTGGAAAGCAGCTAGTT	CCCGTACCGTTAGAGCCGATA	MLSB	efflux
<i>vgaA-02</i>	GACGGGTATTGTGGAAGCAA	TTTCTGTACCATTAGATCCGATAATT	MLSB	efflux
<i>vgb-01</i>	AGGGAGGGTATCCATGCAGAT	ACCAAATGCGCCCCGTTT	MLSB	deactivate
<i>vgbB-01</i>	CAGCCGGATTCTGGTCCCT	TACGATCTCCATTCAATTGGGTAAA	MLSB	efflux
<i>vgbB-02</i>	ATACGAGCTGCCTAATAAAGGATCTT	TGTGAACCACAGGGCATTATCA	MLSB	deactivate
<i>yceE_mdtG-01</i>	TGGCACAAAATATCTGGCAGTT	TTGTGTGGCGATAAGAGCATTAG	other/efflux	efflux
<i>yceE_mdtG-02</i>	TTATCTGTTTTCTGCTCACCTTCTTTT	GCGTGGTGACAAACAGGCTTA	other/efflux	efflux
<i>yceL_mdtH-01</i>	TCGGGATGGTGGGCAAT	CGATAACCGAGCCGATGTAGA	other/efflux	efflux
<i>yceL_mdtH-02</i>	CGCGTGAAACCTTAAGTGCTT	AGACGGCTAAACCCCATATAGCT	other/efflux	efflux
<i>yceL_mdtH-03</i>	CTGCCGTTAAATGGATGTATGC	ACTCCAGCGGGCGATAGG	other/efflux	efflux
<i>yidY_mdtL-01</i>	GCAGTTGCATATCGCCTTCTC	CTTCCCGGCAAACAGCAT	FCA	efflux
<i>yidY_mdtL-02</i>	TGCTGATCGGGATTCTGATTG	CAGGCGCGACGAACATAAT	FCA	efflux

FCA (fluoroquinolone, quinolone, florfenicol, chloramphenicol and amphenicol), MLSB (Macrolide-Lincosamide-Streptogramin B).

Appendix – Chapter 4

Table A4.1 The main physico-chemical characteristics of the pond waters (mean values \pm STD) throughout the study.

Parameters	Oct-2017	Nov-2017	Dec-2017	Jan-2018
Temperature ($^{\circ}$ C)	9.2 \pm 0.5	7.9 \pm 1.0	5.4 \pm 0.7	6.3 \pm 0.4
Conductivity (μ S/cm)	1047 \pm 5	1060 \pm 10	1054 \pm 6	1035 \pm 5
pH	8.07 \pm 0.02	8.05 \pm 0.08	8.15 \pm 0.05	8.30 \pm 0.05
Dissolved Oxygen (mg/L)	5.15 \pm 0.71	7.73 \pm 1.02	8.53 \pm 0.66	7.88 \pm 0.24
Turbidity (NTU)	0.57 \pm 0.08	0.62 \pm 0.05	0.51 \pm 0.10	0.46 \pm 0.17
Absorbance (254 nm)	0.067 \pm 0.015	0.095 \pm 0.022	0.132 \pm 0.010	0.087 \pm 0.008
Nitrite (mg/L)	n.a.	n.a.	n.a.	n.a.
Nitrate (mg/L)	0.147 \pm 0.081	0.402 \pm 0.121	0.709 \pm 0.229	0.987 \pm 0.077
Phosphate (mg/L)	0.216 \pm 0.116	0.389 \pm 0.148	0.324 \pm 0.177	n.a.
Total coliforms (MNP/100 mL)	22400 \pm 1800	19700 \pm 1900	20800 \pm 7400	13500 \pm 1000
<i>E.coli</i> (MNP/100 mL)	6800 \pm 2100	5400 \pm 2000	3600 \pm 2100	4000 \pm 550
Dissolved organic carbon (mg/L)	3.84 \pm 0.17	4.24 \pm 0.52	3.70 \pm 0.28	3.51 \pm 0.19

Table A4.2 The pH values of the influent and effluent samples.

Week	Influent 1	Influent 2	Effluent 1	Effluent 2	Effluent 3	Effluent 4	Effluent 5	Effluent 6	Effluent 7	Effluent 8
			SB	SB	GB	GB	GSB	GSB	ASB	ASB
1	8.04	8.02	8.04	8.17	7.85	7.84	8.11	8.05	8.00	8.02
2	8.1	8.13	8.05	8.09	7.94	7.89	7.99	8.11	8.09	8.06
3	8.12	8.15	7.97	8.02	7.92	7.92	8.00	8.02	8.00	8.09
4	8.11	8.19	8.18	8.13	8.10	8.07	8.29	8.12	8.06	7.96
5	7.91	7.85	7.88	7.89	8.02	8.07	8.01	8.00	7.95	8.01
6	8.03	8.02	8.13	8.21	8.31	8.09	8.22	8.19	8.22	8.23
7	8.15	8.135	8.17	8.18	8.26	8.22	8.25	8.23	8.16	8.18
8	8.35	8.34	8.33	8.36	8.38	8.38	8.42	8.45	8.34	8.31
9	8.21	8.13	8.29	8.29	8.43	8.24	8.27	8.33	8.24	8.25
10	8.23	8.23	8.16	8.05	8.18	8.16	8.15	8.17	8.10	8.17
11	8.48	8.46	8.48	8.47	8.44	8.50	8.44	8.45	8.42	8.47
12	8.20	8.20	8.24	8.24	8.13	8.25	8.21	8.17	8.17	8.12

SB: sand biofilter; GB: GAC biofilter; GSB: GAC sandwich biofilter; ASB: anthracite-sand biofilter.

Table A4.3 The conductivity of the influent and effluent samples.

Week	Influent 1	Influent 2	Effluent 1	Effluent 2	Effluent 3	Effluent 4	Effluent 5	Effluent 6	Effluent 7	Effluent 8
			SB	SB	GB	GB	GSB	GSB	ASB	ASB
1	1050	1047	1042	1034	1036	1035	1056	1044	1043	1048
2	1050	1042	1032	1030	1041	1037	1041	1045	1041	1046
3	1073	1067	1069	1071	1021	1012	1082	1086	1081	1067
4	1070	1071	1062	1062	1066	1070	1076	1074	1067	1066
5	1035	1039	1031	1038	1041	1044	1039	1039	1036	1043
6	1058	1055	1062	1060	1074	1069	1062	1053	1058	1068
7	1038	1029	1021	1031	1053	1059	1052	1037	1038	1048
8	1060	1060	1055	1033	1062	1063	1058	1059	1062	1067
9	1067	1072	1067	1070	1066	1069	1072	1073	1073	1071
10	1036	1034	1034	1046	1070	1055	1041	1074	1064	1064
11	1068	1072	1066	1052	1045	1043	1044	1030	1048	1044
12	1001	1001	1002	997	1000	1009	994	995	1000	1008

SB: sand biofilter; GB: GAC biofilter; GSB: GAC sandwich biofilter; ASB: anthracite-sand biofilter.

Table A4.4 Dissolved oxygen (DO) levels in the influent and effluent samples.

Week	Influent 1	Influent 2	Effluent 1	Effluent 2	Effluent 3	Effluent 4	Effluent 5	Effluent 6	Effluent 7	Effluent 8
			SB	SB	GB	GB	GSB	GSB	ASB	ASB
1	5.05	5.05	4.83	5.04	4.80	4.95	5.03	5.07	5.07	4.99
2	6.62	6.77	6.07	6.19	6.10	6.21	6.32	6.43	6.46	6.44
3	8.18	8.45	7.45	7.46	7.49	7.60	7.72	7.91	7.98	8.01
4	7.41	7.58	6.91	7.04	7.00	7.06	7.19	7.29	7.32	7.30
5	7.18	7.60	7.17	7.27	6.96	7.16	7.70	7.80	7.56	7.58
6	8.30	8.80	7.01	7.17	7.22	7.40	7.65	7.88	8.08	8.23
7	8.94	8.89	8.33	8.98	9.09	8.64	8.59	8.64	8.99	8.59
8	8.48	8.68	8.36	8.34	8.41	8.45	8.50	8.45	8.38	8.50
9	8.05	8.09	7.89	7.74	7.76	7.80	7.79	7.94	7.87	7.79
10	6.99	7.49	6.49	6.70	6.90	6.96	7.08	7.09	7.08	7.04
11	8.65	8.46	8.32	8.53	8.31	8.21	8.38	8.46	8.48	8.46
12	7.86	7.86	8.08	8.27	8.37	8.29	8.04	8.27	8.29	8.39

SB: sand biofilter; GB: GAC biofilter; GSB: GAC sandwich biofilter; ASB: anthracite-sand biofilter.

Table A4.5 Turbidity (NTU) of the influent and effluent samples.

Week	Influent 1	Influent 2	Effluent 1	Effluent 2	Effluent 3	Effluent 4	Effluent 5	Effluent 6	Effluent 7	Effluent 8
			SB	SB	GB	GB	GSB	GSB	ASB	ASB
1	0.622	0.604	0.139	0.172	0.146	0.153	0.179	0.191	0.228	0.239
2	0.513	0.441	0.133	0.245	0.098	0.105	0.128	0.157	0.195	0.222
3	0.774	0.726	0.32	0.272	0.397	0.41	0.217	0.23	0.465	0.376
4	0.511	0.588	0.245	0.260	0.194	0.229	0.183	0.201	0.600	0.427
5	0.693	0.723	0.170	0.153	0.161	0.150	0.161	0.191	0.162	0.173
6	0.673	0.673	0.492	0.248	0.214	0.256	0.212	0.167	0.232	0.252
7	0.653	0.657	0.182	0.159	0.174	0.229	0.158	0.234	0.258	0.178
8	0.534	0.421	0.309	0.274	0.238	0.297	0.210	0.216	0.242	0.324
9	0.205	0.229	0.177	0.142	0.124	0.102	0.091	0.092	0.110	0.136
10	0.215	0.213	0.121	0.094	0.079	0.082	0.070	0.064	0.120	0.136
11	0.446	0.420	0.097	0.104	0.142	0.134	0.072	0.084	0.245	0.114
12	0.989	0.989	0.408	0.390	0.486	0.476	0.414	0.406	0.560	0.448

SB: sand biofilter; GB: GAC biofilter; GSB: GAC sandwich biofilter; ASB: anthracite-sand biofilter.

Table A4.6 The concentration of nitrate (mg/L) in the influent and effluent samples.

Week	Influent 1	Influent 2	Effluent 1	Effluent 2	Effluent 3	Effluent 4	Effluent 5	Effluent 6	Effluent 7	Effluent 8
			SB	SB	GB	GB	GSB	GSB	ASB	ASB
1	0.082	0.114	0.198	0.224	n.a.	n.a.	n.a.	n.a.	0.284	0.355
2	0.060	0.092	0.138	0.250	0.117	0.094	0.165	n.a.	n.a.	0.020
3	0.129	0.189	0.271	n.a.	n.a.	n.a.	n.a.	n.a.	0.490	0.577
4	0.249	0.193	0.526	0.543	n.a.	0.082	0.115	0.110	0.283	0.283
5	0.899	0.632	0.816	0.629	0.222	0.247	0.481	n.a.	0.884	0.382
6	0.808	0.774	0.809	1.003	0.086	0.074	0.426	0.301	1.259	0.840
7	0.244	0.244	0.132	n.a.	0.323	n.a.	0.158	n.a.	n.a.	0.078
8	0.535	0.525	1.069	0.952	0.191	0.079	0.606	0.138	0.728	0.824
9	0.513	0.405	0.601	0.915	0.404	0.425	0.273	0.140	0.259	0.521
10	1.279	1.463	2.827	3.095	1.397	2.682	1.692	1.398	1.551	1.361
11	1.656	1.490	1.302	1.413	0.599	0.541	0.429	0.179	0.851	1.044
12	0.591	0.213	0.353	0.232	0.205	0.541	n.a.	0.049	0.079	0.109

SB: sand biofilter; GB: GAC biofilter; GSB: GAC sandwich biofilter; ASB: anthracite-sand biofilter.

Table A4.7 The concentration of nitrite (mg/L) in the influent and effluent samples.

Week	Influent 1	Influent 2	Effluent 1	Effluent 2	Effluent 3	Effluent 4	Effluent 5	Effluent 6	Effluent 7	Effluent 8
			SB	SB	GB	GB	GSB	GSB	ASB	ASB
1	n.a.									
2	n.a.									
3	n.a.	0.1039	0.1065							
4	n.a.									
5	n.a.	0.0641	0.1073							
6	n.a.	n.a.	n.a.	n.a.	0.1585	n.a.	0.1073	n.a.	0.0493	n.a.
7	n.a.									
8	n.a.									
9	n.a.	n.a.	n.a.	n.a.	n.a.	0.1837	n.a.	n.a.	n.a.	n.a.
10	n.a.									
11	n.a.									
12	n.a.									

SB: sand biofilter; GB: GAC biofilter; GSB: GAC sandwich biofilter; ASB: anthracite-sand biofilter.

Table A4.8 The concentration of phosphate- PO_4^{3-} (mg/L) in the influent and effluent samples.

Week	Influent 1	Influent 2	Effluent 1	Effluent 2	Effluent 3	Effluent 4	Effluent 5	Effluent 6	Effluent 7	Effluent 8
			SB	SB	GB	GB	GSB	GSB	ASB	ASB
1	0.266	0.265	0.294	0.343	0.340	0.280	0.310	0.277	0.235	0.313
2	0.229	0.204	0.245	0.267	0.288	0.213	0.282	0.227	0.218	0.228
3	0.303	0.327	0.343	0.419	0.392	0.348	0.338	0.327	0.252	0.433
4	0.460	0.466	0.468	0.439	0.394	0.398	0.484	0.463	0.434	0.437
5	0.422	0.624	0.407	0.305	0.490	0.210	0.709	0.572	0.562	0.601
6	0.268	0.262	0.661	0.592	0.700	0.586	0.576	0.512	0.504	0.564
7	0.212	0.160	0.278	0.195	0.267	0.381	0.270	n.a.	0.236	0.209
8	n.a.	n.a.	0.122	n.a.	0.140	0.143	n.a.	n.a.	n.a.	n.a.
9	n.a.	n.a.	n.a.	n.a.	0.399	0.454	n.a.	0.482	n.a.	0.171
10	n.a.	n.a.	0.347	n.a.	0.167	n.a.	n.a.	n.a.	0.368	n.a.
11	n.a.	n.a.	0.548	n.a.	0.238	0.197	n.a.	n.a.	n.a.	n.a.
12	n.a.	n.a.	n.a.	n.a.	0.283	0.197	0.132	0.160	0.126	0.125

SB: sand biofilter; GB: GAC biofilter; GSB: GAC sandwich biofilter; ASB: anthracite-sand biofilter.

Table A4.9 The removal of total coliform by the biofilters.

Week	Effluent 1	Effluent 2	Effluent 3	Effluent 4	Effluent 5	Effluent 6	Effluent 7	Effluent 8
	SB	SB	GB	GB	GSB	GSB	ASB	ASB
1	92%	95%	83%	73%	79%	81%	92%	79%
2	85%	81%	96%	88%	97%	96%	95%	95%
3	89%	90%	96%	95%	96%	95%	95%	94%
4	99%	99%	98%	98%	99%	99%	99%	98%
5	98%	97%	100%	99%	99%	98%	98%	94%
6	98%	98%	97%	96%	99%	97%	95%	96%
7	95%	94%	97%	96%	99%	99%	94%	92%
8	99%	98%	100%	98%	99%	100%	93%	94%
9	93%	95%	97%	96%	99%	99%	99%	99%
10	96%	98%	98%	97%	94%	98%	95%	96%
11	95%	93%	100%	89%	99%	100%	100%	98%
12	36%	-28%	85%	97%	40%	58%	-35%	-69%

SB: sand biofilter; GB: GAC biofilter; GSB: GAC sandwich biofilter; ASB: anthracite-sand biofilter.

Table A4.10 The removal of *E. coli* by the biofilters.

Week	Effluent 1	Effluent 2	Effluent 3	Effluent 4	Effluent 5	Effluent 6	Effluent 7	Effluent 8
	SB	SB	GB	GB	GSB	GSB	ASB	ASB
1	93%	91%	88%	88%	90%	86%	91%	89%
2	100%	100%	100%	99%	100%	98%	98%	98%
3	99%	99%	98%	100%	100%	100%	98%	100%
4	99%	99%	100%	100%	100%	99%	100%	99%
5	100%	100%	100%	100%	100%	100%	100%	96%
6	98%	98%	100%	98%	99%	97%	95%	96%
7	98%	97%	99%	98%	100%	99%	98%	95%
8	99%	100%	100%	100%	100%	100%	100%	99%
9	100%	99%	98%	98%	100%	100%	99%	100%
10	98%	100%	99%	99%	98%	98%	98%	100%
11	97%	97%	100%	100%	99%	100%	100%	99%
12	37%	-27%	86%	97%	42%	62%	11%	-27%

SB: sand biofilter; GB: GAC biofilter; GSB: GAC sandwich biofilter; ASB: anthracite-sand biofilter.

Table A4.11 The main physico-chemical characteristics of the raw water from the River Thames (mean values \pm STD) throughout the study.

Parameters	Jun-2018	Jul-2018	Aug-2018	Sep-2018
Temperature ($^{\circ}$ C)	22.2 \pm 0.6	23.7 \pm 1.0	22.2 \pm 2.5	19.1 \pm 1.9
Conductivity (μ S/cm)	1747 \pm 321	2019 \pm 502	3700 \pm 1189	3175 \pm 1218
pH	8.50 \pm 0.03	8.26 \pm 0.25	8.11 \pm 0.19	8.11 \pm 0.09
Dissolved Oxygen (mg/L)	8.59 \pm 0.02	7.13 \pm 3.39	6.43 \pm 0.28	6.23 \pm 0.20
Turbidity (NTU)	8.01 \pm 0.71	12.36 \pm 9.61	19.03 \pm 7.88	17.01 \pm 4.24
Absorbance (254 nm)	0.193 \pm 0.020	0.222 \pm 0.091	0.586 \pm 0.152	0.216 \pm 0.029
COD (mg/L)	23 \pm 4	24 \pm 10	20 \pm 7	21 \pm 4
Nitrite (mg/L)	n.a.	n.a.	n.a.	n.a.
Nitrate (mg/L)	44.9 \pm 5.1	48.8 \pm 7.8	49.3 \pm 7.2	57.9 \pm 5.6
Phosphate (mg/L)	2.65 \pm 0.52	3.10 \pm 0.44	3.57 \pm 0.37	3.86 \pm 0.69
Total coliform (MNP/100 mL)	1.1 \times 10 ⁵ \pm 6.3 \times 10 ⁴	1.9 \times 10 ⁵ \pm 9.7 \times 10 ⁴	3.2 \times 10 ⁵ \pm 3.1 \times 10 ⁵	2.5 \times 10 ⁵ \pm 1.0 \times 10 ⁴
E coli (MNP/100 mL)	1.7 \times 10 ⁴ \pm 2.7 \times 10 ⁴	7.6 \times 10 ³ \pm 2.8 \times 10 ³	3.8 \times 10 ³ \pm 1.7 \times 10 ³	7.0 \times 10 ³ \pm 9.2 \times 10 ²
DOC (mg/L)	4.77 \pm 0.12	5.65 \pm 0.83	5.01 \pm 0.25	4.55 \pm 0.17

COD: chemical oxygen demand; DOC: dissolved organic carbon.

Table A4.12 Mean values of water quality parameters during the maturation stage.

Parameters	Influent	GSB-1	GSB-2	GSB-3	GSB-4	GSB-5	GSB-6	GSB-7	GSB-8
pH	7.99 ± 0.13	8.10 ± 0.07	8.17 ± 0.08	8.13 ± 0.12	8.15 ± 0.08	8.13 ± 0.08	8.18 ± 0.09	8.20 ± 0.07	8.16 ± 0.07
Conductivity (µS/cm)	978 ± 176	973 ± 197	971 ± 191	973 ± 193	974 ± 192	967 ± 191	972 ± 196	972 ± 191	971 ± 193
Turbidity (NTU)	0.75 ± 0.32	0.16 ± 0.03	0.27 ± 0.13	0.26 ± 0.14	0.36 ± 0.29	0.16 ± 0.02	0.34 ± 0.19	0.20 ± 0.02	0.35 ± 0.19
Absorbance (254 nm)	0.085 ± 0.004	0.010 ± 0.007	0.016 ± 0.003	0.014 ± 0.005	0.024 ± 0.010	0.011 ± 0.004	0.017 ± 0.003	0.011 ± 0.004	0.021 ± 0.007
COD (mg/L)	15 ± 2	2 ± 1	5 ± 1	4 ± 1	5 ± 2	3 ± 1	4 ± 2	3 ± 1	7 ± 2
DO (mg/L)	7.32 ± 0.44	6.30 ± 1.73	6.37 ± 1.62	7.15 ± 0.45	7.37 ± 0.61	6.41 ± 1.83	6.36 ± 1.81	6.75 ± 1.11	7.39 ± 0.64
Nitrite (mg/L)	9.54 ± 0.80	5.92 ± 2.08	5.62 ± 0.39	8.30 ± 2.36	8.76 ± 0.83	5.72 ± 2.26	6.03 ± 0.45	6.95 ± 1.15	8.12 ± 0.54
Nitrate (mg/L)	18.0 ± 3.9	26.6 ± 2.4	24.7 ± 2.6	22.8 ± 3.0	20.8 ± 2.8	27.5 ± 4.2	24.3 ± 1.5	23.6 ± 3.4	21.3 ± 2.7
Phosphate (mg/L)	3.96 ± 0.42	4.14 ± 0.53	3.95 ± 0.61	3.41 ± 0.74	3.91 ± 0.77	3.99 ± 0.50	4.07 ± 0.39	3.97 ± 0.41	3.98 ± 0.51
DOC (mg/L)	3.78 ± 0.15	0.79 ± 0.23	0.99 ± 0.12	0.97 ± 0.11	1.00 ± 0.15	0.87 ± 0.16	0.93 ± 0.10	0.86 ± 0.14	1.10 ± 0.25

COD: chemical oxygen demand; DOC: dissolved organic carbon; GSB: GAC sandwich biofilter. Results are presented as mean value ± STD (n = 8).

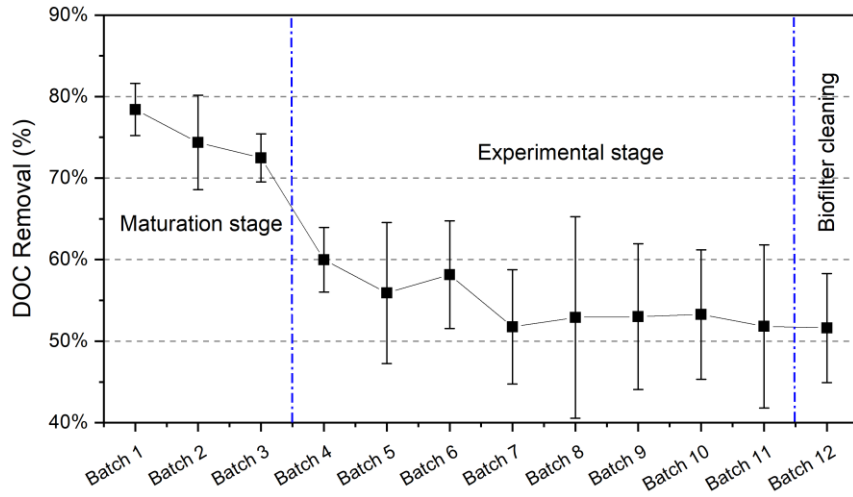


Figure A4.1 Temporal variation of dissolved organic carbon (DOC) removal. The error bars represent STD from the mean value of all biofilters ($n = 8$).

Appendix – Chapter 5

Biofiltration experiment 1

Table A5.1 Matrix effect percentage (%ME) for each antibiotic from different batch samples

Week	SMX	TMP	AMOX	OTC	CTM
5	52%	32%	90%	-2%	-121%
6	59%	1%	88%	36%	-132%
7	56%	-12%	88%	20%	-121%
8	59%	1%	61%	-34%	-174%
9	59%	35%	82%	-59%	-11%
10	59%	10%	89%	26%	-143%
11	51%	45%	92%	13%	-18%
12	58%	34%	91%	21%	-17%

*The matrix effect (%ME) was calculated by the ratio of the signal response of spiked post-extracted raw water samples to that of antibiotic in solvent. A 0% ME indicated no matrix effect; +%ME and -%ME indicated signal suppression and enhancement, respectively. SMX, sulfamethoxazole; TMP: trimethoprim; AMOX: amoxicillin; OTC: oxytetracycline; CTM: clarithromycin.

Table A5.2 Recoveries and the limit of detection (LOD) of the target antibiotics.

Antibiotics	Recovery		LOD
	Ave (%)	STD (n = 3)	ng/L
SMX	85.5	6.0	20
TMP	90.1	7.8	10
AMOX	29.2	10.5	150
OTC	66.7	6.6	40
CTM	115.9	3.9	10

SMX, sulfamethoxazole; TMP: trimethoprim; AMOX: amoxicillin;
OTC: oxytetracycline; CTM: clarithromycin.

Biofiltration experiment 2

Table A5.3 Occurrence of the target antibiotics (mean value \pm STD) in River Thames during the sampling period.

Antibiotics	July-2018	August-2018	September-2018
Trimethoprim	53.3 \pm 39.0	72.3 \pm 29.3	41.4 \pm 4.8
Clarithromycin	46.2 \pm 38.2	9.1 \pm 3.7	n.a.

Table A5.4 Recoveries and the limit of quantification (LOQ) of the target antibiotics.

Antibiotics	Recovery		LOQ
	Ave (%)	STD (n = 3)	ng/L
Sulfamethoxazole	78.0	13.0	15
Trimethoprim	105.8	10.2	10
Amoxicillin	31.4	10.8	200
Oxytetracycline	104.1	14.2	20
Clarithromycin	100.4	17.0	8

Table A5.5 Matrix effect percentage (%ME) for each antibiotic from different batch samples.

Batch	SMX	TMP	AMOX	OTC	CTM
1	65%	53%	88%	33%	-15%
2	62%	38%	79%	24%	-8%
3	47%	31%	85%	50%	-3%
4	38%	20%	82%	39%	6%
5	56%	42%	86%	42%	-9%
6	50%	29%	81%	31%	-1%
7	52%	36%	85%	36%	-9%
8	55%	34%	82%	37%	5%
9	53%	35%	84%	36%	-13%

*The matrix effect (%ME) was calculated by the ratio of the signal response of spiked post-extracted raw water samples to that of antibiotic in solvent. A 0% ME indicated no matrix effect; +%ME and -%ME indicated signal suppression and enhancement, respectively. SMX, sulfamethoxazole; TMP: trimethoprim; AMOX: amoxicillin; OTC: oxytetracycline; CTM: clarithromycin.

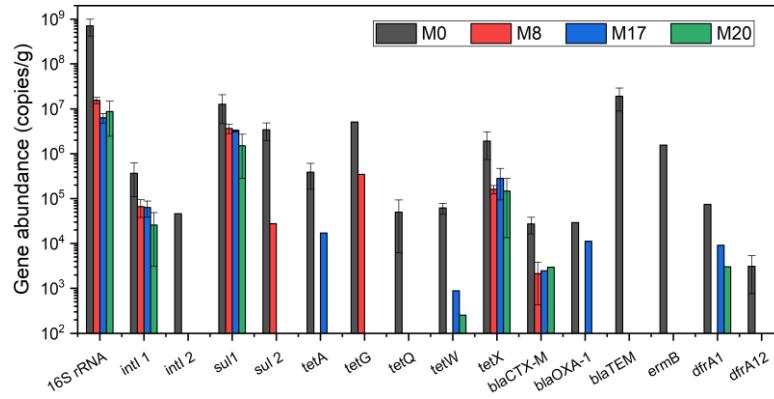
Appendix – Chapter 6

Table A6.1 DNA yield from media samples collected at 4-week and 11-week.

Biofilter	Sample	Position	Media	DNA yield (µg/g) 4-week	DNA yield (µg/g) 11-weeks
SB1	M0	surface	sand	6.355	4.235
	M8	upper	sand	1.727	2.085
	M17	middle	sand	1.365	1.088
	M20	lower	sand	1.394	1.247
SB2	M0	surface	sand	5.225	3.674
	M8	upper	sand	2.058	1.995
	M17	middle	sand	1.519	1.230
	M20	lower	sand	2.232	1.541
GB1	M0	surface	GAC	0.799	3.286
	M8	upper	GAC	0.141	0.215
	M17	middle	GAC	0.085	0.165
	M20	lower	GAC	0.098	0.188
GB2	M0	surface	GAC	0.916	1.663
	M8	upper	GAC	0.145	0.768
	M17	middle	GAC	0.123	0.548
	M20	lower	GAC	0.108	0.342
GSB1	M0	surface	sand	4.945	2.834
	M8	upper	sand	1.939	1.669
	M17	middle	GAC	0.084	0.175
	M20	lower	sand	3.136	1.187
GSB2	M0	surface	sand	4.840	3.060
	M8	upper	sand	1.481	1.631
	M17	middle	GAC	0.118	0.143
	M20	lower	sand	2.828	1.138
ASB1	M0	surface	anthracite	0.577	2.983
	M8	upper	anthracite	0.233	0.542
	M17	middle	anthracite	0.183	0.147
	M20	lower	sand	2.573	1.398
ASB2	M0	surface	anthracite	0.399	1.653
	M8	upper	anthracite	0.254	0.828
	M17	middle	anthracite	0.165	0.289
	M20	lower	sand	1.614	1.759

M0, M8, M17 and M20 refer to biofilm samples collected at different sampling sites (0, 8, 17, and 20cm).
SB: sand biofilter; GB: GAC biofilter; GSB: GAC sandwich biofilter; ASB: anthracite-sand dual biofilter.

4-week



11-week

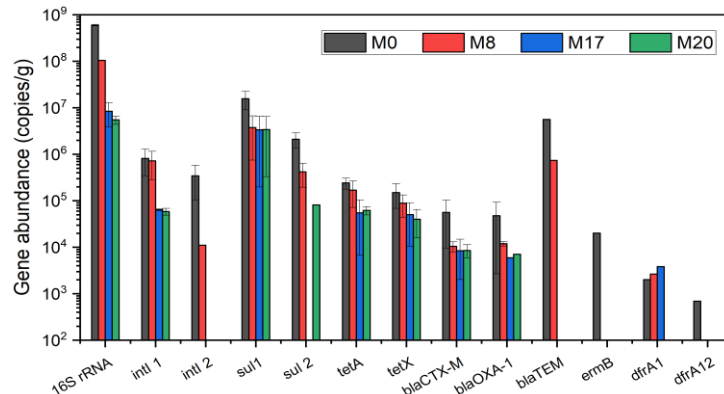
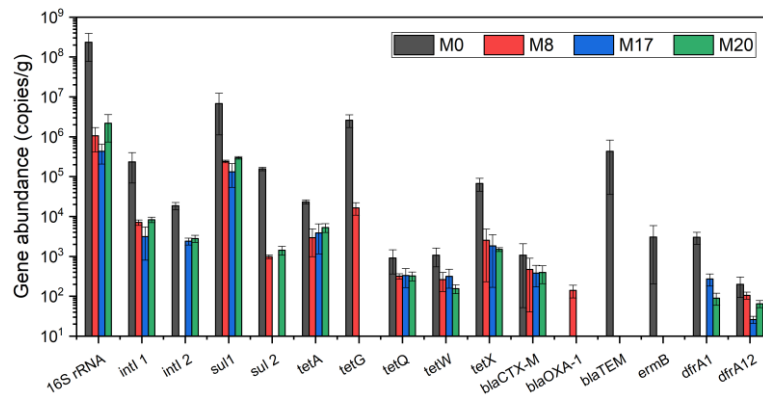


Figure A6.1 Absolute abundance of *16S rRNA*, ARGs and integron in sand biofilm samples collected at 4-week and 11-week. The error bars represent STD from the mean value of qPCR results ($n = 3$).

4-week



11-week

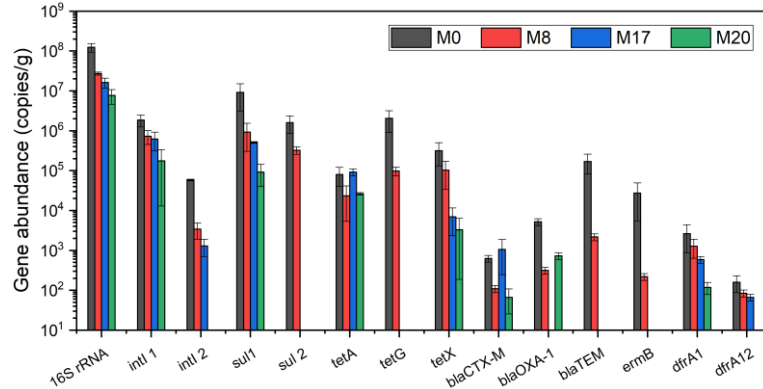
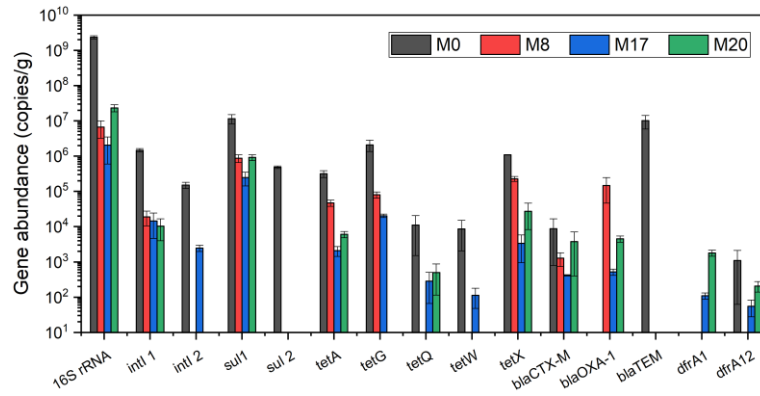


Figure A6.2 Absolute abundance of *16S rRNA*, ARGs and integron in GAC biofilm samples collected at 4-week and 11-week. The error bars represent STD from the mean value of qPCR results ($n = 3$).

4-week



11-week

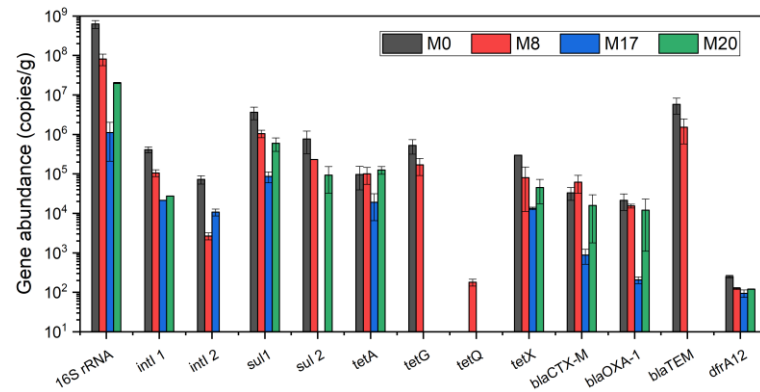
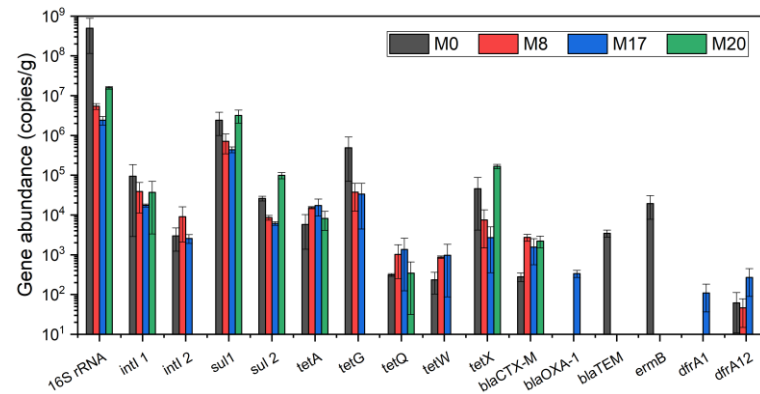


Figure A6.3 Absolute abundance of 16S rRNA, ARGs and integron in GAC sandwich biofilm samples collected at 4-week and 11-week. The error bars represent STD from the mean value of qPCR results (n = 3).

4-week



11-week

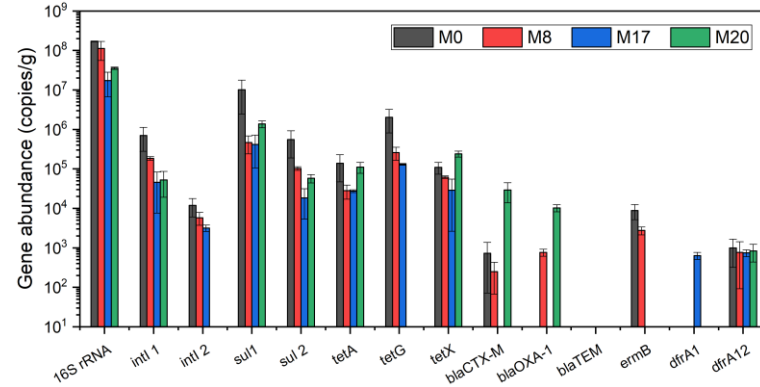


Figure A6.4 Absolute abundance of 16S rRNA, ARGs and integron in anthracite-sand biofilm samples collected at 4-week and 11-week. The error bars represent STD from the mean value of qPCR results (n = 3).

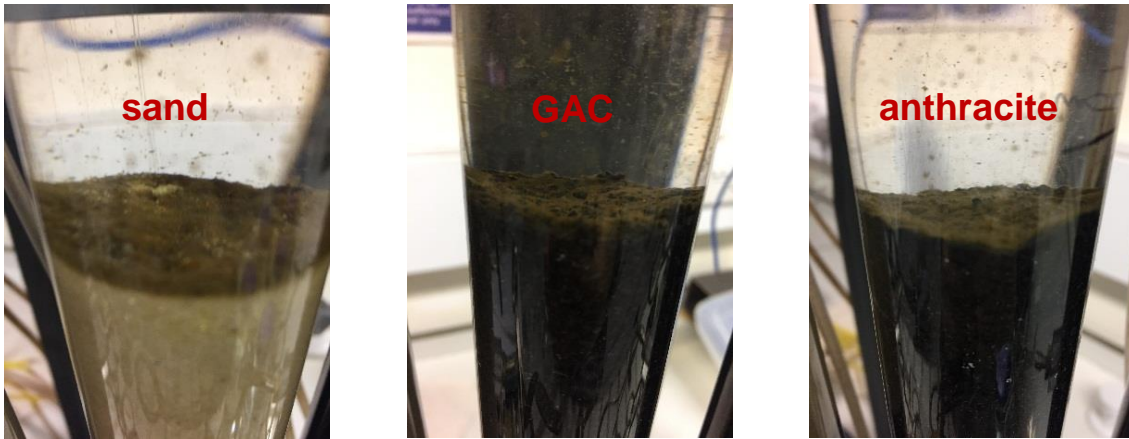


Figure A6.5 The slimy biofilm layer formed on different media surfaces. Photos were taken after 60 days of operation.

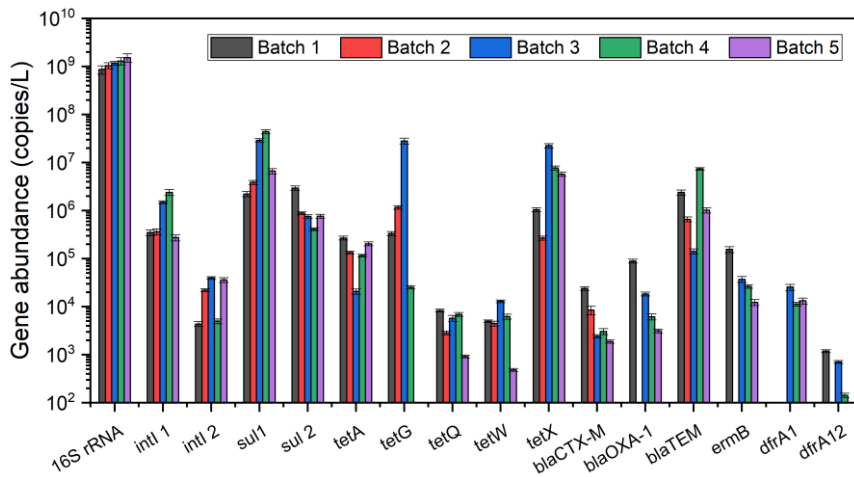
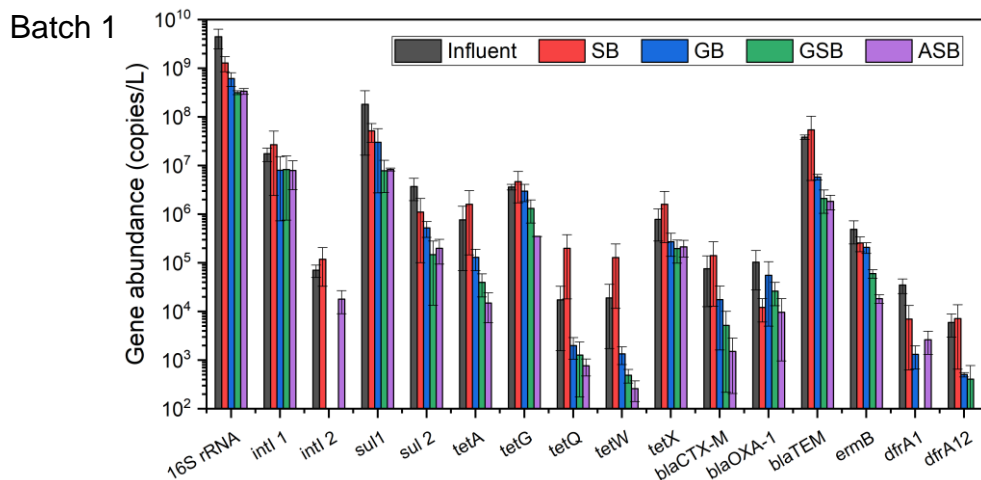


Figure A6.6 The concentration of target genes in lake water samples. The error bars represent STD from the mean value of qPCR results (n = 3).



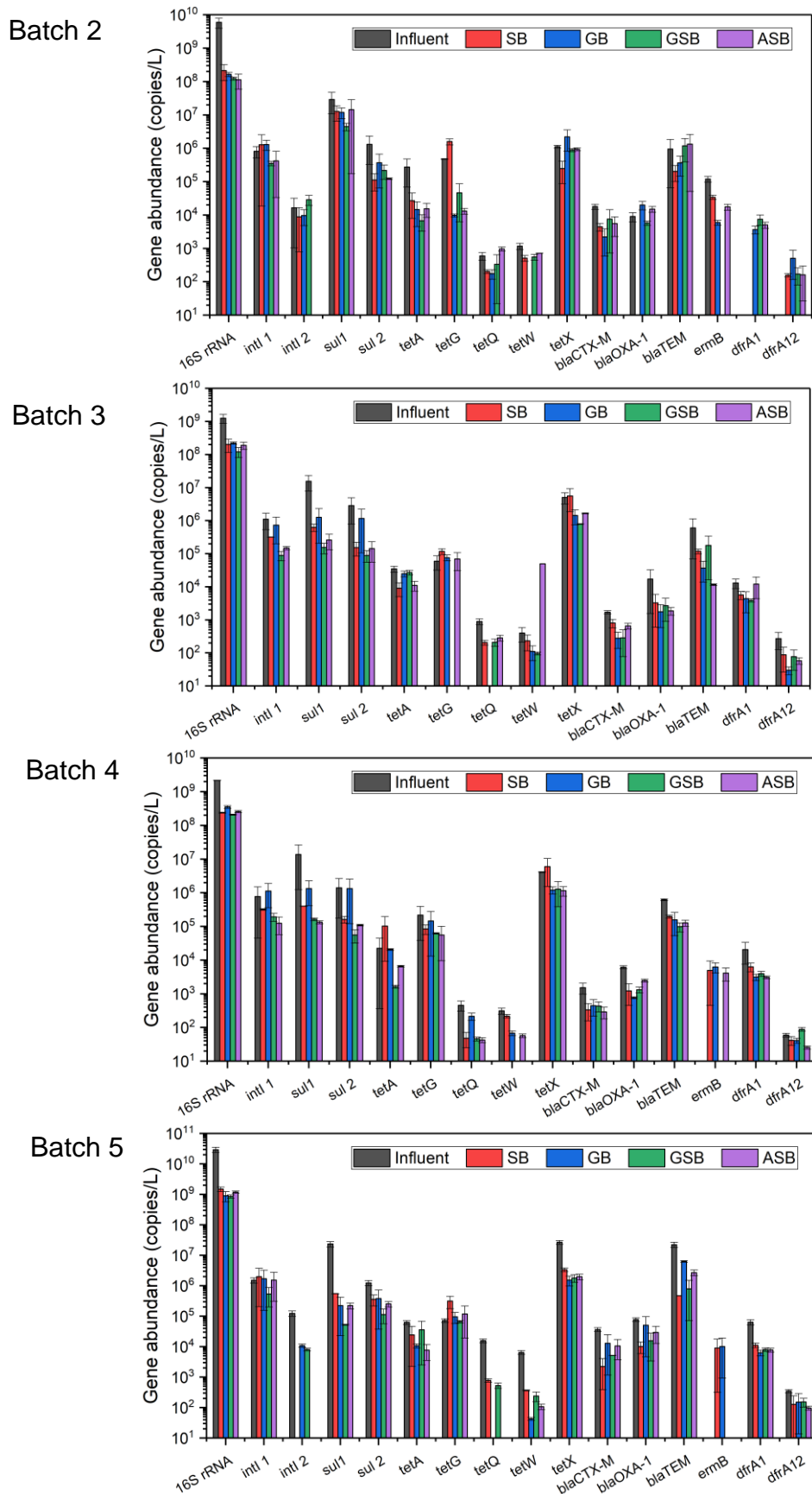


Figure A6.7 The concentration of target genes in the influents and effluents from batch 1-5. The error bars represent STD from the mean value of duplicate biofilters ($n = 2$).

Table A6.2 Correlation among ARGs in biofilm samples (n = 64) by Pearson correlation analysis.

Gene	<i>intl 1</i>	<i>intl 2</i>	<i>sul1</i>	<i>sul2</i>	<i>tetA</i>	<i>tetG</i>	<i>tetQ</i>	<i>tetW</i>	<i>tetX</i>	<i>bla_{CTX-M}</i>	<i>bla_{OXA-1}</i>	<i>bla_{TEM}</i>	<i>ermB</i>	<i>dfrA1</i>	<i>dfrA12</i>	Σint	Σsul	Σtet	Σbla	$\Sigma dfrA$	$\Sigma ARGs$	
<i>intl 1</i>	1.00																					
<i>intl 2</i>	0.45*	1.00																				
<i>sul1</i>	0.61**	0.73**	1.00																			
<i>sul2</i>	0.41**	0.69**	0.76**	1.00																		
<i>tetA</i>	0.47**	0.50**	0.64**	0.59**	1.00																	
<i>tetG</i>	0.41*	0.41	0.82**	0.72**	0.74**	1.00																
<i>tetQ</i>	0.17	0.22	0.30	0.53*	0.84**	0.75**	1.00															
<i>tetW</i>	0.22	0.23	0.56**	0.86**	0.84**	0.75**	0.89**	1.00														
<i>tetX</i>	-0.06	0.24	0.04	0.56**	0.49**	0.63**	0.43*	0.05	1.00													
<i>bla_{CTX-M}</i>	0.14	0.67**	0.35**	0.35*	0.45**	0.04	0.62**	0.96**	-0.04	1.00												
<i>bla_{OXA-1}</i>	0.03	0.88**	0.20	0.63**	0.41*	-0.06	0.88*	0.93*	0.08	0.19	1.00											
<i>bla_{TEM}</i>	-0.19	-0.04	0.12	0.44	0.79**	0.69**	0.99**	0.91**	0.43*	0.11	0.07	1.00										
<i>ermB</i>	-0.19	-0.02	0.03	0.51	0.83**	0.66*	1.00**	1.00**	0.93*	0.25	0.05	1.00**	1.00									
<i>dfrA1</i>	-0.07	-0.03	0.22	0.53*	0.87**	0.85**	1.00**	1.00**	0.06	0.25	0.13	1.00**	1.00**	1.00								
<i>dfrA12</i>	0.14	0.11	0.37*	0.47**	0.82**	0.66*	0.98**	0.93**	0.39*	0.23	0.28	0.96**	0.93**	0.99**	1.00							
Σint	0.99**	0.58**	0.66**	0.46**	0.50**	0.43*	0.18	0.22	-0.06	0.22	0.09	-0.18	-0.18	-0.06	0.15	1.00						
Σsul	0.60**	0.75**	1.00**	0.82**	0.65**	0.85**	0.35	0.63**	0.03	0.37**	0.19	0.18	0.10	0.27	0.40**	0.65**	1.00					
Σtet	0.44**	0.06	0.54**	0.34*	0.64**	1.00**	0.78**	0.63**	0.97*	0.07	0.00	0.68**	0.70**	0.85**	0.66**	0.43**	0.54**	1.00				
Σbla	0.06	0.07	0.25*	0.49**	0.70**	0.62**	0.99**	0.93**	0.01	0.25	0.05	1.00**	1.00**	0.99**	0.89**	0.07	0.29*	0.64**	1.00			
$\Sigma dfrA$	0.00	0.03	0.14	0.37*	0.63**	0.63**	0.98**	0.82**	0.11	0.19	0.03	0.97**	1.00**	1.00**	0.85**	0.01	0.18	0.65**	0.96**	1.00		
$\Sigma ARGs$	0.25*	0.25	0.52**	0.66**	0.81**	0.78**	0.96**	0.95**	0.23*	0.32*	0.09	0.97**	0.97**	0.97**	0.90**	0.27*	0.56**	0.75**	0.96**	0.89**	1.00	

Values indicate the Pearson correlation coefficient (r). The bold number means the significant level at the 0.05 level (2-tailed *) and 0.01 level (2-tailed **), otherwise means $P > 0.05$. Σint : total concentration of integron genes (*intl 1* and *intl 2*); Σsul : total concentration of sulfonamide resistance genes (*sul1* and *sul2*); Σtet : total concentration of tetracycline resistance genes (*tetA*, *tetG*, *tetQ*, *tetW*); Σbla : total concentration of β -lactams resistance genes; $\Sigma dfrA$: total concentration of resistance trimethoprim genes (*dfrA1* and *dfrA12*). $\Sigma ARGs$: total concentration of all ARGs detected in this study.

Table A6.3 Correlation among ARGs in aqueous samples (n = 54) by Pearson correlation analysis.

Gene	<i>intl1</i>	<i>intl2</i>	<i>sul1</i>	<i>sul2</i>	<i>tetA</i>	<i>tetG</i>	<i>tetQ</i>	<i>tetW</i>	<i>tetX</i>	<i>bla_{CTX-M}</i>	<i>bla_{OXA-1}</i>	<i>bla_{TEM}</i>	<i>ermB</i>	<i>dfrA1</i>	<i>dfrA12</i>	Σ <i>int</i>	Σ <i>sul</i>	Σ <i>tet</i>	Σ <i>bla</i>	Σ <i>dfrA</i>	Σ ARGs	
<i>intl1</i>	1.00																					
<i>intl2</i>	0.80**	1.00																				
<i>sul1</i>	0.50**	0.39	1.00																			
<i>sul2</i>	0.29*	0.25	0.28	1.00																		
<i>tetA</i>	0.89**	0.77**	0.53**	0.28	1.00																	
<i>tetG</i>	0.22	0.20	0.17	0.10	0.20	1.00																
<i>tetQ</i>	0.86**	0.77**	0.21	0.19	0.93**	0.19	1.00															
<i>tetW</i>	0.85**	0.77**	0.26	0.18	0.93**	0.22	1.00**	1.00														
<i>tetX</i>	-0.08	0.35*	-0.03	-0.03	-0.05	0.19	0.01	0.01	1.00													
<i>bla_{CTX-M}</i>	0.91**	0.83**	0.52**	0.31*	0.98**	0.20	0.94**	0.93**	-0.03	1.00												
<i>bla_{OXA-1}</i>	0.24	0.15	0.23	0.51**	0.06	0.08	-0.01	-0.04	-0.01	0.19	1.00											
<i>bla_{TEM}</i>	0.91**	0.87**	0.47**	0.38**	0.93**	0.21	0.91**	0.90**	-0.01	0.97**	0.28	1.00										
<i>ermB</i>	0.57**	0.49	0.51*	0.81**	0.39	0.13	0.35	0.35	-0.21	0.47*	0.74**	0.60**	1.00									
<i>dfrA1</i>	0.19	0.55*	0.43**	0.36*	0.19	0.23	0.09	0.13	0.31*	0.26	0.50**	0.31*	0.30	1.00								
<i>dfrA12</i>	0.94**	0.79**	0.53**	0.34*	0.99**	0.24	0.94**	0.94**	-0.01	0.99**	0.11	0.97**	0.72**	0.19	1.00							
Σ <i>int</i>	1.00**	0.80**	0.50**	0.29*	0.89**	0.22	0.86**	0.85**	-0.08	0.91**	0.24	0.91**	0.57**	0.19	0.94**	1.00						
Σ <i>sul</i>	0.50**	0.39	1.00**	0.30*	0.53**	0.17	0.21	0.26	-0.03	0.52**	0.24	0.48**	0.55**	0.43**	0.53**	0.50**	1.00					
Σ <i>tet</i>	0.35*	0.31	0.24	0.16	0.33*	0.99**	0.32*	0.35*	0.94**	0.33*	0.11	0.33*	0.19	0.26	0.38**	0.35**	0.24	1.00				
Σ <i>bla</i>	0.91**	0.87**	0.47**	0.39**	0.93**	0.21	0.91**	0.90**	0.00	0.97**	0.29*	1.00**	0.61**	0.30*	0.97**	0.91**	0.48**	0.34*	1.00			
Σ <i>dfrA</i>	0.26	0.70**	0.46**	0.21	0.35*	0.24	0.28	0.33*	0.32*	0.40**	0.13	0.43**	-0.06	0.98**	0.36*	0.26	0.46**	0.29*	0.43**	1.00		
Σ ARGs	0.75**	0.64**	0.94**	0.37**	0.76**	0.27	0.52**	0.55**	0.14	0.77**	0.29*	0.74**	0.62**	0.43**	0.77**	0.75**	0.94**	0.37**	0.74**	0.50**	1.00	

Values indicate the Pearson correlation coefficient (r). The bold number means the significant level at the 0.05 level (2-tailed *) and 0.01 level (2-tailed **), otherwise means P > 0.05. Σ int: total concentration of integron genes (*intl1* and *intl2*); Σ sul: total concentration of sulfonamide resistance genes (*sul1* and *sul2*); Σ tet: total concentration of tetracycline resistance genes (*tetA*, *tetG*, *tetQ*, *tetW*); Σ bla: total concentration of β -lactams resistance genes; Σ dfrA: total concentration of resistance trimethoprim genes (*dfrA1* and *dfrA12*). Σ ARGs: total concentration of all ARGs detected in this study.

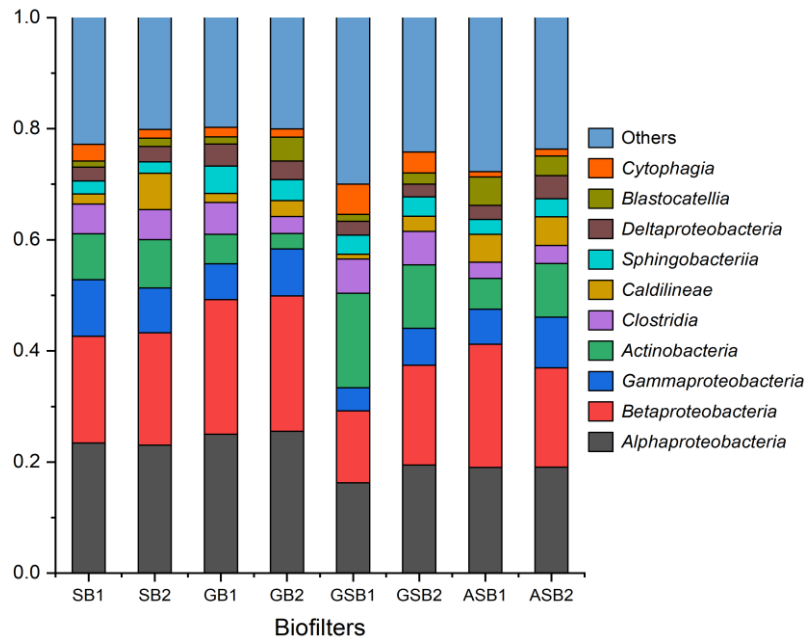


Figure A6.8 Structure of bacterial community (> 1% in any samples) at class level. SB: sand biofilter; GB: GAC biofilter; GSB: GAC sandwich biofilter; ASB: anthracite-sand biofilter.

Table A6.4 Correlation between ARGs and environmental variables in effluent samples (n = 40) by Pearson correlation analysis.

Gene	pH	Conductivity	Turbidity	DO	DOC	Nitrate	Phosphate	Antibiotics
<i>intl1</i>	-0.17	0.27	-0.05	-0.07	0.21	-0.05	0.46*	0.05
<i>sul1</i>	0.12	0.38	0.09	0.19	0.11	0.11	0.18	-0.09
<i>sul2</i>	0.10	0.29	-0.28	-0.14	-0.40	-0.03	0.14	0.28
<i>tetA</i>	-0.02	0.26	-0.10	-0.20	0.23	0.18	0.21	-0.10
<i>tetG</i>	-0.08	0.32	0.04	-0.22	0.14	0.03	0.33	0.02
<i>tetQ</i>	-0.08	0.12	0.01	-0.18	0.25	0.07	0.07	-0.12
<i>tetW</i>	-0.23	0.17	-0.12	-0.27	0.18	-0.06	-0.14	-0.22
<i>tetX</i>	-0.10	-0.02	-0.21	-0.37	0.11	0.12	-0.19	-0.18
<i>bla_{CTX-M}</i>	0.01	0.16	0.09	0.02	0.12	0.06	0.09	-0.03
<i>bla_{OXA-1}</i>	-0.06	0.09	0.16	0.21	-0.11	-0.26	0.09	0.20
<i>bla_{TEM}</i>	-0.07	0.17	0.06	-0.11	0.20	0.03	0.17	-0.04
<i>dfrA1</i>	0.03	0.30	-0.31	-0.09	-0.16	0.04	-0.25	-0.10
<i>dfrA12</i>	0.02	0.26	-0.03	-0.10	0.04	-0.07	0.11	0.05

Values indicate the Pearson correlation coefficient (r). The bold number means the significant level at the 0.05 level (2-tailed *), otherwise means $P > 0.05$. *Intl 2* and *ermB* were excluded from the analysis due to the low detection frequency. DO: dissolved oxygen; DOC: dissolved organic carbon.

Table A6.5 Correlation between ARGs and major bacterial phyla in biofilm samples (n = 8) by Pearson correlation analysis.

Genes	<i>Proteobacteria</i>	<i>Firmicutes</i>	<i>Actinobacteria</i>	<i>Acidobacteria</i>	<i>Bacteroidetes</i>	<i>Chloroflexi</i>	<i>Nitrospirae</i>
<i>intl1</i>	0.65*	-0.52	-0.68*	0.75**	-0.27	-0.36	0.40
<i>intl2</i>	0.63*	-0.41	-0.31	0.03	-0.48	-0.40	-0.34
<i>sul1</i>	0.55	0.15	-0.76**	0.60*	-0.31	-0.21	0.74**
<i>sul2</i>	0.75**	-0.39	-0.70*	0.42	-0.24	-0.52	0.33
<i>tetA</i>	0.35	0.44	-0.65*	0.63*	-0.50	0.04	0.72**
<i>tetG</i>	0.43	0.17	-0.70*	0.68*	-0.22	-0.25	0.78**
<i>tetX</i>	0.54	-0.32	-0.54	0.33	0.01	-0.55	0.36
<i>bla_{CTX-M}</i>	-0.09	0.12	0.36	-0.45	-0.09	-0.29	-0.59
<i>bla_{OXA-1}</i>	0.07	0.04	0.21	-0.42	-0.07	-0.42	-0.51
<i>bla_{TEM}</i>	-0.46	0.21	0.69*	-0.60	0.31	-0.47	-0.68*
<i>ermB</i>	0.41	-0.14	-0.38	-0.01	0.17	-0.46	0.28
<i>dfrA1</i>	0.45	-0.19	-0.36	-0.05	0.08	-0.56	0.14
<i>dfrA12</i>	0.01	0.57	-0.43	0.60	-0.24	0.34	0.82**

Values indicate the Pearson correlation coefficient (r). The bold number means the significant level at the 0.05 level (2-tailed *) and 0.01 level (2-tailed **), otherwise means $P > 0.05$. *tetQ* and *tetW* were excluded from the analysis due to the low detection frequency.

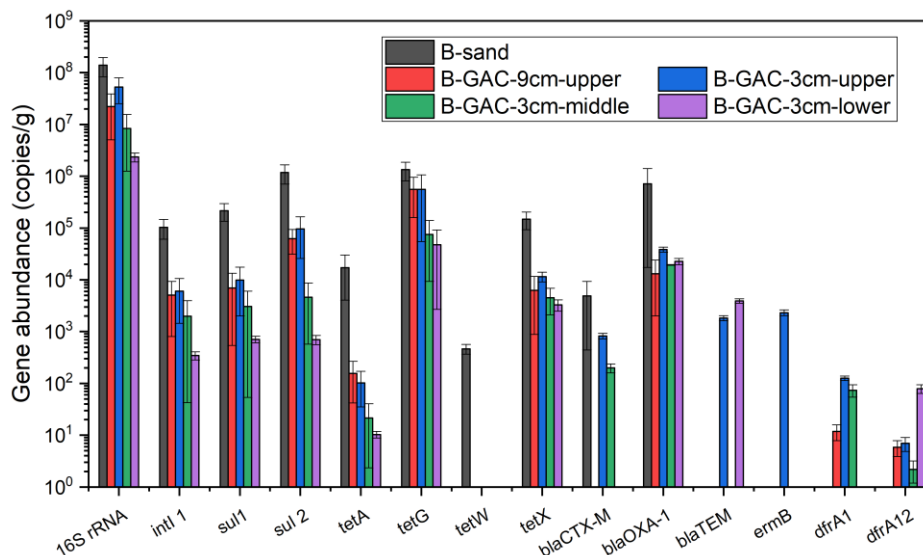


Figure A6.9 Absolute abundance of 16S rRNA, ARGs and integron in biofilm samples collected at 3-week. B-sand: surface sand biofilm; B-GAC: GAC biofilms collected at different positions.

The error bars represent STD from the mean value of duplicate biofilm samples (n = 2).

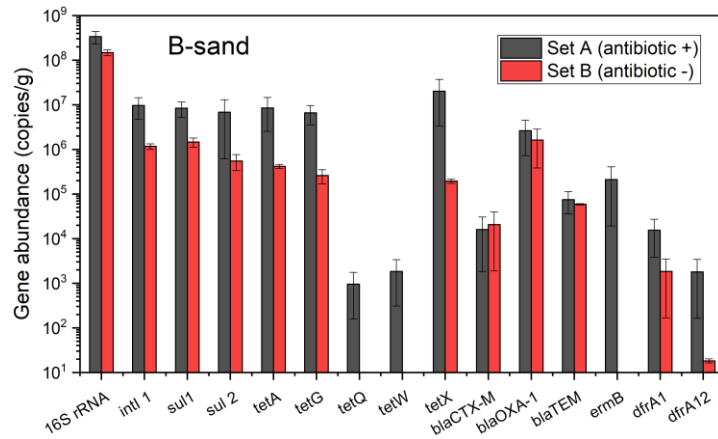


Figure A6.10 Absolute abundance of 16S rRNA, ARGs and integron in surface sand biofilm (B-sand) samples collected at 11-week. The error bars represent STD from the mean value of biofilm samples from Set A and B (n = 4).

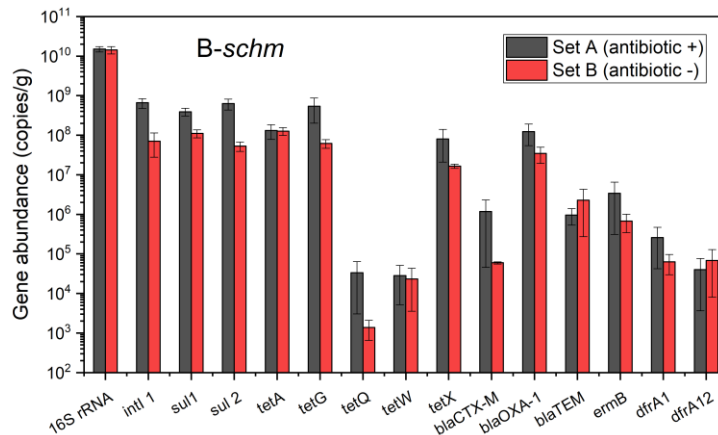


Figure A6.11 Absolute abundance of 16S rRNA, ARGs and integron in schmutzdecke layer (B-schm) biofilms collected at 11-week. The error bars represent STD from the mean value of biofilm samples from Set A and B (n = 4).

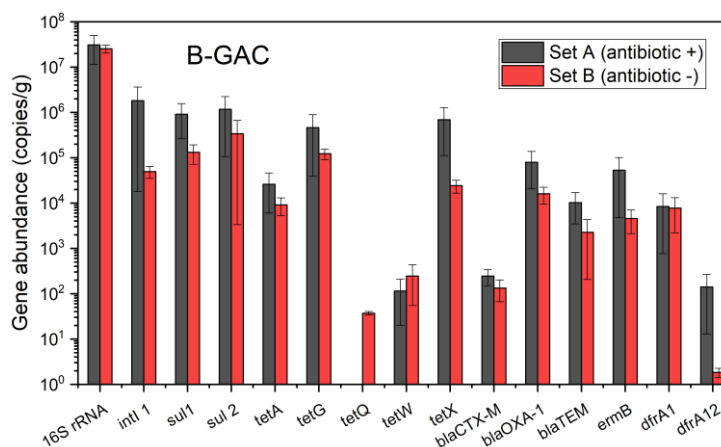


Figure A6.12 Absolute abundance of 16S rRNA, ARGs and integron in GAC biofilm (B-GAC) samples collected at 11-week. The error bars represent STD from the mean value of biofilm samples from Set A and B (n = 4).

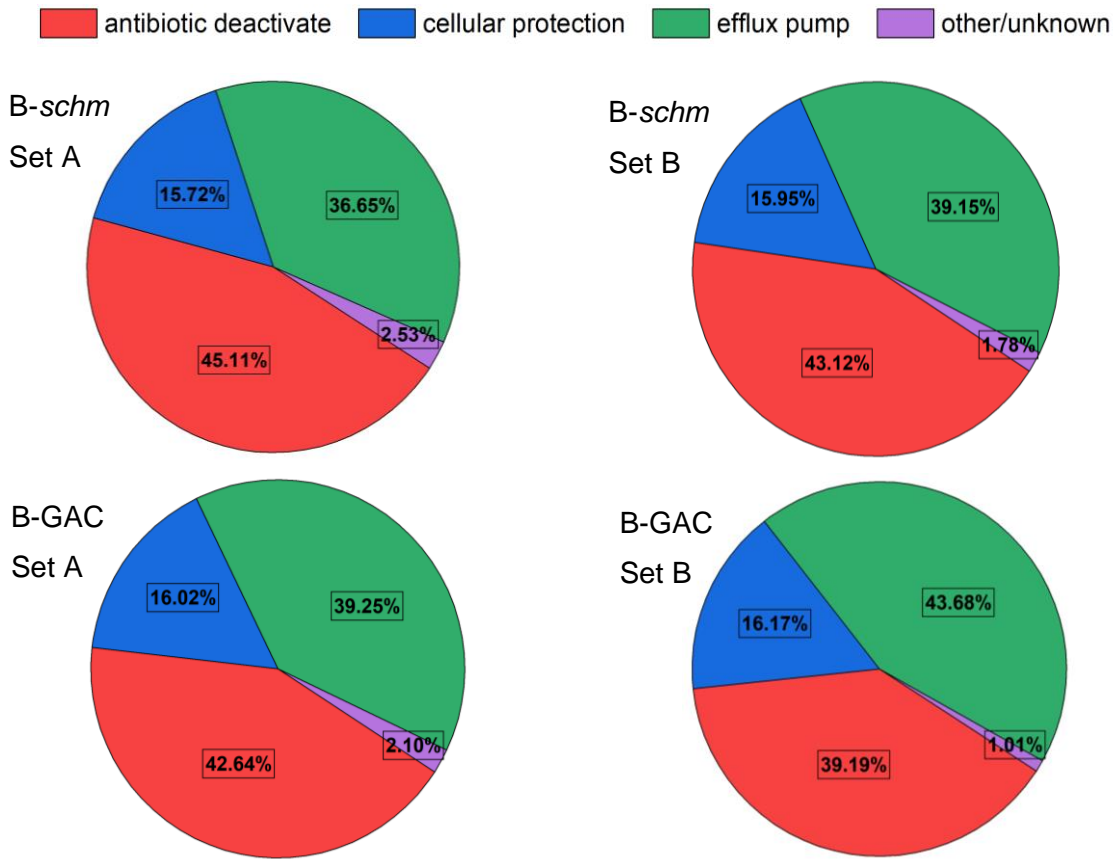
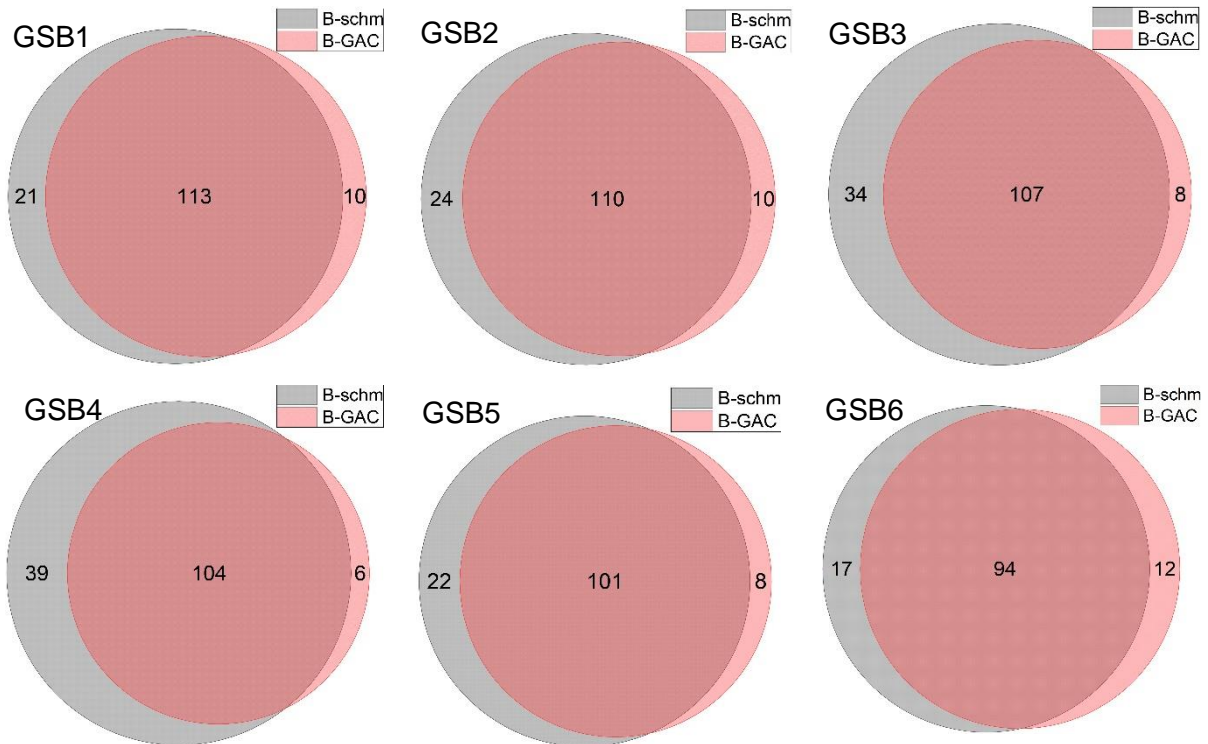


Figure A6.13 Resistance genes detected in B-schm (*schmutzdecke*) and B-GAC samples were classified based on the mechanism of resistance.



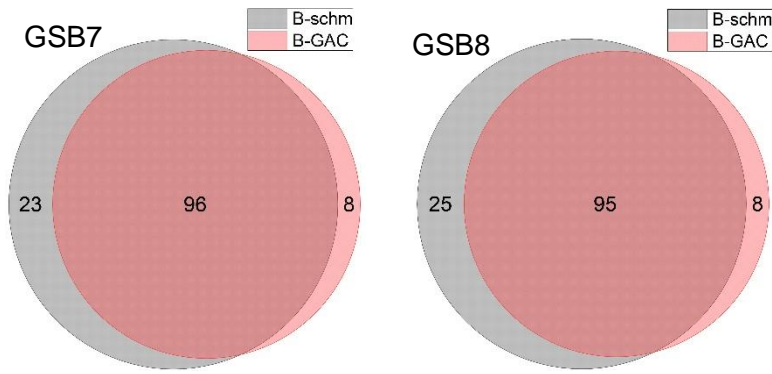


Figure A6.14 Venn diagram showing the number of detected ARGs among B-schm (*schmutzdecke*) and B-GAC biofilm samples in each GAC sandwich biofilter (GSB).

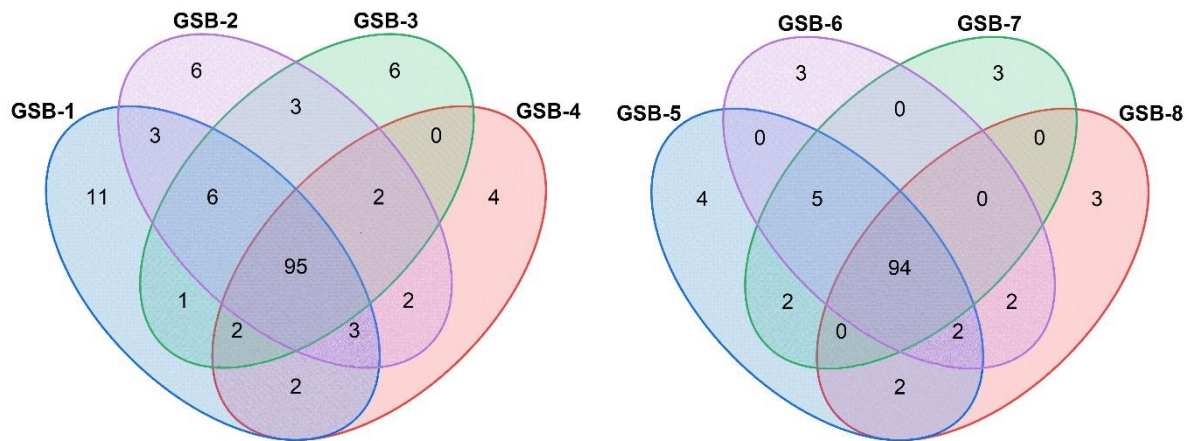
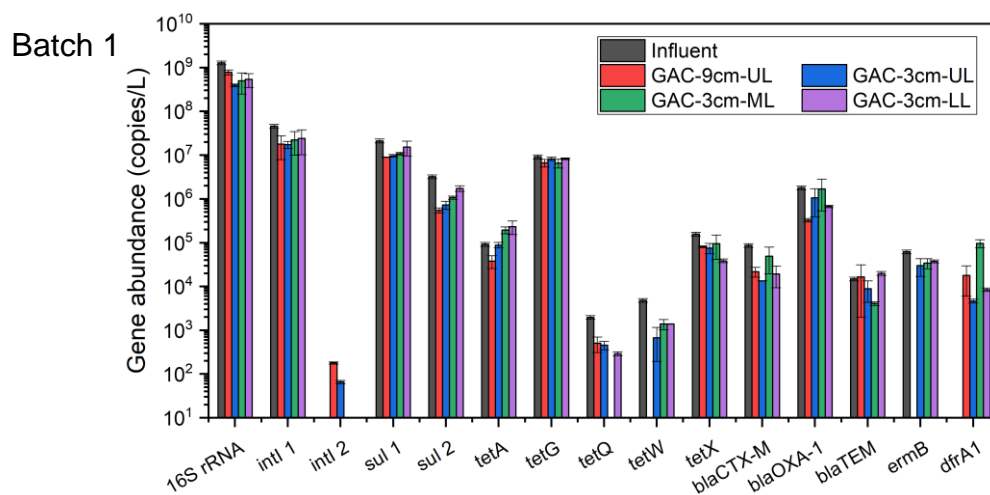
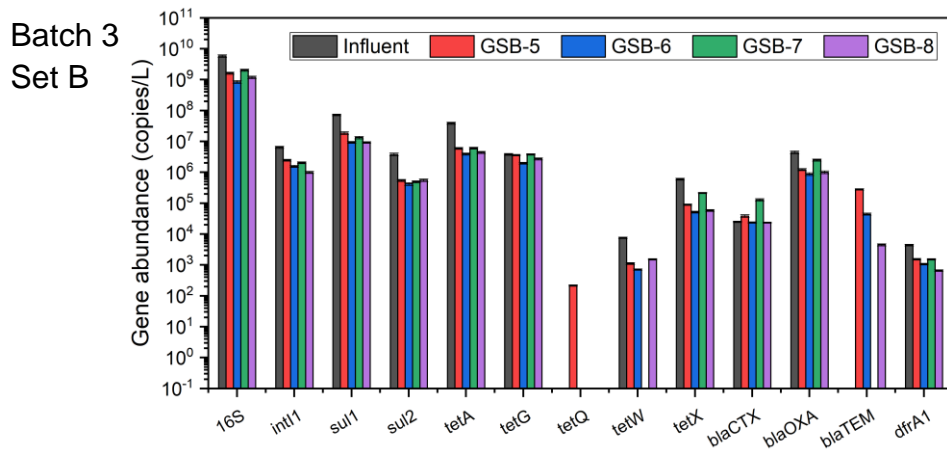
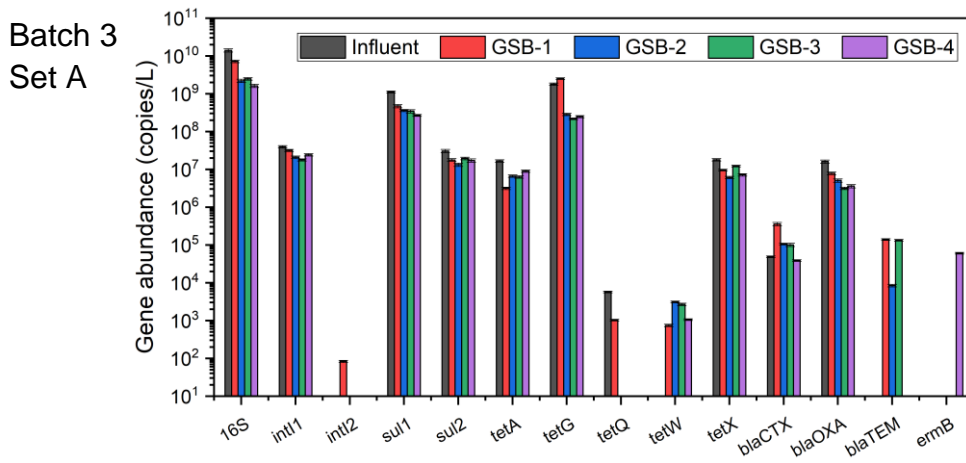
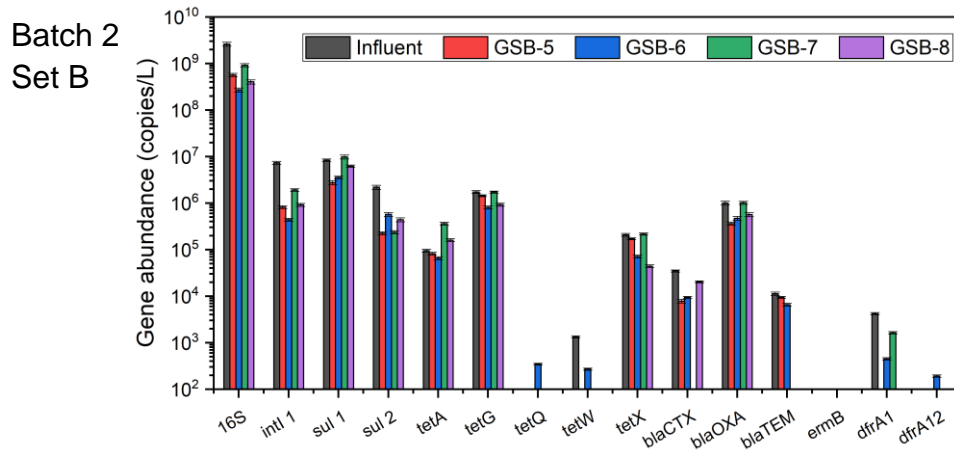
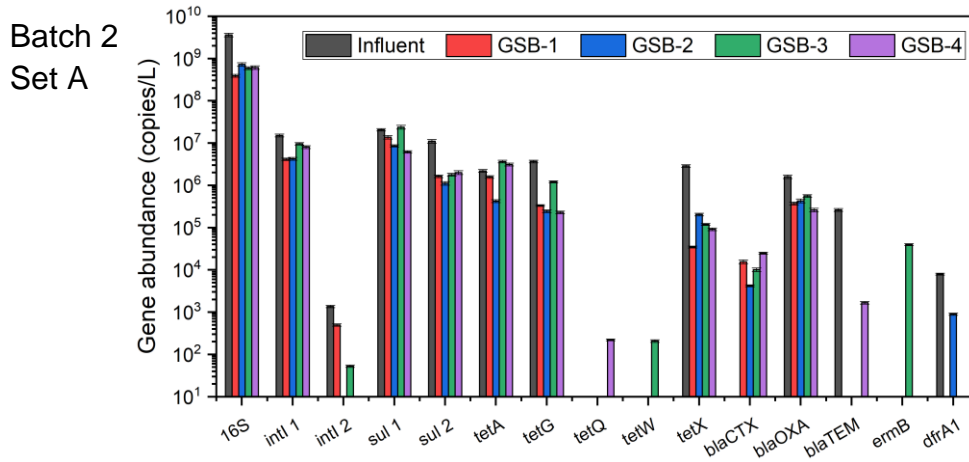
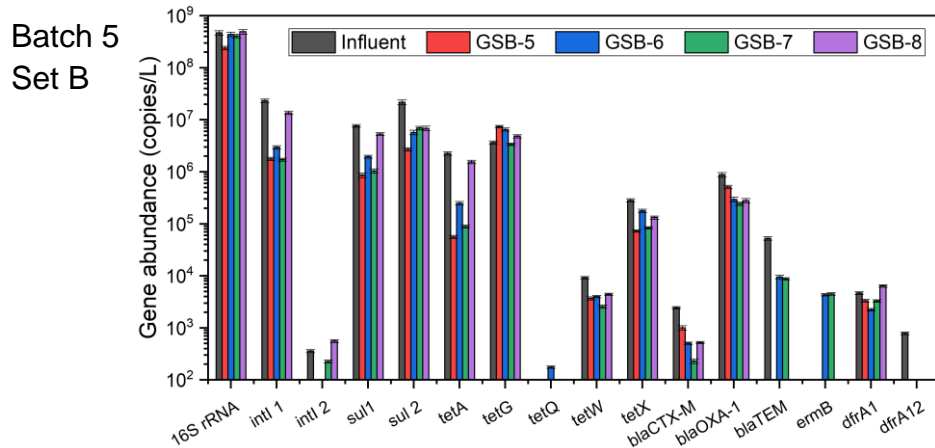
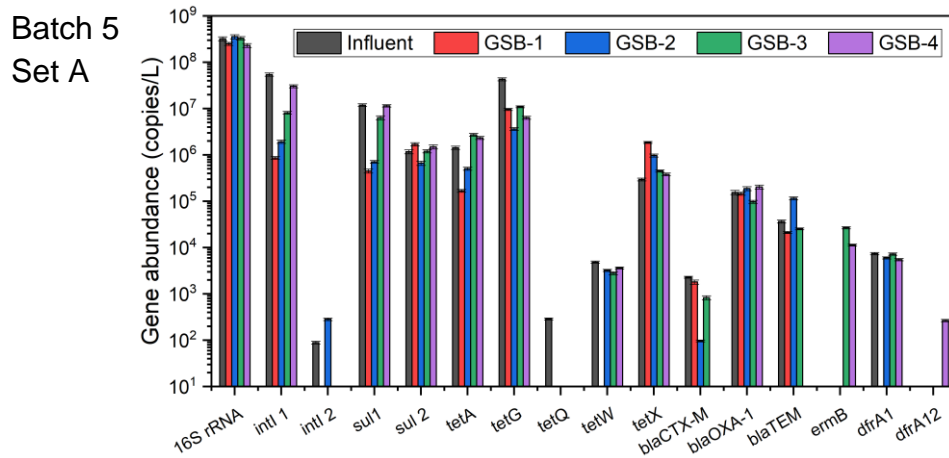
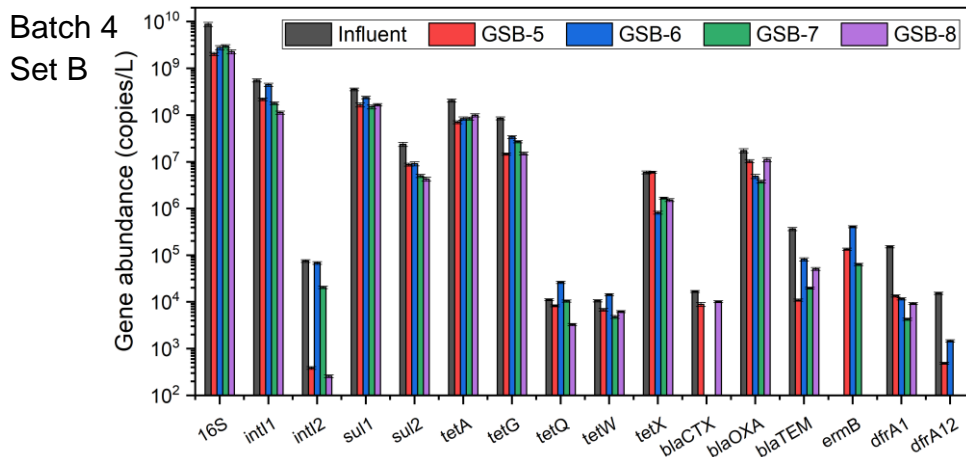
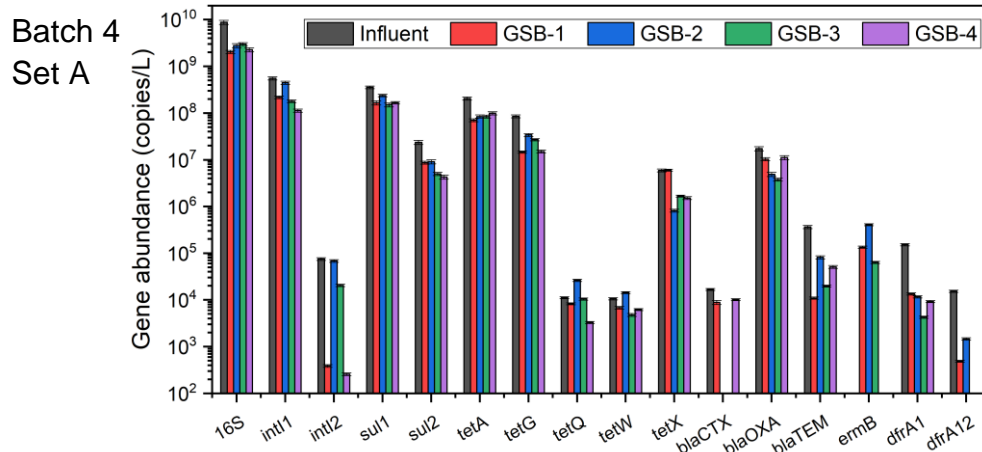


Figure A6.15 Venn diagram showing the number of detected ARGs in GAC biofilms in Set A (left) and B (right). GSB: GAC sandwich biofilter.







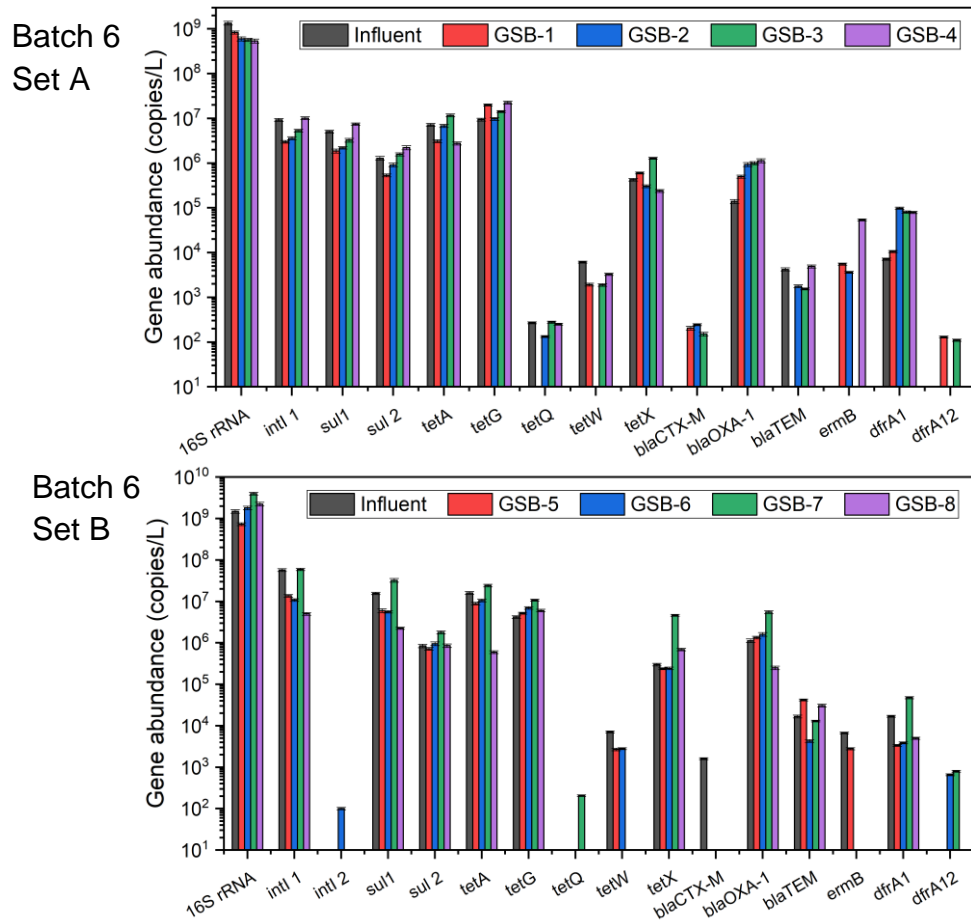


Figure A6.16 Absolute abundance of 16S rRNA, ARGs and integron in influent and effluent samples collected at different batches. Set A: biofilters spiked with 10 µg/L antibiotics; Set B: control biofilters without antibiotic addition. The error bars represent STD from the mean value of qPCR replicates (n = 3).

Table A6.6 The Pearson correlation of the relative abundance of ARGs between B-schm (schmutzdecke layer), B-sand (surface sand biofilm), B-GAC (GAC layer biofilm), raw water, influent and effluent samples.

Sample type	B-schm	B-sand	B-GAC	Raw water	Influent	Effluent
B-schm	1					
B-sand	0.969	1				
B-GAC	0.904	0.930	1			
Raw water	0.775	0.787	0.878	1		
Influent	0.962	0.928	0.901	0.873	1	
Effluent	0.962	0.953	0.891	0.829	0.972	1

All P values less than 0.001.

Table A6.7 Number of total tags, taxonomic tags and OTUs in B-schm (*schmutzdecke* layer) and GAC (B-GAC) biofilm samples.

Sample type	Samples	Total tags	Taxonomic tags	OTUs
B-schm	GSB-1	90758	80822	2924
	GSB-2	115143	103324	3118
	GSB-3	170741	151858	3551
	GSB-4	187347	164542	3729
	GSB-5	181194	164456	3188
	GSB-6	92857	86482	1774
	GSB-7	141897	126536	3198
	GSB-8	128321	107399	3640
B-GAC	GSB-1	83734	76165	2417
	GSB-2	86451	77368	2774
	GSB-3	68874	62092	2393
	GSB-4	137855	111801	2401
	GSB-5	44487	38123	2373
	GSB-6	48219	40572	2741
	GSB-7	96364	86039	3088
	GSB-8	89171	78376	3026

GSB: GAC sandwich biofilter. OUT: operational taxonomic unit.

Table A6.8 The percentage relative abundance of genera associated with opportunistic human pathogens in *schmutzdecke* biofilms.

Genera	GSB-1	GSB-2	GSB-3	GSB-4	GSB-5	GSB-6	GSB-7	GSB-8
<i>Acinetobacter</i>	0.042	0.037	0.079	0.091	0.043	0.200	0.107	0.098
<i>Aeromonas</i>	0.012	0.017	0.017	0.023	0.013	0.161	0.008	0.034
<i>Bacillus</i>	0.364	0.169	1.198	1.060	16.30	34.93	19.35	2.94
<i>Clostridium</i>	0.032	0.028	0.207	0.019	0.020	0.021	0.020	0.454
<i>Corynebacterium</i>	0.005	0	0.001	0.001	0.001	0	0.006	0.008
<i>Escherichia</i>	0.002	0.022	0.020	0.459	0.003	0.027	0.005	0.023
<i>Haemophilus</i>	0.002	0	0	0	0.060	0	0.002	0.004
<i>Legionella</i>	0.588	0.557	0.159	0.231	0.427	0.969	0.540	0.410
<i>Mycobacterium</i>	0.195	0.210	0.168	0.244	0.544	0.946	0.544	0.386
<i>Pseudomonas</i>	0.088	0.083	0.040	0.112	0.296	0.090	0.043	0.044
<i>Staphylococcus</i>	0.014	0	0	0.001	0	0.016	0.002	0.014
<i>Streptococcus</i>	0.002	0.002	0.015	0.034	0.107	0.006	0.073	0.011

GSB: GAC sandwich biofilter.

Table A6.9 The percentage relative abundance of genera associated with opportunistic human pathogens in GAC biofilms.

Genera	GSB-1	GSB-2	GSB-3	GSB-4	GSB-5	GSB-6	GSB-7	GSB-8
<i>Acinetobacter</i>	0.146	0.071	0.031	0.020	0.168	0.133	0.835	0.223
<i>Aeromonas</i>	0.004	0.017	0.016	0.003	0.010	0.042	0.467	0.108
<i>Bacillus</i>	1.178	0.246	1.234	0.662	1.991	0.705	0.185	0.179
<i>Clostridium</i>	0.007	0.018	0.019	0.098	0.034	0.513	0.128	0.057
<i>Corynebacterium</i>	0	0.001	0.002	0.002	0	0.007	0	0
<i>Escherichia</i>	0.009	0.403	0.003	0.020	0.018	0.027	0.019	0.054
<i>Haemophilus</i>	0.001	0	0.063	0.002	0.005	0.010	0.005	0.003
<i>Legionella</i>	0.126	0.570	0.763	0.236	0.758	0.961	2.491	1.372
<i>Mycobacterium</i>	0.181	0.133	0.166	0.094	0.186	0.281	0.182	0.227
<i>Pseudomonas</i>	0.277	0.120	0.362	0.202	0.063	0.047	0.053	0.080
<i>Staphylococcus</i>	0	0	0	0.001	0	0.007	0.001	0.008
<i>Streptococcus</i>	0.034	0.037	0.140	0.007	0.108	0.005	0.001	0.004

GSB: GAC sandwich biofilter.

Table A6.10 Correlation between operational parameters and the relative abundance of ARGs.

	<i>intl1</i>	<i>sul1</i>	<i>sul2</i>	<i>tetA</i>	<i>tetG</i>	<i>tetX</i>	<i>bla_{CTX-M}</i>	<i>bla_{OXA-1}</i>	<i>bla_{TEM}</i>	<i>ermB</i>	<i>dfrA1</i>
pH	-0.21	0.17	-0.32	-0.33	0.26	-0.04	0.46**	-0.10	-0.04	-0.01	0.19
Conductivity	0.23	0.14	0.28	0.53**	-0.06	0.21	-0.50**	0.40*	0.16	0.08	-0.30
Turbidity	0.53**	0.39*	-0.08	0.71**	0.48**	0.51**	-0.13	0.10	-0.09	0.29	-0.03
DO	-0.13	0.12	0.06	-0.12	0.16	0.08	0.36*	-0.04	0.16	-0.13	0.01
COD	0.11	0.07	0.13	0.36*	-0.05	0.17	-0.24	-0.17	0.08	-0.24	-0.30
DOC	0.06	0.44**	0.17	0.37*	0.26	0.36*	-0.29	-0.15	0.16	-0.13	-0.44
Nitrate	0.09	-0.19	-0.39*	0.09	-0.35	0.44**	0.02	0.64**	-0.29	0.43	0.01
Phosphate	0.21	-0.22	-0.06	-0.12	-0.24	-0.23	0.15	0.31	-0.16	0.10	0.38*

Values indicate the Pearson correlation coefficient (r). The bold number means the significant level at the 0.05 level (2-tailed *) and 0.01 level (2-tailed **), otherwise means P > 0.05.

Table A6.11 Correlation among ARGs (relative abundance) in effluent samples (n = 48) by Pearson correlation analysis.

ARGs	<i>intl1</i>	<i>sul1</i>	<i>sul2</i>	<i>tetA</i>	<i>tetG</i>	<i>tetQ</i>	<i>tetW</i>	<i>tetX</i>	<i>bla_{CTX-M}</i>	<i>bla_{OXA-1}</i>	<i>bla_{TEM}</i>	<i>ermB</i>	<i>dfrA1</i>
<i>sul1</i>	0.52**												
<i>sul2</i>	0.42**	0.18											
<i>tetA</i>	0.30	0.49**	0.15										
<i>tetG</i>	0.30	0.35*	0.50**	-0.07									
<i>tetQ</i>	0.52*	0.53*	0.20	0.46	-0.20								
<i>tetW</i>	0.29	-0.33	0.33	0.05	-0.22	0.71**							
<i>tetX</i>	0.17	0.25	0.50**	0.28	0.63**	0.18	-0.05						
<i>bla_{CTX-M}</i>	-0.01	0.45**	-0.37*	-0.16	0.04	-0.52	-0.67**	-0.26					
<i>bla_{OXA-1}</i>	0.27	0.48**	0.01	0.19	0.07	0.77**	0.22	-0.03	0.16				
<i>bla_{TEM}</i>	-0.25	-0.31	-0.05	-0.05	0.11	-0.08	0.16	0.16	-0.41	-0.14			
<i>ermB</i>	0.41	0.60**	-0.63**	0.21	-0.13	0.72**	0.02	-0.11	0.58*	0.52*	0.26		
<i>dfrA1</i>	0.51**	-0.07	0.37*	-0.28	0.36*	0.12	0.62**	0.10	-0.31	0.01	0.07	0.23	

Values indicate the Pearson correlation coefficient (r). The bold number means the significant level at the 0.05 level (2-tailed *) and 0.01 level (2-tailed **), otherwise means P > 0.05.

Table A6.12 Correlation between ARGs types (relative abundance) and taxonomic genus in in *schmutzdecke* and GAC biofilm samples by Pearson correlation analysis.

	Aminoglycoside	Beta-Lactamase	FCA	MLSB	Multidrug	Other	Sulfonamide	Tetracycline	Vancomycin	<i>intl</i>	Transposase
<i>Sulfuritalea</i>	0.04	0.13	0.04	0.43	-0.10	-0.05	-0.07	-0.44	0.05	0.36	-0.27
<i>Bacillus</i>	-0.25	0.10	-0.42	-0.41	-0.60	0.83**	-0.40	0.57*	-0.39	-0.36	0.70**
<i>Denitratisoma</i>	-0.12	-0.14	0.06	0.13	-0.32	-0.33	-0.01	-0.56*	0.06	0.38	-0.41
<i>Noviherbaspirillum</i>	-0.26	-0.08	-0.47	-0.39	-0.53	0.88**	-0.44	0.51*	-0.40	-0.38	0.83**
<i>Bradyrhizobium</i>	-0.29	-0.40	-0.01	-0.25	-0.02	-0.30	-0.24	-0.58*	-0.09	-0.05	-0.44
<i>Hyphomicrobium</i>	0.39	0.15	0.10	0.15	-0.08	-0.01	0.36	0.01	0.42	0.13	-0.11
<i>Methyloversatilis</i>	0.80**	0.60*	0.10	0.53*	0.42	-0.08	0.68**	0.37	0.73**	0.24	-0.12
<i>Sphingopyxis</i>	-0.09	0.16	-0.45	-0.26	-0.49	0.83**	-0.28	0.56*	-0.17	-0.31	0.76**
<i>Lysobacter</i>	0.66**	0.66**	-0.01	0.53*	0.16	0.01	0.53*	0.58*	0.82**	0.09	0.28
<i>Nitrospira</i>	0.83**	0.68**	0.10	0.58*	0.33	0.02	0.64**	0.55*	0.79**	0.12	0.10

The bold number means the significant level at the 0.05 level (2-tailed *) and 0.01 level (2-tailed **), otherwise means P > 0.05.

Table A6.13 Correlation among ARGs types (relative abundance) in *schmutzdecke* and GAC biofilm samples by Pearson correlation analysis.

	Aminoglycoside	Beta-Lactamase	FCA	MLSB	Multidrug	Other	Sulfonamide	Tetracycline	Vancomycin	<i>intl</i>	Transposase
Aminoglycoside	1.00										
Beta_Lactamase	0.64**	1.00									
FCA	0.47	-0.12	1.00								
MLSB	0.62**	0.71**	0.07	1.00							
Multidrug	0.56*	0.28	0.46	0.43	1.00						
Other	-0.11	0.08	-0.36	-0.32	-0.41	1.00					
Sulfonamide	0.62**	0.42	0.49	0.31	0.49	-0.31	1.00				
Tetracycline	0.25	0.33	-0.05	-0.26	-0.14	0.49	0.36	1.00			
Vancomycin	0.72**	0.69**	0.21	0.56*	0.44	-0.29	0.69**	0.22	1.00		
<i>intl</i>	0.38	0.48	0.00	0.83**	0.15	-0.32	0.27	-0.37	0.30	1.00	
Transposase	-0.11	0.00	-0.36	-0.30	-0.51	0.55*	-0.34	0.60*	-0.28	-0.31	1.00

The bold number means the significant level at the 0.05 level (2-tailed *) and 0.01 level (2-tailed **), otherwise means P > 0.05.

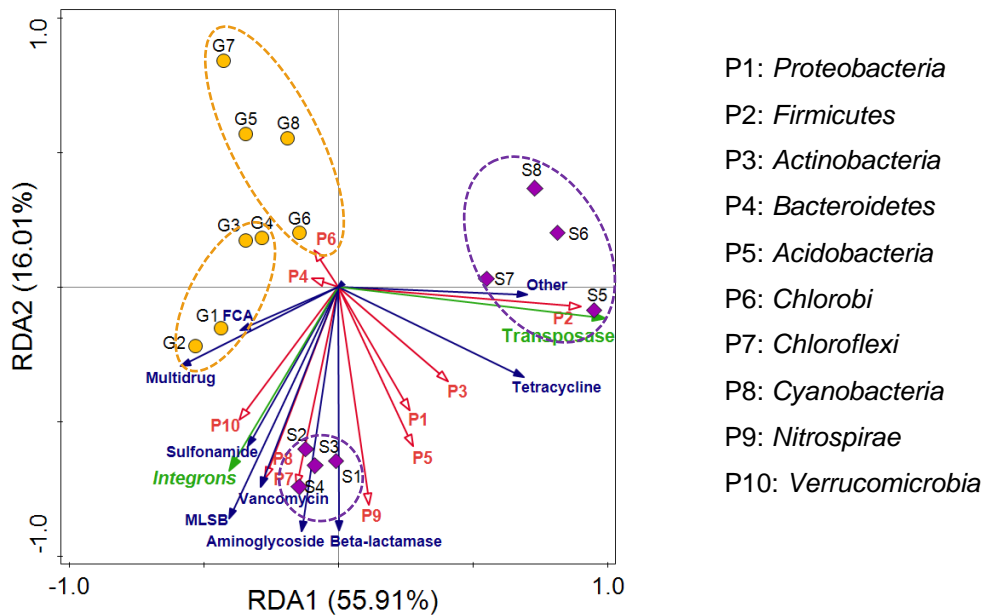


Figure A6.17 Redundancy analysis (RDA) of the correlation between major phyla (top 10) and relative abundance of ARGs types in biofilm samples. MLSB = Macrolide-Lincosamide-Streptogramin B resistance genes; FCA = fluoroquinolone, quinolone, florfenicol, chloramphenicol and amphenicol resistance genes. Purple and diamond scatters S1-4: *schmutzdecke* biofilms exposed to antibiotics; S5-8: *schmutzdecke* biofilms unexposed to antibiotics; Yellow and circle scatters G1-4: GAC biofilms exposed to antibiotics; G5-8: GAC biofilms unexposed to antibiotics.

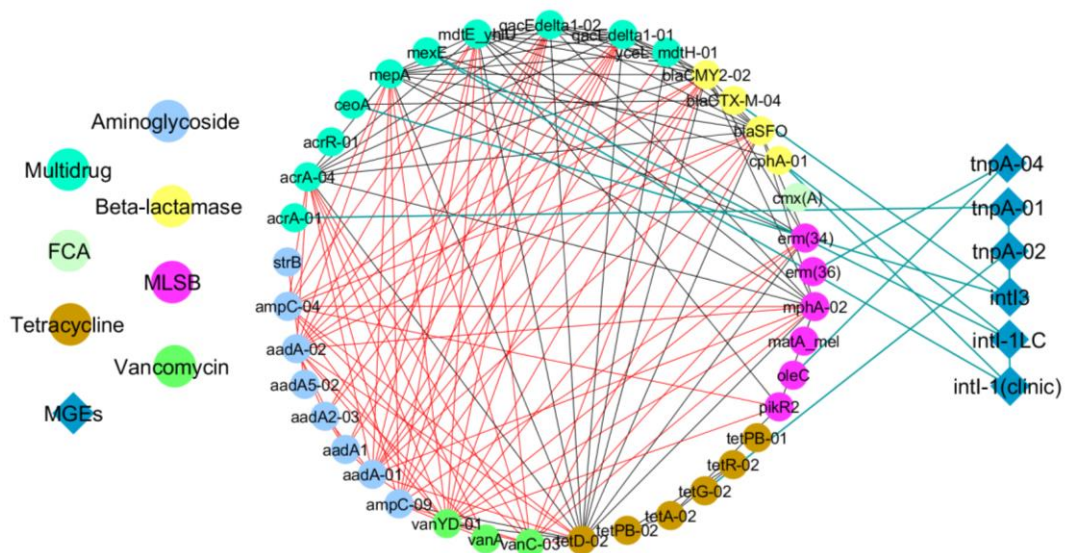


Figure A6.18 Network analysis revealing the co-occurrence patterns between ARG subtypes and MGEs, including transposons and integrons. The nodes were coloured according to ARGs types. The connection between ARGs subtypes represents a strong (Pearson's $r > 0.8$) and significant ($P < 0.01$) correlation. Red edges indicate the connection between aminoglycoside/vancomycin and other ARG subtypes; black edges are the connections among the rest ARG subtypes; and green edges indicate the connection between MGEs and ARG subtypes. MLSB = Macrolide-Lincosamide-Streptogramin B resistance genes; FCA = fluoroquinolone, quinolone, florfenicol, chloramphenicol and amphenicol resistance genes.

Appendix – Chapter 7

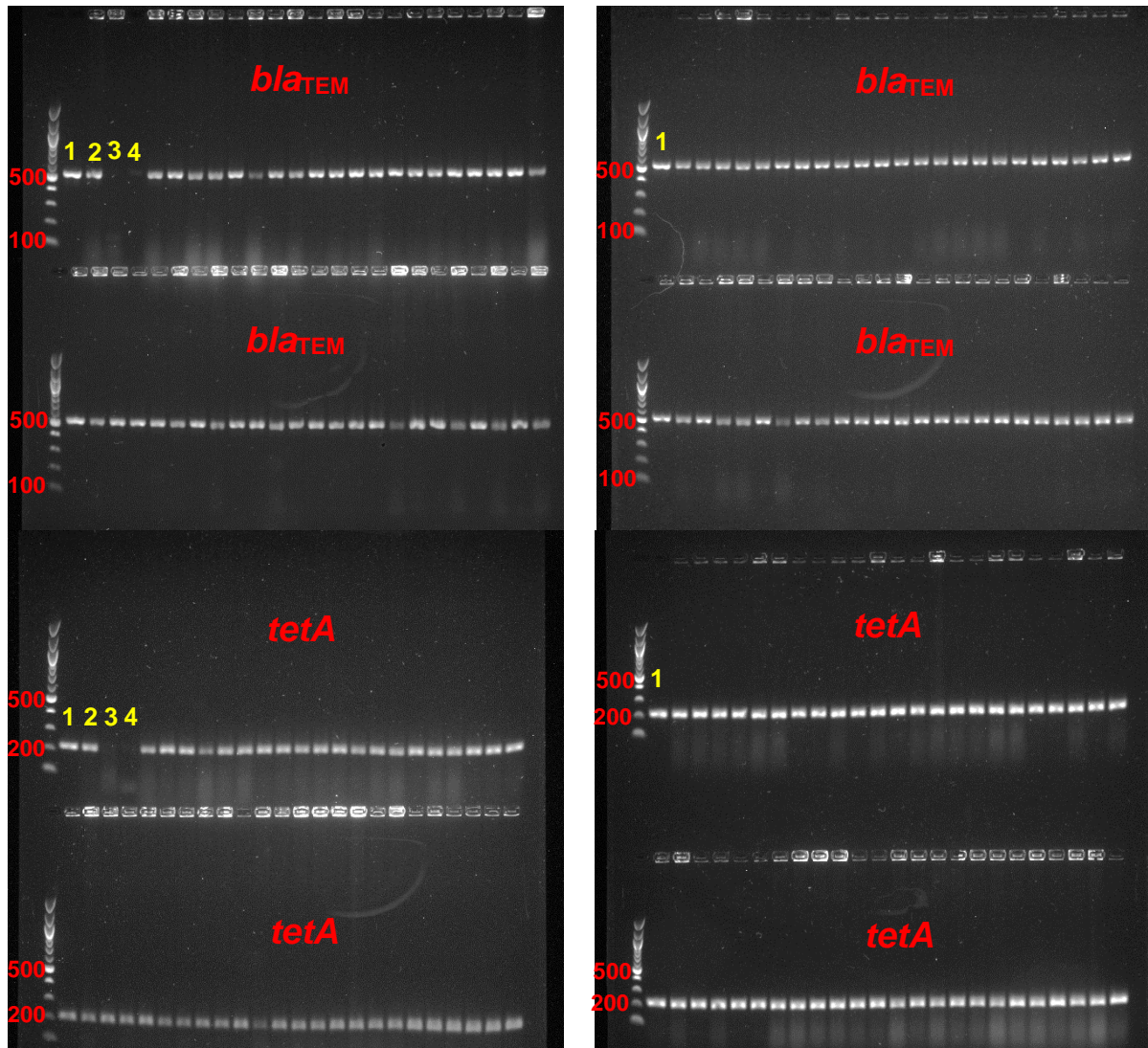


Figure A7.1 Gel images showed the presence of *bla*_{TEM} (516 bp) and *tetA* (210 bp) in all of the transconjugants. Lane 1: RP1 plasmid as positive control; Lane 2: donor cell (*E. coli* J53); Lane 3: recipient cell (*E. coli* HB101); Lane 4: PCR negative control. The rest of the lanes are colonies randomly selected from the plates on which transconjugants grew.